UNIVERSITY OF CALIFORNIA
RIVERSIDE

Toxicogenomic Assessment of Particulate Matter (PM)-Induced Health Effects

A Dissertation submitted in partial satisfaction
of the requirements for the degree of

Doctor of Philosophy

in

Environmental Toxicology

by

C. M. Sabbir Ahmed

June 2021

Dissertation Committee:
Dr. Ying-Hsuan Lin, Chairperson
Dr. David A. Eastmond
Dr. Roya Bahreini

The Dissertation of C. M. Sabbir Ahmed is approved:

_____

_____

_____

Committee Chairperson

University of California, Riverside

Acknowledgements

First and foremost, this dissertation would not have been possible without the generous support, assistance, and insightful feedback from many people. I would like to express my sincerest thanks to my advisor, Dr. Ying-Hsuan Lin, for her trust, encouragement, and unconditional support over the years that have really helped me go further and successfully completed this dissertation. She always guided and encouraged me to come up with new and simple solutions to complex problems. I always had the moral support and the freedom to work on interesting problems during Ph.D. I have learned a lot from her expertise and immense knowledge in the field of atmospheric chemistry and toxicology. I will carry her teachings with me, not just as a researcher but also as a human being, for the rest of my life and will try to improve myself from the time I had her as a guardian.

I would also like to thank my proposal and dissertation committee: Dr. David A. Eastmond, Dr. Roya Bahreini, Dr. Georgios Karavalakis, Dr. William C. Porter, and Dr. Tara M. Nordgren, for their valuable time, encouragement, and insightful comments. Particularly, I am grateful to Dr. Eastmond and Dr. Bahreini for their valuable suggestion, unconditional support and useful discussion on my dissertation and career goal.

I have been extremely fortunate to work with super supportive and friendly research groups in the ETOX program and ENSC department. I would like to thank my past and present lab members: Huanhuan Jiang, Jin Chen, Cody Cullen, Alexa Canchola, and Kunpeng Chen, who have contributed significantly to this dissertation. I have benefited so much from their insightful suggestions on both experiments and manuscript writing.

I am very grateful to many of my wonderful and faithful friends, especially Jawadul H Bappy, Risul Islam, Omar Faruk Rokon, Sudipta Paul, Farzana Rahman Rimi, Biplab Chandra Paul, Rakib Hyder, Ahmed Maksud, Lufor Rahman, Imtiaz Karim, and Towhid Rahman for always being there to constantly encouraging me.

Last but not the least, I would like to thank my family for their inspiration, profound love, and continuous support to pursue Ph.D. study. My little child Arham A. Chowdhury provides me joyful companion during this journey. I am also grateful to my brother Md. Zakaria Hasan Chowdhury for his support and love during my Ph.D. journey. Most importantly, I wish to thank my loving and supportive wife, Riste Ara Khandakar, who gave me perpetual inspiration. I also like to thank my mother-in-law and brother-in-law for their guidance and motivation.

Two most beautiful women:
my mom (the memory of my mom in heaven) and my wife

ABSTRACT OF THE DISSERTATION

Toxicogenomic Assessment of Particulate Matter (PM)-Induced Health Effects

by

C. M. Sabbir Ahmed

Doctor of Philosophy, Graduate Program in Environmental Toxicology
University of California, Riverside, June 2021
Dr. Ying-Hsuan Lin, Chairperson

Particulate Matter (PM) is a complex mixture of organic and inorganic chemicals, which can trigger systemic health effects including chronic obstructive pulmonary disease (COPD), lung cancer, cardiovascular dysfunction, obesity, and diabetes. The exact mechanisms by which disease progression occurs, however, remain unclear. Therefore, proper chemical characterization of PM and their effects on the development of diseases are required to fully understand PM-induced health effects. In this dissertation, we investigated the toxicological responses and disease progression pathways through transcriptomic analysis to probe the potential molecular mechanisms leading to PM-induced health outcomes. First, the toxicological potency of PM emitted from a modern vehicle equipped with a gasoline direct injection (GDI) engine was examined using eight different fuel blends with varying aromatic hydrocarbon and ethanol contents. Second, the potential health impacts of dimethyl selenide (DMSe)-derived secondary organic aerosols (SOA) were investigated by RNA sequencing (RNA-seq). Third, the lncRNA-mRNA co-

expression analysis was conducted to investigate the role of lncRNAs in altered gene expression following DMSe-SOA exposure.

Results from these studies indicate that gasoline exhaust particles from eight different fuel blends imbalance the gene expression related to oxidative stress and inflammation. RNA-seq data reveal major biological pathways perturbed by DMSe-derived SOA associated with elevated genotoxicity, DNA damage, and p53-mediated stress responses, as well as downregulated glycolysis and interleukin IL-4/IL-13 signaling that regulate diabetogenesis and allergic airway inflammation, respectively. In addition, we found that four *trans*-acting lncRNAs known to be associated with human carcinogenesis, including *PINCR*, *PICART1*, *DLGAP1-AS2*, and *LINC01629*, also differentially expressed in human airway epithelial cells treated with DMSe-derived SOA. Overall, using toxicogenomic approaches, this dissertation contributes to an improved understanding of potential biomarkers in early biological responses to PM exposure derived from traffic and natural sources.

Table of Contents

List of Figures

List of Tables

Chapter I: Introduction and Literature Review

Partially reproduced with the permission from Atmosphere, 2018; 9 (9), 336.

1.1 Air Pollutants in the 21st Century

In the twentieth century, the health effects of air pollution entered the world's consciousness. However, the relationship between poor air quality and human disease has been recognized since antiquity.[1] Air pollutants are defined as any substances in the air, which may harm humans, animals, vegetation or material. Air pollutants can be grouped into four categories: (i) gaseous pollutants (e.g., sulfur dioxide-SO_2, nitrogen oxide-NO_x, carbon monoxide-CO, ozone-O_3, volatile organic compounds-VOCs); (ii) persistent organic pollutants (e.g., dioxins); (iii) heavy metals (e.g., lead, mercury); and (iv) particulate matter (PM).[2] The lethality of air pollution was initially recognized in December 1952 when 3000 deaths occurred in London, England over a 3-week period due to "dense smog" containing sulfur dioxide and smoke particulates.[3] Meanwhile, the photochemical smog episodes in Los Angeles, United States resulting from uncontrolled emissions of NO_x and hydrocarbons in the presence of sunlight during 1940s also raised serious public health concerns. To address the growing air pollution issues and to set limits on emissions of air pollutants, the Clean Air Act (CAA) was established in 1970 in the United States.[4] The National Ambient Air Quality Standards (NAAQS) have been defined by the 1970 CAA for six primary pollutants (also known as "criteria air pollutants") found in air, including CO, lead, NO_x, O_3, SO_2, and PM, which have been widely studied over the decades.[5, 6] For its key role in climate, air quality, and adverse health effects, PM is considered as an

important pollutant in the atmosphere.[7, 8] In 2013, the Environmental Protection Agency (EPA) published a new guideline for its PM standard. The annual primary standards was set at 12 $\mu g\ m^{-3}$ for $PM_{2.5}$ and the daily (24-hour) standard at 35 and 150 $\mu g\ m^{-3}$ for $PM_{2.5}$ and PM_{10}, respectively.[5] In most developing countries, the PM concentrations usually exceed the latest air quality guidelines set by the World Health Organization (WHO), which is based on annual exposures to PM_{10}; 20 $\mu g\ m^{-3}$.[6] and become major contributors to the global burden of PM-induced health risks.

1.2 PM Sources, Compositions, and Sizes

PM is a complex mixture of small solid particles or liquid droplets suspended in the air made up with numerous organic and inorganic components that varies continuously in size and chemical composition in time and space.[1, 9, 10] The major chemical constituents of PM include organic compounds (e.g., polycyclic aromatic hydrocarbons, PAH); biological compounds (e.g., endotoxin, cell fragments), sulfates, nitrates, elemental and organic carbon, and metals (e.g., iron, copper, nickel, zinc, and vanadium).[6] The size of PM is generally described by its "aerodynamic equivalent diameter" (AED),[1] where PM with the same AED tends to have the same settling velocity. Because the size of PM controls it deposition, three subgroups of PM fractions: <10, <2.5, and <0.1 μm (PM_{10}, $PM_{2.5}$, and $PM_{0.1}$, respectively) are of particular concerns.[1] In general, a diameter between 2.5 and 10 μm ($PM_{2.5–10}$) is defined as "inhalable coarse particles," less than 2.5 μm as "fine particles," and less than 0.1 μm as "ultrafine particles".[1] When compared, $PM_{2.5}$ has lifetimes up to day to weeks and PM_{10} has minutes to hour. Additionally, traveling distance of $PM_{2.5}$ and PM_{10} are 100-1000 km and 1-10 km, respectively.[6]

Sources of PM can be both natural and anthropogenic. Natural sources include forest fires, volcanoes, dust storms, and aerosolized sea salt. Manmade sources of PM include traffic emissions, combustion in mechanical and industrial processes, and tobacco smoke.[1, 2] Furthermore, among all of the major emission sources, traffic-related PM could contribute to ca. 25% of the ambient $PM_{2.5}$ globally, and up to 37% in regions with highly populated urban centers.[9] For example, it has been estimated that 12.4 tons/day of $PM_{2.5}$ are directly emitted from vehicles in the LA Basin.[11] In addition, secondary organic aerosols (SOA) can be generated from both anthropogenic and natural sources.[12] In the presence of atmospheric oxidants (e.g., O_3, OH, NO_3 radical), SOA can be generated through the transformation of volatile organic compound (VOC) precursors.[13] Globally there is a large contribution of these SOA to atmospheric PM.[8, 14] For example, isoprene (C_5H_8) and α-pinene ($C_{10}H_{16}$) are dominantly emitted into the atmosphere by many species of trees, undergoing complex chemical reactions and leading to the formation of biogenic SOA.[8, 15] In addition, from microbial methylation and plant metabolism, selenium (Se) can be volatilized and released into the atmosphere in methylated forms, such as dimethyl selenide (DMSe) or dimethyl diselenide (DMDSe).[16, 17] Compared to a structural analog of DMSe, dimethyl sulfide (DMS) has been reported as a major precursor leading to secondary aerosol formation in marine atmospheric environments.[18] Atmospheric lifetimes of DMSe against oxidation by O_3, OH, and NO_3 have been reported, ranging from minutes to hours at typical respective oxidant concentrations.[19] Therefore, SOA from atmospheric oxidation of DMSe could potentially contribute to atmospheric PM as a natural source.

1.3 Routes and Target Organ of PM Exposure

Atmospheric PM enters the human body primarily via inhalation and ingestion, while the dermal contact represents a minor route of exposure.[20] The sizes of PM are directly linked to adverse health effects through inhalation. In general, particles with AED of greater than 10 μm can be largely filtered out by the nose and upper airways.[1, 9] $PM_{2.5}$ and $PM_{0.1}$ can deposit deeply into the lungs, and they cannot be easily cleared by the respiratory system.[21] These small particles may even directly penetrate the bloodstream to enter the circulation system and reach various target organs (e.g., lung, heart, liver and brain), which can trigger systemic health effects.[22]

1.4 Health Effects of PM from Traffic and Natural Emissions

It has been reported by the WHO that 4.2 million premature deaths occurred due to exposure to ambient $PM_{2.5}$ in 2016.[23] The International Agency for Research on Cancer (IARC) has classified the diesel exhaust as carcinogenic (Group 1) and gasoline exhaust as possibly carcinogenic (Group 2B) to humans in consideration of diesel exhaust's strong positive association with an increased risk for lung cancer.[24, 25] As a case study, a systematic review was conducted on traffic-related PM and cardiometabolic syndrome.[9] We searched peer-reviewed journal articles that had been published between 1 January 1980 and 20 June 2018. Reviews of published literature were conducted using four of the most commonly accessed databases for scientific journals, including Google Scholar, Web of Science, PubMed, and JSTOR.[9] In each database, we used a stepwise strategy to search the most relevant studies by entering the keywords in the following order: "Traffic-related air pollution", "Particulate matter", "Human health", and "Metabolic syndrome".

After applying the eligibility criteria, the key findings of our search results were summarized based on the study design, the characteristics of subject groups, the exposure metrics, and health outcomes. This resulted in 25 independent research studies for the final review. Key findings from both epidemiological and toxicological revealed consistent correlations between traffic-related PM exposure and the measured cardiometabolic health endpoints.[9] The active components in fresh traffic-related PM could be attributed to metals, black carbon, elemental carbon, PAHs, and diesel exhaust particles. Existing evidence indicates that the development of cardiometabolic symptoms can occur through chronic systemic inflammation and increased oxidative stress (Figure 1.1). The elderly (especially for women), children, genetically susceptible individuals, and people with pre-existing conditions are identified as vulnerable groups.[9] Correlations between systolic blood pressure and exposure to traffic-related $PM_{2.5}$ have also been reported previously by Brook et al.[26] and Langrish et al.[27] Notably, it has been reported that even at low levels, traffic-related $PM_{2.5}$ may dysregulate metabolic insulin sensitivity, and eventually contribute to the development of diabetes.[28] However, the roles of traffic-related PM and exact molecular mechanisms modulating toxicological responses and/or disease progression are not fully understood. Thus, more studies are required to explore the roles of genetic and epigenetic factors in influencing health outcomes by integrating multi-omics approaches (e.g., genomics, epigenomics, and transcriptomics) to provide a comprehensive assessment of biological perturbations caused by traffic-related PM.[9]

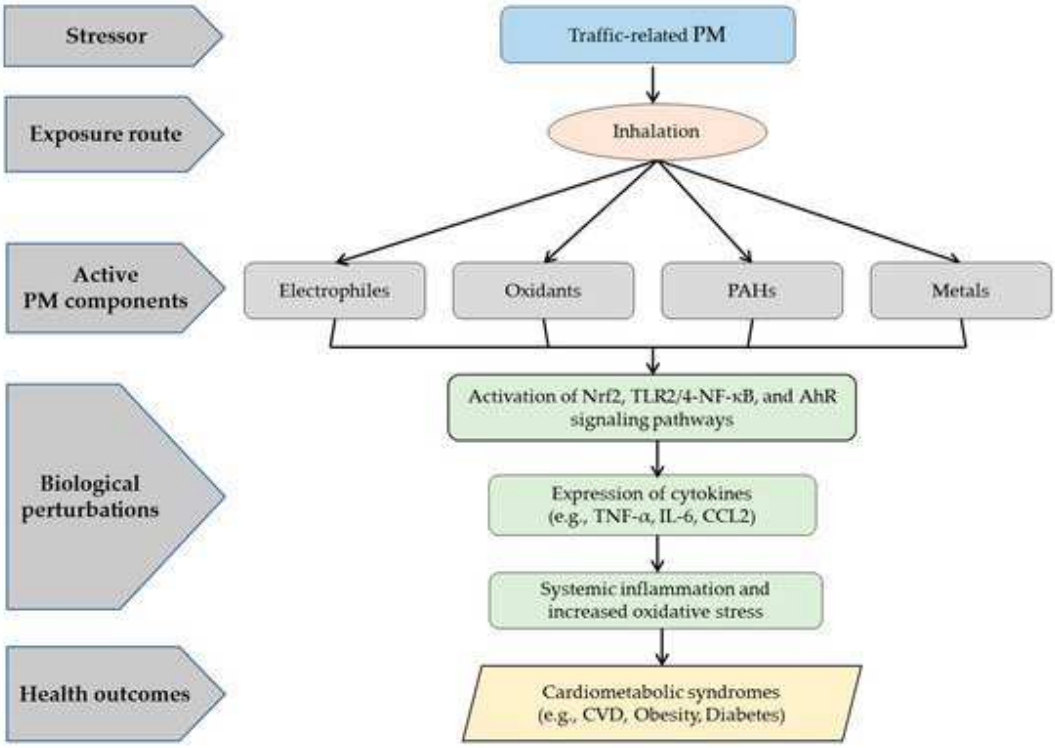

Figure 1.1: A conceptual diagram of traffic-related particulate matter (PM)-induced cardiometabolic syndrome, connecting sources, exposure, biological perturbations, and outcomes.[9]

Despite their abundance in the atmosphere, the health effects of PM and SOA emitted by natural sources have been less studied, but they may also pose potential health risks. PM and SOA from natural sources vary largely in chemical compositions and toxicity depending on their precursors and surrounding environments that influence the atmospheric transformation processes and result in different characteristics of SOA products.[2, 7, 14] For example, recent studies have found that the isoprene-derived SOA con contribute to reactive oxygen species (ROS) generation and alter oxidative stress-related gene expression through the nuclear factor E2-related factor 2 (Nrf2) pathway.[8, 29] Such evidence indicates that some SOA constituents, such organic hydroperoxides, may be redox active and can act as exogeneous ROS.

1.5 PM-induced Toxicity Assessment Techniques

The toxicity of PM can be evaluated on a variety of levels, ranging from molecular and cellular to whole-organism effects of exposure. Particulate matter (PM)-induced adverse health effects may be based on a common theme, which has been hypothesized that PM generates ROS.[30, 31] The ability of PM to generate ROS is called oxidative potential (OP).[32] To date, measurement of OP provides the initial ideas about PM's potential to generate ROS and adverse health effects in biological systems.[33, 34] The most common and popular OP measurement of PM is conducted with an acellular dithiothreitol (DTT, $HSCH_2(CH(OH))_2CH_2SH$) assay, where DTT shares some similarities with glutathione.[32, 34-37] Cell-free DTT assay provides faster output than cell-based assay and incorporates less-controlled environments. Therefore, DTT assay is widely used for measuring OP of PM.[34, 38] In living organisms, ROS is generally produced in mitochondria and endoplasmic reticulum (ER). Where cellular reductants like NADP/NADPH provide electrons enabling the reduction of molecular oxygen (O_2) to superoxide anion (O^{-2}).[34, 39] The rate of DTT consumption is proportional to the amount of redox-active species in PM. Other acellular assays available for OP measurements are the dichlorofluorescein (DCFH) and ascorbic acid (AA)-based tests. The DCFH assay determines OP from the rapid oxidation of DCFH to the fluorescent DCF species in the presence of horseradish peroxidase (HRP).[40, 41]In contrast, the AA assay evaluates OP by measuring the consumption of O_2 using an oxygen-specific electrode.[40, 42]

In many scientific disciplines, cell-based (or *in vitro*) assays provide a common strategy to support toxicity testing. Typically, *in vitro* models traditionally used over past

decades were a monolayer of cells grown in media and provided a means of examining morphological and biochemical signaling processes while avoiding many of the limitations of animal models.[43, 44]. However, compared to *in vivo* conditions, *in vitro* models cannot accurately depict and simulate the rich environment and complex processes due to their simplicity.[45]

Several diseases such as asthma, chronic obstructive pulmonary diseases (COPD), cardiovascular disease, diabetes, and cancer have been found to associated with PM-induced health effects. Instead, a combination of genetic and environmental factors usually interacts to influence an individual's risk of disease.[9, 46, 47] The "-omics" approaches (e.g., genomics, epigenomics and transcriptomics) can provide a comprehensive assessment of biological perturbations caused by PM exposure, and facilitate an understanding of adverse outcome pathways.[9] Using microarrays and emerging methods such as next generation sequencing (e.g., DNA-seq, RNA-seq) enable investigators to profile genomics, epigenomics and transcriptomics changes across the entire genome.[46] Epigenetics can regulate gene expression without alteration of the genetic code itself. Epigenetic modifications provide plausible connections between the environmental stressors and alterations in gene expression that might lead to diseases.[48] Examples include DNA methylation, histone modifications, chromatin remodeling, non-coding RNAs (ncRNA) including microRNA (miRNA), and long non-coding RNA (lncRNAs) expression. In transcriptome studies, messenger RNA (mRNA) has been the primary target and RNA-seq technology has revealed that the human genome is pervasively transcribed, resulting in

thousands of novel non-coding RNA genes. As a result, attention is expanding to the most common, yet the most poorly understood RNA species: lncRNAs.[49]

The lncRNAs are defined as transcribed RNA molecules greater than 200 nucleotides in length with little or no protein coding capability. As opposed to microRNAs (miRNAs) which are involved in transcriptional and post-transcriptional gene silencing via specific base pairing with their targets, lncRNAs regulate gene expression by diverse mechanisms.[47, 50] In addition, lncRNAs have been used as effective biomarkers and are believed to be critical in the manifestation of diverse diseases.[47]

Therefore, ncRNAs or their inhibitors may be potential targets during the treatment of PM-induced diseases. Currently, the effects of epigenetic changes on altered gene expression regulated by lncRNAs are still poorly understood. Additionally, no exact molecular mechanism has been revealed to bridge the gap between the traffic and natural sources of PM exposure and physiological alteration and/or disease progression. Thus, toxicogenomic approaches may be valuable in understanding the potential molecular mechanisms contributing to the increased risk of PM-related health outcomes.

1.6 Overview of Research Aims and Objectives

As discussed above, toxicogenomic approaches can be a valuable tool to study PM-induced health effects exposed to both anthropogenic and natural emissions. The transcriptomic profiling can provide a broad overview of disease mechanisms and progressions at early stages by analyzing differential gene expression. Thus, the overall objective of this research is to conduct a toxicogenomic assessment of PM from traffic and natural sources, as well as their health consequences.

The study described in Chapter II aims to link gasoline fuel compositions and PM emissions to the observed toxicological responses in human airway epithelial cells (BEAS-2B), as well as the measured aerosol oxidative potential of gasoline exhaust from 8 different fuel blends. The study described in Chapter III evaluates the potency of PM formation from DMSe through oxidation by O_3 and OH. Also, transcriptome-wide gene expression changes by RNA-seq in BEAS-2B cells exposed to DMSe-derived SOA are assessed in this chapter. To date, the potential to produce inhalable DMSe-derived secondary organic aerosols (SOA) has not been investigated. We hypothesized that atmospheric oxidation of DMSe could be an important source for secondary aerosol production. The Se-containing aerosols may pose increased health risks upon inhalation due to their redox-active chemical properties. In Chapter IV, we studied the role of lncRNA in gene regulation in BEAS-2B cells exposed to DMSe-derived SOA. Integrative analysis of lncRNA-mRNA co-expression showed that lncRNAs could potentially regulate gene expression via both *cis* and *trans* mechanisms. Finally, in Chapter V, the conclusions and implications of this dissertation are summarized to highlight the overall findings of this dissertation.

Chapter II: Toxicological responses in human airway epithelial cells (BEAS-2B) exposed to particulate matter emissions from gasoline fuels with varying aromatic and ethanol levels

2.1 Introduction

Ambient particulate matter (PM) has been recognized as an important cause of adverse health effects leading to increased pulmonary, cardiovascular and cancer mortalities.[51, 52] According to the recent report published by the World Health Organization (WHO), exposure to outdoor air pollution has been linked to about 4.2 million deaths worldwide in 2016.[53] These health outcomes are greatly influenced by traffic-related air pollution resulting from rapid urbanization and increased traffic loads within the past few decades. The traffic sector is a significant contributor of pollutant emissions in the atmosphere, including carbon monoxide (CO), volatile organic compounds (VOCs), polycyclic aromatic hydrocarbons (PAHs), nitrogen oxides (NO_x), and PM.[52, 54, 55] The International Agency for Research on Cancer (IARC) has classified the diesel exhaust as carcinogenic (Group 1) and gasoline exhaust as possibly carcinogenic (Group 2B) to humans in consideration of its strong positive association with an increased risk for lung cancer.[25, 56, 57]

Modern gasoline engines, such as gasoline direct injection (GDI), have been introduced to the U.S. market to meet growing environmental demands, such as those of greenhouse gas (GHG) emissions reduction and improved engine efficiency.[58]

However, due to the direct fuel injection in the combustion chamber, GDI engines generate a substantial amount of PM emissions.[59, 60] Previous works have shown that GDI vehicles produce higher PM mass and black carbon emissions than the traditional port-fuel injection vehicles or diesel vehicles equipped with diesel particulate filters (DPFs).[61-63] Several studies have shown that fuel type, including chemical composition, volatility, and oxygen content will affect the physical and chemical properties of PM emissions from GDI engines.[63-65] There is a widespread concern that gasoline aromatic levels significantly contribute to the formation of both primary PM emissions and secondary organic aerosols (SOA).[66-68] The development of the PM Index (PMI) provides a modeling tool for the prediction of primary PM emissions from gasoline engines by linking gasoline PM with gasoline composition and properties, such as the vapor pressure and double bond equivalent (DBE) of each hydrocarbon component in the fuel.[69, 70] Studies have shown that gasoline aromatics (aromatics have higher DBE values than paraffins or other hydrocarbons) have significant effects on exhaust PM emissions and demonstrate a tendency for greater PM emissions with high PMI gasoline fuels.[63, 71-73] For example, Fushimi et al. [74] reported higher PM mass emissions for the fuels containing more aromatics with high boiling points and DBE values from GDI and port fuel injection (PFI) vehicles. On the other hand, a number of studies have shown the beneficial impacts of ethanol in reducing tailpipe emissions from GDI engines.[65, 75, 76]

Many epidemiological and toxicological studies have indicated that human lungs are vulnerable to PM exposure.[2, 51, 77] A number of studies are currently investigating the toxicological characteristics of PM emissions from GDI engines, with fewer studies

emphasizing the fuel effect on PM toxicity from GDI engines.[78-81] Maikawa et al. [82] reported the metabolism of PAHs and upregulated expression of oxidative stress-related genes (i.e., increased levels of gene expression products) in cultured lung slices from mouse tissues in response to GDI engine exhaust exposure. Similarly, Libalova et al. [83] showed that exposure to PM emissions from the combustion of butanol-gasoline blends resulted in alteration of stress signaling in BEAS-2B cells, including oxidative stress, metabolism of PAHs and pro-inflammatory responses. However, Bisig et al. [84] found no significant cellular responses after the exposure to PM emissions from the combustion of gasoline or gasoline-ethanol blends in multi-cellular human lung cells. Exposure to PAHs in polluted air is known to generate reactive intermediates and lead to the formation of DNA adducts through bioactivation.[85, 86] The metabolism of PAHs has been linked to the oxidative DNA damage, activation of the aryl hydrocarbon receptor and reactive oxygen species (ROS) generation.[87-89] Excessive production of ROS is a known cause leading to oxidative stress (an imbalance between ROS and antioxidants) that will eventually damage to biomolecules (e.g., DNA, lipid, and protein) and result in a wide variety of diseases, such as cardiovascular diseases and cancer.[90] PAH derivatives, such as nitrated and oxygenated PAHs generated from the operation of GDI engines, may also contribute to multiple toxic events induced by gasoline exhaust particles.[91]

This study aims to link gasoline composition and PM emissions to the observed toxicological responses in human lung cells. This is a companion study to a major research program designed to investigate fuel compositional effects on the tailpipe emissions and secondary aerosols from GDI vehicles.[68, 92]

Testing was performed on a current technology GDI vehicle when operated on eight different fuel blends over the LA92 driving cycle using a chassis dynamometer. The extracted PM components were analyzed using the DTT assay and applied to human airway epithelial cells (BEAS-2B) to assess the oxidative potential and exposure-induced toxicological responses. Multivariate principal component analysis (PCA) and multiple linear regression (MLR) analysis were conducted to understand the associations among fuel formulations, aerosol oxidative potential, and PM-induced biological alterations.

2.2 Materials and Methods

2.2.1. Testing Protocol and Emissions Analysis

Emissions testing was performed at the University of California, Riverside Center for Environmental Research and Technology (CE-CERT). Details on the testing protocols and emissions analysis techniques are described elsewhere.[68, 92] Briefly, the test vehicle was exercised over duplicate LA92 cycles using a Burke E. Porter 48-inch single-roll electric dynamometer. All gaseous and particulate emissions were determined according to the U.S. EPA protocols for light-duty emission testing as given in the CFR, Title 40, Part 86.

The test vehicle was a Tier 3 or California LEV III compliant passenger car equipped with wall-guided direct fuel injection system and a three-way catalyst (TWC). The vehicle was operated on eight different gasoline fuels that were created to meet nominal total aromatics targets of 20 vol% and 30 vol% and ethanol levels ranged from 0 vol% to 20 vol%. More details on fuel blending and major physicochemical properties are provided in.[68]

The main physicochemical properties of the test fuels are listed in Table S2.1, Supplementary Information (SI). PM samples were collected onto 47 mm Teflon membrane filters and stored at -20°C until analysis. Filters were extracted with 23 mL of methanol followed by 50 min of sonication. After sonication, the extracted solution was then transferred to another vial and used for the analyses of PM chemical composition and subsequent cell exposures.

2.2.2. DTT Assay

Dithiothreitol (DTT), 5-5'-dithiobis (2-nitrobenzoic acid) (DTNB), 1,4-naphthoquinone (1,4-NQ) and dimethyl sulfoxide (DMSO) were purchased from Sigma-Aldrich (St. Louis, MO, USA). The potassium phosphate monobasic/sodium hydroxide buffer solution (KH_2PO_4, pH 7.4) was purchased from Fisher Scientific. The DTT assay procedures were adapted from published protocols [93] using clear flat bottom 96-well microplates. For each experiment, 0.5 mM DTT was made fresh in the phosphate buffer solution. A 1 mg/mL of 1,4-NQ was prepared in DMSO, and further diluted with buffer solutions to make a 0.01 mg mL^{-1} working solution to serve as positive controls. Two sets of reactions were performed to examine the effects of solubility on measured DTT activities. For the first set of reactions, the reaction mixture consisted of 100 μL aqueous phosphate buffer, 20 μL of fuel extracts (containing 0.5-1 μg of PM mass), and 5 μL of 0.5 mM DTT. Then, the microplate was sealed and incubated at 37ºC for 30 min. After incubation, 10 μL DTNB (1mM) was added to titrate the remaining reduced DTT and form a 2-nitro-5-thiobenzoic acid (TNB). The final reaction volume for each well was 135 μL.

The second set of reactions was carried out in the same manner, except 50 μL of aqueous phosphate buffer was replaced with 50 μL of methanol to increase the solubility of organic matter in the assay. Each PM sample was prepared in triplicate. Absorbance of the resultant TNB was measured at 405 nm using a TECAN SpectraFluor Plus microplate reader with 620 nm as the reference wavelength. The absorbance was further corrected by subtracting the light absorption of PM sample itself. The final DTT activity (nmol/min/μg) was calculated using the consumption of DTT normalized by the incubation time and PM mass (Table S2.2, SI).

2.2.3. Cell Culture

BEAS-2B cells were obtained from the American Type Culture Collection (ATCC). Cells were cultured in Gibco® LHC-9 medium (1X) (Invitrogen), which is serum-free LHC basal medium supplemented with retinoic acid, epinephrine and gentamicin. The cells were grown at 37 °C and 5% CO_2 in a humidified incubator.

2.2.4. Cell Exposure

In 24-well plates, cells were seeded at a density of 2.5×10^4 cells per well in 250 μL of LHC-9 medium for 2 days prior to exposure. Upon the time of exposure, cells reached around 60−70% confluence. PM extracts were dried off under a gentle nitrogen stream and reconstituted with the LHC-9 medium. Cells were washed with the phosphate buffered saline (PBS) buffer and then exposed to 50 μg/mL of PM extracts in the LHC-9 medium for 24 hr. Experiments were conducted in triplicate per treatment group.

2.2.5. Cytotoxicity Assay

To assess the viability of cells, the lactate dehydrogenase (LDH) cytotoxicity assay was performed following the manufacturer's protocol (Roche). Supernatants were collected 24 h after exposure. Triton X-100 (0.1%) was used as a positive control to simulate 100% cell death. The absorbance was measured using a TECAN SpectraFluor Plus microplate reader at 490 nm, with a reference wavelength at 620 nm.

2.2.6. RNA Isolation and Purification

At the end of exposure, cells were lysed with 350 μL of TRI Reagent (Zymo Research) for the total RNA isolation. Isolated RNA samples were further purified using the spin column-based Direct-zol RNA MiniPrep kit (Zymo Research). RNA quality and concentrations were determined using a NanodropND-1000 spectrophotometer (Thermo Fisher Scientific). The 260 /280 nm absorbance ratios of all samples were determined to be >1.8. Extracted RNA samples were stored at -80°C until processing.

2.2.7. Gene Expression Analysis

Gene expression of selected biomarkers, including heme oxygenase 1 (*HMOX-1*), interleukin-6 (*IL-6*), tumor necrosis factor-alpha (*TNF-α*), chemokine ligand 5 (*CCL5*) and nitric oxide synthase 2 (*NOS2*), was measured using the one-step QuantiFast SYBR Green® RT-PCR kit (Qiagen). The QuantiTect Primer Assays (Qiagen) of *HMOX-1*, *IL-6*, *TNF-α*, *CCL5*, and *NOS2* were used in this study. Results were normalized to a housekeeping gene beta-actin (*ACTB*) and expressed as fold changes over the unexposed controls.

Thermal cycling conditions for RT-PCR were set as follows: 10 min at 50 °C for reverse transcription, 5 min at 95 °C for initial denaturation and 40 cycles of amplification (10 s at 95 °C and 30 s at 60 °C).

2.2.8. Statistical Analysis

The one-way analysis of variance (ANOVA) with Tukey's multiple comparison test was performed to determine whether there are statistically significant differences in measured DTT activities between the fuels (GraphPad Prism 4). The Pearson correlation and PCA were conducted for calculating correlation coefficients and the dimension reduction of measured fuel properties, respectively, using the SPSS (v24, IBM) software. After PCA analysis, the K-Means clustering algorithm was performed on the reduced dataset using the Python platform (Python 3.5.5). The cluster number was 3, number of initial seed = 10, maximum number of iterations of the algorithm = 300 and tolerance = 1×10^{-4}. The centroids of the clusters were measured using the formula: (xc, yc) = ((x1+x2+.... +xk)/k, (y1+y2+.... +yk)/k), where k is the number of points in a cluster. Associations among principle components (PCs), DTT activity and biological responses (i.e., fold changes of gene expression) were further analyzed by MLR within the SPSS (v24, IBM).

2.3. Results and Discussion

2.3.1. Oxidative Potential of PM

The results of the DTT assays conducted in both aqueous buffer solutions and mixed methanol-buffer solutions to assess the oxidative potential of PM emissions from different fuels are shown in Figure 2.1.

Overall, significant differences of DTT activities were found between the fuels in either aqueous buffer solutions or mixed methanol-buffer solutions, as shown in Table S2.3 and Table S2.4 in SI. Fuel 2 (0% ethanol and 30% aromatics) showed the highest oxidative potential of PM emissions compared to Fuel 4 and Fuel 7 (0.039 nmol/min/μg in the mixed methanol-buffer solution and 0.030 nmol/min/μg in the aqueous buffer) (Figure 2.1). Fuel 2, Fuel 3, and Fuel 7 showed statistically significant increases in oxidative potential (0.016-0.03 nmol/min/μg) for PM mass compared to Fuel 1 (0.0077 nmol/min/μg) (Table S2.3 and Table S2.4, SI). The higher oxidative potential for these fuels can be attributed to the higher levels of total aromatics for Fuel 2 and Fuel 7 compared to Fuel 1.

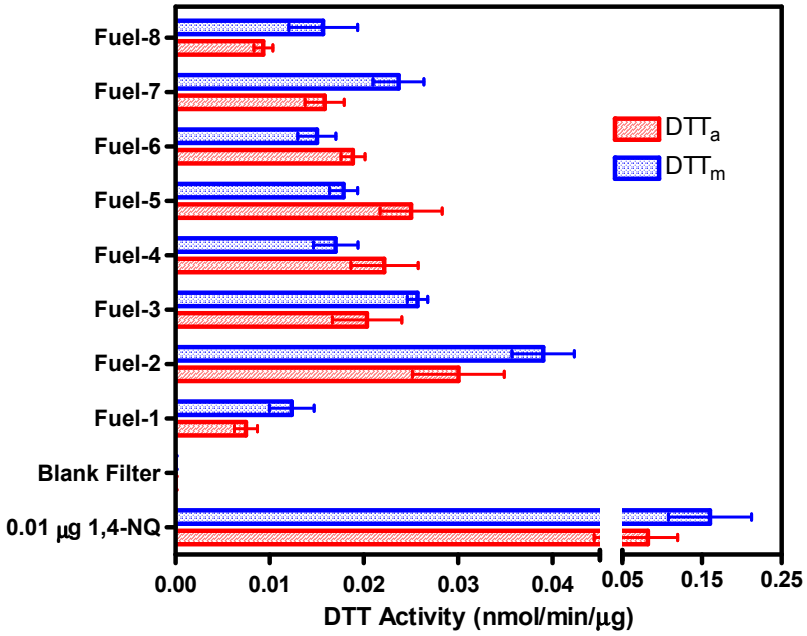

Figure 2.1. DTT activity (nmol/min/μg) of PM samples emitted from eight fuel blends, blank filter for the negative control, and 1,4-NQ as the positive control. Red represents the DDT activity assessed in the 100% aqueous buffer solutions (DTTa) and blue represents the DDT activity assessed in 50%/50% (v/v) methanol/buffer solutions (DTTm).

The higher oxidative potential for Fuel 3 compared to Fuel 1 could likely be due to the higher concentration of heavier C10+ aromatics for this fuel, as indicated by its relatively higher PMI compared to Fuel 1.

To examine the effects of gasoline aromatics on PM emissions and the resulting toxicity, the test fuels have been categorized into high PMI fuels (Fuel 2, Fuel 4, and Fuel 7) and low PMI fuels (Fuel 1, Fuel 3, Fuel 5, Fuel 6, and Fuel 8). Strong positive correlations were found between high PMI fuels and elevated oxidative potential of PM mass emissions (both DTTa and DTTm as shown in Figure 2.2 (a-b). For the high PMI fuels, Fuel 2, which had higher concentrations of C9/C10+ aromatics and higher PMI value compared to Fuel 4 and Fuel 7, showed the highest DTT activity. This finding indicates that the presence of heavier aromatics with higher DBEs in the fuel resulted in poor fuel evaporation during the combustion process and in the formation of PAHs responsible for PM emissions. PM-bound PAH species, including oxygenated PAHs such as quinones since unsubstituted PAHs are not redox active, are known to strongly correlate with DTT [94, 95]. Although PAH emission measurements were not made possible for this study, it is safe to theorize that high PMI fuels produced higher PM-bound PAH emissions, especially quinones (i.e., 1,4-naphthoquinone). Despite the fact that Yang et al. [68] showed an inverse correlation of PM mass emissions and PMI for the high PMI fuels due to ethanol's higher heat of vaporization (higher PMI fuels with higher ethanol produced more PM), this study showed reduced oxidative potential of PM for the high PMI fuels as ethanol increased.

Although the PM mass was higher for these fuels (i.e., Fuel 4 and Fuel 7), the oxygenated fraction in the fuel resulted in the generation of PM constituents that did not

participate in the DTT oxidation (i.e., less oxygenated PAHs). It is therefore reasonable to assume that the presence of ethanol had a more prominent role in the oxidative potential of PM emissions, at least for the high PMI fuels. For the low PMI fuels, the splash blend Fuel 8 (20% ethanol and 19% aromatics) showed the least oxidative potential, which can be ascribed to the dilution of aromatics in the fuel, leading to lower aromatic levels and to lower rates of aromatic soot precursor formation.

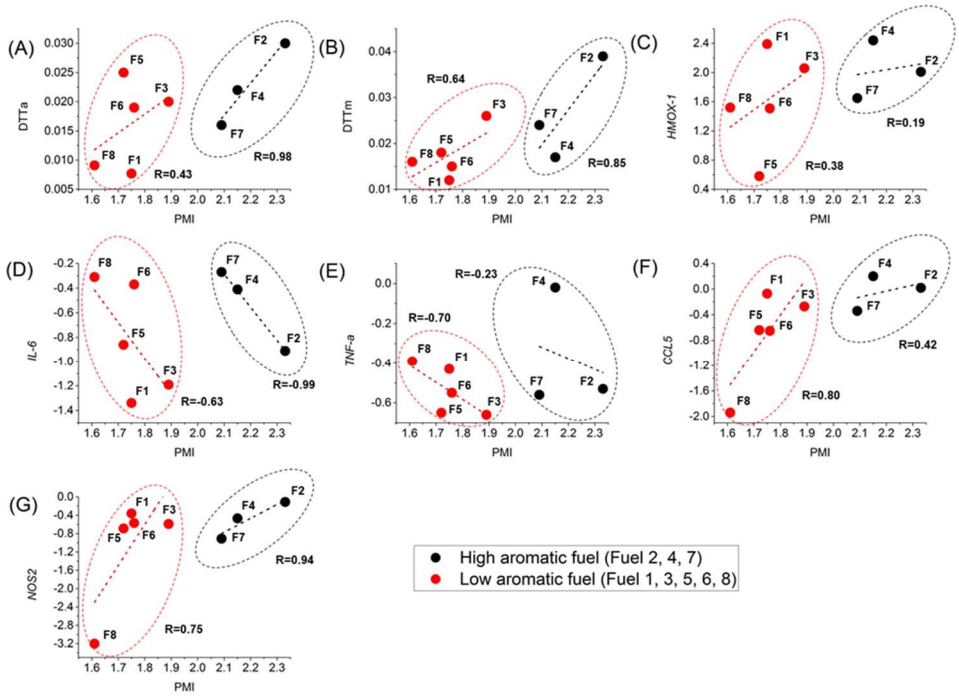

Figure 2.2: Correlations between DTT activities, biomarker responses and PMI. Analyses were carried out based on aromatic levels in fuels. High aromatic fuels include: F2 (PMI: 2.22, Total aromatic: 30%), F4 (PMI: 2.15, Total aromatic: 30%), and F7 (PMI: 2.09, Total aromatic: 30%). Low aromatic fuels include: F1 (PMI: 1.75, Total aromatic: 20%), F3 (PMI:1.89, Total aromatic: 20%), F5 (PMI: 1.72, Total aromatic 20.30%), F6 (PMI: 1.76, Total aromatic: 20%), and F8 (PMI: 1.61, Total aromatic: 19%). Strong correlations were found between higher aromatic levels versus DTTa (A), DTTm (b), *IL-6* (D), and *NOS2* (G). Black color represents higher aromatic levels, and red color represents lower aromatic levels.

Additionally, the presence of oxygen in the fuel will promote the oxidation of soot precursors such as PAHs [96], which are known to be especially active in eliciting oxidative stress responses in PM emissions.[97, 98] As discussed earlier, the relatively higher DTT activity for Fuel 3 was due to the increased levels of heavier aromatics compared to the other low PMI fuels.

Table 2.1: Pearson correlation table among fuel compositions, DTT activities, and toxicological responses.

	Total aromatics	C10+	DTTa	DTTm	PMI	Ethanol	*HMOX-1*	*IL-6*	*TNF-α*	*CCL5*	*NOS2*
Total aromatics	1										
C10+	0.99	1									
DTTa	-0.02	0.06	1								
DTTm	0.40	0.50	0.39	1							
PMI	0.95	0.98	0.08	0.63	1						
Ethanol	-0.35	-0.39	-0.07	-0.25	-0.50	1					
HMOX-1	0.41	0.40	-0.56	0.04	0.45	-0.62	1				
IL-6	0.28	0.21	-0.01	-0.10	0.05	0.71	-0.25	1			
TNF-α	0.36	0.27	-0.41	-0.27	0.24	-0.08	0.56	0.34	1		
CCL5	0.64	0.65	0.05	0.18	0.70	-0.73	0.52	-0.41	0.17	1	
NOS2	0.46	0.50	0.35	0.21	0.55	-0.68	0.28	-0.47	-0.10	0.93	1

The oxidative potential for PM mass emissions of the test fuels measured in the aqueous solutions ranged from 0.007-0.030 nmol/min/μg and were found to be at similar levels compared to those values reported by Cheung et al. [99] (0.012 nmol/min/μg) and Geller et al. [100] (0.025 nmol/min/μg). However, the DTT consumption of PM emissions from a previous study conducted with GDI vehicles showed an average of 0.056 nmol/min/μg, which was higher than our reported DTT activities in both aqueous and methanol solutions (0.007-0.039 nmol/min/μg).[81]

Also, the difference between DTTm and DTTa values demonstrates the significance of solubility of PM constituents in measured aerosol oxidative potential, which may have implications for their bioavailability, which depends on several factors including solubility in lung fluids, permeability across cell membrane, and dissolution rate of exposed PM constituents [101, 102].

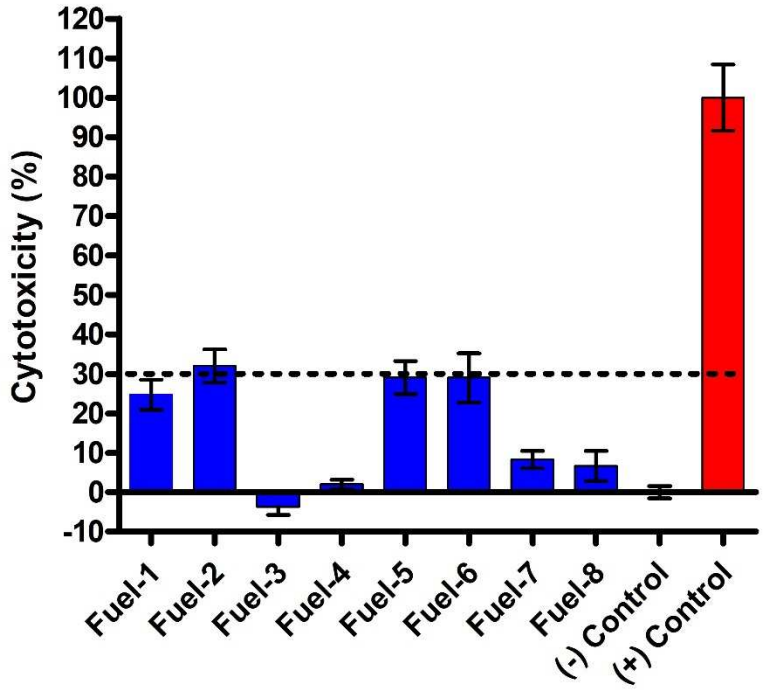

Figure 2.3. Cytotoxicity evaluated by the LDH assay. BEAS-2B cells were exposed to PM emissions from eight different fuel blends at the concentration of 50 μg mL^{-1} for 24 h. Results were expressed as percentage of LDH release relative to negative controls of unexposed cells maintained in the cell medium and positive controls treated with Triton X-100 (0.1% v/v).

A more in-depth correlation analysis was performed to evaluate the relationship between DTT (both DTTa and DTTm) and fuel composition, as shown in Table 2.1. DTTm showed moderate correlations with C10+ aromatics (R = 0.50) and total aromatics (R = 0.40), and a moderate to strong correlation with PMI (R = 0.63) (Table 2.1). Due to the

higher solubility of non-polar PM constituents in methanol, our results suggest that higher aromatics could contribute to higher DTTm. Similarly, Bates et al. [103] reported a positive correlation (R = 0.34) between DTTm versus $PM_{2.5}$ emissions from light-duty gasoline vehicles.

2.3.2. Cytotoxicity Assay

Cytotoxicity was assessed using the LDH assay after 24 h exposure to PM emissions from all test fuels. About ≤ 30% cytotoxicity indicated that cells were stressed after exposure, and the exposure conditions were not overly toxic that could allow further evaluation of gene expression changes [104]. Overall, as shown in Figure 2.3, there was no significant cytotoxicity (≤30%) observed in cells exposed to PM emissions at the level of 50 μg/mL. Thus, the concentration of 50 μg/mL was used as the non-lethal dose for the following gene expression analysis in this study, which is comparable to the level of emissions applied in other studies [83, 105]. Notably, Fuel 2 PM emissions induced relatively higher cytotoxicity than the other fuel blends, along with its higher DTTa and DTTm (Figure 2.1), which might be related to its higher aromatic content and the absence of ethanol.

2.3.3. Gene Expression Analysis

The relative levels of gene expression for the exposure and control groups, expressed as fold changes, were calculated using the comparative cycle threshold ($2^{-\Delta\Delta CT}$) method.[106] Fold changes (Log_2) of *HMOX-1*, *TNF-α, IL-6, CCL5,* and *NOS2* gene expression are shown in Figure 2.4 and Table S2.2, SI. With the exposure to PM emission extracts from different fuels at the concentration of 50 μg/mL for 24 hrs, expression of

oxidative stress-related gene *HMOX-1* was upregulated, whereas expression of inflammation-related genes, including *TNF-α, IL-6, CCL5* and *NOS2*, were downregulated in BEAS-2B cells.

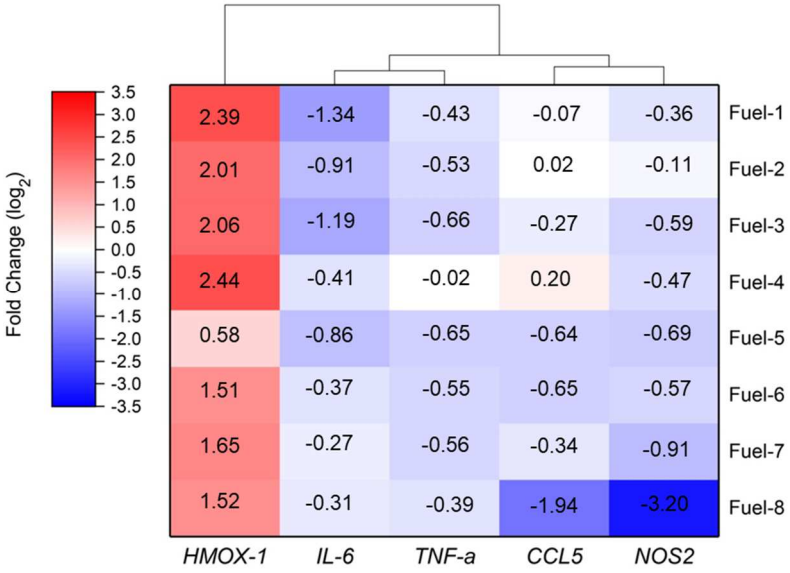

Figure 2.4. Heatmap of differential gene expression in BEAS-2B cells exposed to PM emissions from eight different fuel blends. Results are expressed as fold change (log_2) over unexposed controls and normalized to a housekeeping gene *ACTB*. In the diagram above, the red color represents upregulation and the blue color represents downregulation.

Overall, under non-lethal conditions (cytotoxicity ≤30%, Figure 2.3), we found that the expression of *HMOX-1* gene, which is widely used as a biomarker for oxidative stress, was significantly upregulated after exposure to all fuel PM samples (Figure 2.4). The results reported here agree with recent studies of gasoline exhaust exposure reporting significantly upregulated *HMOX-1* [83, 84, 105]. The Pearson correlation analysis indicated that *HMOX-1* has a strong negative correlation with ethanol content (R = -0.62) and moderate positive correlations with total aromatics (R = 0.41) and C10+ aromatics (R = 0.40) (Table

2.1). When we grouped the fuels into high and low levels of aromatics to correlate PMI with the *HMOX-1* expression again, we did not find significant subgroup effects on *HMOX-1* expression (Figure 2.2 c). Correlations from total aromatics, PMI, and ethanol level suggest that higher ethanol fueling may potentially reduce the *HMOX-1* expression, while total aromatics and C10+ aromatics may potentially contribute to upregulation of *HMOX-1*.

Conversely, cytokines such as *TNF-α* and *IL-6* were downregulated after exposure to PM emissions from different fuels. High PMI fuels with higher ethanol levels showed an inverse strong correlation with *IL-6* (Figure 2.2 d). For the low PMI fuels, the high ethanol blend Fuel 8 having the lowest PMI value showed an increase in the cytokine IL-6. These findings reveal that PMI and the presence of heavy aromatics in the fuel may not significantly affect cytokine IL-6 production, whereas an increase in ethanol concentration in the fuel may result in more reactive PM components that can trigger the downregulation of cytokine *IL-6* production. No strong correlations were seen for *TNF-α* as a function of fuel composition; however, a strong positive correlation was identified showing decreased downregulation of *IL-6* for the higher ethanol content fuels (R= 0.71, Table 2.1).

Addition of ethanol in gasoline fuels has been reported to reduce the concentrations of PAH species in PM exhaust from GDI engines [107, 108], which can potentially explain our observation on the decreased downregulation of *IL-6*. PAH is a class of aryl hydrocarbon receptor (AhR) agonists that can suppress *IL-6* expression [109, 110]. The PAH-mediated suppressed expression of *TNF-α* and *IL-6* could be correlated with the cellular injury and pathogenesis of chronic inflammatory diseases including cancer, celiac disease, vasculitis,

lupus, chronic obstructive pulmonary disease (COPD), atherosclerosis, rheumatoid arthritis, and psoriasis [111]. Thus, the increased ethanol content in fuels appears to neutralize the immunosuppressive effect caused by PAHs. Notably, our observations of downregulation of both *TNF-α* and *IL-6* cytokines at the transcriptional level agree with Manzano-León et. al. [112] that reported PAH-containing $PM_{2.5}$ downregulated *TNF-α* and *IL-6* expression in THP-1 cells (a human monocytic cell line) at the translational level.

The proinflammatory chemokine CCL5/RANTES (regulated upon activation, normal T-cell expressed, and secreted) and the chemokine modulator NOS2 were also found to be downregulated in the PM emissions from all test fuels (Figure 2.4). CCL5 plays a key role in recruiting a variety of leukocytes into inflammatory sites including T cells, macrophages, eosinophils, and basophils in collaboration with certain cytokines such as IL-2.[113] Additionally, *NOS2* can activate the NF-κB factor through tissue damage and airway inflammation of asthma.[114-116] In the inflammatory states, *NOS2* produces nitric oxide, which plays a critical factor in the pathogenesis of inflammatory lung diseases.[117]

CCL5 and *NOS2* gene expression showed positive correlations with aromatic content in fuels; however, the fuels with higher ethanol blending showed negative correlations (i.e., downregulation) with the *CCL5* and *NOS2* biomarkers (Table 2.1). There is also a significant effect of PMI on *CCL5* and *NOS2* gene expression for the high aromatic and low aromatic fuel groups (Figure 2.2 f-g). Correlation analysis indicated moderate to strong negative correlations between ethanol content and expression of *CCL5* and *NOS2* (Table 2.1, R= -0.73 and -0.68 for *CCL5* and *NOS2*, respectively), suggesting that reactive PM constituents were likely produced by ethanol-containing fuels that trigger *CCL5* and

NOS2 downregulation. Our results agree with a recent study that showed a downregulation of *CCL5* responded to ethanol blends from a GDI vehicle.[80] The opposite direction of correlations (aromatics and *CCL5/NOS2* versus ethanol and *CCL5/NOS2*) indicate the potential antagonistic effects in BEAS-2B cell in response to GDI PM emissions exposure.

The observed downregulation of pro-inflammatory cytokines and chemokines in this study is consistent with many previous studies that reported exposure to high concentrations of PAHs in PM can induce immunosuppressive effects (e.g., reduced levels of cytokines and low inflammatory activities).[118-120] Yang et al. [91] showed that GDI vehicles can produce substantial amounts of both vapor- and particle-phase nitro-PAHs and oxygenated-PAHs emissions. Therefore, it is possible that the negative regulation of inflammatory responses induced by fuels with varying aromatic and ethanol levels is linked to PAHs and their derivatives in the PM emissions.

When comparing the expression of biomarkers with the DTT results, it is generally expected that DTT activities (i.e., the oxidizing components in PM) would be positively correlated with oxidative stress and inflammatory-associated gene expression in response to particle-bound ROS generation [98]. Under the present test conditions, no positive correlation was found, with the inducible oxidative stress biomarker *HMOX-1* showing a moderate negative correlation with the measured DTTa (R = -0.55) and no correlation with DTTm (R = 0.04) consumptions (Table 2.2). Previous research showed a positive correlation between DTT activity with *HMOX-1* expression in BEAS-2B cells exposed to ambient particles from the Los Angeles basin [98]. A recent study, on the other hand, showed no significant positive correlations between DTT responses and cellular biomarkers (e.g.,

TNF-α, IL-6) from secondary organic aerosol samples [121]. Thus, whether DTT activities are good indicators of cellular responses remains inconclusive. Compared to the DTT assay, which is an isolated chemical reaction, cellular response involves a complicated biological system. We do not consider the DTT consumption originated from the particles as the only source of ROS production, since various intracellular processes could also produce endogenous ROS, which suggests that the cellular oxidative stress in response to GDI PM emissions from different fuels may be driven by different mechanisms not accounted by DTT consumption [90, 122].

Table 2.2. A multiple linear regression model to predict the altered gene expression of biomarkers and DTT activities by principal components (PCs).

	Parameters	*HMOX-1*	*TNF-α*	*IL-6*	*CCL5*	*NOS2*	DTT_a	DTT_m
	Pearson *R*	0.680	0.363	0.893	0.861	0.731	0.100	0.416
PC1	Standardized coefficient, β1	0.413	0.360	0.284	0.675	0.495	-0.055	0.338
	p-value	0.263	0.427	0.218	0.031*	0.166	0.907	0.443
PC2	Standardized coefficient, β2	-0.540	0.045	0.846	-0.534	-0.537	-0.083	-0.242
	p-value	0.160	0.919	0.008*	0.066	0.139	0.859	0.578

*$p < 0.05$

2.3.4. Principle Component Regression

PCA was performed to evaluate the influence of specific fuel properties on the DTT activity and the gene expression of biomarkers. Two principal components were extracted, explaining 87.41% of the total variance (Table S2.5, SI). After reducing the dimension of fuel properties, two principal components (PC1 and PC2) were identified. The two extracted components corresponded to two groups of hydrocarbon compounds (Figure 2.5), with PC1 representing the hydrophobic hydrocarbons (aromatic compounds) and PC2 representing the hydrophilic hydrocarbons (oxygenated compounds). The points inside each ellipse indicate a similar group of chemical constituents (Figure 2.5). Table S2.5, SI shows that the most significant contributors to PC1 were total aromatics (94.8%), C10+

aromatics (95.5%), and PMI (95.7%), while oxygen/carbon ratio (77%) and ethanol (78%) contributed mostly to PC2.

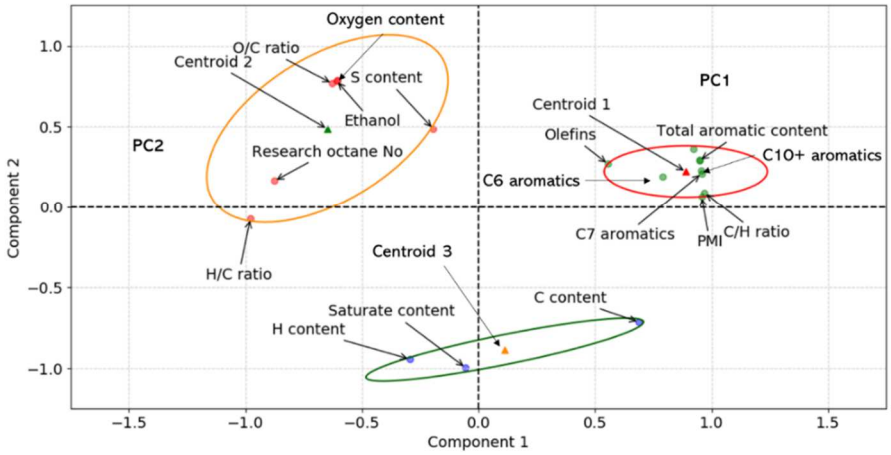

Figure 2.5. Principal component plots for fuel properties. Red ellipse represents PC1 (aromatics group), orange ellipse represents PC2 (oxygenated group) and green ellipse represents other chemicals, respectively. Triangle in each ellipse represents the centroid.

The multiple linear regression model with the Pearson *R* values was used to predict the gene expression alterations and DTT activities by PCs (Table 2.2). Significant associations between biomarkers and PCs were observed. Overall, aromatics-dominated PC1 is associated with the expression of *CCL5* ($p = 0.031$) and oxygenates-dominated PC2 is associated with the *IL-6* ($p = 0.008$) gene. Both gasoline aromatics and ethanol levels have significant impacts on inflammatory gene regulation, which could potentially suggest airway inflammation associated disease progression caused by exposure to GDI PM emissions from these fuels. Significant associations between oxygenates-dominated PC2 and *IL-6* also support that the presence of ethanol in gasoline will likely reduce PAH emissions and their derivatives in PM and neutralize the downregulation of the inflammatory biomarkers.

2.4. Conclusions

This study used a current technology GDI vehicle when operated on eight gasoline fuels with two different levels of aromatics and different ethanol contents over the LA92 cycle to assess the impacts of fuel composition to the toxicological responses in human lung cells. Our results showed the gasoline aromatics and ethanol concentrations were linked to exhaust PM emissions and the up-down regulation of biomarkers. We showed that the method of PM extraction, prior to exposure, may have an impact on the selective enrichment of certain type of PM constituents because of the solubility in the solvents. For this reason, exposure at an air-liquid interface (ALI) without solvent extraction may be considered in future studies to represent a more relevant exposure scenario for lung epithelial cells.[123]

Moreover, future studies examining dose- and time-dependent responses to traffic-related PM are required to provide a more comprehensive picture for traffic-induced toxicological effects. Lastly, our findings indicate that fuel composition influenced the amount of PM mass emissions and altered the expression of oxidative stress and inflammation-related genes in BEAS-2B cells. High PMI fuels led to higher aerosol oxidative potential (DTT_m), more significant PAH-mediated immunosuppressive effects on *IL-6* expression, and reduced levels on *CCL5/NOS2* downregulation. On the other hand, higher ethanol content contributed to decreased levels of *IL-6* downregulation and more significant *CCL5/NOS2* downregulation. These different patterns of correlations reveal that fuel compositions play an important role in determining the chemical and toxicological properties of PM emissions. Future studies are required to further investigate the

underlying molecular mechanisms to gain a more comprehensive understanding of health effects induced by gasoline exhaust.

2.5. Supplementary Information

Table S2.1: The main physicochemical properties of the test fuels.

Property	Test Method	Fuel 1	Fuel 2	Fuel 3	Fuel 4	Fuel 5	Fuel 6	Fuel 7	Fuel 8
Octane Rating		88.1	87.2	87.8	87.0	89.8	88.6	87.4	91.5
Sulfur Content (ppm)	ASTM D5453	8.6	8.0	8.2	8.5	8.9	8.7	8.9	8.3
PM Index (PMI)		1.748	2.330	1.888	2.152	1.722	1.765	2.093	1.613
Total Aromatic Content (vol %)	ASTM D5769	21.2	29.4	21.4	29.1	20.3	21.8	29.3	19.1
Olefins (vol %)	GAGE-MS	7.9	6.5	7.0	8.1	6.5	7.3	8.6	6.0
Saturate Content (vol %)		70.9	64.1	61.7	53.1	58.5	56.1	47.4	55.3
Hydrogen Content (wt %)	ASTM D5291	14.06	13.65	13.79	13.13	13.51	13.38	13.02	13.54
Carbon Content (wt %)	ASTM D5291	85.94	86.35	82.52	83.29	81.07	81.19	81.52	79.26
Oxygen Content (wt %)	ASTM D4815	0.00	0.00	3.69	3.57	5.42	5.43	5.48	7.20
C/H Ratio (wt/wt)		6.111	6.326	5.984	6.342	6.002	6.066	6.260	5.852
H/C Ratio (mole/mole)		1.950	1.884	1.991	1.879	1.986	1.965	1.904	2.036
O/C Ratio (mole/mole)		0.000	0.000	0.034	0.032	0.050	0.050	0.050	0.068
Density @ 15.56 °C (g/cc)	ASTM D4052	0.7409	0.7537	0.7448	0.7557	0.7474	0.7497	0.7592	0.7499
RVP @ 100 F (psi)	ASTM D5191	8.86	8.76	8.97	9.20	8.77	9.09	9.09	8.59
Ethanol Content (vol %)	ASTM D4815	0	0	9.98	9.62	14.72	14.77	14.74	19.61

Table S2.2. Summary of the measured DTT activities and log_2 fold changes of gene expression.

Properties	Fuel 1	Fuel 2	Fuel 3	Fuel 4	Fuel 5	Fuel 6	Fuel 7	Fuel 8
Aerosol oxidative potential (nmol/min/μg)								
DTT Activity (aqueous buffer)	7.7×10^{-3}	3.0×10^{-2}	2.0×10^{-2}	2.2×10^{-2}	2.5×10^{-2}	1.9×10^{-2}	1.6×10^{-2}	9.1×10^{-3}
DTT Activity (50% methanol)	1.2×10^{-2}	3.9×10^{-2}	2.6×10^{-2}	1.7×10^{-2}	1.8×10^{-2}	1.5×10^{-2}	2.4×10^{-2}	1.6×10^{-2}
Gene expression (Log_2 fold change)								
HMOX-1	2.39	2.01	2.06	2.44	0.58	1.51	1.65	1.52
TNF-α	-0.43	-0.53	-0.66	-0.02	-0.65	-0.55	-0.56	-0.39
IL6	-1.34	-0.91	-1.19	-0.41	-0.86	-0.37	-0.27	-0.31
CCL5	-0.07	0.02	-0.27	0.20	-0.64	-0.65	-0.34	-1.94
NOS2	-0.36	-0.11	-0.59	-0.47	-0.69	-0.57	-0.91	-3.20

Table S2.3. ANOVA and Tukey's Multiple Comparison Test of fuel blends for DTT activity in aqueous buffer solution.

P value	$p<0.0001$		
P value summary	***		
Are means significantly different? (P < 0.05)	Yes		
R squared	0.64		
ANOVA Table	SS	df	MS
Treatment (between columns)	0.004	8	0.00047
Residual (within columns)	0.002	42	4.9E-05

Tukey's Multiple Comparison Test	**Mean Diff.**	**q**	***p* value**
Fuel 1 vs Fuel 2	-0.02	7.86	*p < 0.001*
Fuel 1 vs Fuel 4	-0.02	5.12	*p < 0.05*
Fuel 1 vs Fuel 5	-0.02	6.11	*p < 0.01*
Fuel 2 vs Fuel 7	0.01	4.95	*p < 0.05*
Fuel 2 vs Fuel 8	0.02	7.22	*p < 0.001*
Fuel 5 vs Fuel 8	0.02	5.47	*p < 0.05*

Table S2.4: ANOVA and Tukey's Multiple Comparison Test of fuel blends for DTT activity in mixed methanol-buffer solutions.

P value	$p<0.0001$		
P value summary	***		
Are means significantly different? (P < 0.05)	Yes		
R squared	0.76		
ANOVA Table	SS	df	MS
Treatment (between columns)	0.005	8	0.00059
Residual (within columns)	0.002	42	3.6E-05

Tukey's Multiple Comparison Test	**Mean Diff.**	**q**	***p* value**
Fuel 1 vs Fuel 2	-0.03	10.90	*p < 0.001*
Fuel 1 vs Fuel 3	-0.01	5.45	*p < 0.05*
Fuel 1 vs Fuel 7	-0.01	4.63	*p < 0.05*
Fuel 2 vs Fuel 3	0.01	5.45	*p < 0.05*
Fuel 2 vs Fuel 4	0.02	8.99	*p < 0.001*
Fuel 2 vs Fuel 5	0.02	8.65	*p < 0.001*
Fuel 2 vs Fuel 6	0.02	9.81	*p < 0.001*
Fuel 2 vs Fuel 7	0.02	6.27	*p < 0.01*
Fuel 2 vs Fuel 8	0.02	9.54	*p < 0.001*

Table S2.5. Principal component extraction explaining 87.41% of the total variance for principal component analysis (PCA) and multiple linear regression.

Component Matrix[a]		
	Component	
	1	2
Research Octane No	-0.875	0.165
Sulfur	-0.195	0.488
Total aromatics	0.948	0.292
C6 (benzene)	0.791	0.189
C7 (toluene)	0.957	0.210
C8	0.949	0.296
C9	0.921	0.365
C10+	0.955	0.227
Olefins	0.555	0.270
Saturate	-0.056	-0.995
H	-0.295	-0.943
C	0.688	-0.714
O_2	-0.604	0.789
C/H	0.969	0.091
H/C	-0.979	-0.073
O/C	-0.629	0.769
PMI	0.957	0.067
Ethanol	-0.609	0.784

Extraction Method: Principal Component Analysis.

[a]. 2 components extracted.

Chapter III: Exposure to dimethyl selenide (DMSe)-derived secondary organic aerosol alters transcriptomic profiles in human airway epithelial cells

3.1. Introduction

Selenium (Se) is a trace element existing in natural environments and also a micronutrient essential for human health.[17, 124] The oxidation states of Se are critical to determine its solubility, mobility, bioavailability and toxicity.[125] The average Se concentration in soils is ~0.4 mg kg^{-1}, with elevated levels up to 5000 mg kg^{-1} in certain regions including the United States, Canada, China, Japan, Venezuela, and India.[17] The occurrence of Se in these regions depends upon the type of soil, extent of soil erosion, organic matter and rainfall. In addition, the elevated Se levels can be associated with overuse of Se-containing fertilizers.[17, 125] Atmospheric deposition and soil drainage make Se available in water bodies.[17, 124] In underground water, Se concentrations increase due to the use of Se-containing fertilizers in agricultural lands.[125] Oxyanions of Se^{4+} and Se^{6+} along with a number of selenides (Se^{2-}) are predominately present in aquatic environments.[126] A significant transitory reservoir for Se element is the air.[126, 127] Microbial transformation in both terrestrial and aquatic systems contributes to volatilization of Se and its release into the atmosphere in methylated forms, such as dimethyl selenide (DMSe), dimethyl diselenide (DMDSe), methaneselenol, or the inorganic selenium dioxide (SeO_2). Presence of volatile DMSe has been reported in bottled water at concentration ranges of 4-20 ng L^{-1}.[128] Plants metabolically release Se into the atmosphere in the form of hydrogen

selenide and selenates, as well as methylated Se and selenites.[17, 126] As Se is chemically similar to sulfur, the sulfate transporters in the plant's roots facilitate the Se transport and distribution.[17, 126, 129] Atmospheric input of Se is largely influenced by natural emissions from aquatic and terrestrial environments (including volcanic eruptions) and also anthropogenic emissions from industrial processes.[126, 130, 131]

In the human body, Se plays an important role in regulating oxidative stress and the immune system.[17] It also acts as the catalytic center of several seleno-proteins, including glutathione peroxidase and thioredoxin reductase.[132] Deficiencies of Se in the human diet can cause thyroid dysfunction, growth retardation and impaired bone metabolism.[133] On the other hand, selenosis (i.e., the condition of Se toxicity) can lead to pulmonary edema, garlic breath, gastrointestinal disorders, neurological damage, hair loss, and sloughing of nails.[17] Se has a relatively narrow range for optimal human consumption, with toxic levels reported at >400 μg per day and dietary deficiency at < 40 μg per day.[125] It has been reported that the methylated forms of Se (e.g., DMSe) are less toxic than the inorganic Se species.[134] However, with the doses of 0.05 and 0.1 mg Se/kg of body weight, DMSe intratracheal instillation in mice has been reported to cause lung injury and inflammation.[135] Inhalation of DMSe can also result in damage to centrilobular liver cells and acute tubular injury of the kidney.[135]

The chemical fate and transport of Se in natural environments and its interactions with plants have been widely studied.[126, 129] Atmospheric lifetimes of DMSe against oxidation by ozone (O_3), hydroxyl radical (OH), and nitrate radical (NO_3) have been

reported, ranging from minutes to hours at typical respective oxidant concentrations.[136] However, limited details for gas-phase products of DMSe oxidation are available.

Dimethyl selenoxide ($(CH_3)_2SeO$) has been identified as the major gaseous product in O_3 oxidation of DMSe, while both OH and NO_3 radical oxidation of DMSe are thought to predominantly proceed by breaking the Se-C bond, leading to formation of formaldehyde.[137] Although not directly identified, formation of methaneseleninic acid ($CH_3Se(O)OH$) and dimethyl selenoxide as intermediates and precursors of nitrate salts is also expected from its OH and NO_3 oxidation. As a structural analog of DMSe, dimethyl sulfide (DMS) has been reported as a major precursor leading to secondary aerosol formation in marine atmospheric environments.[18] To date, the potential of DMSe to produce inhalable secondary organic aerosol (SOA) through atmospheric oxidation has not been investigated. SOA represents a highly complex and reactive mixture of oxidized species. The dynamic nature of SOA makes characterization of its health impacts challenging. Given the wide range of emission sources of DMSe, we hypothesized that DMSe may be a ubiquitous precursor leading to SOA formation, thereby increasing the toxicity of ambient aerosols due to the redox-active properties of Se-containing components.

In this study, we characterized the chemical properties of SOA generated from OH and O_3 oxidation of DMSe in the presence of nitric oxides (NO_x) in controlled chamber experiments, and assessed the transcriptome-wide gene expression changes in human airway epithelial cells (BEAS-2B) exposed to DMSe-derived SOA. Gene expression profiling was carried out using RNA sequencing (RNA-Seq) followed by pathway

enrichment analyses to identify perturbed biological pathways to provide a mechanistic understanding of DMSe-derived SOA-induced health effects.

3.2. Materials and Methods

3.2.1. Chamber Experiments

DMSe oxidation experiments were carried out in a ~1.3 m^3 fluorinated ethylene propylene (FEP) Teflon environmental chamber, filled with Zero Air (ZA). In the OH oxidation experiment, nitrous acid (HONO) vapors generated by dropwise addition of sodium nitrite to sulfuric acid were first introduced in the chamber, followed by flowing NO to achieve ~170-300 ppbv of NO by start of irradiation. DMSe was injected into the chamber by flowing ZA over ~1.2 μL of DMSe in a glass bulb, to achieve a mixing ratio of ~300 ppbv in the chamber. After allowing the content of the bag to mix for 10 min, black lights (peak radiation intensity at ~350 nm) surrounding the chamber were turned on to initiate photooxidation. Based on previous characterization experiments of octane oxidation, the expected OH concentration in the chamber is at least 3×10^7 molecules cm^{-3}.[138] In the O_3 oxidation experiment, O_3 was first introduced in the chamber by flowing ZA through a λ=185 nm lamp source (UVP Ltd.). After reaching ~250 ppbv of O_3 in the chamber, O_3 injection was stopped, and vapors of DMSe (1.2 μL) were injected into the bag. Once O_3 mixing ratio decreased to 50 ppbv, additional O_3 was injected to the bag in a similar manner to maintain a mixing ration of ~50-150 ppbv. During the O_3 oxidation experiment, background NO_x in the chamber before the reaction was less than 2 ppbv. Relative humidity in the chamber was low (< 25 %) in both experiments. A summary of the experimental conditions is provided in Table S3.1.

During the experiments, gas phase mixing ratios of O_3 and NO_x were monitored by a UV photometric ozone analyzer (Thermo, Model 49*i*) and a chemiluminescence analyzer (Thermo, Model 42*i*), respectively. Aerosol size distributions were measured by a Scanning Electrical Mobility Spectrometer (SEMS, Brechtel Manufacturing Inc.) while aerosol composition was measured by a mini aerosol mass spectrometer (mAMS) with a compact time-of-flight mass spectrometer detector (Aerodyne Research, Inc.). DMSe-derived SOA mass concentrations were determined by standard analysis of the unit-mass resolution spectra of mAMS (using SQUIRREL ToF-AMS Analysis Toolkit, v.1.61) as well as size distribution measurements by SEMS.[139, 140] DMSe-derived SOA densities used in SEMS mass calculations were determined by comparing vacuum aerodynamic-based mass distributions from the mAMS with mobility-based volume distributions of the SEMS.[141] Given the performance of mAMS during the experiments (mass spectrometer resolution of ~1100 and mass accuracy of better than 1.2 ppm at *m/z* 40 and better than 3 ppm at *m/z* 184), multi-peak fitting routines written for high-resolution analysis of mAMS spectra were applied to *m/z* < 113 amu (using PIKA ToF-AMS Analysis Toolkit, v.1.21) to gain more detailed insights into the composition of DMSe-derived SOA.[142] It is worth noting that >97% of the detected aerosol mass in both experiments was at *m/z* < 113 amu. The high-resolution ion-list of PIKA was adjusted to include Se-containing fragments (and their corresponding isotopic fragments) in the fitting routine.

3.2.2. Aerosol Sample Collection and Extraction

At the end of each experiment, DMSe-derived SOA samples were collected onto 47 mm Teflon membrane filters and stored at -20 °C for two weeks until extraction. Filters were extracted with 23 ml of high-purity methanol (HPLC grade, Fisher Scientific), followed by 50 min of sonication. After sonication, the extracted solution was transferred to a clean vial and methanol solvent was dried off under a gentle stream of nitrogen gas. Then, the extracted DMSe-derived SOA constituents were stored at -20 °C (typically for a day) until further analysis.

3.2.3. Dithiothreitol (DTT) Assay

DTT assays were conducted to measure the oxidative potential (i.e., thiol reactivity) of DMSe-derived SOA products from both O_3 and OH oxidation experiments. The DTT assay procedures were carried out based on those published by Kramer et al.[93] Briefly, an aqueous buffer solution was made with potassium phosphate monobasic/ sodium hydroxide (0.05 M, pH 7.4) and 1 mM ethylenediaminetetraacetic acid (EDTA). The reaction mixtures (n=3) containing 1 μg of DMSe-derived SOA extracts and 2.5 nmol of DTT were incubated at 37 °C for 30 min; then the remaining DTT was quenched with 10 nmol of DTNB to make the final volume of 135 μL. The reaction between DTNB and DTT produced 5-thio-2-nitrobenzoic acid (TNB) that can be measured by its absorbance at 412 nm using a UV-Vis spectrophotometer (Beckman DU-640). The DTT consumption rate (expressed as nmol DTT consumed per min per μg of sample) was quantified in comparison with blank filter samples. To examine the potential for sample degradation during storage,

filter samples from O_3 and OH oxidation experiments were also analyzed immediately after collection.

3.2.4. Cell Culture and Exposure

BEAS-2B cells, obtained from the American Type Culture Collection (ATCC), were originally derived from the normal bronchial epithelium of a healthy individual. Cells were transformed by infection with a replication-defective SV40/adenovirus 12 hybrid and cloned to create an immortalized cell line.[143] Cells were cultured in commercially purchased Gibco® LHC-9 medium (1X) (invitrogen) and grown at 37 °C and 5% CO_2 in a humidified incubator. Cells were seeded in 24-well plates at a density of 2.5×10^4 cells per well in 250 μL of LHC-9 medium for 2 days prior to exposure. At the time of exposure, cells reached 60−70% confluence. Dried DMSe-derived SOA extracts were reconstituted with LHC-9 medium. Cells were washed with phosphate-buffered saline (PBS), and then exposed to DMSe-derived SOA extracts from the O_3 and OH oxidation experiments at the concentration of 10 μg ml^{-1} for 24 hr. Cells exposed to extracts of blank filters were included as negative controls.

3.2.5. RNA Isolation and Sequencing

After 24 hr of exposure, cells were lysed with 350 μL of TRI Reagent (Zymo Research) for total RNA isolation. Isolated RNA samples were further purified using the spin column-based Direct-zol RNA MiniPrep kit (Zymo Research). Extracted RNA samples were stored at -80 °C until processing. Nanodrop ND-1000 spectrophotometer (Thermo Fisher Scientific, Wilmington, DE) and Agilent 2100 Bioanalyzer (Agilent, Santa Clara, CA) were used to measure the RNA quality and concentrations. The 260/280 nm

absorbance ratios of all samples were determined to be >1.8. The RNA integrity number (RIN) scores from Bioanalyzer were >7. Following the manufacturer's recommendations, RNA-Seq libraries were prepared using NEBNext ultra II Directional RNA Library Prep Kit for Illumina NextSeq 500 high output 75bp single end analysis. RNA-Seq was performed at the University of California, Riverside- Institute for Integrative Genome Biology (IIGB). The read data were deposited in the sequence read archive (SRA) BioSample database (SRA accession number: PRJNA539990).

3.2.6. RNA-Seq Data Analysis

After sequencing, FastQC (version 0.11.7)[144] was used for read quality assessment. Trimming was obtained using Trimmomatic (version 0.35).[145] Bases before positions 13 and after 72 were cropped with CROP:72 and HEADCROP:13 parameters. Reads that are at least 50 bases long were kept using MINLEN:50. Then, raw reads were aligned to the human genome version hg19 with HISAT2 (version 2.1.0).[146] The aligned files were converted to bam files, sorted and indexed with samtools (version 1.9).[147] Subread (version 1.6.2) tool was used for counting reads of the UCSC Genome Browser annotated coding sequence (CDS) using the featureCounts commands.[148] Normalization and differential gene expression analysis was carried out using three different packages, including DESeq2 (version 1.18.1), edgeR (version 3.20.9), and Limma package (version 3.34.9) in R (version 3.4.4).[149-151] The combination of multiple data processing tools that use different models and normalization methods to identify differentially expressed genes (DEGs) improves the sensitivity of DEG identification and provides more reliable and robust results than the individual solutions. [49, 152]

Cut-offs used for DEGs between treated and untreated samples were identified and considered significant if the p-value was ≤0.01, FDR value was ≤0.01, and the absolute Log_2 Fold Change (Log_2 FC) was ≥1. The workflow for RNA-Seq data analysis is provided in Figure S3.1. The Log_2 FC values of selected genes are provided in Figures S3.2-S3.3.

3.2.7. Pathway Enrichment Analysis

For significantly altered genes, pathway enrichment analyses were performed to identify perturbed biological pathways from target gene sets using the ConsensusPathDB database.[153] To interpret the function of altered genes, overrepresentation analyses were carried out. Based on the hypergeometric distribution, the significance level of observed overlap between the members of predefined pathways and the input DEGs were calculated. Criteria of (1) a minimum overlap of two genes between the input list and pathways, and (2) a p value cutoff of 0.01 were set.[154] ClueGO (a Cytoscape app, version 2.5.4) was used for visualization of enriched pathways.[155]

3.3. Results

3.3.1. Aerosol Production and Composition

Both OH and O_3 oxidation experiments resulted in DMSe-derived SOA formation. Despite the intense nucleation during the O_3 experiments (e.g., Figure 1a), the total mass of DMSe-derived SOA formed from the O_3 oxidation (10-20 μg m^{-3}) was significantly lower than in the OH experiments (250-300 μg m^{-3}) at similar oxidation times and with similar amounts of DMSe injected (e.g., Figure 3.1b).

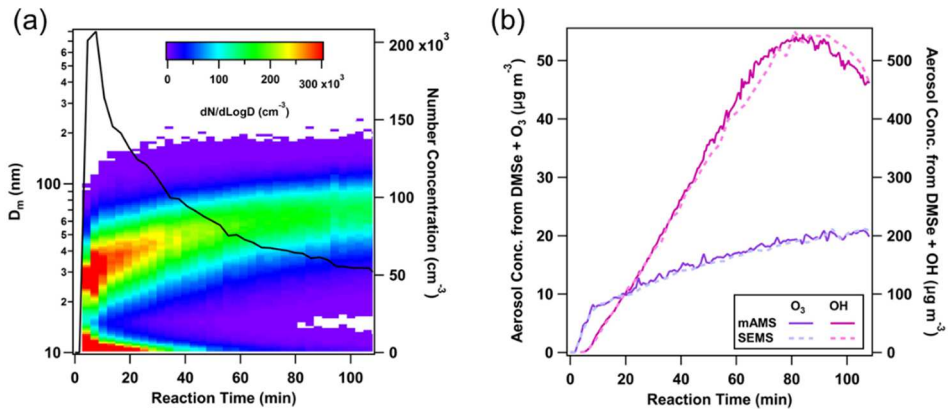

Figure 3.1. (a) Nucleation and growth of DMSe-derived SOA particles during O3 oxidation of DMSe; (b) aerosol mass concentrations during OH and O_3 oxidation experiments, as determined by mAMS and SEMS; aerosol density values of 1.8 g cm^{-3} and 1.6 g cm^{-3} were used in O_3 and OH oxidation experiments, respectively.

Although chamber concentration of DMSe was not monitored during the experiments, given the differences in DMSe oxidation rate constants with OH (6.8×10^{-11} cm^3 $molecule^{-1}$ s^{-1}) [136] and O_3 (6.8×10^{-17} cm^3 $molecule^{-1}$ s^{-1}) [136] and representative oxidant concentrations during the experiments ($[OH]_{average}$= 3×10^7 molecule cm^{-3} and $[O_3]_{average}$= 75-100 ppbv), we expect to have reacted only ~50-60% (~160-180 ppbv) of DMSe with O_3 after 80-100 min (assuming secondary production of OH was negligible), while a negligible fraction should have remained during the same time in the OH oxidation experiment. Further discussion on DMSe's potential to form SOA is provided in Section 3.4.1. As shown in Figure 3.1b, in both experiments, estimated mass concentrations using mAMS unit-mass resolution spectra, along with the standard relative ionization efficiency of organics (RIE_{org}=1.4) and unity collection efficiency, agreed well with the total mass concentrations estimated from the measured size distributions and inferred SOA densities. High-resolution analysis of mAMS spectra with the modified HR-ion list suggests that on average ~ 52-54% of the observed mass concentration in the range of *m/z* <113 was from

fragments containing Se, while ~18-22% of the mass stemmed from organic fragments lacking Se in their structures (Figure 3.2a). The contribution of the Se-containing ions was similar between the O_3 and OH oxidation experiments (Figure 3.2b), suggesting the composition of DMSe-derived SOA is relatively similar for both pathways.

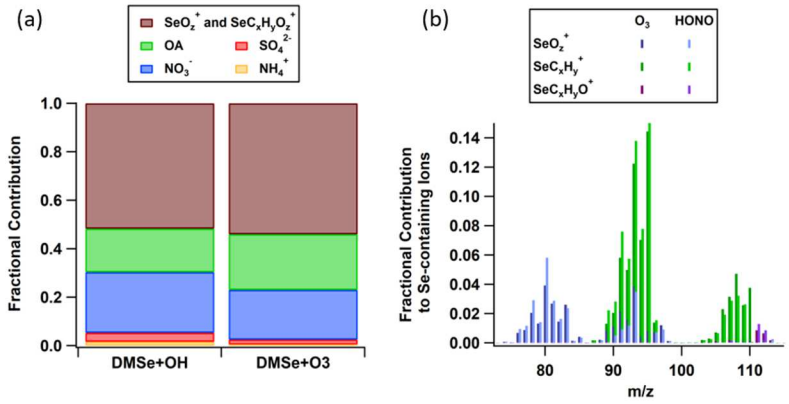

Figure 3.2. (a) Fractional contribution of SOA species to total SOA mass during filter collection. (b) Average HR-MS analysis of Se-containing fragments during the peak mass concentration of O_3 and OH oxidation experiments. Frequency of each atom in the designated ions is specified by integers x, y, and z.

In both experiments, ~20-25% of aerosol mass was from nitrate (Figure 3.2a); however, given the different NO^+/ NO_2^+ ratios, different compounds likely contribute to the nitrate concentrations in the OH and O_3 oxidation experiments (Figure S3.4). During the first ~40 min after start of the reaction, there is evidence for formation of organonitrates in both systems, given the higher ratio of NO^+/ NO_2^+ relative to that of ammonium nitrate. However, during the OH experiment, the ratio decreased to values lower than that of ammonium nitrate after ~60 min while in the O_3 experiment the ratio approached ammonium nitrate calibrations (Figure S3.4). These observations suggest formation of nitrated salts or nitro-organics in the OH experiment and the formation of nitric acid in the O_3 experiment.

3.3.2. Aerosol Oxidative Potential

The oxidative potential of aerosol is expressed as DTT consumption rate normalized to the particulate matter (PM) mass (pmol/min/μg). Both aerosol samples collected from OH and O_3 oxidation experiments have similar DTT consumption rates of ~77 pmol/min/μg, suggesting the presence of common oxidizing moieties in both aerosol systems. Note that the reactive components in DMSe-derived SOA did not seem to decay rapidly under the given storage duration and conditions as evidenced in the similarity of DTT activity between stored and freshly analyzed filter samples (Figure S5). The DTT assay has been widely used as an indicator for total particle-bound oxidants in aerosol constituents.[156] In comparison with other sources of PM, DMSe-derived SOA have DTT consumption rates higher than ambient PM (10–70 pmol/min/μg),[157] SOA from isoprene, toluene and α-pinene (2.1–57.5 pmol/min/μg),[93, 158, 159] and diesel exhaust particles (1–61 pmol/min/μg).[99] The DTT consumption rates of DMSe-derived SOA are comparable to cooking OA (90 ± 51 pmol/min/PM), but less than biomass burning OA (151 ± 20 pmol/min/μg)[157] and naphthalene SOA (153.4 ± 49.2 pmol/min/μg) that potentially constitute redox active quinones.[157]

3.3.3. Differential Gene Expression from RNA-Seq Data

RNA-Seq was performed to detect differential gene expression in BEAS-2B cells exposed to DMSe-derived SOA (from both OH and O_3 oxidation experiments) versus the control groups that were exposed to the blank filter extracts. The lactate dehydrogenase (LDH) assay analysis of the cellular samples indicated no significant cell death after 24 hr of exposure; therefore, RNA-seq results represent the true transcriptional change of the live

cells (Figure S3.6). From RNA-Seq quality analysis, the quality metrics indicated base-composition bias before 13 and after 72 bp positions, which could be due to the unbalanced selection of random primers. Therefore, those base positions were cropped prior to alignment. On average, we obtained 24.8 million mapped reads, with a mapping rate of 90.81% (Table S3.2). From 23,393 UCSC annotated human CDS, we retained ~55% of genes for subsequent analyses with transcriptional signal fpm≥1 in DESeq2. This percentage was the same when using cpm≥1 as a threshold in edgeR and limma.

With the sorting criteria of Log_2 FC |±1|, p value = 0.01, false discovery rate (FDR)-adjusted p value = 0.01, DESeq2, edgeR, and Limma resulted in 2619 and 2616, 2605 and 2687, and 1229 and 1258 DEGs for O_3 and OH, respectively. The three sets of DEGs obtained from DESeq2, edgeR, and limma were intersected to identify common DEGs. As shown in the intersections of Venn diagrams in Fig. 3.3, we identified 1196 common DEGs from exposure to O_3 oxidation products (862 up-regulated and 334 down-regulated) and 1232 common DEGs from exposure to OH oxidation products (875 up-regulated and 357 down-regulated) for the downstream pathway enrichment analysis.

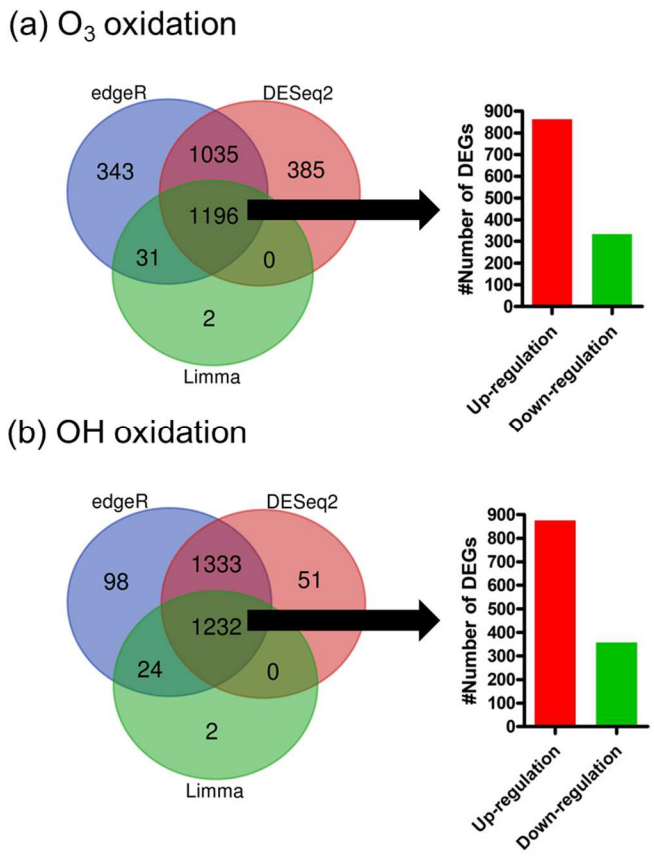

Figure 3.3. DEGs identified from three different tools, including DESeq2, edgeR, and Limma for BEAS-2B cells exposed to DMSe-derived SOA resulting from (a) O3 and (b) OH-initiated oxidation. Sorting criteria: Log_2 FC |±1|, p value = 0.01, FDR/adjusted p value = 0.01, and CPM ≥ 1. Bar graphs represent the number of up-regulated and down-regulated DEGs in the intersections of three gene sets input from DESeq2, edgeR, and Limma.

3.3.4. Perturbed Biological Pathways

Significantly altered biological pathways were identified using the ConsensusPathDB database (Tables S3.3-4). The input of DEGs were categorized into six groups based on up- and down-regulation of genes: (1) up-regulated by both O_3 and OH oxidation products, (2) up-regulated by O_3 only, (3) up-regulated by OH only, (4) down-regulated by both O_3 and OH oxidation products, (5) down-regulated by O_3 only, and (6) down-regulated by OH

only (Fig. S3.7). Figure 3.4 shows the major biological pathways enriched for up-regulated and down-regulated DEGs by both O_3 and OH oxidation products.

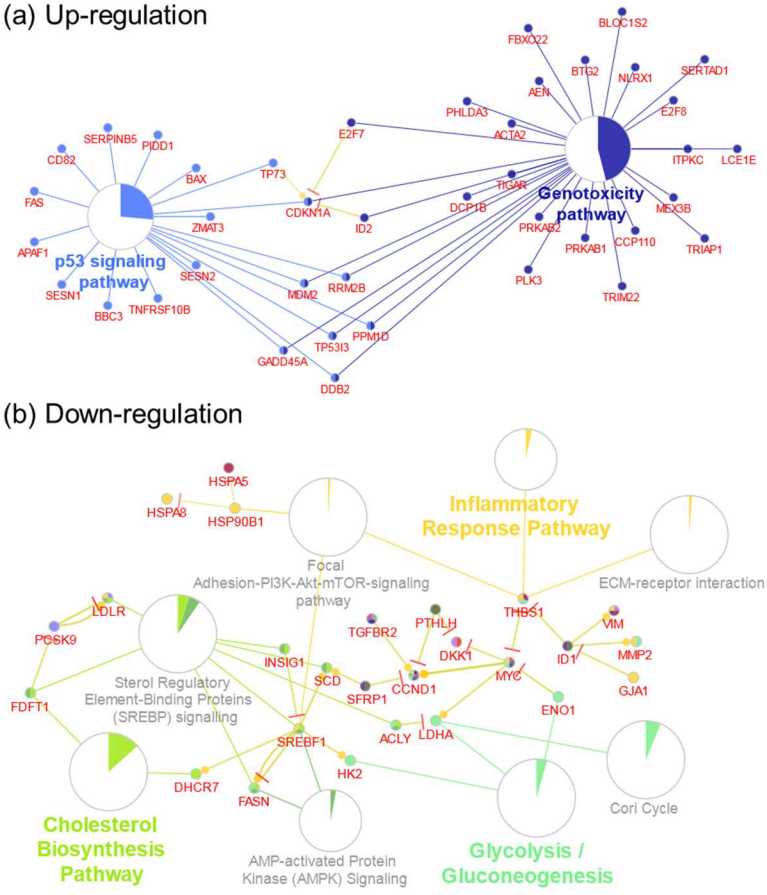

Figure 3.4. Major biological pathways enriched for (a) up-regulated and (b) down-regulated DEGs, FDR < 0.01. Pie charts represent the percentage of visible genes of a pathway. Genes shared between pathways are shown.

Top pathways that are enriched by up-regulated common DEGs from both O_3 and OH oxidation products include genotoxicity, p53 signaling and mitogen-activated protein kinase (MAPK) signaling (Table S3.3). On the other hand, down-regulated common DEGs by both O_3 and OH oxidation products enriched pathways mostly associated with the

metabolic regulation of glucose, as well as the interleukin IL-4 and IL-13 signaling that are related to the pathogenesis of allergic airway disorders (Table S3.4).

3.4. Discussion

3.4.1. DMSe-derived SOA Yields

Both OH and O_3 oxidation of DMSe resulted in formation and growth of DMSe-derived SOA. Considering the estimated amounts of reacted DMSe in each experiment, our results suggest DMSe-derived SOA formation yields of ~23% and ~2% in the OH and O_3 oxidation experiments, respectively (Table S3.1). The significantly lower yields in O_3 oxidation experiments suggest formation of relatively more volatile products under these conditions. These SOA formation yields are in the same range as the yields observed in non-seeded chamber or flow tube photooxidation experiments of other naturally emitted hydrocarbons, such as isoprene and α-pinene.[160-162] Further discussion on the potential abundance of atmospheric DMSe oxidation products is presented in Section 3.4.7. Note that these SOA yields are likely underestimated since vapor and particle losses to the chamber walls were not corrected for, and the observed nitrate components were not considered as DMSe-derived SOA.

Despite the much lower formation yield in the O_3 oxidation experiment, bulk DMSe-derived SOA composition was very similar to that in the OH oxidation experiment, which could potentially explain similar values of aerosol oxidative potential measured for DMSe-derived SOA in the two systems.

3.4.2. PM oxidative potential and DMSe-derived SOA induced oxidative damage

High PM oxidative potential measured by the DTT assay has been associated with the ability of PM to generate reactive oxygen species (ROS).[163] Previously, the DTT activities of ambient PM have been largely attributed to the presence of transition metals and quionones.[164] In this study, the oxidative potential of DMSe-derived SOA was assessed and found to contribute to high DTT consumption rates, which supports our hypothesis that DMSe-derived SOA possesses redox-active properties. Recent studies have also indicated that PM oxidative potential can be directly linked to the reactivity of PM constituents towards thiol functional groups within biomolecules leading to cellular oxidative stress.[8, 165] Cellular oxidative stress can be attributed to an imbalance between ROS production (from both exogenous and endogenous sources) and their elimination through protective mechanisms by antioxidants. Disbalance in these pathways is the leading cause of a variety of injuries, including acute and chronic inflammation, genome instability and mutation, pulmonary fibrosis, obesity, diabetes and atherosclerosis.[166] Prior studies have established that through metabolic processes, Se compounds have the potential to induce genotoxicity via generation of ROS.[167] Relative expression of oxidative stress and antioxidant-related genes are consistent with DTT results (Fig. S3.2). With exposure to DMSe-derived SOA in BEAS-2B cells, several pathways associated with oxidative damage, genotoxicity, glutathione metabolism, biological oxidation, and DNA damage response were perturbed and are discussed in the next sections.

Results from both DTT assays and pathway enrichment analysis suggest that Se-containing moieties in DMSe-derived SOA might be important in ROS-induced oxidative damage.

3.4.3. DNA damage, genotoxicity and activation of p53-mediated stress response

The up-regulated DEGs from both O_3 and OH oxidation experiments revealed the activation of p53 signaling pathway in response to DMSe-derived SOA exposure in BEAS-2B cells (Table S3.3 and Figure 3.4a). Tumor suppressor protein p53 is encoded by the *TP53* gene, which is one of the most commonly mutated genes in human cancer,[168] including lung cancer.[169] More than half of all tumors exhibit mutations in either *TP53* or MDM2 proto-oncogene (*MDM2*) genes, whose protein products control p53 activity.[168, 170] The affinity of p53 for MDM2 is reduced when ataxia-telangiectasia mutated (ATM) protein kinase (Table S3, FDR = 7.22×10^{-2}) phosphorylates p53, which consequently results in reduced p53 degradation by MDM2, and thus enhances p53 protein stability and activity.[171] The functions of p53 are complex; under normal conditions, p53 expression is very low inside the cell, but it is activated in response to oxidative, genotoxic or oncogenic stress; p53 exerts its activities as tumor-suppressive, pro-oxidant, and antioxidant.[168, 172] Under mild stress, activated p53 acts as a pro-oxidant and mediates the activation of tumor protein 53-induced nuclear protein 1 (*TP53INP1*) and cyclin dependent kinase inhibitor 1A (*CDKN1A*) to induce cell cycle arrest in G1 to allow cells to repair and recover from damage. Under prolonged stress or rapid DNA damage, p53 acts as an antioxidant and activates the BCL2 binding component 3 (*BBC3*) and phorbol-12-myristate-13-acetate-induced protein 1 (*PMAIP1*) genes that produce proapoptotic proteins to neutralize the

DNA damage.[168, 172] In addition, p53 can also act as an upstream activator to regulate mitogen-activated protein kinase (MAPK) signaling in response to DNA damage from external insults.[173] Overall, DMSe-derived SOA can activate p53 through the genotoxicity pathway, which could potentially result in various adverse cellular events like DNA damage, heat shock, hypoxia and oncogene overexpression.[174]

3.4.4. Dysregulation of metabolic pathways with p53 activation

The down-regulated DEGs identified from this study revealed the dysregulation of metabolic pathways associated with cholesterol biosynthesis, glycolysis, gluconeogenesis, and fatty acid synthesis (Table S3.4 and Figure 3.4b).[175] Upon activation of p53 under stress, many cellular processes that control energy and metabolism are negatively regulated to maintain homeostasis. Recent studies have shown the connection between p53, energy metabolism, and metabolic diseases, including type II diabetes mellitus.[168, 172] Moreover, p53 can also indirectly control glycolysis by regulating the phosphatidylinositol 3-kinase/protein kinase b (PI3K/Akt) pathways (Table S3.4, FDR = 4.70×10^{-5}). Specifically, the PI3K/Akt pathway can be negatively regulated by the p53 target genes, including the tumor suppressor gene phosphatase and tensin homologue deleted on chromosome 10 (*PTEN*) that is frequently inactivated by mutation.[168] As the PTEN phosphatase activity is the major antagonist of Akt, PTEN could affect the p53 protein levels and stability by keeping Akt inactive, [172, 176] and thus PTEN would be an essential component of the p53 response upon DNA damage.

At the same time, p53 is linked to enhance the transcription of *PTEN*.[177] However, under reduced nutrient or energy levels, the Akt and AMP-activated protein kinase

(AMPK) (Table S3.3, FDR = 1.88×10^{-3}) fail to be activated, which can subsequently induce p53. As a result, it is clear that p53 plays a pivotal role in the metabolic regulation.[172] Through suppression of the peroxisome proliferator-activated receptor-γ coactivator-1α (PGC-1α), p53 also influences the insulin resistance that is critical in the development of type II diabetes and pre-diabetes.[168, 178] Notably, the Warburg effect (FDR = 1.33×10^{-3}) was also found to be significantly enriched in the current study (Table S3.3). The Warburg effect describes the increased usage of glycolysis for ATP synthesis rather than using oxidative phosphorylation, which is a metabolic hallmark of cancer cells that rewire their metabolism to promote growth and survival.[172] It has been suggested that the Warburg effect may provide unifying insights into the progression of cancer and type II diabetes mellitus.[179] Overall, the perturbed biological pathways identified in this study (Tables S3.3-4) are coherent, and conclusively support the potential significance of p53-mediated metabolic dysregulation caused by DMSe-derived SOA exposure.

3.4.5. Signaling Associated with Allergic Airway Inflammation

Down-regulated IL-4/IL-13 signaling (FDR = 6.40×10^{-4}) and neutrophil degranulation (FDR = 1.61×10^{-2}) pathways were both observed in this study (Table S3.4), consistent with previous reports that IL-4 and IL-13 can suppress excessive neutrophil accumulation.[180] Although neutrophils were directly not tested in the current study, genes involved in neutrophil degranulation were found differentially expressed in BEAS-2B.

Among these DEGs, mutation in *SERPINA1* has been linked to low levels of alpha-1-antytrypsin (AAT) in alveolar epithelial cells that may lead to premature development of pulmonary emphysema.[181] Notably, perturbations in various inflammatory responses and

signaling pathways revealed the potential interplay between oxidative damage and inflammation upon DMSe-derived SOA exposure, which may result in the production of soluble mediators to activate the signal transducer and activator of transcription 3 (STAT3) and MAPK that mediate the expression of a variety of genes in response to cellular stimuli.[166, 182] Chronic inflammation can contribute to tumor development through induction of oncogenic mutations, genomic instability, early tumor promotion, and enhanced angiogenesis. In the type 2 inflammatory responses associated with the pathogenesis of asthma and allergies, IL-4 and IL-13 are the signature cytokines that can be triggered by allergens;[183] however, IL-4 and IL-13 play distinct roles in allergic inflammatory states. Briefly, IL-4 regulates Th2 cell proliferation and survival that has been shown to be essential in the initiation of allergic airway responses, while IL-13 contributes to the pathological features of diseases (e.g., mucus production, airway smooth muscle alterations, and sub-epithelial fibrosis).[184] Recent studies have shown that activation of IL-4/IL-13–STAT6 and ROS-epidermal growth factor receptor (EGFR) signaling pathways is associated with airway mucin overproduction induced by foreign stimuli,[185] as well as enhanced epithelial repair in response to lung injury.[186] Together with the significant ROS generation potential (as measured by DTT) and the identified EGFR signaling pathway, our findings highlight the potential significance of DMSe-derived SOA in modulating allergic airway inflammation.

3.5. Potential Limitations

When interpreting the results of the current study, some potential limitations should be considered. First, the oxidative potential of DMSe-SOA was measured using an acellular

DTT assay to approximate the ability of PM to generate ROS or reactivity towards thiols. Recent studies have indicated that DTT activity can only represent part of PM-bound ROS.[187] Measurement of ROS within cells will provide more direct evidence to determine the cellular oxidative stress conditions and warrants future work. Also, the initial concentration of DTT used in the assay has been reported to influence the DTT consumption rates.[188] Caution should be taken when intercomparing the DTT assay results from different studies. In addition, owing to the nature of the hard ionization technique used by mAMS, composition of the highly fragmented DMSe-derived SOA products was obtained. To identify specific moieties or functional groups of DMSe-derived SOA contributing to ROS generation, comprehensive analysis that can retain molecular information is necessary. DMSe-derived SOA samples were extracted with methanol, which may have selectively enriched certain types of DMSe-derived SOA constituents. Furthermore, the use of an immortalized cell line (BEAS-2B) may not faithfully represent the untransformed human airway epithelium, but it provides reproducible results critical to gaining initial insights into cellular response to DMSe-derived SOA exposure. Lastly, as RNA-Seq and pathway enrichment analysis have enabled rapid identification of pathway perturbations at the transcriptional level, functional validation will be required to demonstrate the effects on the changes of phenotypes.

3.6. Atmospheric Implications

Selenium contamination is associated with a broad spectrum of natural and anthropogenic activities, but the sources and sinks are not well constrained in the atmosphere. Concentrations of Se measured in ambient aerosols have been reported to

range from ~1.5-30 ng m^{-3}.[189] A wide range of selenium volatilization rates from terrestrial emissions in California has also been reported (~20 μg Se m^{-2} d^{-1} for bare soil and up to 430 μg Se m^{-2} d^{-1} in biotreated soil).[190, 191] Moreover, Karlson et al. reported that DMSe emissions potentially can increase with the onset of the warmer temperatures, during the summer season.[192] In San Joaquin Valley, DMSe contributes to 90% of volatile Se.[193] Assuming a 1-acre source area, the emissions rates mentioned above translate to ~4-80 pptv d^{-1} emissions of DMSe in a 1.5 km deep planetary boundary layer. Considering typical, non-polluted daytime OH and nighttime O_3 concentrations (4×10^6 molecule cm^{-3} and 50 ppbv, respectively) with the estimates of our DMSe-derived SOA formation yield, at least ~0.2-80 ng m^{-3} of DMSe-derived SOA can be produced in four hours during day or night. Although Se-rich soils might not be in close proximity to populated areas, since fine particles have lifetimes of ~7-10 days, once formed in at the atmosphere, DMSe-derived SOA particles could potentially be transported away and pose health risks in areas downwind of high DMSe emission regions.

Furthermore, if agricultural fields contain high Se in the soil, field workers could potentially be in direct exposure to significant amounts of DMSe-derived SOA, especially during the warmer months. Overall, atmospheric oxidation of DMSe produces SOA with high oxidative potential. Transcriptomic gene expression profiling followed by pathway enrichment analysis revealed that major biological pathways perturbed by DMSe-derived SOA are associated with elevated genotoxicity, DNA damage, and p53-mediated stress responses, as well as dysregulated metabolic activities and cytokine signaling that plays crucial roles in allergic airway inflammation. Future work is required to examine

atmospheric emissions of DMSe and gain a more detailed molecular composition of DMSe-derived SOA. To fully assess environmental health impacts of DMSe-derived SOA, direct measures of ROS production and validation of the perturbed biological functions in primary airway epithelial cells and other cell types would also be valuable.

3.7. Supplementary Information

S3.1: Cytotoxicity Assay

The lactate dehydrogenase (LDH) cytotoxicity assay was performed to assess the viability of cells, following the manufacturer's protocol (Roche). Cells were seeded in 24-well plates at a density of 2.5×10^4 cells per well in 250 µL of LHC-9 medium for 2 days prior to exposure. Supernatants were collected 24 h after exposure. To simulate 100% cell death, Triton X-100 (0.1%) was used as a positive control. The absorbance was measured using a TECAN SpectraFluor Plus microplate reader at 490 nm, with a reference wavelength at 620 nm.

Table S3.1. Summary of smog chamber experimental conditions. Experiments were carried out to oxidize ~300 ppbv of DMSe by OH (k=6.78 × 10^{-11} cm^3/molecule/s) and O_3 (k=6.8× 10^{-17} cm^3/molecule/s).

Oxidant	Irradiation	$[NO]_0$ (ppbv)	$[O_3]_0$ (ppbv)	Yield
OH	Yes (peak λ~350 nm)	300	< 1	26 %
		200	< 2	20 %
		170	< 2	23 %
O_3	none	< 2	200	2.0 %
		<2	270	2.4 %
		<2	220	1.3 %

Table S3.2: Alignment rates of samples with the human reference genome (hg19).

Sample ID	Pre-Trimming #Reads	Post Trimming #Reads	Alignment Rate (%)
Control_#1	67677315	66634166	93.23%
Control_#2	70530339	69950456	92.99%
Control_#3	47054369	46702719	92.51%
O_3_#1	65336736	65035144	89.75%
O_3_#2	60974300	60764347	90.07%
O_3_#3	71361747	70750882	89.61%
OH_#1	36214977	35932064	90.20%
OH_#2	49401319	48271745	89.30%
OH_#3	44435743	44174097	89.82%

Table S3.3: List of the up-regulated pathways in BEAS-2B cells exposed to DMSe-derived SOA.

#	pathway	size	p-value	FDR-value	members_input_overlap	source
	Up-regulated by both O_3 and OH oxidation products					
1	Genotoxicity pathway	64	8.82E-26	1.14E-22	*ACTA2; PLK3; TIGAR; DCP1B; NLRX1; PHLDA3; AEN; SERTAD1; PPM1D; BTG2; GADD45A; TRIAP1; FBXO22; ITPKC; RRM2B; DDB2; CDKN1A; RPS27; PRKAB2; PRKAB1; TRIM22; LCE1E; TP53I3; CCP110; MDM2; MEX3B; BLOC1S2; E2F7; ID2; E2F8*	Wikipathways
2	Direct p53 effectors	143	6.71E-22	4.33E-19	*LIF; SESN1; RPS27; PLK3; TIGAR; BAX; TNFRSF10C; TNFRSF10B; FDXR; BBC3; BTG2; GADD45A; ZNF385A; CD82; TRIAP1; PCBP4; RRM2B; DDB2; GDF15; CDKN1A; APAF1; PRDM1; TYRP1; PRKAB1; TP53I3; TP53INP1; SNAI2; MDM2; SERPINB5; HIC1; ARID3A; E2F2; IRF5; TP73; PIDD1; ATF3; FAS; SCN3B*	PID
3	p53 signaling pathway	72	1.85E-11	7.96E-09	*SESN2; PPM1D; SESN1; TP73; FAS; CDKN1A; CD82; TP53I3; PIDD1; TNFRSF10B; ZMAT3; RRM2B; BAX; GADD45A; DDB2; MDM2; SERPINB5; BBC3; APAF1*	KEGG
4	Validated transcriptional targets of TAp63 isoforms	55	1.52E-09	4.92E-07	*TRAF4; BBC3; EGR2; GADD45A; CDKN1A; SPATA18; DHRS3; BAX; TP53I3; FAS; FDXR; GDF15; SERPINB5; MDM2; AEN*	PID
5	TP53 Regulates Transcription of Cell Death Genes	29	7.14E-08	1.84E-05	*FAS; TP53I3; TRIAP1; TNFRSF10C; TNFRSF10B; TP53INP1; BAX; BBC3; PIDD1; APAF1*	Wikipathways
6	TP53 Regulates Transcription of Cell Cycle Genes	13	1.75E-07	3.77E-05	*E2F7; ARID3A; BTG2; GADD45A; PLK3; PCBP4; CDKN1A*	Wikipathways
8	p73 transcription factor network	79	1.74E-06	2.82E-04	*BBC3; FAS; PLK3; NTRK1; BAX; TP53I3; NSG1; MDM2; TP73; JAG2; GDF15; AEN; CDKN1A; DCP1B*	PID
9	Generic Transcription Pathway	1107	3.03E-06	4.34E-04	*ZNF699; ZNF337; ZNF195; KRBA1; SESN1; SESN2; NUAK1; CDKN1A; SMAD7; TIGAR; BAX; ZNF256; TNFRSF10C; TNFRSF10B; ZNF79; ZNF596; ZNF30; FAS; NR1D1; BBC3; NOTCH3; ZNF383; ZNF746; PPM1D; ZNF606; BTG2; PPM1A; GADD45A; ZNF385A; PRKAB1; PPARGC1A; ZFP2; TRIAP1; ZNF343; PCBP4; RRM2B; ZNF550; DDB2; ZNF473; PLK3; APAF1; FBXW7; E2F7; ZFPM1; PRKAB2; ESRRB; NR4A3; TP53I3; ZNF540; TP53INP1; GLS2; E2F8; ZNF440; MDM2; GATA2; ZNF28; ARID3A; SOCS4; TAF3; ZNF441; NOTCH1; TP73; PIDD1; ZNF468; ZNF425; PRDM1; ZNF274; ZNF750; TNRC6C; ZNF563; NR0B1; ZNF561; ZNF506*	Reactome
10	Transcriptional Regulation by TP53	374	7.49E-06	8.84E-04	*SESN1; SESN2; NUAK1; CDKN1A; TIGAR; BAX; TNFRSF10C; TNFRSF10B; TNRC6C; BBC3; E2F8; BTG2; GADD45A; ZNF385A; TRIAP1; PCBP4; RRM2B; DDB2; PLK3; APAF1; E2F7; PRKAB2; PRKAB1; TP53I3; TP53INP1; MDM2; ARID3A; TAF3; TP73; PIDD1; PRDM1; FAS; GLS2*	Reactome
11	TP53 Regulates Transcription of	14	7.53E-06	8.84E-04	*E2F7; ARID3A; ZNF385A; E2F8; PCBP4; CDKN1A*	Reactome

	Genes Involved in G1 Cell Cycle Arrest					
12	TP53 Regulates Metabolic Genes	9	9.44E-06	9.96E-04	*TIGAR; SESN2; RRM2B; SESN1; GLS2*	Wikipathways
13	DNA Damage Response	68	1.00E-05	9.96E-04	*SESN1; GADD45A; CDKN1A; BAX; PIDD1; TNFRSF10B; RRM2B; FAS; DDB2; MDM2; BBC3; APAF1*	Wikipathways
14	TP53 Regulates Transcription of Cell Cycle Genes	51	2.11E-05	1.95E-03	*ARID3A; E2F7; BTG2; GADD45A; PLK3; BAX; E2F8; PCBP4; CDKN1A; ZNF385A*	Reactome
15	RNA Polymerase II Transcription	1236	7.37E-05	6.35E-03	*ZNF699; ZNF337; ZNF195; KRBA1; SESN1; SESN2; NUAK1; CDKN1A; SMAD7; TIGAR; BAX; ZNF256; TNFRSF10C; TNFRSF10B; ZNF79; ZNF596; ZNF30; FAS; NR1D1; BBC3; NOTCH3; ZNF383; ZNF746; PPM1D; ZNF606; BTG2; PPM1A; GADD45A; ZNF385A; PRKAB1; PPARGC1A; ZFP2; TRIAP1; ZNF343; PCBP4; RRM2B; ZNF550; DDB2; ZNF473; PLK3; APAF1; FBXW7; E2F7; ZFPM1; PRKAB2; ESRRB; NR4A3; TP53I3; ZNF540; TP53INP1; GLS2; E2F8; ZNF440; MDM2; GATA2; ZNF28; ARID3A; SOCS4; TAF3; ZNF441; RPAP2; NOTCH1; TP73; PIDD1; ZNF468; ZNF425; PRDM1; ZNF274; ZNF750; TNRC6C; ZNF563; NR0B1; ZNF561; ZNF506*	Reactome
16	TP53 Network	20	7.96E-05	6.43E-03	*GADD45A; CDKN1A; TP73; BAX; BBC3; MDM2*	Wikipathways
17	miRNA Regulation of DNA Damage Response	89	1.56E-04	1.19E-02	*SESN1; GADD45A; CDKN1A; BAX; PIDD1; TNFRSF10B; RRM2B; FAS; DDB2; MDM2; BBC3; APAF1*	Wikipathways
18	miRNA regulation of p53 pathway in prostate cancer	32	1.81E-04	1.30E-02	*BAX; TNFRSF10B; ZMAT3; DDB2; BBC3; MDM2; APAF1*	Wikipathways
19	Transcriptional activation of cell cycle inhibitor p21	4	2.24E-04	1.45E-02	*PCBP4; ZNF385A; CDKN1A*	Reactome
20	Transcriptional activation of p53 responsive genes	4	2.24E-04	1.45E-02	*PCBP4; ZNF385A; CDKN1A*	Reactome
21	Transcriptional misregulation in cancer	186	3.03E-04	1.86E-02	*TRAF1; DDIT3; LYL1; ETV7; ITGB7; GADD45A; CDKN1A; NUPR1; ID2; NTRK1; BAX; KDM6A; ITGAM; NR4A3; DDB2; MDM2; UTY; NGFR*	KEGG
22	Chromosomal and microsatellite instability in colorectal cancer	73	4.80E-04	2.76E-02	*TGFBR1; RALGDS; TBK1; NTN1; CDKN1A; BAX; DDB2; GADD45A; APC2; BBC3*	Wikipathways
23	MAPK signaling pathway	295	4.96E-04	2.76E-02	*NGF; MAPK8IP2; HSPA6; JUND; NGFR; PGF; AREG; PPM1A; GADD45A; NTRK1; DUSP8; RELB; NFKB2; CACNA1H; TGFBR1; DDIT3; PLA2G4C; KITLG; DUSP16; FGF1; RASGRF1; MAP3K12; FAS; FLNC*	KEGG
24	Apoptosis	87	5.13E-04	2.76E-02	*TRAF1; IRF1; IRF5; FAS; TP73; NFKBIE; TNFRSF10B; BAX; MDM2; BBC3; APAF1*	Wikipathways
25	Gene expression (Transcription)	1373	6.62E-04	3.42E-02	*ZNF699; ZNF337; PRDM1; KRBA1; SESN1; SESN2; NUAK1; CDKN1A; ZFPM1; TIGAR; BAX; ZNF256; TNFRSF10C; TNFRSF10B; ZNF79; TNRC6C; ZNF30; FAS; NR1D1; BBC3; E2F8; ZNF383; ZNF746; PPM1D; ZNF606; BTG2; PPM1A; GADD45A; ZNF385A; PRKAB1; PPARGC1A; ZFP2; TRIAP1; ZNF343; PCBP4; RRM2B; ZNF550; DDB2; ZNF473; PLK3; APAF1; FBXW7;*	Reactome

					E2F7; SMAD7; PRKAB2; ESRRB; NR4A3; DNMT3L; ZNF540; TP53INP1; TP53I3; ZNF440; MDM2; MOV10L1; GATA2; ZNF28; ARID3A; SOCS4; TAF3; ZNF441; NOTCH3; RPAP2; NOTCH1; TP73; PIDD1; ZNF195; ZNF468; ZNF425; ZNF561; ZNF274; ZNF750; ZNF596; ZNF563; NR0B1; GLS2; ZNF506	
26	TP53 Regulates Transcription of Genes Involved in Cytochrome C Release	20	8.15E-04	4.05E-02	*BBC3; TP53INP1; TP73; BAX; TRIAP1*	Reactome
27	TP53 Regulates Transcription of Death Receptors and Ligands	12	8.57E-04	4.10E-02	*TNFRSF10C; FAS; TP73; TNFRSF10B*	Reactome
28	cell cycle: g2/m checkpoint	21	1.04E-03	4.71E-02	*GADD45A; MDM2; RASGRF1; CDKN1A; MYT1*	BioCarta
29	Activation of TRKA receptors	6	1.06E-03	4.71E-02	*ADORA2A; NGF; NTRK1*	Reactome
30	Antiarrhythmic Pathway, Pharmacodynamics	55	1.17E-03	5.00E-02	*CACNA1H; KCNH2; HCN2; ADRB2; SLC8A3; SCN4B; GJD3; SCN3B*	PharmGKB
31	Transcriptional cascade regulating adipogenesis	13	1.20E-03	5.00E-02	*EGR2; DDIT3; GATA2; KLF15*	Wikipathways
32	hypoxia and p53 in the cardiovascular system	22	1.30E-03	5.09E-02	*GADD45A; CDKN1A; MDM2; BAX; HIC1*	BioCarta
33	Nuclear Receptors Meta-Pathway	316	1.30E-03	5.09E-02	*SLC6A4; CPEB4; S100P; BAX; CYP4F12; PPARGC1A; HBEGF; SLC6A13; NFKB2; SQSTM1; JUND; AHRR; CES3; CES2; SNAI2; SERPINB2; IP6K3; ARL5B; CYP1A1; IL11; HMOX1; TNFAIP3; GGT1; PLTP*	Wikipathways
34	Collagen chain trimerization	44	1.38E-03	5.22E-02	*COL15A1; COL7A1; COL9A2; COL9A3; COL5A3; COL2A1; COL20A1*	Reactome
35	MAPK Signaling Pathway	246	1.44E-03	5.22E-02	*CACNA1H; TGFBR1; DUSP16; MAPK8IP2; HSPA6; PPM1A; GADD45A; NGF; JUND; MAP3K12; DDIT3; DUSP8; FAS; PLA2G4C; RELB; NFKB2; FLNC; NTRK1; FGF1; RASGRF1*	Wikipathways
36	TRKA activation by NGF	2	1.50E-03	5.22E-02	*NGF; NTRK1*	Reactome
37	NFG and proNGF binds to p75NTR	2	1.50E-03	5.22E-02	*NGF; NGFR*	Reactome
38	RANKL	23	1.61E-03	5.46E-02	*SQSTM1; NFKB2; TREM2; CYLD; TRAF1*	NetPath
39	ATF-2 transcription factor network	60	2.08E-03	6.88E-02	*DDIT3; GADD45A; JUND; PPARGC1A; DUSP8; ACHE; SERPINB5; ATF3*	PID
40	Hippo signaling pathway - Homo sapiens (human)	154	2.46E-03	7.22E-02	*AREG; TGFBR1; SNAI2; PARD6G; RASSF1; SMAD7; ID2; TP73; WNT4; LATS2; WNT9A; APC2; BBC3; FGF1*	KEGG
41	Hematopoietic Stem Cell Differentiation	49	2.62E-03	7.22E-02	*RIOK3; LYL1; KCNH2; TPO; NOTCH1; KITLG; GATA2*	Wikipathways
42	Protein alkylation leading to liver fibrosis	50	2.95E-03	7.22E-02	*ACTA2; SMAD7; BAX; RELB; NFKB2; APAF1; MMP1*	Wikipathways
43	Inositol phosphate metabolism	50	2.95E-03	7.22E-02	*PLCB1; INPP1; INPP5D; INPP5J; ITPKC; PLCD1; IP6K3*	Reactome

44	Synthesis of IP3 and IP4 in the cytosol	27	3.39E-03	7.22E-02	*PLCB1; INPP5J; INPP5D; ITPKC; PLCD1*	Reactome
45	btg family proteins and cell cycle regulation	9	4.07E-03	7.22E-02	*HOXB9; BTG2; BTG1*	BioCarta
46	p75NTR regulates axonogenesis	10	4.07E-03	7.22E-02	*NGF; NGFR; LINGO1*	Reactome
47	Frs2-mediated activation	9	4.07E-03	7.22E-02	*NGF; NTRK1; FRS2*	Reactome
48	p75NTR recruits signalling complexes	9	4.07E-03	7.22E-02	*SQSTM1; NGF; NGFR*	Reactome
49	Thyroid hormone synthesis	9	4.07E-03	7.22E-02	*TPO; TG; DUOX1*	SMPDB
50	Oxidative Damage	40	4.09E-03	7.22E-02	*TRAF1; GADD45A; CDKN1A; NFKBIE; C5AR1; APAF1*	Wikipathways
51	PLC-gamma1 signalling	3	4.37E-03	7.22E-02	*NGF; NTRK1*	Reactome
52	Signalling to STAT3	3	4.37E-03	7.22E-02	*NGF; NTRK1*	Reactome
53	Ceramide signalling	3	4.37E-03	7.22E-02	*NGF; NGFR*	Reactome
54	Hydrolysis of LPE	3	4.37E-03	7.22E-02	*PLA2G4C; GPCPD1*	Reactome
55	regulation of cell cycle progression by plk3	18	4.41E-03	7.22E-02	*PLK3; APAF1; RASGRF1; BAX*	BioCarta
56	Breast cancer	147	4.64E-03	7.22E-02	*JAG2; E2F2; GADD45A; CDKN1A; NOTCH1; BAX; WNT4; DDB2; WNT9A; APC2; NFKB2; NOTCH3; FGF1*	KEGG
57	Bladder cancer	41	4.64E-03	7.22E-02	*E2F2; RASSF1; CDKN1A; HBEGF; MDM2; MMP1*	KEGG
58	Adipogenesis	131	4.84E-03	7.22E-02	*LIF; DDIT3; LPIN3; KLF15; EGR2; GADD45A; CDKN1A; ID3; PPARGC1A; FRZB; FAS; GATA2*	Wikipathways
59	ATM Signaling Pathway	19	5.41E-03	7.22E-02	*GADD45A; CDKN1A; TP73; PIDD1*	Wikipathways
60	Ketoprofen Action Pathway	30	5.45E-03	7.22E-02	*CYP4F3; CYP4F2; GGT1; ALOX12B; ALOX5*	SMPDB
61	Acetylsalicylic Acid Action Pathway	30	5.45E-03	7.22E-02	*CYP4F3; CYP4F2; GGT1; ALOX12B; ALOX5*	SMPDB
62	Diflunisal Action Pathway	30	5.45E-03	7.22E-02	*CYP4F3; CYP4F2; GGT1; ALOX12B; ALOX5*	SMPDB
63	Acetaminophen Action Pathway	30	5.45E-03	7.22E-02	*CYP4F3; CYP4F2; GGT1; ALOX12B; ALOX5*	SMPDB
64	Sulindac Action Pathway	30	5.45E-03	7.22E-02	*CYP4F3; CYP4F2; GGT1; ALOX12B; ALOX5*	SMPDB
65	Ketorolac Action Pathway	30	5.45E-03	7.22E-02	*CYP4F3; CYP4F2; GGT1; ALOX12B; ALOX5*	SMPDB
66	Naproxen Action Pathway	30	5.45E-03	7.22E-02	*CYP4F3; CYP4F2; GGT1; ALOX12B; ALOX5*	SMPDB
67	Flurbiprofen Action Pathway	30	5.45E-03	7.22E-02	*CYP4F3; CYP4F2; GGT1; ALOX12B; ALOX5*	SMPDB
68	Antrafenine Action Pathway	30	5.45E-03	7.22E-02	*CYP4F3; CYP4F2; GGT1; ALOX12B; ALOX5*	SMPDB
69	Trisalicylate-choline Action Pathway	30	5.45E-03	7.22E-02	*CYP4F3; CYP4F2; GGT1; ALOX12B; ALOX5*	SMPDB
70	Nepafenac Action Pathway	30	5.45E-03	7.22E-02	*CYP4F3; CYP4F2; GGT1; ALOX12B; ALOX5*	SMPDB
71	Phenylbutazone Action Pathway	30	5.45E-03	7.22E-02	*CYP4F3; CYP4F2; GGT1; ALOX12B; ALOX5*	SMPDB
72	Lornoxicam Action Pathway	30	5.45E-03	7.22E-02	*CYP4F3; CYP4F2; GGT1; ALOX12B; ALOX5*	SMPDB

73	Salsalate Action Pathway	30	5.45E-03	7.22E-02	*CYP4F3; CYP4F2; GGT1; ALOX12B; ALOX5*	SMPDB
74	Salicylic Acid Action Pathway	30	5.45E-03	7.22E-02	*CYP4F3; CYP4F2; GGT1; ALOX12B; ALOX5*	SMPDB
75	Salicylate-sodium Action Pathway	30	5.45E-03	7.22E-02	*CYP4F3; CYP4F2; GGT1; ALOX12B; ALOX5*	SMPDB
76	Oxaprozin Action Pathway	30	5.45E-03	7.22E-02	*CYP4F3; CYP4F2; GGT1; ALOX12B; ALOX5*	SMPDB
77	Nabumetone Action Pathway	30	5.45E-03	7.22E-02	*CYP4F3; CYP4F2; GGT1; ALOX12B; ALOX5*	SMPDB
78	Bromfenac Action Pathway	30	5.45E-03	7.22E-02	*CYP4F3; CYP4F2; GGT1; ALOX12B; ALOX5*	SMPDB
79	Mefenamic Acid Action Pathway	30	5.45E-03	7.22E-02	*CYP4F3; CYP4F2; GGT1; ALOX12B; ALOX5*	SMPDB
80	Piroxicam Action Pathway	30	5.45E-03	7.22E-02	*CYP4F3; CYP4F2; GGT1; ALOX12B; ALOX5*	SMPDB
81	Carprofen Action Pathway	30	5.45E-03	7.22E-02	*CYP4F3; CYP4F2; GGT1; ALOX12B; ALOX5*	SMPDB
82	Fenoprofen Action Pathway	30	5.45E-03	7.22E-02	*CYP4F3; CYP4F2; GGT1; ALOX12B; ALOX5*	SMPDB
83	Antipyrine Action Pathway	30	5.45E-03	7.22E-02	*CYP4F3; CYP4F2; GGT1; ALOX12B; ALOX5*	SMPDB
84	Magnesium salicylate Action Pathway	30	5.45E-03	7.22E-02	*CYP4F3; CYP4F2; GGT1; ALOX12B; ALOX5*	SMPDB
85	Tenoxicam Action Pathway	30	5.45E-03	7.22E-02	*CYP4F3; CYP4F2; GGT1; ALOX12B; ALOX5*	SMPDB
86	Tiaprofenic Acid Action Pathway	30	5.45E-03	7.22E-02	*CYP4F3; CYP4F2; GGT1; ALOX12B; ALOX5*	SMPDB
87	Tolmetin Action Pathway	30	5.45E-03	7.22E-02	*CYP4F3; CYP4F2; GGT1; ALOX12B; ALOX5*	SMPDB
88	Suprofen Action Pathway	30	5.45E-03	7.22E-02	*CYP4F3; CYP4F2; GGT1; ALOX12B; ALOX5*	SMPDB
89	Etodolac Action Pathway	30	5.45E-03	7.22E-02	*CYP4F3; CYP4F2; GGT1; ALOX12B; ALOX5*	SMPDB
90	Rofecoxib Action Pathway	30	5.45E-03	7.22E-02	*CYP4F3; CYP4F2; GGT1; ALOX12B; ALOX5*	SMPDB
91	Diclofenac Action Pathway	30	5.45E-03	7.22E-02	*CYP4F3; CYP4F2; GGT1; ALOX12B; ALOX5*	SMPDB
92	Etoricoxib Action Pathway	30	5.45E-03	7.22E-02	*CYP4F3; CYP4F2; GGT1; ALOX12B; ALOX5*	SMPDB
93	Lumiracoxib Action Pathway	30	5.45E-03	7.22E-02	*CYP4F3; CYP4F2; GGT1; ALOX12B; ALOX5*	SMPDB
94	Valdecoxib Action Pathway	30	5.45E-03	7.22E-02	*CYP4F3; CYP4F2; GGT1; ALOX12B; ALOX5*	SMPDB
95	Meloxicam Action Pathway	30	5.45E-03	7.22E-02	*CYP4F3; CYP4F2; GGT1; ALOX12B; ALOX5*	SMPDB
96	Leukotriene C4 Synthesis Deficiency	30	5.45E-03	7.22E-02	*CYP4F3; CYP4F2; GGT1; ALOX12B; ALOX5*	SMPDB
97	Arachidonic Acid Metabolism	30	5.45E-03	7.22E-02	*CYP4F3; CYP4F2; GGT1; ALOX12B; ALOX5*	SMPDB
98	p75(NTR)-mediated signaling	71	5.48E-03	7.22E-02	*SQSTM1; NGF; LINGO1; NTRK1; NGFR; ZNF274; APAF1; MMP1*	PID
99	HDL remodeling	10	5.65E-03	7.29E-02	*LCAT; PLTP; ALB*	Reactome
100	Activation of PPARGC1A (PGC-1alpha) by phosphorylation	10	5.65E-03	7.29E-02	*PRKAB2; PPARGC1A; PRKAB1*	Reactome
101	Colorectal cancer	86	5.94E-03	7.56E-02	*AREG; TGFBR1; RALGDS; GADD45A; CDKN1A; BAX; DDB2; APC2; BBC3*	KEGG
102	Glucocorticoid Receptor Pathway	71	5.97E-03	7.56E-02	*CPEB4; MGAM; S100P; TNFAIP3; IL11; SNAI2; NFKB2; ARL5B*	Wikipathways

103	EGF-Ncore	57	6.19E-03	7.76E-02	*INPP5D; SMAD7; DUSP8; KSR1; MDM2; DUSP16; MAPK8IP2*	Signalink
104	Indomethacin Action Pathway	31	6.29E-03	7.82E-02	*CYP4F3; CYP4F2; GGT1; ALOX12B; ALOX5*	SMPDB
105	Hypertrophy Model	20	6.56E-03	8.00E-02	*HBEGF; JUND; ATF3; NR4A3*	Wikipathways
106	superpathway of D-inositol (1,4,5)-trisphosphate metabolism	20	6.56E-03	8.00E-02	*INPP5J; INPP1; INPP5D; ITPKC*	HumanCyc
107	White fat cell differentiation	32	7.23E-03	8.72E-02	*EGR2; DDIT3; GATA2; ZNF423; KLF15*	Wikipathways
108	Preimplantation Embryo	59	7.47E-03	8.78E-02	*DDIT3; AQP3; CELF3; DNMT3L; ZSCAN4; GATA2; MXD1*	Wikipathways
109	Taurine and hypotaurine metabolism	11	7.54E-03	8.78E-02	*GGT1; GGT6; GAD1*	KEGG
110	NOTCH-Core	11	7.54E-03	8.78E-02	*JAG2; NOTCH1; NOTCH3*	Signalink
111	Prolonged ERK activation events	11	7.54E-03	8.78E-02	*NGF; NTRK1; FRS2*	Reactome
112	p53-Dependent G1 DNA Damage Response	21	7.86E-03	8.99E-02	*MDM2; ZNF385A; CDKN1A; PCBP4*	Reactome
113	p53-Dependent G1/S DNA damage checkpoint	21	7.86E-03	8.99E-02	*MDM2; ZNF385A; CDKN1A; PCBP4*	Reactome
114	Aryl Hydrocarbon Receptor Pathway	46	8.22E-03	9.17E-02	*CYP1A1; JUND; BAX; AHRR; CES3; SERPINB2*	Wikipathways
115	E2F transcription factor network	75	8.28E-03	9.17E-02	*E2F7; HIC1; CDKN1A; TP73; CES3; CES2; APAF1; E2F2*	PID
116	Phase I - Functionalization of compounds	109	8.46E-03	9.17E-02	*CYP1A1; CYP11A1; CYP4F12; AHRR; AOC2; CES3; CES2; FDXR; CYP4F2; CYP4F3*	Reactome
117	Regulation of TP53 Expression and Degradation	4	8.52E-03	9.17E-02	*MDM2; PRDM1*	Wikipathways
118	NGF processing	4	8.52E-03	9.17E-02	*NGF; PCSK5*	Reactome
119	Expression and Processing of Neurotrophins	4	8.52E-03	9.17E-02	*NGF; PCSK5*	Reactome
120	Axonal growth stimulation	4	8.52E-03	9.17E-02	*NGF; NGFR*	Reactome
121	Arachidonic acid metabolism	62	8.95E-03	9.56E-02	*CYP1A1; ALOXE3; ALOX5; GGT1; CYP4F2; CYP4F3; ALOX12B*	Reactome
122	Nucleotide-binding domain, leucine rich repeat containing receptor (NLR) signaling pathways	47	9.12E-03	9.66E-02	*NLRP1; TAB3; TNFAIP3; CYLD; IRAK2; P2RX7*	Reactome
123	Synthesis of Leukotrienes (LT) and Eoxins (EX)	23	9.32E-03	9.79E-02	*ALOX5; CYP4F3; CYP4F2; GGT1*	Reactome
124	Eicosanoids	12	9.77E-03	9.98E-02	*CYP4F12; CYP4F2; CYP4F3*	Reactome
125	TP53 Regulates Transcription of Caspase Activators and Caspases	12	9.77E-03	9.98E-02	*APAF1; TP73; PIDD1*	Reactome
126	Small cell lung cancer	93	9.81E-03	9.98E-02	*TRAF1; TRAF4; E2F2; GADD45A; CDKN1A; BAX; DDB2; LAMC3; APAF1*	KEGG

127	TNF alpha Signaling Pathway	93	9.81E-03	9.98E-02	*TRAF1; TBK1; TAB3; BAX; NFKBIE; TNFAIP3; KSR1; NFKB2; APAF1*	Wikipathways
	Up-regulated by O_3 oxidation products only					
1	Constitutive Signaling by NOTCH1 PEST Domain Mutants	54	1.30E-03	3.58E-02	*NEURL1B; NEURL1; HDAC10*	Reactome
2	Signaling by NOTCH1 PEST Domain Mutants in Cancer	54	1.30E-03	3.58E-02	*NEURL1B; NEURL1; HDAC10*	Reactome
3	Constitutive Signaling by NOTCH1 HD+PEST Domain Mutants	54	1.30E-03	3.58E-02	*NEURL1B; NEURL1; HDAC10*	Reactome
4	Signaling by NOTCH1 HD+PEST Domain Mutants in Cancer	54	1.30E-03	3.58E-02	*NEURL1B; NEURL1; HDAC10*	Reactome
5	Signaling by NOTCH1 in Cancer	54	1.30E-03	3.58E-02	*NEURL1B; NEURL1; HDAC10*	Reactome
6	Constitutive Signaling by NOTCH1 HD Domain Mutants	15	1.60E-03	3.58E-02	*NEURL1B; NEURL1*	Reactome
7	Signaling by NOTCH1 HD Domain Mutants in Cancer	15	1.60E-03	3.58E-02	*NEURL1B; NEURL1*	Reactome
8	Signaling by NOTCH1	74	3.09E-03	5.43E-02	*NEURL1B; NEURL1; HDAC10*	Reactome
9	NOTCH2 Activation and Transmission of Signal to the Nucleus	22	3.45E-03	5.43E-02	*NEURL1B; NEURL1*	Reactome
10	Signaling by NTRK1 (TRKA)	76	3.46E-03	5.43E-02	*RPS6KA1; ADCYAP1R1; SHC2*	Reactome
11	NOTCH3 Activation and Transmission of Signal to the Nucleus	25	4.44E-03	5.92E-02	*NEURL1B; NEURL1*	Reactome
12	ErbB signaling pathway	85	4.74E-03	5.92E-02	*SHC4; BUB1B-PAK6; SHC2*	KEGG
13	Signaling by NTRKs	89	5.39E-03	5.92E-02	*RPS6KA1; ADCYAP1R1; SHC2*	Reactome
14	Alcoholism	180	5.75E-03	5.92E-02	*SHC4; HDAC10; CREB5; SHC2*	KEGG
15	ErbB Signaling Pathway	92	5.91E-03	5.92E-02	*SHC4; BUB1B-PAK6; SHC2*	Wikipathways
16	Ras Signaling	184	6.21E-03	5.92E-02	*SHC4; BUB1B-PAK6; FGFR3; SHC2*	Wikipathways
17	Class B/2 (Secretin family receptors)	96	6.46E-03	5.92E-02	*PTCH2; ADCYAP1R1; WNT11*	Reactome
18	Activated NOTCH1 Transmits Signal to the Nucleus	32	6.78E-03	5.92E-02	*NEURL1B; NEURL1*	Reactome
19	Signaling by NOTCH2	33	7.66E-03	6.17E-02	*NEURL1B; NEURL1*	Reactome

20	Stimuli-sensing channels	102	7.86E-03	6.17E-02	*BEST1; WNK4; TTYH3*	Reactome
21	TNF signaling pathway	110	9.66E-03	7.22E-02	*PTGS2; CREB5; IFNB1*	KEGG
	Up-regulated by OH oxidation products only					
1	SHC-mediated cascade:FGFR3	18	3.16E-03	7.78E-02	*HRAS; FGF2*	Reactome
2	Genes targeted by miRNAs in adipocytes	18	3.16E-03	7.78E-02	*PTBP2; KCNQ1*	Wikipathways
3	SHC-mediated cascade:FGFR4	20	3.90E-03	7.78E-02	*HRAS; FGF2*	Reactome
4	FRS-mediated FGFR3 signaling	20	3.90E-03	7.78E-02	*HRAS; FGF2*	Reactome
5	SHC-mediated cascade:FGFR1	21	4.30E-03	7.78E-02	*HRAS; FGF2*	Reactome
6	FRS-mediated FGFR4 signaling	22	4.71E-03	7.78E-02	*HRAS; FGF2*	Reactome
7	Signaling by FGFR3 point mutants in cancer	22	4.71E-03	7.78E-02	*HRAS; FGF2*	Reactome
8	Signaling by FGFR3 in disease	22	4.71E-03	7.78E-02	*HRAS; FGF2*	Reactome
9	SHC-mediated cascade:FGFR2	23	5.15E-03	7.78E-02	*HRAS; FGF2*	Reactome
10	FRS-mediated FGFR1 signaling	23	5.15E-03	7.78E-02	*HRAS; FGF2*	Reactome
11	FRS-mediated FGFR2 signaling	25	6.07E-03	7.78E-02	*HRAS; FGF2*	Reactome
12	Downstream signaling of activated FGFR3	25	6.07E-03	7.78E-02	*HRAS; FGF2*	Reactome
13	Downstream signaling of activated FGFR4	27	7.06E-03	7.78E-02	*HRAS; FGF2*	Reactome
14	Signaling by FGFR2 in disease	27	7.06E-03	7.78E-02	*HRAS; FGF2*	Reactome
15	Neuronal System	368	7.32E-03	7.78E-02	*KCNMB3; CACNB2; HRAS; MYO6; KCNQ1; DLGAP1*	Reactome
16	Phase 2 - plateau phase	28	7.58E-03	7.78E-02	*CACNB2; KCNQ1*	Reactome
17	TP53 Regulates Transcription of Cell Death Genes	29	8.11E-03	7.78E-02	*TNFRSF10A; PMAIP1*	Wikipathways
18	Downstream signaling of activated FGFR2	30	8.67E-03	7.78E-02	*HRAS; FGF2*	Reactome
19	Ovarian Infertility Genes	31	9.24E-03	7.78E-02	*GDF9; DMC1*	Wikipathways
20	Downstream signaling of activated FGFR1	31	9.24E-03	7.78E-02	*HRAS; FGF2*	Reactome

Table S3.4: List of the down-regulated pathways in BEAS-2B cells exposed to DMSe-derived SOA.

#	Pathway	Size	p-value	FDR-value	Members_input_overlap	source
Down-regulated by both O_3 and OH oxidation products						
1	Activation of gene expression by SREBF (SREBP)	26	7.15E-15	3.65E-12	*HMGCS1; SCD; IDI1; DHCR7; ELOVL6; SREBF1; FASN; LSS; HMGCR; CYP51A1; FDFT1; SQLE*	Reactome
2	Activation of gene expression by SREBF (SREBP)	20	7.81E-15	3.65E-12	*HMGCS1; SCD; IDI1; DHCR7; ELOVL6; FASN; LSS; HMGCR; CYP51A1; FDFT1; SQLE*	Wikipathways
3	Regulation of cholesterol biosynthesis by SREBP (SREBF)	31	9.64E-14	3.00E-11	*HMGCS1; SCD; IDI1; DHCR7; ELOVL6; SREBF1; FASN; LSS; HMGCR; CYP51A1; FDFT1; SQLE*	Reactome
4	Cholesterol Biosynthesis Pathway	15	8.10E-13	5.72E-11	*MSMO1; HMGCS1; IDI1; DHCR7; LSS; HMGCR; CYP51A1; FDFT1; SQLE*	Wikipathways
5	Pravastatin Action Pathway	22	1.65E-12	5.72E-11	*MSMO1; HMGCS1; IDI1; LSS; HMGCR; CYP51A1; LIPA; FDFT1; SQLE; DHCR24*	SMPDB
6	Atorvastatin Action Pathway	22	1.65E-12	5.72E-11	*MSMO1; HMGCS1; IDI1; LSS; HMGCR; CYP51A1; LIPA; FDFT1; SQLE; DHCR24*	SMPDB
7	Rosuvastatin Action Pathway	22	1.65E-12	5.72E-11	*MSMO1; HMGCS1; IDI1; LSS; HMGCR; CYP51A1; LIPA; FDFT1; SQLE; DHCR24*	SMPDB
8	Lovastatin Action Pathway	22	1.65E-12	5.72E-11	*MSMO1; HMGCS1; IDI1; LSS; HMGCR; CYP51A1; LIPA; FDFT1; SQLE; DHCR24*	SMPDB
9	Cerivastatin Action Pathway	22	1.65E-12	5.72E-11	*MSMO1; HMGCS1; IDI1; LSS; HMGCR; CYP51A1; LIPA; FDFT1; SQLE; DHCR24*	SMPDB
10	Fluvastatin Action Pathway	22	1.65E-12	5.72E-11	*MSMO1; HMGCS1; IDI1; LSS; HMGCR; CYP51A1; LIPA; FDFT1; SQLE; DHCR24*	SMPDB
11	Simvastatin Action Pathway	22	1.65E-12	5.72E-11	*MSMO1; HMGCS1; IDI1; LSS; HMGCR; CYP51A1; LIPA; FDFT1; SQLE; DHCR24*	SMPDB
12	Hyper-IgD syndrome	22	1.65E-12	5.72E-11	*MSMO1; HMGCS1; IDI1; LSS; HMGCR; CYP51A1; LIPA; FDFT1; SQLE; DHCR24*	SMPDB
13	Cholesteryl ester storage disease	22	1.65E-12	5.72E-11	*MSMO1; HMGCS1; IDI1; LSS; HMGCR; CYP51A1; LIPA; FDFT1; SQLE; DHCR24*	SMPDB
14	Lysosomal Acid Lipase Deficiency (Wolman Disease)	22	1.65E-12	5.72E-11	*MSMO1; HMGCS1; IDI1; LSS; HMGCR; CYP51A1; LIPA; FDFT1; SQLE; DHCR24*	SMPDB
15	Mevalonic aciduria	22	1.65E-12	5.72E-11	*MSMO1; HMGCS1; IDI1; LSS; HMGCR; CYP51A1; LIPA; FDFT1; SQLE; DHCR24*	SMPDB
16	Wolman disease	22	1.65E-12	5.72E-11	*MSMO1; HMGCS1; IDI1; LSS; HMGCR; CYP51A1; LIPA; FDFT1; SQLE; DHCR24*	SMPDB
17	Smith-Lemli-Opitz Syndrome (SLOS)	22	1.65E-12	5.72E-11	*MSMO1; HMGCS1; IDI1; LSS; HMGCR; CYP51A1; LIPA; FDFT1; SQLE; DHCR24*	SMPDB
18	Chondrodysplasia Punctata II, X Linked Dominant (CDPX2)	22	1.65E-12	5.72E-11	*MSMO1; HMGCS1; IDI1; LSS; HMGCR; CYP51A1; LIPA; FDFT1; SQLE; DHCR24*	SMPDB
19	CHILD Syndrome	22	1.65E-12	5.72E-11	*MSMO1; HMGCS1; IDI1; LSS; HMGCR; CYP51A1; LIPA; FDFT1; SQLE; DHCR24*	SMPDB

20	Desmosterolosis	22	1.65E-12	5.72E-11	*MSMO1; HMGCS1; IDI1; LSS; HMGCR; CYP51A1; LIPA; FDFT1; SQLE; DHCR24*	SMPDB
21	Hypercholesterolemia	22	1.65E-12	5.72E-11	*MSMO1; HMGCS1; IDI1; LSS; HMGCR; CYP51A1; LIPA; FDFT1; SQLE; DHCR24*	SMPDB
22	Steroid Biosynthesis	22	1.65E-12	5.72E-11	*MSMO1; HMGCS1; IDI1; LSS; HMGCR; CYP51A1; LIPA; FDFT1; SQLE; DHCR24*	SMPDB
23	Alendronate Action Pathway	22	1.65E-12	5.72E-11	*MSMO1; HMGCS1; IDI1; LSS; HMGCR; CYP51A1; LIPA; FDFT1; SQLE; DHCR24*	SMPDB
24	Risedronate Action Pathway	22	1.65E-12	5.72E-11	*MSMO1; HMGCS1; IDI1; LSS; HMGCR; CYP51A1; LIPA; FDFT1; SQLE; DHCR24*	SMPDB
25	Pamidronate Action Pathway	22	1.65E-12	5.72E-11	*MSMO1; HMGCS1; IDI1; LSS; HMGCR; CYP51A1; LIPA; FDFT1; SQLE; DHCR24*	SMPDB
26	Zoledronate Action Pathway	22	1.65E-12	5.72E-11	*MSMO1; HMGCS1; IDI1; LSS; HMGCR; CYP51A1; LIPA; FDFT1; SQLE; DHCR24*	SMPDB
27	Ibandronate Action Pathway	22	1.65E-12	5.72E-11	*MSMO1; HMGCS1; IDI1; LSS; HMGCR; CYP51A1; LIPA; FDFT1; SQLE; DHCR24*	SMPDB
28	superpathway of cholesterol biosynthesis	25	7.98E-12	2.57E-10	*MSMO1; HMGCS1; IDI1; DHCR7; LSS; HMGCR; CYP51A1; FDFT1; SQLE; DHCR24*	HumanCyc
29	Cholesterol biosynthesis	25	7.98E-12	2.57E-10	*MSMO1; HMGCS1; IDI1; DHCR7; LSS; HMGCR; CYP51A1; FDFT1; SQLE; DHCR24*	Reactome
30	Cori Cycle	16	1.16E-10	3.51E-09	*HK1; SLC2A4; GPI; G6PD; GAPDH; PGAM1; LDHA; PGK1*	Wikipathways
31	Glycolysis Pathway D (2)	23	1.17E-10	3.51E-09	*HK2; HK1; GAPDH; ENO1; PGAM1; ALDOA; ALDOC; LDHA; PGK1*	Wikipathways
32	Metabolic reprogramming in colon cancer	42	1.40E-10	4.09E-09	*GPI; ENO1; SLC16A3; G6PD; GAPDH; PAICS; FASN; PGAM1; ACLY; LDHA; PGK1*	Wikipathways
33	glycolysis	25	1.84E-10	5.19E-09	*GPI; HK2; HK1; GAPDH; ENO1; PGAM1; ALDOA; ALDOC; PGK1*	HumanCyc
34	Sterol Regulatory Element-Binding Proteins (SREBP) signalling	68	2.07E-10	5.68E-09	*HMGCS1; SCD; IDI1; CYP51A1; LDLR; SREBF1; FASN; LSS; HMGCR; INSIG1; ACLY; FDFT1; SQLE*	Wikipathways
35	Glycolysis and Gluconeogenesis	45	3.17E-10	8.46E-09	*HK1; GPI; HK2; SLC2A4; GAPDH; ENO1; PGAM1; ALDOA; ALDOC; LDHA; PGK1*	Wikipathways
36	Steroid biosynthesis	19	6.47E-10	1.68E-08	*MSMO1; LIPA; DHCR7; LSS; CYP51A1; FDFT1; SQLE; DHCR24*	KEGG
37	cholesterol biosynthesis I	13	9.06E-10	2.17E-08	*MSMO1; DHCR7; LSS; CYP51A1; FDFT1; SQLE; DHCR24*	HumanCyc
38	cholesterol biosynthesis II (via 24,25-dihydrolanosterol)	13	9.06E-10	2.17E-08	*MSMO1; DHCR7; LSS; CYP51A1; FDFT1; SQLE; DHCR24*	HumanCyc
39	cholesterol biosynthesis III (via desmosterol)	13	9.06E-10	2.17E-08	*MSMO1; DHCR7; LSS; CYP51A1; FDFT1; SQLE; DHCR24*	HumanCyc
40	Cholesterol biosynthesis, regulation and transport	9	2.64E-09	6.16E-08	*HMGCS1; IDI1; DHCR7; LSS; FDFT1; SQLE*	Wikipathways
41	Pathways in clear cell renal cell carcinoma	86	4.30E-09	9.81E-08	*PDGFB; GPI; HK2; HK1; GAPDH; ENO1; PLOD2; FASN; ALDOA; ACLY; ALDOC; LDHA; PGK1*	Wikipathways
42	Glycolysis Gluconeogenesis	46	5.67E-09	1.26E-07	*GPI; HK2; HK1; GAPDH; ENO1; PGAM1; ALDOA; ALDOC; LDHA; PGK1*	INOH
43	Glycolysis / Gluconeogenesis - Homo sapiens (human)	68	3.32E-08	7.21E-07	*GPI; HK2; ACSS2; HK1; GAPDH; ENO1; PGAM1; ALDOA; ALDOC; LDHA; PGK1*	KEGG
44	FOXM1 transcription factor network	42	4.71E-08	1.00E-06	*CCNB1; LAMA4; PLK1; CENPF; CENPA; CCND1; GAS1; MYC; MMP2*	PID

45	Metabolism of steroids	127	6.90E-08	1.43E-06	*MSMO1; HMGCS1; SCD; IDI1; DHCR7; ELOVL6; SREBF1; FASN; LSS; HMGCR; CYP51A1; FDFT1; SQLE; DHCR24*	Reactome
46	superpathway of conversion of glucose to acetyl CoA and entry into the TCA cycle	48	1.33E-07	2.70E-06	*GPI; HK2; HK1; GAPDH; ENO1; PGAM1; ALDOA; ALDOC; PGK1*	HumanCyc
47	Glycolysis	15	1.43E-07	2.73E-06	*GPI; HK2; GAPDH; ENO1; PGAM1; ALDOA*	SMPDB
48	Glycogenosis, Type VII. Tarui disease	15	1.43E-07	2.73E-06	*GPI; HK2; GAPDH; ENO1; PGAM1; ALDOA*	SMPDB
49	Fanconi-bickel syndrome	15	1.43E-07	2.73E-06	*GPI; HK2; GAPDH; ENO1; PGAM1; ALDOA*	SMPDB
50	gluconeogenesis	26	2.11E-07	3.94E-06	*GPI; GAPDH; ENO1; PGAM1; ALDOA; ALDOC; PGK1*	HumanCyc
51	Steroids metabolism	16	2.26E-07	4.14E-06	*IDI1; DHCR7; LSS; HMGCR; FDFT1; SQLE*	INOH
52	Extracellular matrix organization	294	3.84E-07	6.90E-06	*PDGFB; ITGB5; ITGB4; FN1; ITGB6; EFEMP1; NID2; SPARC; COL8A1; THBS1; ITGA5; LAMB1; LOXL2; PLOD2; ADAM15; LAMC2; LAMA4; LOX; MMP2; LAMA5*	Reactome
53	Glycolysis	71	4.75E-07	8.36E-06	*GPI; HK2; HK1; GAPDH; ENO1; PGP; PGAM1; ALDOA; ALDOC; PGK1*	Reactome
54	SREBF and miR33 in cholesterol and lipid homeostasis	18	5.08E-07	8.79E-06	*HMGCS1; SCD; LDLR; SREBF1; FASN; HMGCR*	Wikipathways
55	Non-integrin membrane-ECM interactions	42	7.06E-07	1.20E-05	*PDGFB; LAMA4; ITGB4; THBS1; LAMB1; LAMC2; ITGB5; LAMA5*	Reactome
56	Gluconeogenesis	22	1.92E-06	2.85E-05	*GPI; HK2; GAPDH; ENO1; PGAM1; ALDOA*	SMPDB
57	Glycogenosis, Type IA. Von gierke disease	22	1.92E-06	2.85E-05	*GPI; HK2; GAPDH; ENO1; PGAM1; ALDOA*	SMPDB
58	Glycogenosis, Type IC	22	1.92E-06	2.85E-05	*GPI; HK2; GAPDH; ENO1; PGAM1; ALDOA*	SMPDB
59	Glycogen Storage Disease Type 1A (GSD1A) or Von Gierke Disease	22	1.92E-06	2.85E-05	*GPI; HK2; GAPDH; ENO1; PGAM1; ALDOA*	SMPDB
60	Triosephosphate isomerase	22	1.92E-06	2.85E-05	*GPI; HK2; GAPDH; ENO1; PGAM1; ALDOA*	SMPDB
61	Fructose-1,6-diphosphatase deficiency	22	1.92E-06	2.85E-05	*GPI; HK2; GAPDH; ENO1; PGAM1; ALDOA*	SMPDB
62	Phosphoenolpyruvate carboxykinase deficiency 1 (PEPCK1)	22	1.92E-06	2.85E-05	*GPI; HK2; GAPDH; ENO1; PGAM1; ALDOA*	SMPDB
63	Glycogenosis, Type IB	22	1.92E-06	2.85E-05	*GPI; HK2; GAPDH; ENO1; PGAM1; ALDOA*	SMPDB
64	Gluconeogenesis	35	2.05E-06	3.00E-05	*GPI; GAPDH; ENO1; PGAM1; ALDOA; ALDOC; PGK1*	Reactome
65	ECM-receptor interaction - Homo sapiens (human)	82	2.12E-06	3.04E-05	*LAMA4; LAMA5; FN1; ITGB6; ITGA5; THBS1; LAMC2; LAMB1; ITGB5; ITGB4*	KEGG
66	Focal Adhesion-PI3K-Akt-mTOR-signaling pathway	302	2.44E-06	3.46E-05	*IL7R; PDGFB; LPAR1; DDIT4; ITGB4; FN1; ITGB6; LAMA4; SLC2A4; ITGA5; HSP90B1; IRS1; GYS1; LAMC2; SREBF1; LAMB1; ITGB5; THBS1; LAMA5*	Wikipathways
67	Laminin interactions	23	2.56E-06	3.57E-05	*LAMA4; LAMA5; LAMB1; NID2; LAMC2; ITGB4*	Reactome
68	Beta1 integrin cell surface interactions	66	2.68E-06	3.63E-05	*TGM2; LAMA4; LAMA5; FN1; ITGA5; THBS1; LAMB1; CD14; LAMC2*	PID
69	HIF-1-alpha transcription factor network	66	2.68E-06	3.63E-05	*EGLN3; CA9; HK2; HK1; ENO1; ALDOA; BNIP3; LDHA; PGK1*	PID
70	PI3K-Akt Signaling Pathway	340	3.52E-06	4.70E-05	*IL7R; PDGFB; DDIT4; ITGB4; FN1; IRS1; CCND1; ITGB6; ITGA5; HSP90B1; THBS1; GYS1; LAMC2; LAMA4; TLR4; LAMB1; ITGB5; MYC; LPAR1; LAMA5*	Wikipathways

71	Nuclear Receptors Meta-Pathway	316	4.74E-06	6.24E-05	*CCL2; TGFBR2; PDGFB; ANGPTL4; SCNN1A; SERPINA1; CCND1; SCD; SLC2A4; SLC39A10; PRDX1; NAV3; SREBF1; FASN; FGFBP1; MYC; TNS4; G6PD; DNER*	Wikipathways
72	Glucose metabolism	91	4.99E-06	6.47E-05	*GPI; HK2; HK1; GAPDH; ENO1; PGP; PGAM1; ALDOA; ALDOC; PGK1*	Reactome
73	Pathogenic Escherichia coli infection	55	5.95E-06	7.61E-05	*ACTG1; TUBA1C; TUBB4B; TUBA1A; CD14; NCL; TLR4; ACTB*	KEGG
74	PI3K-Akt signaling pathway	354	6.47E-06	8.17E-05	*IL7R; PDGFB; DDIT4; ITGB4; FN1; ITGB6; CCND1; IRS1; HSP90B1; THBS1; GYS1; ITGA5; LAMA5; TLR4; LAMB1; ITGB5; MYC; LPAR1; LAMC2; LAMA4*	KEGG
75	Pathogenic Escherichia coli infection	56	6.83E-06	8.51E-05	*ACTG1; TUBA1C; TUBB4B; TUBA1A; CD14; NCL; TLR4; ACTB*	Wikipathways
76	Beta3 integrin cell surface interactions	44	1.25E-05	1.54E-04	*TGFBR2; PDGFB; LAMA4; FN1; THBS1; LAMB1; THY1*	PID
77	Fructose Mannose metabolism	30	1.36E-05	1.64E-04	*GPI; HK2; HK1; MPI; ALDOA; ALDOC*	INOH
78	Focal Adhesion	198	1.46E-05	1.73E-04	*PDGFB; ITGB5; ITGB4; FN1; ITGB6; CCND1; ITGA5; THBS1; LAMB1; LAMC2; LAMA4; ACTB; ACTG1; LAMA5*	Wikipathways
79	a6b1 and a6b4 Integrin signaling	45	1.46E-05	1.73E-04	*PMP22; LAMA4; LAMA5; LAMB1; LAMC2; CD9; ITGB4*	PID
80	Focal adhesion - Homo sapiens (human)	199	1.55E-05	1.80E-04	*PDGFB; ITGB5; ITGB4; FN1; ITGB6; CCND1; ITGA5; THBS1; LAMC2; LAMB1; LAMA4; ACTB; ACTG1; LAMA5*	KEGG
81	prion pathway	19	1.75E-05	2.02E-04	*LAMC2; LAMB1; LAMA4; LAMA5; HSPA5*	BioCarta
82	Platelet degranulation	129	2.19E-05	2.49E-04	*SERPINA1; PDGFB; FN1; HSPA5; TMSB4X; THBS1; LGALS3BP; SPARC; ALDOA; PCDH7; CD9*	Reactome
83	Vitamin D Receptor Pathway	184	2.98E-05	3.36E-04	*CA9; SFRP1; G6PD; CCND1; SLC2A4; PTHLH; ID1; CD14; S100A9; SLC8A1; MYC; CD9; DNER*	Wikipathways
84	Alpha6 beta4 integrin-ligand interactions	11	3.12E-05	3.43E-04	*LAMC2; LAMB1; LAMA5; ITGB4*	PID
85	Response to elevated platelet cytosolic Ca2+	134	3.12E-05	3.43E-04	*SERPINA1; PDGFB; FN1; HSPA5; TMSB4X; PCDH7; LGALS3BP; SPARC; ALDOA; THBS1; CD9*	Reactome
86	miR-targeted genes in muscle cell - TarBase	400	3.96E-05	4.30E-04	*SLC38A5; TGFBR2; CTSC; ITGB4; GJA1; CCND1; G6PD; IRS1; C1QBP; THBS1; PLK1; SPARC; NCL; ANPEP; ARHGDIA; LAMC2; CYP51A1; IPO4; FADS2; NRP1*	Wikipathways
87	Arrhythmogenic right ventricular cardiomyopathy (ARVC)	72	4.49E-05	4.82E-04	*GJA1; ITGB5; ACTG1; ITGB6; ITGA5; SLC8A1; ACTB; ITGB4*	KEGG
88	Squalene and cholesterol biosynthesis	37	4.77E-05	5.07E-04	*MSMO1; IDI1; DHCR7; HMGCR; FDFT1; SQLE*	EHMN
89	Amoebiasis	96	5.41E-05	5.68E-04	*LAMA4; LAMA5; FN1; LAMC2; CD14; TLR4; LAMB1; SERPINB3; SERPINB4*	KEGG
90	Arrhythmogenic Right Ventricular Cardiomyopathy	74	5.48E-05	5.69E-04	*GJA1; ITGB5; ACTG1; ITGB6; ITGA5; SLC8A1; ACTB; ITGB4*	Wikipathways
91	Mitotic G2-G2-M phases	5	5.69E-05	5.77E-04	*PLK1; CENPF; CCNB1*	Wikipathways
92	Pentose Phosphate Pathway (Erythrocyte)	5	5.69E-05	5.77E-04	*HK1; GPI; G6PD*	PharmGKB
93	Interleukin-4 and Interleukin-13 signaling	97	6.37E-05	6.40E-04	*ANXA1; CCL2; LAMA5; FN1; CCND1; HSPA8; VIM; MYC; MMP2*	Wikipathways
94	Mammary gland development pathway - Puberty (Stage 2 of 4)	13	6.56E-05	6.52E-04	*CCND1; MYC; FN1; VIM*	Wikipathways

95	Proteoglycans in cancer	201	7.45E-05	7.33E-04	*TFAP4; FZD2; ITGB5; ACTG1; FN1; CCND1; ITGA5; THBS1; MSN; TLR4; MYC; MMP2; ACTB*	KEGG
96	HIF-1 signaling pathway	100	8.10E-05	7.88E-04	*EGLN3; HK2; HK1; GAPDH; ENO1; TLR4; ALDOA; LDHA; PGK1*	KEGG
97	p73 transcription factor network	79	8.78E-05	8.45E-04	*TP63; CCNB1; BUB1; SERPINA1; PLK1; TUBA1A; FASN; MYC*	PID
98	TGF-B Signaling in Thyroid Cells for Epithelial-Mesenchymal Transition	14	9.05E-05	8.54E-04	*CDH6; VIM; FN1; ID1*	Wikipathways
99	fig-met-1-last-solution	14	9.05E-05	8.54E-04	*HK1; G6PD; FASN; LDHA*	Wikipathways
100	MET promotes cell motility	27	1.08E-04	1.01E-03	*LAMC2; LAMB1; LAMA4; LAMA5; TNS4*	Reactome
101	Demo complete	6	1.12E-04	1.03E-03	*FDFT1; SQLE; HMGCR*	Wikipathways
102	Phosphorylation of Emi1	6	1.12E-04	1.03E-03	*PLK1; CCNB1; CDC20*	Reactome
103	PLK1 signaling events	44	1.30E-04	1.18E-03	*CCNB1; BUB1; PLK1; CENPE; CDC20; AURKA*	PID
104	Warburg Effect	45	1.48E-04	1.33E-03	*GPI; HK2; G6PD; GAPDH; ENO1; PGK1*	SMPDB
105	Central carbon metabolism in cancer	65	1.65E-04	1.47E-03	*G6PD; HK2; SLC16A3; HK1; PGAM1; MYC; LDHA*	KEGG
106	srebp control of lipid synthesis	7	1.94E-04	1.69E-03	*HMGCS1; LDLR; SREBF1*	BioCarta
107	Activation of NIMA Kinases NEK9, NEK6, NEK7	7	1.94E-04	1.69E-03	*PLK1; NEK6; CCNB1*	Reactome
108	Bisphosphonate Pathway, Pharmacodynamics	17	2.06E-04	1.78E-03	*HMGCS1; FDFT1; SQLE; HMGCR*	PharmGKB
109	AMP-activated Protein Kinase (AMPK) Signaling	68	2.20E-04	1.88E-03	*CCNB1; SLC2A4; GYS1; CAMKK1; SREBF1; FASN; HMGCR*	Wikipathways
110	EGFR1	457	2.29E-04	1.94E-03	*SLITRK6; GJA1; CAVIN1; ANXA2; ALDOA; ITGB4; LDHA; KRT6A; VIM; ENO1; LDLR; KRT7; MYC; KRT5; PGAM1; ANXA1; SERPINB3; TNS4; ACTB; GSN*	NetPath
111	MET activates PTK2 signaling	18	2.61E-04	2.20E-03	*LAMC2; LAMB1; LAMA4; LAMA5*	Reactome
112	Small cell lung cancer	93	2.76E-04	2.30E-03	*LAMA4; LAMA5; FN1; CCND1; CKS2; LAMC2; LAMB1; MYC*	KEGG
113	Glucocorticoid Receptor Pathway	71	2.88E-04	2.34E-03	*CCL2; FGFBP1; NAV3; ANGPTL4; SCNN1A; TNS4; DNER*	Wikipathways
114	Fructose and mannose metabolism	33	2.91E-04	2.34E-03	*HK2; ALDOA; ALDOC; HK1; MPI*	KEGG
115	Alpha 6 Beta 4 signaling pathway	33	2.91E-04	2.34E-03	*LAMB1; LAMC2; LAMA5; IRS1; ITGB4*	Wikipathways
116	Inflammatory Response Pathway	33	2.91E-04	2.34E-03	*LAMB1; LAMC2; LAMA5; FN1; THBS1*	Wikipathways
117	epoxysqualene biosynthesis	2	3.26E-04	2.56E-03	*FDFT1; SQLE*	HumanCyc
118	Proprotein convertase subtilisin-kexin type 9 (PCSK9) mediated LDL receptor degradation	2	3.26E-04	2.56E-03	*LDLR; PCSK9*	Wikipathways
119	Evolocumab Mechanism	2	3.26E-04	2.56E-03	*LDLR; PCSK9*	Wikipathways
120	Smooth Muscle Contraction	35	3.87E-04	3.01E-03	*ANXA1; ANXA2; ITGB5; DYSF; ANXA6*	Reactome
121	Phagosome	152	4.18E-04	3.23E-03	*ITGB5; ACTG1; TUBA1C; TUBB4B; TUBA1A; ITGA5; THBS1; CD14; TLR4; ACTB*	KEGG

122	Regulation of Insulin-like Growth Factor (IGF) transport and uptake by Insulin-like Growth Factor Binding Proteins (IGFBPs)	127	4.67E-04	3.58E-03	*SERPINA1; PCSK9; FN1; PDIA6; FAM20C; HSP90B1; PRSS23; LAMB1; MMP2*	Reactome
123	downregulated of mta-3 in er-negative breast tumors	21	4.90E-04	3.72E-03	*TUBA1C; ALDOA; TUBA1A; GAPDH*	BioCarta
124	Regulation of actin cytoskeleton	213	5.01E-04	3.77E-03	*PDGFB; ITGB5; ITGB4; FN1; ITGB6; TMSB4X; ITGA5; MSN; ACTB; LPAR1; ACTG1; GSN*	KEGG
125	Validated transcriptional targets of AP1 family members Fra1 and Fra2	37	5.04E-04	3.77E-03	*CCND1; CCL2; MMP2; ITGB4; GJA1*	PID
126	ECM proteoglycans	57	5.51E-04	4.09E-03	*ITGB5; LAMA5; ITGB6; SPARC; LAMB1; LAMA4*	Reactome
127	Fatty Acid Biosynthesis	22	5.90E-04	4.34E-03	*ACLY; SCD; FASN; ACSS2*	Wikipathways
128	mevalonate pathway	10	6.38E-04	4.62E-03	*IDI1; HMGCR; HMGCS1*	HumanCyc
129	Liver X Receptor Pathway	10	6.38E-04	4.62E-03	*SCD; SREBF1; FASN*	Wikipathways
130	inactivation of gsk3 by akt causes accumulation of b-catenin in alveolar macrophages	40	7.28E-04	5.23E-03	*CCND1; GJA1; CD14; TLR4; DKK1*	BioCarta
131	Hypertrophic cardiomyopathy (HCM)	83	7.48E-04	5.34E-03	*ITGB5; ITGB4; ITGB6; ITGA5; SLC8A1; ACTB; ACTG1*	KEGG
132	Post-translational protein phosphorylation	110	8.04E-04	5.69E-03	*SERPINA1; PCSK9; FN1; PDIA6; FAM20C; HSP90B1; PRSS23; LAMB1*	Reactome
133	Aurora B signaling	41	8.17E-04	5.70E-03	*NCL; BUB1; AURKA; CENPA; VIM*	PID
134	Regulation of lipid metabolism by Peroxisome proliferator-activated receptor alpha (PPARalpha)	41	8.17E-04	5.70E-03	*HMGCS1; TNFRSF21; ANGPTL4; FDFT1; HMGCR*	Wikipathways
135	Pentose phosphate cycle	24	8.34E-04	5.77E-03	*ALDOA; ALDOC; G6PD; GPI*	INOH
136	Statin Pathway, Pharmacodynamics	25	9.79E-04	6.72E-03	*LDLR; FDFT1; SQLE; HMGCR*	PharmGKB
137	Validated targets of C-MYC transcriptional activation	87	9.91E-04	6.76E-03	*CCNB1; GAPDH; ENO1; NCL; MYC; LDHA; PEG10*	PID
138	Metabolism of carbohydrates	264	1.01E-03	6.83E-03	*HK1; CHST15; GPI; HK2; G6PD; GAPDH; GYS1; ENO1; PGP; PGAM1; ALDOA; ALDOC; PGK1*	Reactome
139	Toxoplasmosis	113	1.02E-03	6.84E-03	*LAMA4; LAMA5; HSPA8; LAMC2; LDLR; MAP2K6; TLR4; LAMB1*	KEGG
140	miR-targeted genes in epithelium - TarBase	333	1.09E-03	7.26E-03	*TGFBR2; ANXA2; ITGB4; GJA1; CCND1; TUBA1A; CTSC; C1QBP; PLK1; G6PD; NCL; ARHGDIA; CYP51A1; IPO4; NRP1*	Wikipathways
141	miRNA targets in ECM and membrane receptors	44	1.13E-03	7.39E-03	*LAMA4; THBS1; ITGB5; FN1; ITGB6*	Wikipathways
142	Prostaglandin Synthesis and Regulation	44	1.13E-03	7.39E-03	*ANXA1; ANXA3; ANXA2; PTGER2; ANXA6*	Wikipathways
143	Dilated cardiomyopathy (DCM)	90	1.13E-03	7.39E-03	*ITGB5; ITGB4; ITGB6; ITGA5; SLC8A1; ACTB; ACTG1*	KEGG
144	superpathway of geranylgeranyldiphosphate biosynthesis I (via mevalonate)	12	1.14E-03	7.39E-03	*HMGCS1; HMGCR; IDI1*	HumanCyc
145	Integrated Breast Cancer Pathway	66	1.21E-03	7.77E-03	*ANXA1; IRS1; AURKA; HMGCR; TFPI; MYC*	Wikipathways

146	VEGFA-VEGFR2 Signaling Pathway	236	1.23E-03	7.87E-03	*ANXA1; GJA1; F3; ITGB5; CCND1; DKK1; CTGF; NCL; MAP2K6; SLC8A1; CCL2; MMP2*	Wikipathways
147	miR-targeted genes in lymphocytes - TarBase	489	1.44E-03	9.17E-03	*TGFBR2; PTRH1; CTSC; CCND1; TUBA1A; G6PD; IRS1; C1QBP; GYS1; PLK1; ANXA2; NCL; ANPEP; ARHGDIA; LAMC2; CYP51A1; IPO4; FADS2; NRP1*	Wikipathways
148	Transcriptional regulation by RUNX3	13	1.46E-03	9.22E-03	*CCND1; CTGF; MYC*	Wikipathways
149	AMPK signaling pathway	120	1.50E-03	9.41E-03	*CCND1; SCD; SLC2A4; IRS1; GYS1; SREBF1; FASN; HMGCR*	KEGG
150	Prefoldin mediated transfer of substrate to CCT/TriC	28	1.52E-03	9.45E-03	*TUBA1C; TUBB4B; ACTB; TUBA1A*	Reactome
151	Assembly of collagen fibrils and other multimeric structures	48	1.69E-03	1.04E-02	*LAMC2; LOXL2; COL8A1; LOX; ITGB4*	Reactome
152	RHO GTPases Activate Formins	123	1.76E-03	1.08E-02	*BUB1; ACTG1; PLK1; CENPF; CENPE; CENPA; CDC20; ACTB*	Reactome
153	Alpha6Beta4Integrin	71	1.76E-03	1.08E-02	*ITGB4; IRS1; VIM; LAMB1; LAMC2; LAMA5*	NetPath
154	Pentose Phosphate Pathway	14	1.83E-03	1.09E-02	*ALDOA; G6PD; GPI*	SMPDB
155	Glucose-6-phosphate dehydrogenase deficiency	14	1.83E-03	1.09E-02	*ALDOA; G6PD; GPI*	SMPDB
156	Ribose-5-phosphate isomerase deficiency	14	1.83E-03	1.09E-02	*ALDOA; G6PD; GPI*	SMPDB
157	Transaldolase deficiency	14	1.83E-03	1.09E-02	*ALDOA; G6PD; GPI*	SMPDB
158	Integrin	124	1.85E-03	1.09E-02	*COL8A1; ITGB5; ITGB4; FN1; ITGB6; ITGA5; LAMC2; ACTB*	INOH
159	Cholesterol biosynthesis via desmosterol	4	1.91E-03	1.11E-02	*DHCR7; DHCR24*	Reactome
160	Cholesterol biosynthesis via lathosterol	4	1.91E-03	1.11E-02	*DHCR7; DHCR24*	Reactome
161	Metabolism of lipids	664	1.94E-03	1.12E-02	*MSMO1; UGCG; TNFAIP8L3; IDI1; DHCR7; CYP51A1; SQLE; SCD; PLIN3; LPCAT4; FASN; LSS; LPCAT1; FDFT1; HMGCS1; PCYT2; HMGCR; GGT5; FADS2; DHCR24; ELOVL6; SREBF1; ACLY*	Reactome
162	miR-targeted genes in leukocytes - TarBase	154	1.94E-03	1.12E-02	*PTRH1; ANXA2; G6PD; TUBA1A; CTSC; THBS1; GYS1; ANPEP; ARHGDIA*	Wikipathways
163	Pentose phosphate pathway	30	1.98E-03	1.13E-02	*ALDOA; ALDOC; G6PD; GPI*	KEGG
164	Primary Focal Segmental Glomerulosclerosis FSGS	73	2.04E-03	1.16E-02	*LAMA5; DKK1; TLR4; PTPRO; VIM; ITGB4*	Wikipathways
165	Statin Pathway	31	2.24E-03	1.27E-02	*LDLR; FDFT1; SQLE; HMGCR*	Wikipathways
166	Regulation of sister chromatid separation at the metaphase-anaphase transition	15	2.26E-03	1.27E-02	*CENPE; BUB1; CDC20*	Wikipathways
167	Sorafenib Metabolism Pathway	15	2.26E-03	1.27E-02	*PDIA6; PDIA4; HSPA5*	SMPDB
168	Metabolism	1972	2.40E-03	1.33E-02	*MSMO1; UGCG; TNFAIP8L3; IDI1; GLRX; SMS; GAPDH; DHCR7; NDUFAF3; PGAM1; PYCR3; PLIN3; LPCAT1; ALDOC; SCD; SQLE; PAICS; LPCAT4; FASN; LSS; PGP; CYP51A1; KYAT1; FDFT1; LDHA; PGK1; HMGCS1; HK1; GPI; HK2; ACSS2; PCYT2; GYS1; ENO1; LDLR; HMGCR; GGT5; ALDOA; UCP2; FADS2; DHCR24; CA9; CHST15; CDA;*	Reactome

					SLC16A3; G6PD; ELOVL6; BTD; SREBF1; ACLY; LRP8; SLC19A1	
169	L1CAM interactions	103	2.49E-03	1.38E-02	*DPYSL2; HSPA8; ITGA5; MSN; LAMB1; SCN5A; NRP1*	Reactome
170	Syndecan-4-mediated signaling events	32	2.52E-03	1.38E-02	*TFPI; ITGA5; FN1; THBS1*	PID
171	FoxO signaling pathway	132	2.61E-03	1.42E-02	*IL7R; TGFBR2; CCNB1; PLK1; SLC2A4; IRS1; CCND1; BNIP3*	KEGG
172	Apoptosis-related network due to altered Notch3 in ovarian cancer	53	2.63E-03	1.42E-02	*IL7R; TNFRSF21; VIM; HSPA5; THBS1*	Wikipathways
173	Cardiac Progenitor Differentiation	53	2.63E-03	1.42E-02	*SCN5A; THY1; NOG; ANPEP; DKK1*	Wikipathways
174	Polo-like kinase mediated events	16	2.75E-03	1.45E-02	*PLK1; CENPF; CCNB1*	Reactome
175	Regulation of TLR by endogenous ligand	16	2.75E-03	1.45E-02	*CD14; S100A9; TLR4*	Reactome
176	Morphine Metabolism Pathway	16	2.75E-03	1.45E-02	*PDIA6; PDIA4; HSPA5*	SMPDB
177	CRMPs in Sema3A signaling	16	2.75E-03	1.45E-02	*SEMA3A; DPYSL2; NRP1*	Reactome
178	Cooperation of Prefoldin and TriC/CCT in actin and tubulin folding	33	2.83E-03	1.48E-02	*TUBA1C; TUBB4B; ACTB; TUBA1A*	Reactome
179	Neutrophil degranulation	490	3.14E-03	1.61E-02	*SERPINA1; CTSC; LPCAT1; GPI; TUBB4B; HSPA8; RHOF; CD14; ANXA2; S100A9; ANPEP; PGAM1; ALDOA; ACLY; SERPINB3; GSN; ALDOC; CDA*	Reactome
180	Neomycin, kanamycin and gentamicin biosynthesis	5	3.14E-03	1.61E-02	*HK2; HK1*	KEGG
181	Extrinsic Pathway of Fibrin Clot Formation	5	3.14E-03	1.61E-02	*F3; TFPI*	Reactome
182	ATF6 (ATF6-alpha) activates chaperone genes	5	3.14E-03	1.61E-02	*HSPA5; HSP90B1*	Wikipathways
183	Canonical and Non-Canonical TGF-B signaling	17	3.29E-03	1.68E-02	*TGFBR2; LOXL2; LOX*	Wikipathways
184	Resolution of Sister Chromatid Cohesion	109	3.62E-03	1.84E-02	*CCNB1; BUB1; PLK1; CENPF; CENPE; CENPA; CDC20*	Reactome
185	Mammary gland development pathway - Embryonic development (Stage 1 of 4)	18	3.90E-03	1.90E-02	*CCND1; MYC; SFRP1*	Wikipathways
186	Fructose intolerance, hereditary	18	3.90E-03	1.90E-02	*ALDOA; HK1; MPI*	SMPDB
187	Fructose and Mannose Degradation	18	3.90E-03	1.90E-02	*ALDOA; HK1; MPI*	SMPDB
188	Fructosuria	18	3.90E-03	1.90E-02	*ALDOA; HK1; MPI*	SMPDB
189	Beta5 beta6 beta7 and beta8 integrin cell surface interactions	18	3.90E-03	1.90E-02	*ITGB5; FN1; ITGB6*	PID
190	Photodynamic therapy-induced HIF-1 survival signaling	36	3.90E-03	1.90E-02	*HK1; PGK1; LDHA; BNIP3*	Wikipathways
191	Elastic fibre formation	36	3.90E-03	1.90E-02	*EFEMP1; ITGB5; ITGA5; ITGB6*	Reactome
192	Starch and sucrose metabolism	36	3.90E-03	1.90E-02	*HK2; GYS1; HK1; GPI*	KEGG
193	Glutaminolysis and Cancer	37	4.31E-03	2.09E-02	*SLC38A5; ACLY; MYC; LDHA*	SMPDB
194	ESR-mediated signaling	19	4.57E-03	2.16E-02	*CCND1; MYC; KPNA2*	Wikipathways
195	Etoposide Action Pathway	19	4.57E-03	2.16E-02	*PDIA6; PDIA4; HSPA5*	SMPDB

196	Etoposide Metabolism Pathway	19	4.57E-03	2.16E-02	*PDIA6; PDIA4; HSPA5*	SMPDB
197	LDL clearance	19	4.57E-03	2.16E-02	*LIPA; LDLR; PCSK9*	Reactome
198	GDP-mannose biosynthesis	6	4.66E-03	2.16E-02	*GPI; MPI*	HumanCyc
199	GDP-glucose biosynthesis II	6	4.66E-03	2.16E-02	*HK2; HK1*	HumanCyc
200	Fibronectin matrix formation	6	4.66E-03	2.16E-02	*ITGA5; FN1*	Reactome
201	zymosterol biosynthesis	6	4.66E-03	2.16E-02	*MSMO1; CYP51A1*	HumanCyc
202	Fatty acyl-CoA biosynthesis	38	4.75E-03	2.20E-02	*ELOVL6; ACLY; FASN; SCD*	Reactome
203	Signaling by MET	61	4.85E-03	2.23E-02	*LAMC2; LAMB1; LAMA4; LAMA5; TNS4*	Reactome
204	Signaling by Rho GTPases	435	5.12E-03	2.35E-02	*BUB1; ACTG1; PLK1; CENPF; CENPE; CENPA; RHOF; KIF14; ARHGDIB; ARHGEF39; ARHGDIA; ACTB; CDC20; ARHGAP29; ARHGAP18; DEPDC1B*	Reactome
205	Gap junction	88	5.18E-03	2.36E-02	*GJA1; PDGFB; TUBA1C; TUBB4B; TUBA1A; LPAR1*	KEGG
206	O-glycosylation of TSR domain-containing proteins	39	5.22E-03	2.37E-02	*ADAMTS12; ADAMTSL1; ADAMTSL4; THBS1*	Reactome
207	Glutathione metabolism	20	5.30E-03	2.37E-02	*G6PD; ANPEP; GGT5*	Wikipathways
208	Aminosugars metabolism	20	5.30E-03	2.37E-02	*HK2; HK1; MPI*	INOH
209	Syndecan interactions	20	5.30E-03	2.37E-02	*ITGB5; ITGB4; THBS1*	Reactome
210	Spinal Cord Injury	117	5.34E-03	2.37E-02	*ANXA1; GJA1; CCND1; VIM; CCL2; TLR4; MYC*	Wikipathways
211	Bladder Cancer	40	5.72E-03	2.53E-02	*CCND1; MYC; MMP2; THBS1*	Wikipathways
212	Lung fibrosis	64	5.94E-03	2.62E-02	*CCL2; SERPINA1; PDGFB; MMP2; CTGF*	Wikipathways
213	Regulation of Apoptosis by Parathyroid Hormone-related Protein	21	6.11E-03	2.68E-02	*MYC; ITGB4; PTHLH*	Wikipathways
214	Regulation of Actin Cytoskeleton	151	6.17E-03	2.69E-02	*PDGFB; ACTG1; FN1; TMSB4X; MSN; CD14; ACTB; GSN*	Wikipathways
215	Bladder cancer	41	6.25E-03	2.69E-02	*CCND1; MYC; MMP2; THBS1*	KEGG
216	APC/C-mediated degradation of cell cycle proteins	41	6.25E-03	2.69E-02	*PLK1; CCNB1; AURKA; CDC20*	Reactome
217	Regulation of mitotic cell cycle	41	6.25E-03	2.69E-02	*PLK1; CCNB1; AURKA; CDC20*	Reactome
218	Collagen formation	92	6.43E-03	2.75E-02	*LOXL2; ITGB4; PLOD2; COL8A1; LAMC2; LOX*	Reactome
219	Mevalonate pathway	7	6.44E-03	2.75E-02	*HMGCS1; HMGCR*	Wikipathways
220	Hippo signaling pathway	154	6.66E-03	2.83E-02	*TGFBR2; FZD2; ACTG1; CCND1; ID1; CTGF; MYC; ACTB*	KEGG
221	Mitotic Prometaphase	186	6.76E-03	2.85E-02	*CCNB1; BUB1; PLK1; CENPF; TUBA1A; CENPA; CDC20; TUBB4B; CENPE*	Reactome
222	Glycolysis and Gluconeogenesis	67	6.77E-03	2.85E-02	*ENO1; SLC16A3; HK1; GPI; PGAM1*	EHMN
223	Hair Follicle Development- Induction (Part 1 of 3)	42	6.81E-03	2.85E-02	*TP63; CTGF; NOG; MYC*	Wikipathways
224	Terpenoid backbonesapiens (human)	22	6.98E-03	2.91E-02	*HMGCS1; HMGCR; IDI1*	KEGG
225	Pathways in cancer	526	7.21E-03	2.98E-02	*IL7R; TGFBR2; FZD2; LAMA4; LAMA5; FN1; CCND1; CKS2; PDGFB; HSP90B1;*	KEGG

					LAMC2; PTGER2; LAMB1; MYC; LPAR1; MMP2; EGLN3; HHIP	
226	Integrin cell surface interactions	67	7.21E-03	2.98E-02	*ITGB6; ITGB5; ITGA5; FN1; THBS1*	Reactome
227	Platelet activation, signaling and aggregation	260	7.77E-03	3.15E-02	*SERPINA1; PDGFB; FN1; HSPA5; TMSB4X; PCDH7; LGALS3BP; SPARC; ALDOA; THBS1; CD9*	Reactome
228	Amplification of signal from unattached kinetochores via a MAD2 inhibitory signal	96	7.87E-03	3.15E-02	*BUB1; PLK1; CENPF; CENPE; CENPA; CDC20*	Reactome
229	Amplification of signal from the kinetochores	96	7.87E-03	3.15E-02	*BUB1; PLK1; CENPF; CENPE; CENPA; CDC20*	Reactome
230	TLR ECSIT MEKK1 p38	23	7.92E-03	3.15E-02	*CD14; MAP2K6; TLR4*	INOH
231	Signaling events mediated by the Hedgehog family	23	7.92E-03	3.15E-02	*GAS1; PTHLH; HHIP*	PID
232	Ibuprofen Metabolism Pathway	23	7.92E-03	3.15E-02	*PDIA6; PDIA4; HSPA5*	SMPDB
233	Irinotecan Action Pathway	23	7.92E-03	3.15E-02	*PDIA6; PDIA4; HSPA5*	SMPDB
234	Irinotecan Metabolism Pathway	23	7.92E-03	3.15E-02	*PDIA6; PDIA4; HSPA5*	SMPDB
235	Post-chaperonin tubulin folding pathway	23	7.92E-03	3.15E-02	*TUBA1C; TUBB4B; TUBA1A*	Reactome
236	miR-targeted genes in squamous cell - TarBase	158	8.03E-03	3.17E-02	*TGFBR2; ANXA2; TUBA1A; THBS1; GYS1; NCL; ANPEP; NRP1*	Wikipathways
237	Urokinase-type plasminogen activator (uPA) and uPAR-mediated signaling	44	8.04E-03	3.17E-02	*ITGB5; NCL; ITGA5; FN1*	PID
238	sucrose degradation	8	8.49E-03	3.25E-02	*ALDOA; ALDOC*	HumanCyc
239	HIF1A and PPARG regulation of glycolysis	8	8.49E-03	3.25E-02	*GAPDH; LDHA*	Wikipathways
240	RUNX3 regulates WNT signaling	8	8.49E-03	3.25E-02	*CCND1; MYC*	Reactome
241	oleate biosynthesis	8	8.49E-03	3.25E-02	*SCD; FADS2*	HumanCyc
242	Hypothetical Craniofacial Development Pathway	8	8.49E-03	3.25E-02	*TP63; ARHGAP29*	Wikipathways
243	RUNX2 regulates genes involved in cell migration	8	8.49E-03	3.25E-02	*ITGA5; ITGBL1*	Reactome
244	Ligand-receptor interactions	8	8.49E-03	3.25E-02	*GAS1; HHIP*	Reactome
245	Epithelial to mesenchymal transition in colorectal cancer	160	8.64E-03	3.29E-02	*TGFBR2; FZD2; FN1; ITGA5; ID1; SPARC; MAP2K6; MMP2*	Wikipathways
246	Muscle contraction	195	9.08E-03	3.44E-02	*ANXA1; ANXA2; ITGB5; DYSF; ANXA6; ASPH; VIM; SLC8A1; SCN5A*	Reactome
247	AGE-RAGE signaling pathway in diabetic complications	99	9.10E-03	3.44E-02	*CCL2; TGFBR2; F3; FN1; CCND1; MMP2*	KEGG
248	Type II diabetes mellitus	46	9.39E-03	3.54E-02	*HK2; SLC2A4; HK1; IRS1*	KEGG
249	Angiopoietin Like Protein 8 Regulatory Pathway	131	9.73E-03	3.65E-02	*SCD; SLC2A4; IRS1; GYS1; SREBF1; FASN; MAP2K6*	Wikipathways
Down-regulated by O_3 oxidation products only						
1	Aryl hydrocarbon receptor signalling	7	1.47E-04	1.81E-02	*HSP90AB1; PTGES3*	Reactome
2	Metallothioneins bind metals	12	4.57E-04	1.82E-02	*MT1X; MT1A*	Reactome
3	Benzodiazepine Pathway, Pharmacodynamics	14	6.29E-04	1.82E-02	*DBI; VDAC1*	PharmGKB

4	Response to metal ions	15	7.24E-04	1.82E-02	*MT1X; MT1A*	Reactome
5	Cellular responses to external stimuli	414	7.38E-04	1.82E-02	*MT1X; PTGES3; UBE2C; HMGA2; HSP90AB1; MT1A*	Reactome
6	HSP90 chaperone cycle for steroid hormone receptors (SHR)	19	1.17E-03	2.40E-02	*PTGES3; HSP90AB1*	Reactome
7	Post-chaperonin tubulin folding pathway	23	1.72E-03	2.71E-02	*TUBA1B; TUBA4A*	Reactome
8	Alanine Aspartate Asparagine metabolism	25	2.03E-03	2.71E-02	*ADSS; PKM*	INOH
9	VEGFR3 signaling in lymphatic endothelium	25	2.03E-03	2.71E-02	*ITGA4; VEGFC*	PID
10	Formation of tubulin folding intermediates by CCT/TriC	26	2.20E-03	2.71E-02	*TUBA1B; TUBA4A*	Reactome
11	Attenuation phase	28	2.55E-03	2.74E-02	*HSP90AB1; PTGES3*	Reactome
12	Phase I - Functionalization of compounds	109	2.93E-03	2.74E-02	*HSP90AB1; PTGES3; CYP4B1*	Reactome
13	Biological oxidations	231	3.06E-03	2.74E-02	*HSP90AB1; PTGES3; MAT2A; CYP4B1*	Reactome
14	HSF1 activation	31	3.12E-03	2.74E-02	*HSP90AB1; PTGES3*	Reactome
15	Cooperation of Prefoldin and TriC/CCT in actin and tubulin folding	33	3.53E-03	2.75E-02	*TUBA1B; TUBA4A*	Reactome
16	Cell Cycle	564	3.58E-03	2.75E-02	*UBE2C; HSP90AB1; DKC1; TUBA4A; CDCA8; PHLDA1*	Reactome
17	TCR	245	4.02E-03	2.86E-02	*HSP90AB1; TUBA4A; PKM; CALM1*	NetPath
18	HSF1-dependent transactivation	36	4.19E-03	2.86E-02	*PTGES3; HSP90AB1*	Reactome
19	Zinc homeostasis	37	4.43E-03	2.86E-02	*MT1X; MT1A*	Wikipathways
20	Platelet degranulation	129	4.96E-03	3.05E-02	*TUBA4A; VEGFC; CALM1*	Reactome
21	Response to elevated platelet cytosolic Ca2+	134	5.52E-03	3.18E-02	*TUBA4A; VEGFC; CALM1*	Reactome
22	G2/M Transition	137	5.87E-03	3.18E-02	*HSP90AB1; TUBA4A; PHLDA1*	Reactome
23	Mitotic G2-G2/M phases	139	6.11E-03	3.18E-02	*HSP90AB1; TUBA4A; PHLDA1*	Reactome
24	Prostaglandin Synthesis and Regulation	44	6.21E-03	3.18E-02	*S100A10; AKR1C2*	Wikipathways
25	Mineral absorption	51	8.27E-03	4.07E-02	*MT1X; MT1A*	KEGG
26	Cell Cycle, Mitotic	481	8.76E-03	4.14E-02	*HSP90AB1; TUBA4A; CDCA8; PHLDA1; UBE2C*	Reactome
27	Copper homeostasis	55	9.57E-03	4.20E-02	*MT1X; MT1A*	Wikipathways
28	Pathogenic Escherichia coli infection	55	9.57E-03	4.20E-02	*TUBA1B; TUBA4A*	KEGG
29	Pathogenic Escherichia coli infection	56	9.91E-03	4.20E-02	*TUBA1B; TUBA4A*	Wikipathways
Down-regulated by OH oxidation product only						
1	Prostaglandin Synthesis and Regulation	44	3.70E-05	3.36E-03	*ABCC4; PTGER4; PLA2G4A; SOX9*	Wikipathways

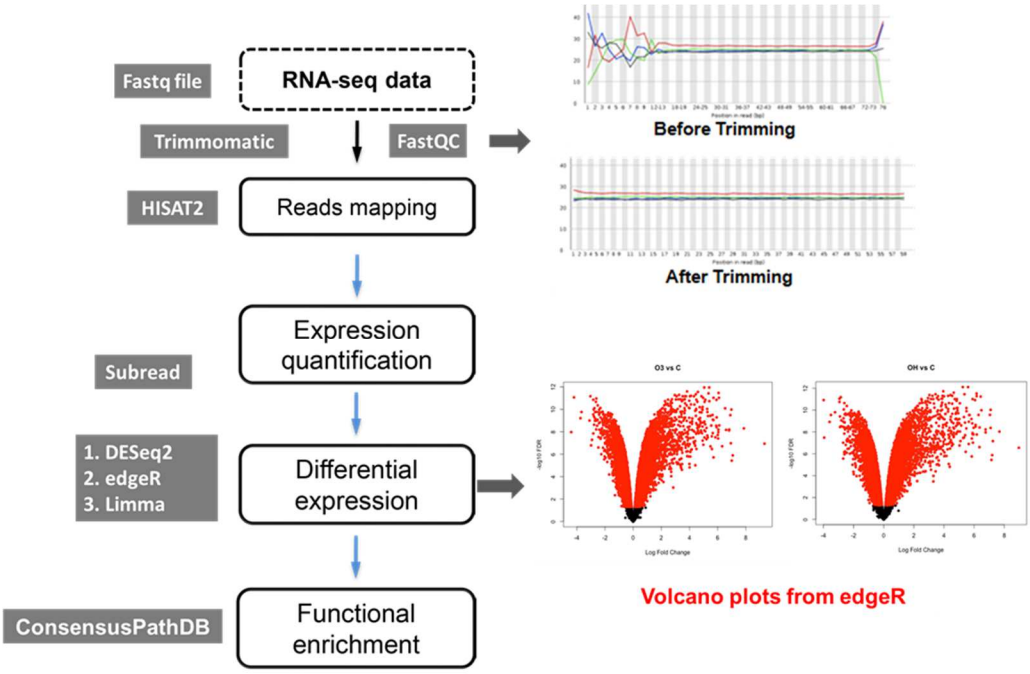

Figure S3.1. Pipeline for RNA-Seq data analysis. For DESeq2, fragments per million (fpm≥1 in at least two samples) was used to normalize library size and to filter out lowly expressed genes. For edgeR and limma packages, counts per million (cpm≥1 in at least two samples) was used. In edgeR, trimmed mean of M-values (TMM) was also used to normalize for composition bias, and gene-wise negative binomial generalized linear fit models with quasi-likelihood tests were used to count data using the glmQLFTest function. In limma, minimum total count of 25 reads in two samples was used for removing lowly expressed genes which was equivalent to cpm≥1 in average. Then, the voom function was used to transform count data to ready-to-use for linear modelling. The linear modeling was carried out by lmFit and contrasts.fit functions.

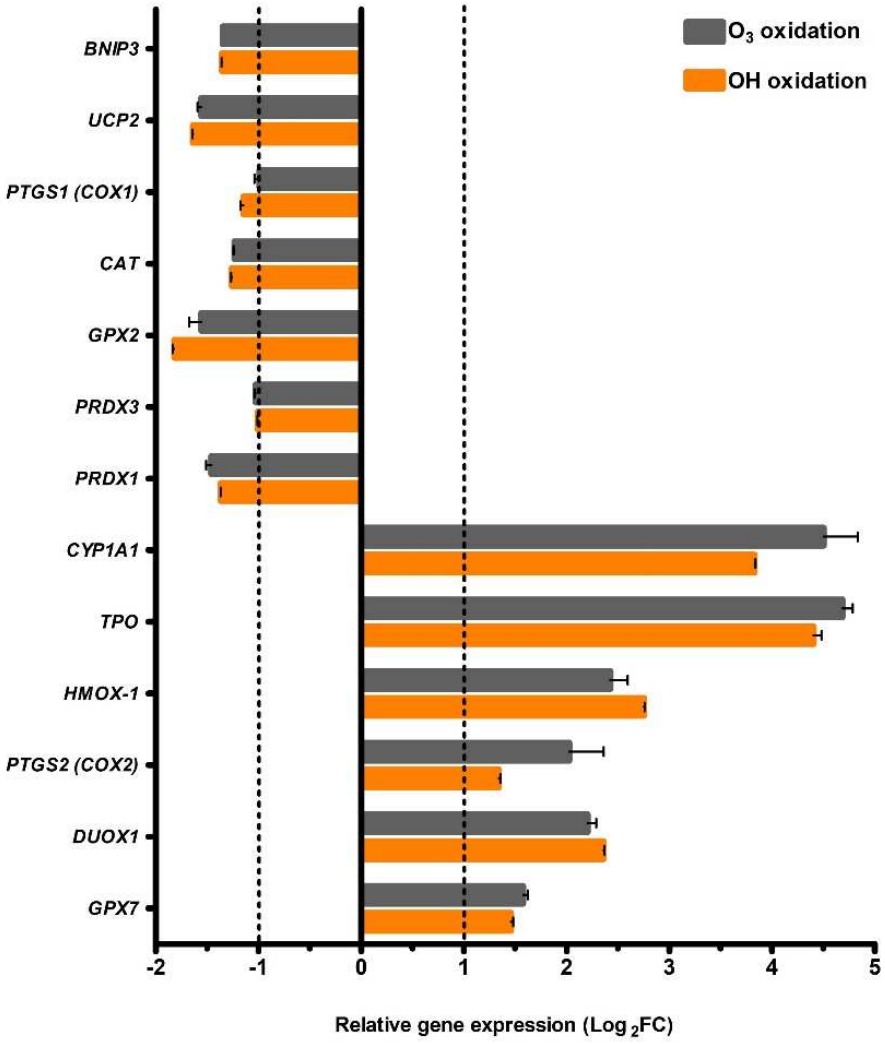

Figure S3.2. List of identified DEGs related to oxidative stress, ROS generation or antioxidant enzymes at the cellular level. Most of the antioxidant-related genes were downregulated while oxidative responsive genes were upregulated. Some of the oxidative stress responsive genes (e.g., *HMOX-1, DUOX1, TPO,* and *CYP1A1*) showed higher range of relative expression levels (log_2FC, 2.5-4.5). The relative expression of oxidative stress-related genes clearly correlates with our DTT results that measured the oxidative potential of DMSe-derived SOA.

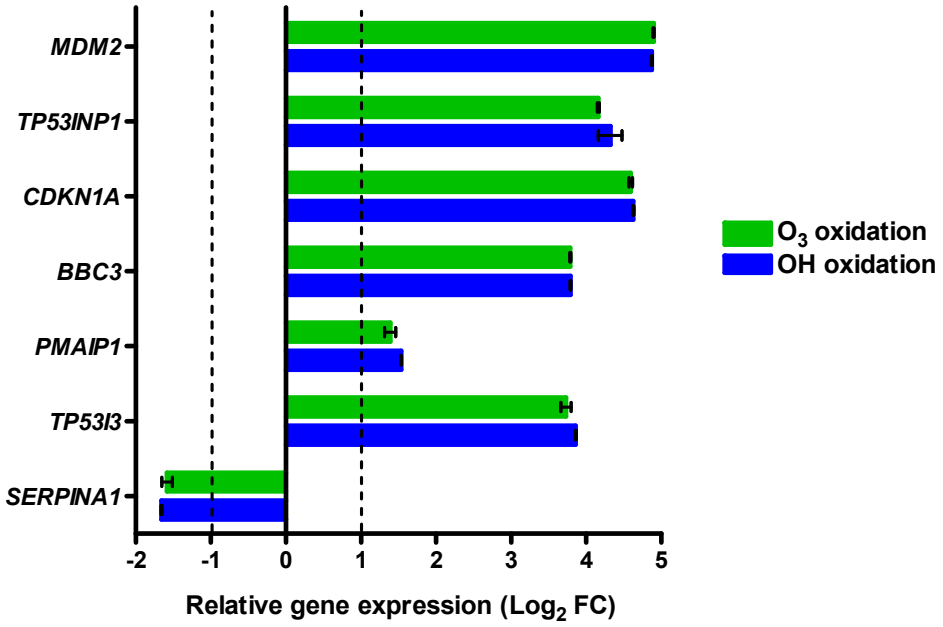

Figure S3.3: The relative expression of highlighted genes in the discussion.

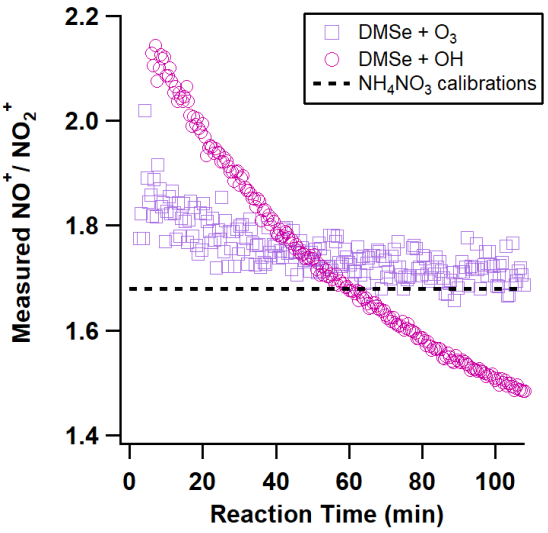

Figure S3.4. Time trend of the ratio of common nitrate ions during DMSe oxidation experiments in comparison with the ratio observed during ammonium nitrate calibrations.

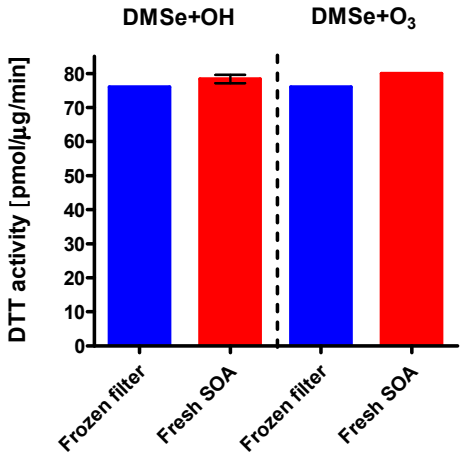

Figure S3.5. DTT activity (pmol/µg/min) for both frozen and fresh SOA samples from OH and O3 oxidation of DMSe. Compared to fresh SOA samples, frozen filters (stored in dark in a -20 °C freezer for about two weeks) showed minimal decay (~5%) of DTT activity for SOA generated from O_3 oxidation, while no significant differences were observed for SOA generated from OH oxidation ($p > 0.05$).

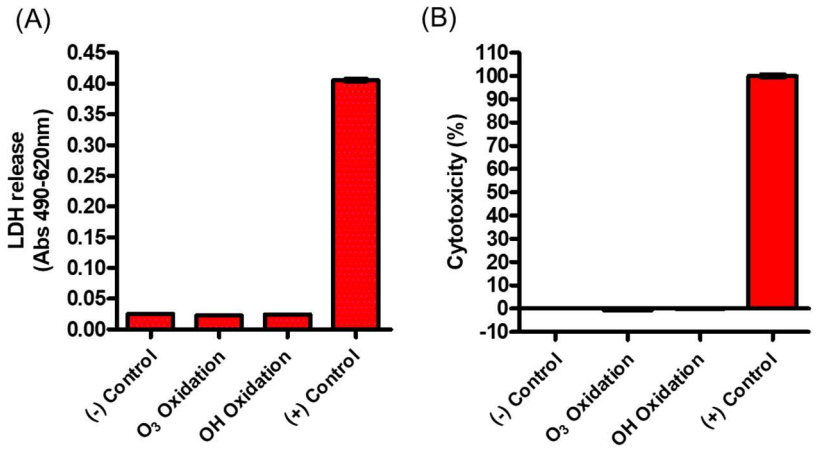

Figure S3.6. (A) LDH release and (B) cytotoxicity (%) induced by extracts of DMSe-derived SOA from O3 and OH oxidation at a concentration 10 µg/mL. The negative (-) control represents cells exposed to the blank filter extracts, and positive (+) control represents cells exposed to 1% Triton X-100.

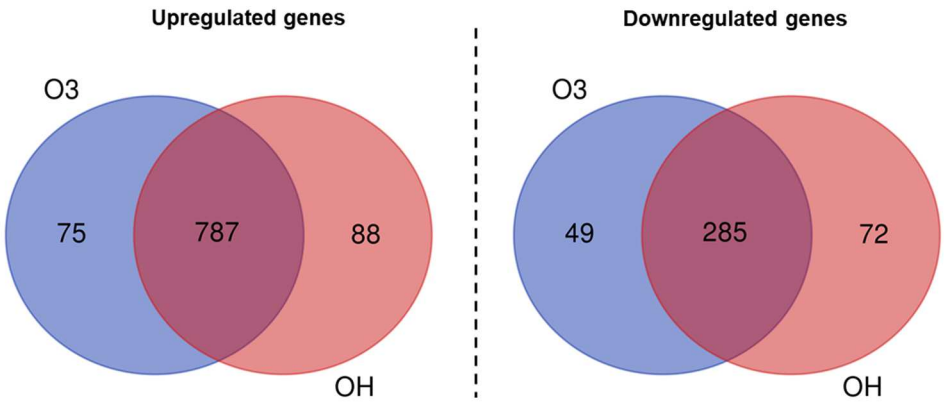

Figure S3.7. Number of common and unique DEGs induced by SOA generated by O3 and OH oxidation products: (A) common DEGs, (B) DEGs induced by O_3 oxidation products only, and (C) DEGs induced by OH oxidation products only.

Chapter IV: Integrative analysis of lncRNA-mRNA co-expression in human lung epithelial cells exposed to dimethyl selenide (DMSe)-derived secondary organic aerosols

4.1. Introduction

Selenium (Se) is a trace element cycling in the natural environment and a micronutrient essential for human health.[194] Excess Se intake from dietary or environmental exposure has been linked to several human diseases, including cancer, diabetes mellitus, cardiovascular disease, and disorders of central nervous system.[195-197] Se is readily found in soil, water, and air.[194, 198] Both biotic and abiotic processes govern the fate and transport of Se in the environment. Through microbial methylation and plant metabolism, inorganic Se can be transformed to volatile organoselenium compounds.[194, 199] Previous studies suggested that alkylated Se compounds, such as dimethylselenide (DMSe) and dimethyl diselenide (DMDSe), are volatile and less toxic compared to the inorganic Se species.[200] However, it has been recently revealed that the atmospheric oxidation (with O_3 and OH) of DMSe leads to the formation of secondary organic aerosol (SOA), which could potentially pose health risks in areas with high DMSe emissions (e.g., Se-rich fields) and their downwind regions during summer months.[199] The resultant DMSe-derived SOA has been shown to be a potent stressor in human airway epithelial cells (BEAS-2B) that can perturb several biological pathways, including genotoxicity, DNA

damage, p53-mediated stress responses, cholesterol biosynthesis, glycolysis, and interleukin IL-4/IL-13 signaling.[199]

Long noncoding RNAs (lncRNAs) are a class of transcripts that typically have more than 200 nucleotide (nt) in length,[201, 202] but they contain no functional open reading frame that may or may not be polyadenylated and do not have protein coding capacity.[202, 203] In human tissues, most lncRNAs are expressed at lower levels compared to protein-coding RNAs.[204] However, recent studies have reported that lncRNAs play a critical role in regulating gene expression and cellular homeostasis.[47, 205, 206] Based on the position relative to protein-coding genes, lncRNAs are classified as intergenic (between genes), intragenic/intronic (within genes) and antisense.[207] In response to internal or environmental stimuli, lncRNAs show cell type-specific expression, suggesting that their expression is under considerable transcriptional control and can potentially be disturbed under stress.[206, 208] In general, lncRNAs can directly interact with DNAs or RNAs by base pairing and form a strong duplex or a triplex.[202, 209] Through epigenetic, transcriptional and posttranscriptional mechanisms, lncRNAs can also control the expression of their adjacent genes in *cis* (near the site of lncRNA production) or modulate gene transcription in *trans* (to distant target genes),[202] and recruit chromatin-modifying enzymes for gene regulation.[208]

Aberrant expression of certain lncRNAs has been found in different types of human cancers.[202] LncRNAs can contribute in multiple ways to the regulation of DNA damage repair, while failures in DNA damage response can cause mutation and cancer transformation.[210, 211] Recent studies have reported that several lncRNAs are transcribed

after DNA damage in response to external stimuli.[212] Specifically, some lncRNAs have been found to regulate transcriptional response of the tumor suppressor protein p53,[213] which has critical functions in response to DNA damage to prevent mutations from being passed on down the lineage.[214] For example, long intergenic non-coding RNA-p21 (*lincRNA-p21*), which is located upstream of *CDKN1A* gene, can interact with hnRNA-K (heterogeneous nuclear ribonucleoprotein K) to regulate apoptosis and act as a transcriptional repressor in the canonical p53 pathway.[213] The lncRNA *DINO* (damage-induced noncoding), which is also transcribed upstream of the *CDKN1A* gene, is inducible in a p53 dependent-manner to promote cell cycle arrest or apoptosis.[215] The lncRNA *GUARDIN* is shown to be p53-responsive to sustain the genome stability by acting as a decoy to sequester *miRNA-23a* and maintain the expression of *TRF2* (telomeric repeat factor 2) to prevent chromosome end-to-end fusion.[216, 217] The lncRNA *PANDA* (p21-associated ncRNA DNA damage-activated) can be directly activated by p53after DNA damage,[212] and negatively regulates apoptosis through interaction with the transcription factor NF-YA (nuclear factor Y).[215] Additionally, lncRNA *DDSR1* (DNA damage-sensitive RNA1) is induced in an ATM-dependent manner and regulated by the NF-κB transcription factor (nuclear factor "kappa-light-chain enhancer" of activated B cells) in response to DNA damage.[217] Overall, lncRNAs play an essential role in the regulation of DNA damage response and cell cycle control to protect cells from malignant transformation.[210, 216]

We have recently demonstrated that DMSe-derived SOA is a potent stressor in BEAS-2B cells that can lead to genotoxicity and p53-mediated DNA damage responses at

the mRNA expression level.[199] The role of lncRNAs in regulation of gene expression via epigenetic mechanisms and their contributions to the observed perturbations remain unclear. Given the increasing evidence suggesting the potential involvement of lncRNAs in lung carcinogenesis,[205, 218] this study aims at identifying lncRNAs responsible for oncogenic dysregulation in BEAS-2B cells exposed to DMSe-derived SOA. We performed integrative analyses of the lncRNA and mRNA transcriptome to investigate the role of differentially expressed (DE) lncRNAs in regulating gene expression via *cis* and *trans* mechanisms. Results from this study provide an improved understanding of lncRNAs-mediated stress response induced by DMSe-derived SOA exposure.

4.2. Experimental Methods

4.2.1. DMSe-derived SOA Generation and Sample Collection

To generate DMSe-derived SOA, a ~1.3 m^3 fluorinated ethylene propylene (FEP) Teflon chamber was used as a controlled atmosphere. Prior to each experiment, the chamber was filled with zero air. Detailed operating procedures for this chamber experiment and sample collection have been described previously.[199] Briefly, oxidation of DMSe with atmospheric oxidants such as O_3 and OH was initiated separately. In the O_3 oxidation experiments, ~300 ppbv of DMSe vapors (1.2 μL) were introduced into the chamber to react with ~250 ppbv of O_3 to generate SOA. In the OH oxidation experiments, nitrous acid (HONO) vapors were first generated in the chamber by the dropwise addition of sodium nitrite to sulfuric acid. Then, DMSe was introduced into the chamber by flowing zero air over ~1.2 μL of DMSe in a glass bulb to achieve a mixing ratio of ~300 ppbv.

Black lights (peak radiation intensity at ~350 nm) surrounding the chamber were turned on to initiate photooxidation after allowing the content of the bag to mix for 10 min. DMSe-derived SOA samples were collected onto 47 mm Teflon membrane filters with a sampling flow rate of 10 L min^{-1} at the end of each experiment. Collected filter samples were stored at −20 °C immediately. To preserve the integrity of SOA constituents, filter samples were extracted within two weeks with 23 mL of high-purity methanol (>99.9%, Fisher Chemical™) by 50 min of sonication. The extracted solution was transferred to a clean vial after sonication, and then blown dry under a gentle stream of nitrogen gas. Finally, the extracted DMSe-derived SOA constituents were stored at −20 °C until cell exposure.

4.2.2. Cell Culture and Exposure

BEAS-2B cells were obtained from the American Type Culture Collection (ATCC). Cells were cultured in Gibco® LHC-9 medium (1×) (Invitrogen) grown at 37 °C and 5% CO_2 in a humidified incubator. Cells were seeded in 24-well plates at a density of 2.5×10^4 cells per well in 250 μL of LHC-9 medium for 48 hours prior to exposure. Upon the time of exposure, cells reached around 60–70% confluence. Extracted DMSe-derived SOA materials were reconstituted with the LHC-9 cell culture medium. Cells were washed with phosphate-bu□ered saline (PBS) and then exposed to DMSe-derived SOA extracts collected from the O_3 and OH oxidation experiments at the concentration of 10 μg mL^{-1} for 24 h. The exposure concentration was selected based on comparison to prior studies using similar approaches to test other types of aerosol samples (e.g., isoprene SOA[219] or gasoline exhaust[220, 221]) to elicit transcriptional changes in BEAS-2B cells under non-

cytotoxic conditions. Cells exposed to the extracts of blank filters were included as negative controls. Experiments were conducted in triplicate per treatment group. After 24 h of exposure, supernatants were collected for assessment of cytotoxicity using the lactate dehydrogenase (LDH) assay (Roche) to ensure that the exposure conditions were not highly cytotoxic to interfere with the downstream lncRNA expression analyses. Details of the LDH assay has been described elsewhere.[199] To isolate the total RNA, cells were lysed with 350 μL of TRI reagent (Zymo Research).

4.2.3. RNA Extraction, Library Construction, and Sequencing

The lysed cell solutions were further purified using the spin column-based Direct-zol RNA MiniPrep kit (Zymo Research). Immediately after extraction, RNA samples were stored at −80 °C until further analysis. RNA quality and concentrations were measured using a Nanodrop ND-1000 spectrophotometer (Thermo Fisher Scientific, Wilmington, DE) and an Agilent 2100 Bioanalyzer (Agilent, Santa Clara, CA). The 260/280 nm absorbance ratios of all RNA samples were >1.8 and the RNA integrity number (RIN) scores from Bioanalyzer were >7. RNA-Seq was performed at the University of California, Riverside-Institute for Integrative Genome Biology (UCR IIGB). Detailed methods of library preparation and RNA sequencing have been published previously.[199] The RNA-seq read data were deposited in the sequence read archive (SRA) BioSample database (SRA accession number: PRJNA539990).

4.2.4. Processing of RNA-seq Data

RNA-seq raw data (raw reads) in fastq format were checked for quality through FastQC (version 0.11.7)[144] and pre-processed by Trimmomatic (version 0.35).[145] In these steps,

clean data (clean reads) were obtained by removing reads containing adapters, reads containing poly-N, and low-quality reads from raw data. All downstream analyses were based on the high-quality clean data.

4.2.5. Read Mapping and Quantification for lncRNA Analysis

Raw reads were aligned to the human genome version hg19 [Genome Reference Consortium Human Build 37 (GRCh37)] using HISAT2 (version 2.1.0).[146] The aligned files were converted to bam files, sorted, and indexed with samtools (version 1.9).[147] Subread (version 1.6.2) tool was used for counting reads of the GENCODE annotated coding and long noncoding transcript using the featureCounts commands.[148] Normalization and di□erential lncRNA expression analysis were carried out using DESeq2 (version 1.18.1)[149] in R (version 3.6.3). Cuto□s used for DE lncRNAs between exposed and unexposed samples were identified and considered significant if the p value was ≤0.01, false discovery rate (FDR) value was ≤0.01, and the absolute log2 fold change (log2 FC) was ≥ |±1|. The workflow for RNA-Seq data analysis for lncRNAs is provided in Figure S4.1.

4.2.6. Prediction of *cis* and *trans* lncRNA Target Genes

LncRNA target genes were divided into two categories: *cis*-target and *trans*-regulated genes. Target genes within 10 kb upstream or downstream of the lncRNA were considered as *cis* target genes were identified using bedtools (version 2.29.2). *Cis* acting lncRNAs and their corresponding target genes were further analyzed for their differential gene expression using R (version 3.6.3). The top 20 DE lncRNAs (determined with the smallest FDR values) were used to predict the *trans*-regulated genes using rtools (http://rtools.cbrc.jp/cgi-

bin/RNARNA/index.pl).[222] Top 100 predicted *trans* target genes were selected based on the minimum energy of lncRNA and mRNA interaction. From a total of 2,000 genes, DE genes (log2FC > |±2|) were selected for construction of the *trans*-regulatory network using network (version 1.16.0) and ggnet (version 0.1.0) packages in R (version 3.6.3)

4.2.7. Gene Ontology (GO) and Gene Set Enrichment Analysis (GSEA)

DE *cis*-target protein-coding genes were further analyzed for the GO enrichment using R package goseq (version 1.38.0). DE lncRNAs were analyzed for the enrichment of human cancer-associated lncRNAs obtained from the public database Lnc2Cancer 2.0 (http://www.bio-bigdata.net/lnc2cancer) for GSEA by using the fgsea package (version 1.12.0).[223, 224]

4.2.8. Code Availability

Data analysis and codes are available at (https://github.com/biplabua/lncRNA_Analysis_2020).

4.3. Results

4.3.1. Differential Expression of lncRNAs

Our prior study has shown that genes associated with genotoxicity and DNA damage responses are enriched in BEAS-2B cells in response to the DMSe-derived SOA exposure.[199] The RNA-seq results highlighted the true transcriptional changes of the live cells, as the exposed cells did not show significant cytotoxicity (assessed by LDH release) with the concentration of 10 μg mL^{-1} after 24 h of exposure.[199] On average, we obtained 27, 28, and 17 million mapped reads in control, O_3, and OH treatment groups for mRNA and 1.5, 1.7, and 1.1 million mapped reads for lncRNA, respectively (Table S4.1). We

hypothesized that lncRNAs could modulate gene expression involved in BEAS-2B cells in response to the DMSe-derived SOA exposure. Though differential expression analysis we detected lncRNAs in BEAS-2B cells exposed to DMSe-derived SOA from both OH and O_3 oxidation experiments.

With the criteria of log2 FC > |±1| and the FDR < 0.01, the DESeq2 identified 716 and 837 DE known lncRNAs for O_3 and OH experiments, respectively, which are highlighted in Figure 4.1a-b. In addition, we found 646 up-regulated and 191 down-regulated DE lncRNAs from OH oxidation experiments, and 554 up-regulated and 162 down-regulated DE lncRNAs from O_3 oxidation experiments (Figure 4.1c-d). Total 461 of upregulated and 121 down-regulated lncRNAs were common between BEAS-2B cells exposed to O_3 and OH oxidation products (Figure 4.1c-d; Figure S4.2). This finding is consistent with our prior report of similar SOA composition (i.e., Se-containing fragments) and common mRNA expression patterns that are associated with genotoxicity from both O_3 and OH experiments. Thus, co-expressed lncRNAs and mRNAs identified in this study revealed possible epigenetic controls of gene expression by lncRNAs.

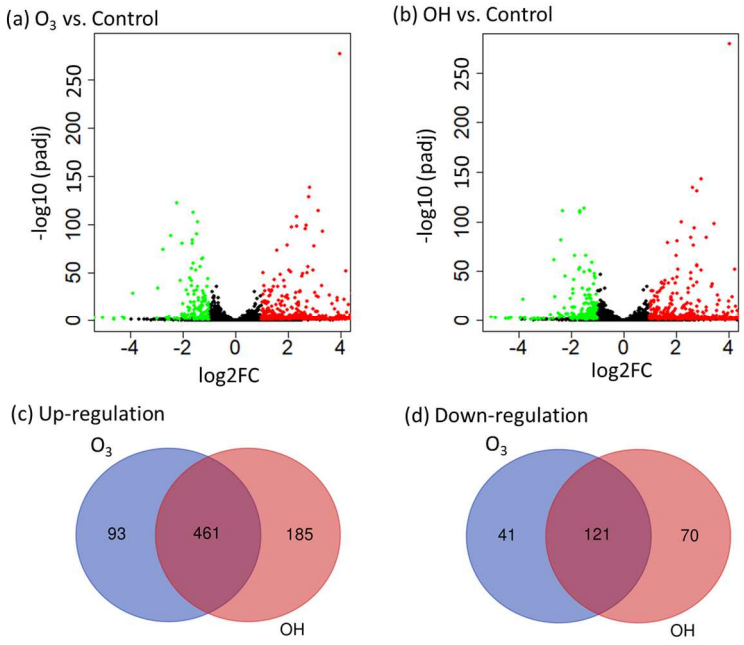

Figure 4.1. Differential expression of lncRNAs in BEAS-2B cells. (a-b) The Volcano plots of DE lncRNAs in control vs. DMSe-derived SOA from O_3 oxidation and control vs. DMSe-derived SOA from OH treated BEAS-2B cells, respectively. X-axis represents log2 (fold-change), and Y-axis represents -log10 (padj). Red dots denote the significantly up-regulated lncRNAs and green dots denote the significantly down-regulated lncRNAs. Black dots denote the non-differentially expressed lncRNAs. (c-d) Venn diagram shows the number of the DE up-regulated and down-regulated lncRNAs in O_3 and OH, respectively.

4.3.2. GSEA of Cancer-related lncRNAs

Since our previous study found alteration of cancer-associated mRNAs,[199] DE lncRNAs were further analyzed to examine the enrichment of cancer-associated lncRNAs using GSEA (Figure 4.2 a-d). The GSEA shows that a large fraction of up-regulated lncRNAs is cancer-related (Figure 4.2a and c). However, the GSEA analysis also showed some lncRNAs are downregulated and associated with cancer (Figure 4.2b and d). This finding is consistent with our previous study on gene expression profiling.

We found genotoxicity, DNA damage, and p53-mediated stress response pathways significantly enriched, which collectively leads to carcinogenesis.[199] In addition, many of the lncRNAs in the database were experimentally validated and mechanistically linked to cancer development and progression.[223, 225] Thus, both up- and down-regulated lncRNAs found in this study could potentially contribute to carcinogenesis.

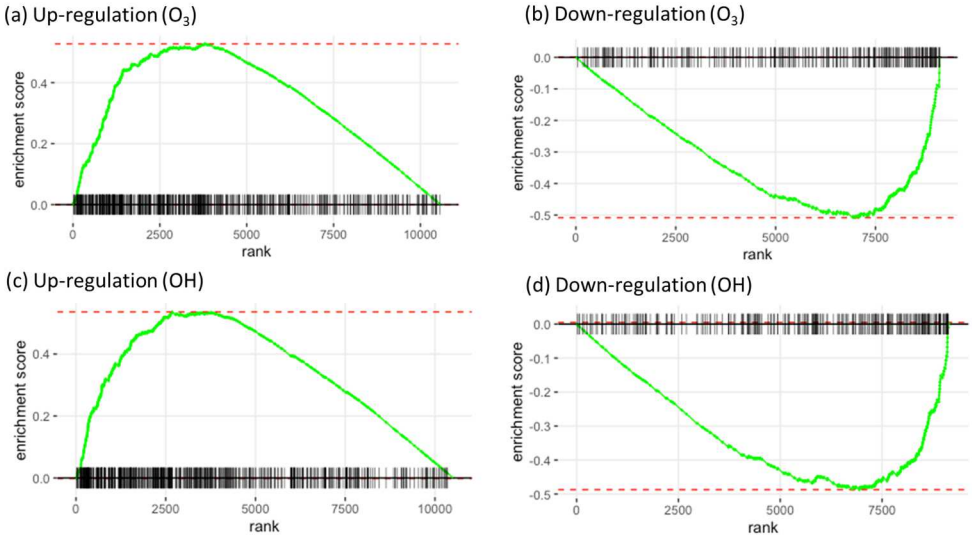

Figure 4.2. GSEA of cancer-related lncRNAs. (a-b) represents GSEA of DMSe-derived SOA from O_3 for up and down-regulation, respectively, and (c-d) represents DMSe-derived SOA from OH for up and down-regulation, respectively.

4.3.3. *Cis*-targeted Genes Prediction of the DE-lncRNAs

Differential co-expression of cancer-associated lncRNAs and mRNAs provides a putative network of lncRNA-mediated expression changes. We further investigated how DE lncRNAs can interact with the nearest target genes to regulate DMSe-derived SOA-induced gene regulation responses at the cellular level. To answer this question, we analyzed DE lncRNA and the mRNA within 10 kb upstream and downstream.

The hierarchical clustering of lncRNA and their respective mRNA showed that most up-regulation of lncRNA in both samples are correlated with the upregulation of their nearest coding genes (Figure 4.3a). Among these nearest genes, 279 and 285 genes were differentially expressed in cells exposed to O_3 and OH oxidation products from the neighboring lncRNAs (Figure 4.3b). In addition, 214 DE genes were common for both O_3 and OH oxidation products (Figure 4.3b). Among the *cis* acting nearby DE genes (Figure 4.3b), 196 and 191 genes showed the same expression trend with nearby lncRNAs for O_3 and OH, while 18 and 23 genes showed the opposite expression trend with neighboring lncRNAs for O_3 and OH, respectively (Figure S4.2-3). GO analysis of common 214 DE genes showed significantly enriched GO terms including T cell homeostasis, signal transduction involved in DNA damage checkpoint, signal transduction by p53 class mediator, regulation of SREBP signaling pathway, regulation of apoptotic signaling pathway, MAPK cascade, intrinsic apoptotic signaling pathway by p53 class mediator, cellular response to stress, and cell death (Figure 4.3c and Table S4.4). These results indicated that lncRNAs may participate in gene regulation related to p53-mediated signal transduction, DNA damage, cell death, apoptosis, cellular stress response, and MAPK cascade in BEAS-2B cells via *cis*-acting mechanisms.

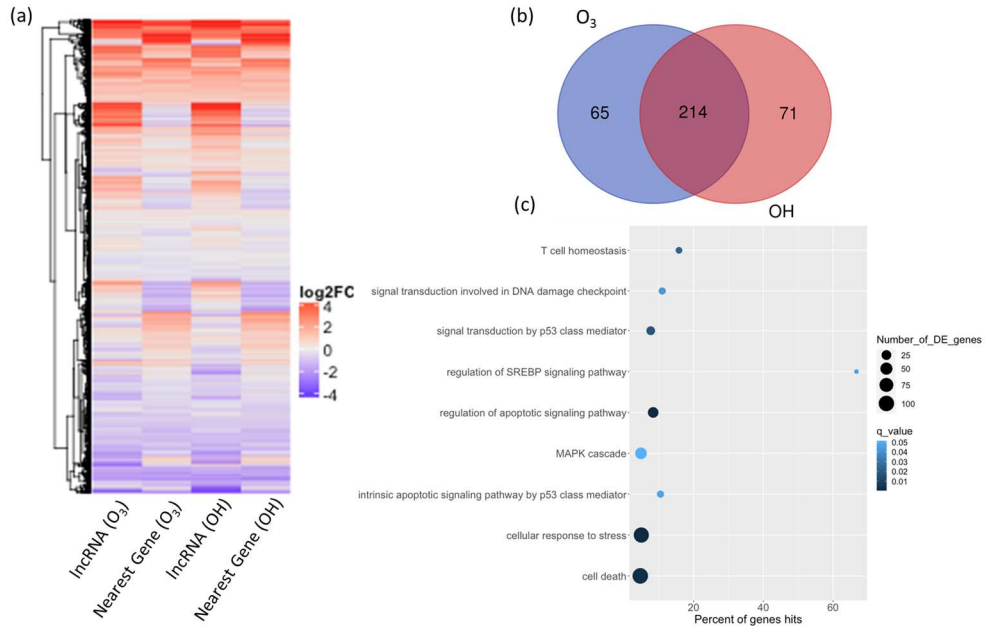

Figure 4.3. Predicted cis-targeted genes of the differentially expressed lncRNAs. (a) A heatmap generated from the log2FC values from RNA-Seq results to visualize the expression patterns of responsive lncRNAs and their neighboring genes in BEAS-2B cells exposed to DMSe-derived SOA from O_3 and OH oxidation products. (b) The number of *cis*-targeted DE genes predicted by DE lncRNAs. (c) GO enrichment analyses of the DE genes adjacent to the DE lncRNAs. The color of the dots represents *q* (FDR) values, and the size of the dot represents the number of DE genes mapped to the reference pathways.

4.3.4. Prediction of *trans*-targeted Genes of the DE lncRNAs

Previous studies have suggested that lncRNAs can regulate the expression of neighboring protein-coding genes, as well as genes located on other chromosomes via a *trans* mechanism.[226, 227] In this study, we predicted the potential *trans*-targeted genes of the top 20 DE lncRNAs common for both O_3 and OH oxidation products. A total of 2,000 *trans*-targeted genes were selected to construct the interaction network. The top 20 DE lncRNAs have a total of 239 potential *trans*-targeted genes ($\log2FC \geq |\pm1|$) (Table S4.5).

Among the 239 *trans*-acting DE genes for both O_3 and OH oxidation products, 124 genes showed the same expression trend (for up and down regulation) and 115 genes showed the opposite expression trend with the *trans*-acting lncRNAs (Figure S4.5). The interactions between lncRNAs and their DE target genes (log2FC > |±2|) are shown in Figure 4.4. Most coding genes are regulated by distinct lncRNA. Notably, a few coding genes (e.g., *TSPAN11, TNNI1, ACHE, HOXB9, SRCIN1, IGF2, MEX3B, PGPEP1, KCNA7, POPDC2, IQSEC3, ZNF662*) could be regulated by multiple lncRNAs (Figure 4.4 and Table S4.5).

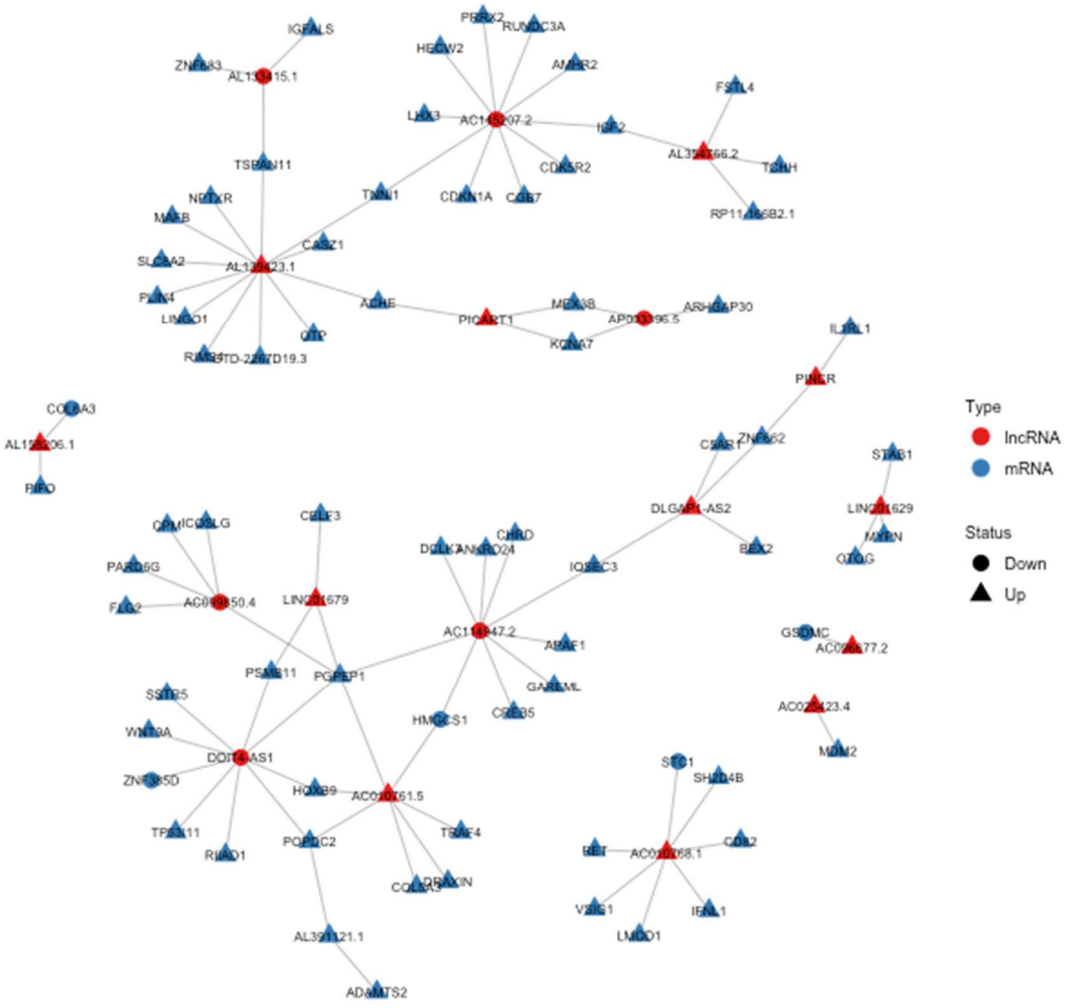

Figure 4.4. Predicted trans-targeted genes (log2FC>|±2|) and regulatory network of the differentially expressed lncRNAs. The regulatory network of top 20 DE lncRNAs (with the lowest FDRs) was built by R package (version 3.6.3) for both O_3 and OH oxidation products. The colors represent type of RNAs. Blue: mRNA; red: lncRNA. The triangles denote up-regulation, and the dots represent the downregulation.

4.4. Discussion

The lncRNA response to DMSe-derived SOA exposure is consistent with our previous findings, showing that common O_3 and OH oxidation products (typically Se-containing aerosol constituents) interplay with cellular responses.[199]

However, the exact association between lncRNAs and gene expression in this context remains to be elucidated fully. Growing evidence suggests that lncRNAs can regulate gene expression at epigenetic, transcriptional, and post-transcriptional levels, and are widely involved in various physiological and pathological processes.[206, 228, 229] Our previous study indicated that DMSe-derived SOA induced differential gene expression associated with p53-mediated stress response, genotoxicity, and DNA damage pathways in BEAS-2B cells.[199] These pathways are collectively responsible for carcinogenesis. Here, we demonstrate that cancer-related lncRNAs (as documented in the public database[223]) are differentially expressed in response to DMSe-SOA exposure.

Increasing evidence has revealed that altered expression of many lncRNAs can be found in various types of human cancers. Dysregulated lncRNAs may behave like tumor suppressors or oncogenes via interaction with the promoter or enhancer regions of a gene and modulate the gene expression.[230] Therefore, a further exploration of the roles and mechanisms of lncRNAs involved in different stages of cancer development (i.e., initiation, promotion and progression) is critical to provide novel lncRNA-based strategies for the treatment of human cancers. Some well-studied lncRNAs have been reported as oncogenes (e.g., *HOTAIR*[231] and *MALAT1*[232]), and tumor suppressors (e.g., *MEG3*[233]). We anticipate that the DE lncRNAs identified in this study could provide valuable information for lncRNA-based biomarkers for cancer diagnosis and prognosis. A recent study reported that after DNA damage, a p53-regulated lncRNA *PINCR* (p53-induced noncoding RNA) was induced nearly100-fold and exerted a pro-survival function in human colorectal cancer cells *in vitro* and tumor growth *in vivo*.[234]

In addition, a novel lncRNA *PICART1* (p53-inducible cancer-associated RNA transcript 1) was identified and found to be upregulated by p53.[235] *PICART1* expression was found to be decreased in breast and colorectal cancer cells and tissues. Their study suggests that *PICART1* is a novel p53-inducible tumor-suppressor lncRNA.[235] In this study, we found DE *PINCR* (log2FC 4.88) and *PICART1* (log2FC 3.16) (Fig 4.4, Table S4.5), which potentially suggest that *PINCR* and *PICART1* might be involved in p53-mediated gene regulation when exposed to DMSe-derived SOA.

On the other hand, our study identified lncRNA *LINC01629* (log2FC 4.97) (Table S4.5), which has been reported as a potential biomarker associated with oral squamous cell carcinoma (one of the most common malignancies worldwide).[236] In addition, lncRNA DLGAP1 antisense RNA 2 (*DLGAP1-AS2*) (log2FC 2.34) (Table S4.5) was found in our study, which has been reported to be up-regulated significantly in glioma.[237] It has been confirmed that loss of *DLGAP1-AS2* in glioma cells could induce cell apoptosis, resulting in the suppression of the progression of glioma.[237] Another study reported that lncRNA *DLGAP1-AS2* knockdown may inhibit hepatocellular carcinoma cell migration and invasion by regulating miR-154-5p methylation.[238] Therefore, our above-identified lncRNAs could potentially act as mediators for modulating cancer development following exposure to DMSe-derived SOA.

High mortality and low survival rates for cancers mainly result from the delay in diagnosis.[239] Recently, lncRNAs have been explored as potential biomarkers for early detection of cancers.[239] In fact, increasing investigations show that lncRNAs are cell- and tumor-specific, and play critical roles in many biological processes.

Thus, lncRNAs could be used as diagnostic markers or therapeutic targets in various cancer types.[239, 240] Studies suggest that *PANDA* is overexpressed in many tumors and may potentially act as a biomarker for cancer diagnosis.[241] In addition, *NEAT1* (Nuclear Enriched Abundant Transcript 1) was identified as a direct p53-target gene and it drove tumor initiation and progression, and thus could serve as a diagnostic biomarker.[242] Overall, our identified DE cancer-related lncRNAs could also potentially be used as biomarkers for early detection of DMSe SOA-induced health outcomes.

We used the RNA-Seq technique to profile the DE lncRNAs in BEAS-2B cells exposed to DMSe-SOA. In contrast to the known mRNA functions, one major challenge in lncRNA profiling is that the functions of most lncRNAs have not been determined, and no existing database is currently available to identify their functional annotations.[227] Mounting evidence demonstrates that lncRNAs can regulate the expression of neighboring (*cis*) and distant (*trans*) target genes, and the expression of lncRNAs is highly correlated with expression of neighboring (*cis*) and distant (*trans*) target genes.[227, 243] In our study, GO analysis of the DE *cis*-target genes showed connections with the following pathways: signal transduction involved in DNA damage checkpoint, signal transduction by p53 class mediator, regulation of SREBP signaling pathway, regulation of apoptotic signaling pathway, MAPK cascade, intrinsic apoptotic signaling pathway by p53 class mediator, cellular response to stress, and cell death in DMSe-derived SOA exposed BEAS-2B cells (Table S4.4). Most of these pathways were found in our previous study.[199]

Here, we found a clear pattern that DMSe-derived SOA is potentially responsible for DNA damage and p53 signaling pathways, and that co-expressed DE lncRNAs could

regulate these biological processes via *cis* mechanisms. LncRNAs can interact with associated mRNAs via the formation of complementary hybrids and it can work from both nearby and distant sites.[244] In this study, the top 20 DE-lncRNAs and their potential *trans*-targeted genes were identified (Figure 4.4). Some genes (e.g., *SRCIN1, MEX3B, TSPAN11, ZNF662*) were found to be associated with multiple lncRNAs (Figure 4.4). Many of these have been reported to be associated with cancer pathogenesis in previous studies. For example, *SRCIN1* (SRC kinase signaling inhibitor 1), which translates a docking/adaptor protein is co-expressed with both lncRNA *AC145207.2* and *PICART1* (Figure 4.4). *SRCIN1* behaves as a tumor suppressor in breast cancer, and recent studies reported that this is also correlated with delaying tumor progression for colorectal cancer.[245] Additionally, *MEX3B* (muscle excess 3 RNA binding family member B) is associated with lncRNA *PICART1* and *AP003396.5* (Figure 4.4). This gene is involved in the process of apoptosis, increased invasion of gastric cancer cells, and tumorigenesis.[246] The *HOXB9* (homeobox superfamily, cluster B 9) gene is involved with both lncRNA *DDIT4-AS1* and *AC010761.5*. This gene can regulate lung adenocarcinoma progression.[247] Furthermore, *TSPAN11* (Tetraspanin 11) is co-expressed with both *AL139423.1* and *AL133415.1*, which has the potential to influence invasiveness and metastasis of cancer cells.[248]

ZNF662 (zinc finger protein 662), which is the largest family of sequence-specific DNA binding proteins and encoded by 2% of human genes,[249] is co-expressed with both *PINCR* and *DLGAP1-AS2* (Figure 4.4). It has been reported that epigenetic changes of *ZNF662* genes may be associated with the development and progression of oral squamous cell carcinoma.[250] Gene *IGF2* (insulin-like growth factor 2) is involved with both lncRNA

AC145207.2 and *AL354766.2* (Figure 4.4), which can regulate lung tumorigenesis in lung epithelial cells by promoting exocytosis of *IGF2*.[251] All these above findings indicate that lncRNAs may regulate these genes to participate in the regulation of cancer progression via *trans* mechanisms.

While the current study provides novel information at the transcriptomic level regarding cellular responses to DMSe-derived SOA through epigenetic mechanisms, cautions are needed in interpretation of results. First, the exposure was carried out using an immortalized (BEAS-2B) human bronchial epithelial cell line that does not differentiate or develop tight junctions. In addition, many lncRNAs show tissue-specific expression patterns. Future studies are warranted to utilize primary cell cultures or *in vivo* inhalation designs to investigate the transcriptional and epigenetic changes induced by DMSe-derived SOA exposure. Further functional validation at the phenotype level will also be required to demonstrate the e□ects on the changes of DMSe-derived SOA exposure from the epigenetic perspective.

4.5. Conclusion

Taken together, lncRNAs constitute a critical hidden layer of gene regulation in complex organisms that may contribute to lung carcinogenesis and its complications through dysregulation of gene expression.[252-254] By profiling the expression of both lncRNAs and mRNAs, our findings indicate that lncRNAs are potentially involved in the modulation of DNA damage responses in BEAS-2B cells exposed to DMSe-SOA. Specifically, cancer-related lncRNAs were found to be differentially expressed, and these lncRNAs may modulate carcinogenesis via *cis* and *trans* regulatory mechanisms. GO

network analysis of *cis*-targeted genes showed significantly enriched GO terms for DNA damage, apoptosis, and p53-mediated stress response pathways. Among the top 20 potential *trans*-acting lncRNAs, 4 lncRNAs (e.g., *PINCR, PICART1, DLGAP1-AS2, LINC01629*) are linked to human carcinogenesis. Our findings provide a useful resource for further investigation of whether specific lncRNAs or a set of lncRNAs identified here can serve as biomarkers for lung carcinogenesis. Therefore, validation of the affected biological functions is required to confirm their clinical significance.

4.6. Supplementary Information

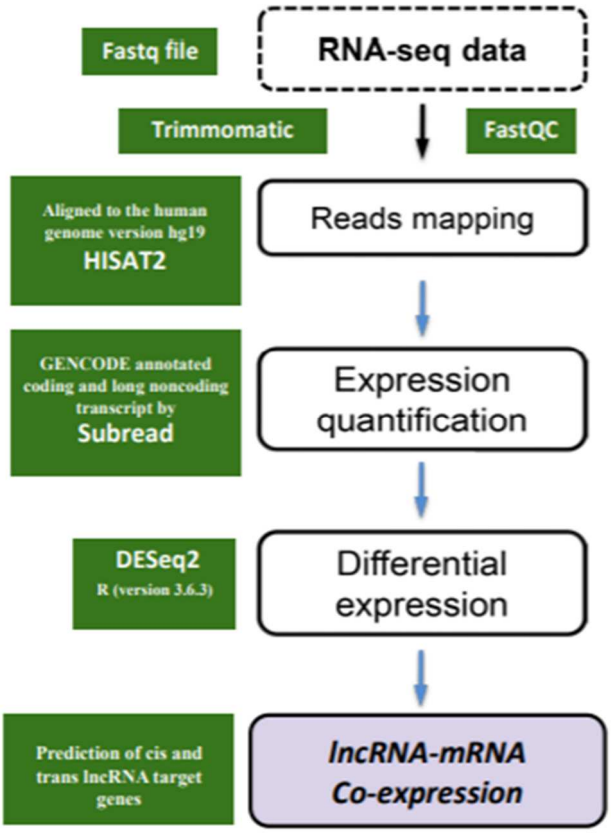

Figure S4.1. The workflow for RNA-Seq data analysis for lncRNAs.

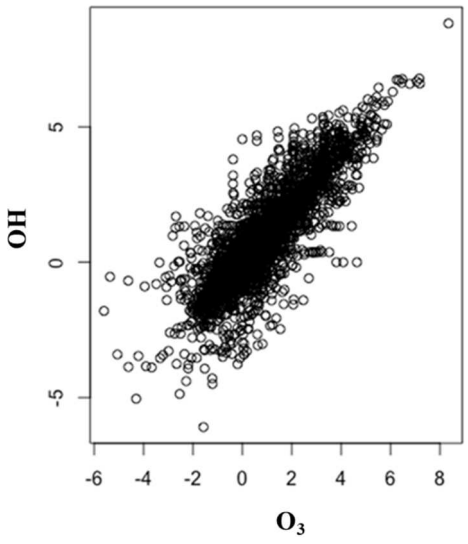

Figure S4.2. Correlation of differentially expressed lncRNAs in BEAS-2B cells exposed to DMSe-derived SOA from O_3 and OH oxidation.

Table S4.1. Number of reads aligned to mRNA and lncRNA.

Sample	**mRNA**	**lncRNA**
Control#1	30991631	1658724
Control#2	32203734	1802536
Control#3	20674281	1216303
O_3#1	28334958	1807673
O_3#2	26522679	1667846
O_3#3	30726267	1930738
OH#1	14129905	906934
OH#2	20597118	1332204
OH#3	19334403	1202592

Table S4.2: Expression information of DE-lncRNAs and nearby protein-coding genes for O3 oxidation.

lncRNAs					Nearby Genes				
lncRNA ID	lncRNA symbol	log2FC	FDR value	status	Gene ID	Gene symbol	log2FC	FDR value	status
ENSG00000272411.1	AC116312.1	4.58	4.46E-03	Up	ENSG00000169247	SH3TC2	-3.00	3.92E-36	Down
ENSG00000256006.1	AC084117.1	-2.54	6.80E-03	Down	ENSG00000134333	LDHA	-2.91	0.00E+00	Down
ENSG00000227220.1	AL133346.1	-2.74	1.67E-74	Down	ENSG00000118523	CTGF	-2.72	0.00E+00	Down
ENSG00000261604.1	AC114947.2	-2.46	6.63E-89	Down	ENSG00000112972	HMGCS1	-2.69	0.00E+00	Down
ENSG00000265415.1	AC099850.4	-2.24	#######	Down	ENSG00000068489	PRR11	-2.26	7.11E-75	Down
ENSG00000228404.1	AP001468.1	-1.63	5.71E-07	Down	ENSG00000160285	LSS	-2.18	2.71E-77	Down
ENSG00000242396.1	AC096536.2	-2.08	3.80E-43	Down	ENSG00000116133	DHCR24	-2.13	6.83E-85	Down
ENSG00000258232.2	AC125611.3	-2.03	1.01E-80	Down	ENSG00000167553	TUBA1C	-2.12	4.99E-183	Down
ENSG00000271795.1	AC011337.1	-1.61	4.95E-08	Down	ENSG00000086570	FAT2	-2.08	2.44E-32	Down
ENSG00000261468.1	AC096921.2	-2.93	3.58E-35	Down	ENSG00000163513	TGFBR2	-1.98	1.08E-73	Down
ENSG00000255202.1	AL049629.1	1.71	1.34E-03	Up	ENSG00000110427	KIAA1549L	-1.97	3.61E-07	Down
ENSG00000259827.1	AC026461.1	-1.86	2.84E-33	Down	ENSG00000187193	MT1X	-1.97	1.33E-50	Down
ENSG00000205890.3	AC108134.1	1.81	3.00E-03	Up	ENSG00000103145	HCFC1R1	-1.95	5.91E-70	Down
ENSG00000272711.1	AC019069.1	-1.57	4.94E-17	Down	ENSG00000159399	HK2	-1.90	4.48E-45	Down
ENSG00000235837.1	AC073333.1	-1.74	1.73E-45	Down	ENSG00000136261	BZW2	-1.87	8.88E-127	Down
ENSG00000243415.2	AC107021.1	-2.51	6.23E-05	Down	ENSG00000152952	PLOD2	-1.84	1.42E-211	Down
ENSG00000253837.1	AC090197.1	-1.71	7.82E-21	Down	ENSG00000134013	LOXL2	-1.83	2.49E-90	Down
ENSG00000238258.1	AL121748.1	-1.80	1.28E-28	Down	ENSG00000099250	NRP1	-1.83	1.76E-58	Down
ENSG00000257042.1	AC008011.2	-1.56	3.61E-12	Down	ENSG00000087494	PTHLH	-1.75	9.73E-35	Down
ENSG00000265168.1	AC005726.3	-1.67	2.28E-55	Down	ENSG00000109107	ALDOC	-1.74	2.77E-85	Down
ENSG00000268262.1	AC011445.1	-1.81	2.89E-07	Down	ENSG00000128011	LRFN1	-1.73	5.08E-20	Down
ENSG00000269926.1	DDIT4-AS1	-1.62	9.60E-85	Down	ENSG00000168209	DDIT4	-1.68	2.58E-210	Down
ENSG00000263873.1	AP003396.5	-1.61	#######	Down	ENSG00000154096	THY1	-1.66	2.06E-107	Down
ENSG00000257225.1	AC079601.2	-1.60	3.77E-60	Down	ENSG00000139174	PRICKLE1	-1.66	6.22E-36	Down
ENSG00000269899.1	AC025857.2	-2.04	3.77E-08	Down	ENSG00000079459	FDFT1	-1.66	4.95E-125	Down
ENSG00000235897.1	TM4SF19-AS1	-1.31	1.13E-16	Down	ENSG00000145107	TM4SF19	-1.65	7.28E-06	Down
ENSG00000257671.1	KRT7-AS	-1.62	3.00E-81	Down	ENSG00000135480	KRT7	-1.64	6.94E-127	Down
ENSG00000257453.1	AC011611.3	-1.65	1.25E-42	Down	ENSG00000139289	PHLDA1	-1.64	7.94E-47	Down
ENSG00000254682.1	AP002387.2	-1.18	6.08E-05	Down	ENSG00000172893	DHCR7	-1.62	2.83E-104	Down
ENSG00000269292.1	AC093503.2	-1.23	2.71E-66	Down	ENSG00000160013	PTGIR	-1.60	1.45E-04	Down
ENSG00000255202.1	AL049629.1	1.71	1.34E-03	Up	ENSG00000085063	CD59	-1.60	9.16E-95	Down
ENSG00000257452.1	AC004551.1	-1.88	1.52E-05	Down	ENSG00000089127	OAS1	-1.59	2.45E-30	Down
ENSG00000233110.1	AC093797.1	-1.93	6.25E-03	Down	ENSG00000154556	SORBS2	-1.58	1.24E-13	Down
ENSG00000226526.1	AL049569.1	-1.56	3.81E-28	Down	ENSG00000159363	ATP13A2	-1.55	5.06E-121	Down
ENSG00000228838.1	AL355483.1	-1.16	1.04E-03	Down	ENSG00000157193	LRP8	-1.55	2.38E-56	Down
ENSG00000262624.1	AC113189.1	-1.67	1.00E-07	Down	ENSG00000181284	TMEM102	-1.54	8.09E-28	Down

ENSG00000205890.3	AC108134.1	1.81	3.00E-03	Up	ENSG00000131652	THOC6	-1.53	9.03E-76	Down
ENSG00000228404.1	AP001468.1	-1.63	5.71E-07	Down	ENSG00000235878	AP001468.1	-1.53	2.76E-09	Down
ENSG00000267898.1	AC026803.2	2.56	1.44E-06	Up	ENSG00000104812	GYS1	-1.52	5.67E-53	Down
ENSG00000234961.1	AL133415.1	-1.48	4.10E-91	Down	ENSG00000026025	VIM	-1.52	1.97E-113	Down
ENSG00000231864.2	AL807752.3	-1.48	1.50E-32	Down	ENSG00000186193	SAPCD2	-1.47	3.05E-28	Down
ENSG00000258424.1	AL512791.1	-1.43	9.82E-37	Down	ENSG00000198668	CALM1	-1.42	5.04E-74	Down
ENSG00000232220.2	AC008440.1	-1.16	5.31E-25	Down	ENSG00000179820	MYADM	-1.42	1.15E-42	Down
ENSG00000261898.2	AC091153.4	-1.34	4.09E-12	Down	ENSG00000161920	MED11	-1.41	1.62E-27	Down
ENSG00000269968.1	AC006064.4	-1.35	7.57E-57	Down	ENSG00000111640	GAPDH	-1.40	2.73E-101	Down
ENSG00000261532.1	AC009065.8	-1.09	2.98E-18	Down	ENSG00000184207	PGP	-1.39	1.54E-51	Down
ENSG00000262413.1	AC145207.2	-1.42	#######	Down	ENSG00000141522	ARHGDIA	-1.39	2.02E-152	Down
ENSG00000244161.1	FLNB-AS1	-1.50	4.62E-53	Down	ENSG00000136068	FLNB	-1.38	2.17E-20	Down
ENSG00000258086.1	AC079313.1	-1.11	3.30E-06	Down	ENSG00000161638	ITGA5	-1.37	4.74E-54	Down
ENSG00000272182.1	AC135507.1	-1.41	8.74E-25	Down	ENSG00000168291	PDHB	-1.37	5.91E-44	Down
ENSG00000267484.1	AC027319.1	-1.18	1.16E-21	Down	ENSG00000105355	PLIN3	-1.33	1.17E-111	Down
ENSG00000235865.2	GSN-AS1	-1.40	3.91E-12	Down	ENSG00000148180	GSN	-1.32	9.49E-95	Down
ENSG00000240963.1	AL645465.1	-1.26	9.52E-21	Down	ENSG00000035687	ADSS	-1.31	5.46E-111	Down
ENSG00000273055.1	AC005046.2	-1.04	3.42E-04	Down	ENSG00000091136	LAMB1	-1.29	5.57E-110	Down
ENSG00000261113.1	AC009034.1	-1.58	3.68E-09	Down	ENSG00000103319	EEF2K	-1.28	4.90E-27	Down
ENSG00000246640.1	PICART1	3.16	#######	Up	ENSG00000005884	ITGA3	-1.27	1.26E-59	Down
ENSG00000265194.1	AL359922.2	-1.20	2.02E-29	Down	ENSG00000099810	MTAP	-1.27	1.09E-40	Down
ENSG00000228037.1	AL139246.3	8.35	1.63E-11	Up	ENSG00000157870	FAM213B	-1.26	8.22E-29	Down
ENSG00000272931.1	AC099568.2	-1.58	1.61E-04	Down	ENSG00000271949	RP11-302M6.4	-1.25	2.84E-03	Down
ENSG00000254829.1	AP003032.2	-1.13	2.00E-24	Down	ENSG00000151364	KCTD14	-1.24	9.86E-23	Down
ENSG00000265579.1	AC023301.1	-1.72	6.41E-14	Down	ENSG00000166342	NETO1	-1.24	1.02E-18	Down
ENSG00000243960.1	AL390195.2	-1.27	2.07E-65	Down	ENSG00000116455	WDR77	-1.24	6.78E-65	Down
ENSG00000254027.1	AC009902.2	-1.29	1.74E-10	Down	ENSG00000164687	FABP5	-1.24	1.00E-17	Down
ENSG00000251072.2	LMNB1-DT	2.13	2.61E-03	Up	ENSG00000113368	LMNB1	-1.23	7.27E-116	Down
ENSG00000237655.1	AC073834.1	-1.68	1.96E-04	Down	ENSG00000197557	TTC30A	-1.21	5.90E-10	Down
ENSG00000253645.1	AC108863.2	-1.12	6.26E-22	Down	ENSG00000169499	PLEKHA2	-1.20	2.44E-11	Down
ENSG00000237768.2	AL731563.3	-1.36	3.57E-15	Down	ENSG00000122884	P4HA1	-1.20	1.12E-86	Down
ENSG00000272129.1	AL359715.3	-1.26	1.23E-03	Down	ENSG00000083123	BCKDHB	-1.20	4.94E-26	Down
ENSG00000233589.1	AL138789.1	-1.15	7.30E-27	Down	ENSG00000024526	DEPDC1	-1.20	1.19E-56	Down
ENSG00000259863.1	SH3RF3-AS1	-1.65	3.66E-37	Down	ENSG00000172985	SH3RF3	-1.19	5.07E-15	Down
ENSG00000271980.1	AC012640.6	-1.04	1.16E-16	Down	ENSG00000150753	CCT5	-1.19	3.36E-58	Down
ENSG00000227279.1	AC110015.1	-1.00	1.96E-13	Down	ENSG00000170558	CDH2	-1.18	1.23E-41	Down
ENSG00000264785.1	AC005722.4	-1.26	1.41E-04	Down	ENSG00000108602	ALDH3A1	-1.18	7.49E-17	Down
ENSG00000268015.1	AC010320.3	-1.16	1.79E-21	Down	ENSG00000105568	PPP2R1A	-1.17	5.31E-101	Down
ENSG00000230698.1	AC105935.2	-1.17	4.43E-05	Down	ENSG00000164078	MST1R	-1.16	2.39E-42	Down
ENSG00000245385.2	AP003396.1	-1.16	3.53E-22	Down	ENSG00000173456	RNF26	-1.16	5.97E-46	Down
ENSG00000265784.1	AC006441.3	-1.04	2.55E-44	Down	ENSG00000002834	LASP1	-1.16	1.83E-33	Down
ENSG00000258377.1	AL139099.2	-1.09	5.80E-37	Down	ENSG00000168282	MGAT2	-1.15	7.85E-54	Down

ENSG00000258177.1	AC008149.1	-1.23	3.99E-21	Down	ENSG00000111145	ELK3	-1.13	7.21E-21	Down
ENSG00000264044.1	AC005726.2	-1.08	2.20E-10	Down	ENSG00000007202	KIAA0100	-1.13	2.38E-25	Down
ENSG00000260944.1	FOXC2-AS1	-1.09	6.65E-04	Down	ENSG00000176692	FOXC2	-1.13	1.45E-18	Down
ENSG00000254821.1	AL136309.3	-1.16	3.28E-03	Down	ENSG00000198721	ECI2	-1.13	2.35E-35	Down
ENSG00000261416.1	AC012645.3	-1.10	2.71E-03	Down	ENSG00000102879	CORO1A	-1.12	4.20E-31	Down
ENSG00000239775.1	AC017116.1	2.17	5.39E-14	Up	ENSG00000136279	DBNL	-1.11	8.44E-54	Down
ENSG00000258749.1	AL110504.1	-1.24	3.32E-32	Down	ENSG00000205476	CCDC85C	-1.10	1.54E-15	Down
ENSG00000270362.1	HMGN3-AS1	-1.02	1.11E-05	Down	ENSG00000118418	HMGN3	-1.09	7.72E-15	Down
ENSG00000256944.1	AP003721.3	-1.75	6.16E-03	Down	ENSG00000110108	TMEM109	-1.09	1.15E-60	Down
ENSG00000224821.5	COL4A2-AS2	-1.54	1.29E-03	Down	ENSG00000134871	COL4A2	-1.08	1.72E-29	Down
ENSG00000251018.2	HMMR-AS1	-1.02	3.36E-16	Down	ENSG00000072571	HMMR	-1.07	4.34E-61	Down
ENSG00000267546.2	AC015802.4	2.46	7.46E-32	Up	ENSG00000161544	CYGB	-1.07	1.09E-62	Down
ENSG00000258777.1	HIF1A-AS1	-1.06	3.27E-11	Down	ENSG00000100644	HIF1A	-1.05	5.24E-48	Down
ENSG00000223947.1	AC016738.1	-1.16	5.40E-10	Down	ENSG00000170485	NPAS2	-1.03	3.57E-14	Down
ENSG00000228404.1	AP001468.1	-1.63	5.71E-07	Down	ENSG00000160284	SPATC1L	-1.03	2.54E-13	Down
ENSG00000268191.1	AC010503.2	-2.19	6.94E-03	Down	ENSG00000104833	TUBB4A	-1.03	2.46E-03	Down
ENSG00000257715.1	AC007298.1	-1.13	1.10E-21	Down	ENSG00000111144	LTA4H	-1.01	5.69E-43	Down
ENSG00000259884.1	NR4A1AS	1.27	2.50E-14	Up	ENSG00000123358	NR4A1	1.01	1.19E-13	Up
ENSG00000245148.2	ARAP1-AS2	1.08	1.27E-09	Up	ENSG00000186635	ARAP1	1.02	1.10E-52	Up
ENSG00000256007.1	ARAP1-AS1	1.08	1.03E-21	Up	ENSG00000186635	ARAP1	1.02	1.10E-52	Up
ENSG00000260593.1	AC009097.2	1.35	2.54E-03	Up	ENSG00000140832	MARVELD3	1.02	3.85E-09	Up
ENSG00000259539.1	AC051619.5	1.27	9.19E-04	Up	ENSG00000138606	SHF	1.03	1.56E-05	Up
ENSG00000255108.1	AP006621.1	1.06	3.67E-51	Up	ENSG00000177666	PNPLA2	1.03	5.41E-63	Up
ENSG00000261054.1	AC036108.2	1.10	5.78E-09	Up	ENSG00000182253	SYNM	1.04	1.00E-10	Up
ENSG00000244268.1	AC117394.2	2.48	4.99E-03	Up	ENSG00000181467	RAP2B	1.09	2.81E-29	Up
ENSG00000260107.1	AC005606.1	1.07	1.29E-28	Up	ENSG00000167962	ZNF598	1.10	9.14E-58	Up
ENSG00000271992.1	AL354872.2	1.79	8.16E-05	Up	ENSG00000116761	CTH	1.12	7.30E-25	Up
ENSG00000249007.1	AL691482.4	1.29	2.90E-06	Up	ENSG00000163435	ELF3	1.12	7.74E-07	Up
ENSG00000253930.1	TNFRSF10A-AS1	1.37	1.60E-32	Up	ENSG00000104689	TNFRSF10A	1.13	2.28E-42	Up
ENSG00000250379.1	AC020659.2	1.28	2.16E-26	Up	ENSG00000137802	MAPKBP1	1.14	3.73E-18	Up
ENSG00000229953.1	AL590666.2	1.24	2.40E-05	Up	ENSG00000132692	BCAN	1.14	7.32E-05	Up
ENSG00000272405.1	AL365181.3	1.18	9.53E-19	Up	ENSG00000132692	BCAN	1.14	7.32E-05	Up
ENSG00000269915.1	AP006621.4	1.15	3.86E-21	Up	ENSG00000177106	EPS8L2	1.15	1.57E-110	Up
ENSG00000234869.1	AL021392.1	2.48	3.74E-06	Up	ENSG00000075275	CELSR1	1.15	5.73E-20	Up
ENSG00000271781.1	AC026740.1	2.68	5.13E-15	Up	ENSG00000268885	AC026740.1	1.15	2.86E-09	Up
ENSG00000259941.1	AC084782.1	1.44	2.75E-07	Up	ENSG00000151575	TEX9	1.16	7.15E-18	Up
ENSG00000260084.1	AC126773.3	2.74	4.56E-04	Up	ENSG00000184939	ZFP90	1.17	9.18E-22	Up
ENSG00000266680.1	AL135905.1	2.74	1.05E-50	Up	ENSG00000112245	PTP4A1	1.18	6.07E-79	Up
ENSG00000268745.1	AL365205.3	1.59	8.29E-04	Up	ENSG00000164663	USP49	1.18	8.82E-07	Up
ENSG00000234478.1	ACBD3-AS1	1.11	2.28E-20	Up	ENSG00000182827	ACBD3	1.18	5.48E-47	Up
ENSG00000259436.1	AC010247.2	4.51	1.56E-03	Up	ENSG00000028277	POU2F2	1.19	2.51E-04	Up
ENSG00000271420.1	AL109936.3	2.66	6.36E-03	Up	ENSG00000125945	ZNF436	1.19	4.04E-17	Up

ENSG00000255992.1	AC131009.1	-1.36	4.75E-04	Down	ENSG00000177169	ULK1	1.19	1.93E-24	Up
ENSG00000243762.1	AC006547.2	1.14	6.45E-32	Up	ENSG00000128191	DGCR8	1.20	1.19E-37	Up
ENSG00000272933.1	AL391121.1	2.15	5.94E-98	Up	ENSG00000171206	TRIM8	1.20	1.14E-53	Up
ENSG00000268108.1	AC008687.2	2.14	3.59E-06	Up	ENSG00000225950	NTF4	1.20	4.23E-10	Up
ENSG00000272356.1	AL080317.2	1.26	4.23E-20	Up	ENSG00000009413	REV3L	1.22	1.44E-21	Up
ENSG00000260088.1	DDX59-AS1	1.59	4.12E-05	Up	ENSG00000118197	DDX59	1.22	6.55E-38	Up
ENSG00000238186.1	AL603839.2	1.22	1.55E-13	Up	ENSG00000164002	EXO5	1.23	7.61E-58	Up
ENSG00000227278.1	AL603839.1	1.30	7.51E-33	Up	ENSG00000164002	EXO5	1.23	7.61E-58	Up
ENSG00000255958.1	AC115676.1	1.70	2.32E-04	Up	ENSG00000139112	GABARAPL1	1.25	1.74E-40	Up
ENSG00000164621.5	SMAD5-AS1	1.65	4.90E-04	Up	ENSG00000113658	SMAD5	1.26	2.51E-20	Up
ENSG00000259416.2	AC021739.3	2.63	3.64E-03	Up	ENSG00000183655	KLHL25	1.26	3.11E-23	Up
ENSG00000257622.1	AL512356.1	1.83	4.63E-43	Up	ENSG00000183828	NUDT14	1.26	1.04E-24	Up
ENSG00000238123.1	MID1IP1-AS1	1.05	3.92E-06	Up	ENSG00000165175	MID1IP1	1.28	8.36E-84	Up
ENSG00000204666.3	AC010624.1	5.42	8.72E-42	Up	ENSG00000142528	ZNF473	1.28	2.14E-92	Up
ENSG00000231080.1	AL592161.1	2.44	1.90E-04	Up	ENSG00000152763	WDR78	1.28	5.00E-10	Up
ENSG00000232358.1	AL050404.1	1.30	1.01E-10	Up	ENSG00000026559	KCNG1	1.29	3.38E-25	Up
ENSG00000246323.2	AC113382.1	1.52	5.65E-08	Up	ENSG00000031003	FAM13B	1.29	1.00E-24	Up
ENSG00000254682.1	AP002387.2	-1.18	6.08E-05	Down	ENSG00000172890	NADSYN1	1.29	4.06E-92	Up
ENSG00000254812.1	AC067930.2	2.08	2.86E-07	Up	ENSG00000183309	ZNF623	1.30	3.69E-43	Up
ENSG00000268729.1	AC020922.2	1.39	1.33E-04	Up	ENSG00000160469	BRSK1	1.32	3.38E-30	Up
ENSG00000267898.1	AC026803.2	2.56	1.44E-06	Up	ENSG00000087088	BAX	1.33	2.25E-61	Up
ENSG00000268292.1	AC006547.3	1.45	3.25E-36	Up	ENSG00000183597	TANGO2	1.34	1.34E-39	Up
ENSG00000256249.1	AC026333.3	2.02	2.17E-24	Up	ENSG00000182782	HCAR2	1.34	2.99E-07	Up
ENSG00000260772.1	AC012321.1	1.36	1.60E-31	Up	ENSG00000102908	NFAT5	1.35	8.04E-04	Up
ENSG00000269989.1	AC036176.3	3.30	3.21E-04	Up	ENSG00000206075	SERPINB5	1.35	1.35E-93	Up
ENSG00000272734.1	ADIRF-AS1	1.09	1.47E-37	Up	ENSG00000173269	MMRN2	1.35	3.09E-04	Up
ENSG00000262899.1	AC004232.1	1.18	8.63E-05	Up	ENSG00000162086	ZNF75A	1.36	2.99E-31	Up
ENSG00000273419.1	AC004877.1	2.39	1.31E-20	Up	ENSG00000106479	ZNF862	1.36	2.33E-13	Up
ENSG00000272720.1	AL022322.1	2.10	5.07E-04	Up	ENSG00000128298	BAIAP2L2	1.37	2.20E-03	Up
ENSG00000255310.2	AF131215.5	1.40	1.25E-15	Up	ENSG00000171044	XKR6	1.38	3.59E-20	Up
ENSG00000269918.1	AF131215.6	1.30	2.26E-11	Up	ENSG00000171044	XKR6	1.38	3.59E-20	Up
ENSG00000272081.1	AC008972.2	2.04	6.63E-05	Up	ENSG00000157107	FCHO2	1.44	2.66E-57	Up
ENSG00000260892.1	AC105020.4	1.25	2.43E-05	Up	ENSG00000173546	CSPG4	1.47	4.19E-18	Up
ENSG00000225057.2	AC012485.1	1.12	8.08E-03	Up	ENSG00000132326	PER2	1.48	7.40E-17	Up
ENSG00000260196.1	AC124798.1	1.71	1.36E-48	Up	ENSG00000188211	NCR3LG1	1.48	1.97E-10	Up
ENSG00000243155.1	AL162431.1	1.59	7.01E-74	Up	ENSG00000135823	STX6	1.50	1.43E-73	Up
ENSG00000267424.1	AC020934.1	2.26	6.44E-04	Up	ENSG00000105613	MAST1	1.51	1.35E-16	Up
ENSG00000268186.1	ZNF114-AS1	3.38	1.57E-03	Up	ENSG00000178150	ZNF114	1.52	2.01E-13	Up
ENSG00000265126.1	AC004448.3	2.90	6.67E-03	Up	ENSG00000128482	RNF112	1.53	2.82E-04	Up
ENSG00000269125.1	AL137002.1	2.71	4.85E-05	Up	ENSG00000126231	PROZ	1.55	2.13E-05	Up
ENSG00000261202.1	Z83847.1	1.87	9.96E-03	Up	ENSG00000133477	FAM83F	1.55	1.74E-41	Up
ENSG00000240291.1	AL450384.2	1.60	3.91E-36	Up	ENSG00000165995	CACNB2	1.55	1.81E-14	Up

ENSG00000228544.1	CCDC183-AS1	1.37	2.35E-04	Up	ENSG00000213213	CCDC183	1.59	9.43E-07	Up
ENSG00000259955.1	AC008741.1	1.62	2.03E-13	Up	ENSG00000155592	ZKSCAN2	1.61	6.75E-26	Up
ENSG00000269082.1	AC010328.3	1.38	4.06E-03	Up	ENSG00000180257	ZNF816	1.63	2.31E-37	Up
ENSG00000268896.1	AC009955.3	2.87	1.39E-05	Up	ENSG00000188760	TMEM198	1.64	2.85E-11	Up
ENSG00000260618.1	AC025917.1	1.37	1.57E-09	Up	ENSG00000047346	FAM214A	1.68	1.32E-84	Up
ENSG00000267510.1	AC011451.1	1.76	1.21E-16	Up	ENSG00000196110	ZNF699	1.69	7.62E-31	Up
ENSG00000225981.1	AC102953.1	6.78	1.26E-06	Up	ENSG00000164877	MICALL2	1.76	2.38E-125	Up
ENSG00000224459.1	SLC25A34-AS1	-1.19	3.13E-06	Down	ENSG00000162461	SLC25A34	1.77	1.79E-03	Up
ENSG00000246130.1	AC107959.2	4.42	3.99E-29	Up	ENSG00000120889	TNFRSF10B	1.79	8.38E-74	Up
ENSG00000253445.1	AC027309.1	1.70	7.79E-12	Up	ENSG00000214357	NEURL1B	1.80	1.08E-12	Up
ENSG00000271420.1	AL109936.3	2.66	6.36E-03	Up	ENSG00000204219	TCEA3	1.80	7.53E-80	Up
ENSG00000249906.1	AC006487.1	1.89	1.25E-16	Up	ENSG00000064300	NGFR	1.81	1.32E-40	Up
ENSG00000255308.1	CSRP3-AS1	1.52	2.58E-06	Up	ENSG00000129173	E2F8	1.82	1.65E-114	Up
ENSG00000255478.1	AP000944.1	2.61	5.30E-06	Up	ENSG00000173825	TIGD3	1.83	1.03E-14	Up
ENSG00000261668.1	AC093591.2	1.92	8.90E-26	Up	ENSG00000164070	HSPA4L	1.84	4.50E-115	Up
ENSG00000267249.1	AP005482.4	1.72	2.40E-18	Up	ENSG00000101624	CEP76	1.84	1.96E-160	Up
ENSG00000253187.2	HOXA10-AS	1.40	1.31E-04	Up	ENSG00000253293	HOXA10	1.86	5.70E-03	Up
ENSG00000272582.1	AL031587.3	4.14	8.79E-23	Up	ENSG00000100139	MICALL1	1.87	6.56E-99	Up
ENSG00000232220.2	AC008440.1	-1.16	5.31E-25	Down	ENSG00000126583	PRKCG	1.87	5.86E-03	Up
ENSG00000263787.1	SKAP1-AS1	4.86	1.23E-03	Up	ENSG00000141293	SKAP1	1.87	9.94E-03	Up
ENSG00000241111.1	AC092040.2	1.64	6.83E-22	Up	ENSG00000163637	PRICKLE2	1.89	6.00E-18	Up
ENSG00000226017.2	PRICKLE2-AS3	2.68	7.89E-07	Up	ENSG00000163637	PRICKLE2	1.89	6.00E-18	Up
ENSG00000272940.1	U62317.3	5.04	9.19E-04	Up	ENSG00000008735	MAPK8IP2	1.89	1.14E-25	Up
ENSG00000263171.1	AC026954.3	1.88	2.04E-36	Up	ENSG00000213859	KCTD11	1.90	1.12E-41	Up
ENSG00000272183.1	AC005041.3	1.73	9.34E-05	Up	ENSG00000179528	LBX2	1.91	2.81E-15	Up
ENSG00000257702.3	LBX2-AS1	2.03	1.72E-53	Up	ENSG00000179528	LBX2	1.91	2.81E-15	Up
ENSG00000243155.1	AL162431.1	1.59	7.01E-74	Up	ENSG00000135835	KIAA1614	1.95	6.21E-12	Up
ENSG00000232586.1	KIAA1614-AS1	2.96	1.32E-53	Up	ENSG00000135835	KIAA1614	1.95	6.21E-12	Up
ENSG00000243888.1	AL355140.1	2.52	3.25E-04	Up	ENSG00000107282	APBA1	1.96	6.17E-05	Up
ENSG00000267727.1	AC008738.5	2.01	2.43E-05	Up	ENSG00000245848	CEBPA	1.96	2.18E-07	Up
ENSG00000267580.1	AC008738.3	2.42	4.50E-17	Up	ENSG00000245848	CEBPA	1.96	2.18E-07	Up
ENSG00000232530.1	LIF-AS1	2.32	1.35E-08	Up	ENSG00000128342	LIF	2.00	1.99E-55	Up
ENSG00000271781.1	AC026740.1	2.68	5.13E-15	Up	ENSG00000171368	TPPP	2.02	4.09E-09	Up
ENSG00000257622.1	AL512356.1	1.83	4.63E-43	Up	ENSG00000184916	JAG2	2.02	2.23E-187	Up
ENSG00000233485.1	FHAD1-AS1	2.21	7.24E-03	Up	ENSG00000142621	FHAD1	2.03	2.36E-07	Up
ENSG00000240801.1	AC132217.1	2.64	6.60E-10	Up	ENSG00000167244	IGF2	2.03	4.35E-04	Up
ENSG00000232259.1	AL158166.2	1.79	4.98E-07	Up	ENSG00000132334	PTPRE	2.03	3.12E-124	Up
ENSG00000239775.1	AC017116.1	2.17	5.39E-14	Up	ENSG00000164708	PGAM2	2.04	2.23E-12	Up
ENSG00000259539.1	AC051619.5	1.27	9.19E-04	Up	ENSG00000137857	DUOX1	2.06	4.43E-42	Up
ENSG00000271787.1	AC104794.5	2.26	2.19E-25	Up	ENSG00000172059	KLF11	2.10	8.48E-33	Up
ENSG00000269275.1	AC020922.3	2.35	5.49E-04	Up	ENSG00000095752	IL11	2.12	3.35E-71	Up
ENSG00000229299.2	AL121845.1	2.74	4.86E-21	Up	ENSG00000130584	ZBTB46	2.13	8.42E-19	Up

ENSG00000255441.1	AC008750.2	1.69	9.80E-05	Up	ENSG00000142512	SIGLEC10	2.18	8.12E-10	Up
ENSG00000254760.1	AC008750.1	2.17	7.78E-04	Up	ENSG00000142512	SIGLEC10	2.18	8.12E-10	Up
ENSG00000258086.1	AC079313.1	-1.11	3.30E-06	Down	ENSG00000161642	ZNF385A	2.18	4.58E-154	Up
ENSG00000273216.1	AC002059.1	2.50	4.15E-04	Up	ENSG00000100276	RASL10A	2.23	2.48E-03	Up
ENSG00000266872.1	AC015688.6	2.11	7.41E-52	Up	ENSG00000141068	KSR1	2.27	5.00E-38	Up
ENSG00000265840.1	AC010761.5	2.34	#######	Up	ENSG00000076604	TRAF4	2.30	2.64E-301	Up
ENSG00000265474.1	AC010761.4	1.96	5.93E-79	Up	ENSG00000076604	TRAF4	2.30	2.64E-301	Up
ENSG00000256249.1	AC026333.3	2.02	2.17E-24	Up	ENSG00000255398	HCAR3	2.31	4.03E-28	Up
ENSG00000270751.1	FBXW7-AS1	2.44	3.43E-31	Up	ENSG00000109670	FBXW7	2.36	5.98E-156	Up
ENSG00000266957.1	AC012254.1	4.60	2.00E-03	Up	ENSG00000167216	KATNAL2	2.41	2.08E-06	Up
ENSG00000225905.1	AL391244.1	2.71	5.14E-03	Up	ENSG00000235098	ANKRD65	2.42	2.21E-27	Up
ENSG00000241886.1	AC112496.1	3.05	1.37E-10	Up	ENSG00000198814	GK	2.46	1.33E-94	Up
ENSG00000243055.1	GK-AS1	2.48	9.22E-31	Up	ENSG00000198814	GK	2.46	1.33E-94	Up
ENSG00000232010.1	DNMT3L-AS1	7.06	9.56E-08	Up	ENSG00000160223	ICOSLG	2.47	1.14E-37	Up
ENSG00000232363.1	AL021391.1	4.74	1.79E-03	Up	ENSG00000128408	RIBC2	2.49	5.01E-27	Up
ENSG00000225057.2	AC012485.1	1.12	8.08E-03	Up	ENSG00000144485	HES6	2.50	5.56E-116	Up
ENSG00000255438.2	AL354813.1	2.31	2.64E-30	Up	ENSG00000196562	SULF2	2.53	7.59E-132	Up
ENSG00000255092.1	AC010768.2	4.60	4.08E-03	Up	ENSG00000085117	CD82	2.58	2.31E-231	Up
ENSG00000254693.1	AC010768.1	2.68	1.33E-96	Up	ENSG00000085117	CD82	2.58	2.31E-231	Up
ENSG00000257202.1	AC084398.2	2.56	4.37E-50	Up	ENSG00000136048	DRAM1	2.59	1.75E-145	Up
ENSG00000265750.1	AC090772.3	1.39	3.66E-33	Up	ENSG00000154040	CABYR	2.60	1.38E-145	Up
ENSG00000230415.1	LINC01786	1.73	3.16E-05	Up	ENSG00000162572	SCNN1D	2.60	1.62E-59	Up
ENSG00000261888.1	AC144831.1	5.85	4.59E-23	Up	ENSG00000176845	METRNL	2.62	1.59E-208	Up
ENSG00000269275.1	AC020922.3	2.35	5.49E-04	Up	ENSG00000160472	TMEM190	2.63	1.81E-05	Up
ENSG00000272582.1	AL031587.3	4.14	8.79E-23	Up	ENSG00000128346	C22orf23	2.63	3.88E-98	Up
ENSG00000203362.2	POLH-AS1	2.40	7.85E-19	Up	ENSG00000170734	POLH	2.66	1.72E-131	Up
ENSG00000231542.1	TAB3-AS1	2.54	9.62E-09	Up	ENSG00000157625	TAB3	2.66	7.14E-73	Up
ENSG00000235512.1	TAB3-AS2	2.53	3.79E-47	Up	ENSG00000157625	TAB3	2.66	7.14E-73	Up
ENSG00000265408.1	AC009084.1	2.79	#######	Up	ENSG00000172831	CES2	2.67	6.27E-281	Up
ENSG00000237341.1	SYP-AS1	3.38	3.96E-04	Up	ENSG00000102003	SYP	2.84	1.42E-18	Up
ENSG00000256633.1	AP005019.1	1.75	5.83E-04	Up	ENSG00000186642	PDE2A	2.88	4.59E-29	Up
ENSG00000261996.1	AC004706.1	4.20	6.63E-53	Up	ENSG00000212734	C17orf100	2.90	1.70E-41	Up
ENSG00000266456.1	AP001178.3	2.32	2.64E-18	Up	ENSG00000176912	C18orf56	2.92	2.69E-32	Up
ENSG00000263727.1	AP001178.1	2.86	1.31E-03	Up	ENSG00000176912	C18orf56	2.92	2.69E-32	Up
ENSG00000272078.1	AL139423.1	2.71	2.12E-99	Up	ENSG00000130940	CASZ1	2.97	2.15E-159	Up
ENSG00000261215.1	AL162231.4	1.43	1.62E-11	Up	ENSG00000213927	CCL27	3.04	1.33E-05	Up
ENSG00000253389.2	AC113133.1	5.28	1.94E-04	Up	ENSG00000029534	ANK1	3.07	3.20E-49	Up
ENSG00000271730.1	AL390208.1	2.99	3.38E-78	Up	ENSG00000080546	SESN1	3.13	3.27E-305	Up
ENSG00000261863.1	LINC01996	4.63	7.04E-03	Up	ENSG00000188176	SMTNL2	3.16	3.08E-03	Up
ENSG00000177699.4	AC011944.1	2.51	5.91E-07	Up	ENSG00000058335	RASGRF1	3.16	6.52E-24	Up
ENSG00000255404.1	AP001266.1	3.86	5.12E-25	Up	ENSG00000172818	OVOL1	3.23	1.17E-11	Up
ENSG00000272321.1	AP003355.2	2.88	4.40E-03	Up	ENSG00000156486	KCNS2	3.24	4.86E-04	Up

ENSG00000246526.2	LINC002481	2.82	4.82E-03	Up	ENSG00000163993	S100P	3.25	1.34E-16	Up
ENSG00000246130.1	AC107959.2	4.42	3.99E-29	Up	ENSG00000173535	TNFRSF10C	3.26	2.52E-47	Up
ENSG00000255478.1	AP000944.1	2.61	5.30E-06	Up	ENSG00000162241	SLC25A45	3.27	2.05E-34	Up
ENSG00000224818.1	AC096677.2	3.34	6.84E-94	Up	ENSG00000174307	PHLDA3	3.28	3.58E-221	Up
ENSG00000266456.1	AP001178.3	2.32	2.64E-18	Up	ENSG00000079101	CLUL1	3.29	1.29E-25	Up
ENSG00000249641.2	HOXC13-AS	4.84	6.84E-07	Up	ENSG00000123364	HOXC13	3.32	2.79E-04	Up
ENSG00000242902.1	FLNC-AS1	3.12	2.35E-10	Up	ENSG00000128591	FLNC	3.33	3.74E-122	Up
ENSG00000225062.1	CATIP-AS1	1.86	4.78E-05	Up	ENSG00000158428	C2orf62	3.37	9.45E-15	Up
ENSG00000211683.3	AP000346.1	2.85	1.37E-03	Up	ENSG00000189269	C22orf43	3.38	9.05E-05	Up
ENSG00000272482.1	AC254633.1	5.30	9.61E-09	Up	ENSG00000162496	DHRS3	3.53	9.19E-110	Up
ENSG00000226510.1	UPK1A-AS1	2.37	5.59E-06	Up	ENSG00000105668	UPK1A	3.56	7.28E-09	Up
ENSG00000256897.1	AC018410.1	1.82	7.91E-03	Up	ENSG00000134574	DDB2	3.68	0.00E+00	Up
ENSG00000273361.1	AC021016.3	-1.41	2.55E-04	Down	ENSG00000018280	SLC11A1	3.80	1.61E-04	Up
ENSG00000262001.1	DLGAP1-AS2	2.34	3.61E-99	Up	ENSG00000170579	DLGAP1	3.83	1.98E-06	Up
ENSG00000233611.3	AC019068.1	3.23	3.21E-03	Up	ENSG00000168505	GBX2	3.91	9.98E-07	Up
ENSG00000260912.1	AL158206.1	3.99	#######	Up	ENSG00000177076	ACER2	3.92	7.82E-71	Up
ENSG00000266872.1	AC015688.6	2.11	7.41E-52	Up	ENSG00000168961	LGALS9	3.93	5.51E-07	Up
ENSG00000266990.1	AC004528.1	5.08	2.15E-03	Up	ENSG00000116032	GRIN3B	3.98	1.15E-64	Up
ENSG00000273110.1	AL162591.2	3.94	1.40E-03	Up	ENSG00000169291	SHE	4.02	1.13E-03	Up
ENSG00000256462.1	AL732437.1	3.90	2.12E-09	Up	ENSG00000178363	CALML3	4.02	9.82E-08	Up
ENSG00000257181.1	AC025423.4	4.41	0.00E+00	Up	ENSG00000135678	CPM	4.04	0.00E+00	Up
ENSG00000262966.2	AC005695.1	5.40	5.79E-05	Up	ENSG00000065320	NTN1	4.13	5.42E-70	Up
ENSG00000253715.1	AC083841.2	4.25	9.55E-04	Up	ENSG00000167656	LY6D	4.16	7.46E-05	Up
ENSG00000246740.2	PLA2G4E-AS1	3.08	1.58E-03	Up	ENSG00000188089	PLA2G4E	4.17	3.32E-05	Up
ENSG00000268108.1	AC008687.2	2.14	3.59E-06	Up	ENSG00000196337	CGB7	4.23	5.99E-19	Up
ENSG00000272347.1	AC116351.2	7.19	4.32E-08	Up	ENSG00000145506	NKD2	4.39	8.18E-66	Up
ENSG00000253653.1	AC009185.1	4.36	2.31E-07	Up	ENSG00000055163	CYFIP2	4.42	0.00E+00	Up
ENSG00000253196.1	AC083841.1	5.18	3.84E-03	Up	ENSG00000180155	LYNX1	4.54	1.49E-51	Up
ENSG00000272508.1	AL136982.6	4.77	1.03E-03	Up	ENSG00000188100	FAM25A	4.57	2.80E-03	Up
ENSG00000259546.1	AC027808.1	1.66	7.96E-05	Up	ENSG00000259649	RP11-351M8.1	4.65	1.59E-03	Up
ENSG00000265408.1	AC009084.1	2.79	#######	Up	ENSG00000172828	CES3	4.66	4.09E-144	Up
ENSG00000257181.1	AC025423.4	4.41	0.00E+00	Up	ENSG00000135679	MDM2	4.85	0.00E+00	Up
ENSG00000256325.1	AC025423.1	3.85	1.49E-05	Up	ENSG00000135679	MDM2	4.85	0.00E+00	Up
ENSG00000244953.1	AC087521.1	5.52	3.33E-05	Up	ENSG00000187479	C11orf96	4.89	5.78E-29	Up
ENSG00000246877.1	DNM1P35	3.69	1.85E-18	Up	ENSG00000182950	ODF3L1	5.03	8.56E-28	Up
ENSG00000257702.3	LBX2-AS1	2.03	1.72E-53	Up	ENSG00000115297	TLX2	5.13	1.48E-04	Up
ENSG00000240219.1	AL512306.2	4.65	2.55E-19	Up	ENSG00000170382	LRRN2	5.13	6.79E-06	Up
ENSG00000254933.1	AP000785.1	5.00	1.40E-03	Up	ENSG00000085741	WNT11	5.29	6.32E-06	Up
ENSG00000267131.1	AC005746.2	4.91	6.89E-04	Up	ENSG00000121068	TBX2	5.35	8.44E-93	Up
ENSG00000268650.3	AC005759.1	5.75	8.24E-83	Up	ENSG00000105650	PDE4C	5.43	4.21E-124	Up
ENSG00000260650.1	AC010542.1	5.89	8.93E-08	Up	ENSG00000140932	CMTM2	5.46	1.08E-06	Up
ENSG00000231964.1	AL731567.1	5.47	3.60E-05	Up	ENSG00000012779	ALOX5	5.60	9.28E-64	Up

ENSG00000232010.1	DNMT3L-AS1	7.06	9.56E-08	Up	ENSG00000142182	DNMT3L	5.79	1.64E-07	Up
ENSG00000228917.1	AL591806.1	5.65	5.58E-07	Up	ENSG00000143217	PVRL4	5.85	2.98E-237	Up
ENSG00000255648.1	AC087242.1	5.37	1.94E-04	Up	ENSG00000177938	CAPZA3	5.87	1.67E-05	Up
ENSG00000264125.1	AC104984.2	4.17	4.87E-04	Up	ENSG00000108576	SLC6A4	6.49	2.47E-09	Up
ENSG00000254338.1	MAFA-AS1	2.42	3.67E-03	Up	ENSG00000182759	MAFA	6.51	1.82E-38	Up
ENSG00000253645.1	AC108863.2	-1.12	6.26E-22	Down	ENSG00000169495	HTRA4	6.57	2.18E-07	Up

Table S4.3: Expression information of DE-lncRNAs and nearby protein-coding genes for OH oxidation.

lncRNAs					Nearby Genes				
lncRNA ID	lncRNA symbol	log2FC	FDR value	status	Gene ID	Gene symbol	log2FC	FDR value	status
ENSG00000265784.1	AC006441.3	-1.11	1.09E-48	Down	ENSG00000002834	LASP1	-1.29	9.73E-40	Down
ENSG00000260510.1	AC004381.1	4.80	9.66E-04	Up	ENSG00000005187	ACSM3	1.23	2.93E-17	Up
ENSG00000246640.1	PICART1	2.66	9.09E-77	Up	ENSG00000005884	ITGA3	-1.27	5.10E-59	Down
ENSG00000264044.1	AC005726.2	-1.21	1.73E-12	Down	ENSG00000007202	KIAA0100	-1.27	7.57E-32	Down
ENSG00000272940.1	U62317.3	4.65	3.16E-03	Up	ENSG00000008735	MAPK8IP2	2.00	4.11E-27	Up
ENSG00000272356.1	AL080317.2	1.33	1.13E-21	Up	ENSG00000009413	REV3L	1.25	1.11E-22	Up
ENSG00000268189.2	AC005785.1	1.29	1.24E-29	Up	ENSG00000011243	AKAP8L	1.27	2.87E-107	Up
ENSG00000231964.1	AL731567.1	5.87	9.07E-06	Up	ENSG00000012779	ALOX5	5.77	2.92E-67	Up
ENSG00000244738.1	AC026316.3	4.75	4.64E-03	Up	ENSG00000013297	CLDN11	-1.30	1.31E-56	Down
ENSG00000273361.1	AC021016.3	-1.25	2.67E-03	Down	ENSG00000018280	SLC11A1	4.22	2.75E-05	Up
ENSG00000233589.1	AL138789.1	-1.01	9.59E-19	Down	ENSG00000024526	DEPDC1	-1.08	1.08E-43	Down
ENSG00000234961.1	AL133415.1	-1.65	4.97E-112	Down	ENSG00000026025	VIM	-1.65	2.11E-133	Down
ENSG00000232358.1	AL050404.1	1.04	7.49E-07	Up	ENSG00000026559	KCNG1	1.11	1.78E-18	Up
ENSG00000253389.2	AC113133.1	5.96	2.32E-05	Up	ENSG00000029534	ANK1	3.42	2.23E-60	Up
ENSG00000246323.2	AC113382.1	1.51	2.07E-07	Up	ENSG00000031003	FAM13B	1.36	2.41E-27	Up
ENSG00000240963.1	AL645465.1	-1.21	4.27E-18	Down	ENSG00000035687	ADSS	-1.18	2.11E-85	Down
ENSG00000260618.1	AC025917.1	1.75	1.24E-14	Up	ENSG00000047346	FAM214A	1.65	3.49E-77	Up
ENSG00000270012.1	AC232271.1	-1.27	2.09E-05	Down	ENSG00000049769	PPP1R3F	1.63	5.25E-21	Up
ENSG00000253653.1	AC009185.1	4.41	2.13E-07	Up	ENSG00000055163	CYFIP2	4.64	0.00E+00	Up
ENSG00000177699.4	AC011944.1	2.42	2.97E-06	Up	ENSG00000058335	RASGRF1	3.06	1.50E-21	Up
ENSG00000249906.1	AC006487.1	1.72	5.74E-13	Up	ENSG00000064300	NGFR	1.67	5.21E-33	Up
ENSG00000262966.2	AC005695.1	5.77	1.77E-05	Up	ENSG00000065320	NTN1	4.39	4.96E-78	Up
ENSG00000273123.1	AC020634.2	4.69	9.22E-03	Up	ENSG00000065534	MYLK	3.66	1.32E-151	Up
ENSG00000265415.1	AC099850.4	-2.34	4.90E-112	Down	ENSG00000068489	PRR11	-2.44	5.63E-81	Down
ENSG00000265840.1	AC010761.5	2.62	2.85E-135	Up	ENSG00000076604	TRAF4	2.45	0.00E+00	Up
ENSG00000265474.1	AC010761.4	2.04	4.14E-81	Up	ENSG00000076604	TRAF4	2.45	0.00E+00	Up
ENSG00000266456.1	AP001178.3	2.42	3.83E-19	Up	ENSG00000079101	CLUL1	3.45	1.89E-27	Up
ENSG00000269899.1	AC025857.2	-2.19	6.98E-08	Down	ENSG00000079459	FDFT1	-1.67	1.51E-125	Down
ENSG00000271730.1	AL390208.1	3.16	2.43E-85	Up	ENSG00000080546	SESN1	3.22	0.00E+00	Up
ENSG00000255202.1	AL049629.1	1.63	3.41E-03	Up	ENSG00000085063	CD59	-1.20	1.68E-53	Down
ENSG00000255092.1	AC010768.2	5.13	1.30E-03	Up	ENSG00000085117	CD82	2.49	1.06E-210	Up
ENSG00000254693.1	AC010768.1	2.70	6.77E-95	Up	ENSG00000085117	CD82	2.49	1.06E-210	Up
ENSG00000254933.1	AP000785.1	4.72	3.41E-03	Up	ENSG00000085741	WNT11	4.14	7.01E-04	Up
ENSG00000271795.1	AC011337.1	-1.95	1.02E-08	Down	ENSG00000086570	FAT2	-2.75	1.48E-46	Down
ENSG00000267898.1	AC026803.2	3.07	6.07E-09	Up	ENSG00000087088	BAX	1.55	3.84E-82	Up
ENSG00000257042.1	AC008011.2	-1.96	6.31E-15	Down	ENSG00000087494	PTHLH	-1.92	9.26E-35	Down
ENSG00000273356.1	LINC02019	2.16	8.67E-07	Up	ENSG00000088538	DOCK3	1.69	4.42E-03	Up

ENSG00000257452.1	AC004551.1	-1.52	1.02E-03	Down	ENSG00000089127	OAS1	-2.11	1.04E-39	Down
ENSG00000273055.1	AC005046.2	-1.15	3.68E-04	Down	ENSG00000091136	LAMB1	-1.42	9.69E-131	Down
ENSG00000235119.1	AL138895.1	4.04	6.95E-03	Up	ENSG00000095397	DFNB31	2.97	1.03E-110	Up
ENSG00000238258.1	AL121748.1	-1.92	1.49E-28	Down	ENSG00000099250	NRP1	-1.91	5.64E-61	Down
ENSG00000272582.1	AL031587.3	4.01	5.59E-21	Up	ENSG00000100139	MICALL1	1.77	4.80E-88	Up
ENSG00000258938.1	AL162311.3	1.06	4.70E-08	Up	ENSG00000100916	BRMS1L	1.04	8.10E-26	Up
ENSG00000267249.1	AP005482.4	1.76	4.08E-18	Up	ENSG00000101624	CEP76	2.00	4.97E-186	Up
ENSG00000237341.1	SYP-AS1	3.67	1.26E-04	Up	ENSG00000102003	SYP	2.89	1.69E-18	Up
ENSG00000261416.1	AC012645.3	-1.81	1.26E-05	Down	ENSG00000102879	CORO1A	-1.21	9.43E-34	Down
ENSG00000260772.1	AC012321.1	1.34	5.14E-30	Up	ENSG00000102908	NFAT5	1.77	7.97E-06	Up
ENSG00000261113.1	AC009034.1	-2.26	1.48E-13	Down	ENSG00000103319	EEF2K	-1.52	2.22E-32	Down
ENSG00000253930.1	TNFRSF10A-AS1	1.38	3.83E-31	Up	ENSG00000104689	TNFRSF10A	1.33	1.38E-57	Up
ENSG00000235191.1	NUCB1-AS1	-1.05	8.88E-28	Down	ENSG00000104805	NUCB1	-1.02	6.17E-61	Down
ENSG00000267898.1	AC026803.2	3.07	6.07E-09	Up	ENSG00000104812	GYS1	-1.59	1.87E-54	Down
ENSG00000268287.1	AC008687.3	1.41	9.06E-03	Up	ENSG00000104848	KCNA7	7.43	7.31E-09	Up
ENSG00000267484.1	AC027319.1	-1.26	1.81E-23	Down	ENSG00000105355	PLIN3	-1.42	6.54E-117	Down
ENSG00000267424.1	AC020934.1	2.36	5.03E-04	Up	ENSG00000105613	MAST1	1.23	2.59E-10	Up
ENSG00000268650.3	AC005759.1	5.81	1.05E-83	Up	ENSG00000105650	PDE4C	5.61	9.95E-132	Up
ENSG00000226510.1	UPK1A-AS1	2.60	9.06E-07	Up	ENSG00000105668	UPK1A	4.10	2.51E-11	Up
ENSG00000273419.1	AC004877.1	1.96	2.28E-13	Up	ENSG00000106479	ZNF862	1.12	8.50E-09	Up
ENSG00000270823.1	AC007938.2	-1.28	1.09E-13	Down	ENSG00000106484	MEST	-1.41	1.32E-30	Down
ENSG00000243888.1	AL355140.1	2.47	6.75E-04	Up	ENSG00000107282	APBA1	2.10	2.39E-05	Up
ENSG00000236662.1	AL133215.1	-1.75	6.23E-03	Down	ENSG00000107815	C10orf2	-1.18	3.81E-43	Down
ENSG00000264125.1	AC104984.2	4.70	7.67E-05	Up	ENSG00000108576	SLC6A4	6.53	2.20E-09	Up
ENSG00000264785.1	AC005722.4	-2.14	8.08E-08	Down	ENSG00000108602	ALDH3A1	-1.40	6.84E-21	Down
ENSG00000265168.1	AC005726.3	-1.71	1.88E-52	Down	ENSG00000109107	ALDOC	-1.87	3.46E-92	Down
ENSG00000270751.1	FBXW7-AS1	2.80	1.19E-39	Up	ENSG00000109670	FBXW7	2.68	4.37E-198	Up
ENSG00000255202.1	AL049629.1	1.63	3.41E-03	Up	ENSG00000110427	KIAA1549L	-2.62	2.25E-08	Down
ENSG00000258177.1	AC008149.1	-1.19	1.65E-17	Down	ENSG00000111145	ELK3	-1.18	8.32E-22	Down
ENSG00000269968.1	AC006064.4	-1.29	9.22E-52	Down	ENSG00000111640	GAPDH	-1.42	6.47E-104	Down
ENSG00000266680.1	AL135905.1	2.58	4.22E-43	Up	ENSG00000112245	PTP4A1	1.29	8.08E-94	Up
ENSG00000261604.1	AC114947.2	-2.39	1.69E-82	Down	ENSG00000112972	HMGCS1	-2.92	0.00E+00	Down
ENSG00000254293.1	AC026688.2	2.34	8.02E-03	Up	ENSG00000113196	HAND1	4.07	1.09E-05	Up
ENSG00000164621.5	SMAD5-AS1	1.66	6.96E-04	Up	ENSG00000113658	SMAD5	1.17	1.77E-17	Up
ENSG00000230454.1	U73166.1	2.55	3.78E-12	Up	ENSG00000114353	GNAI2	-1.02	2.17E-62	Down
ENSG00000225610.1	AC007679.2	1.60	1.29E-05	Up	ENSG00000114933	INO80D	1.34	3.05E-04	Up
ENSG00000257702.3	LBX2-AS1	2.07	7.48E-53	Up	ENSG00000115297	TLX2	5.48	5.02E-05	Up
ENSG00000266990.1	AC004528.1	6.02	2.23E-04	Up	ENSG00000116032	GRIN3B	3.88	7.55E-60	Up
ENSG00000242396.1	AC096536.2	-2.21	4.33E-46	Down	ENSG00000116133	DHCR24	-2.42	3.58E-107	Down
ENSG00000228703.1	AL355310.2	-1.07	2.35E-12	Down	ENSG00000116337	AMPD2	-1.08	2.20E-30	Down
ENSG00000243960.1	AL390195.2	-1.07	4.10E-44	Down	ENSG00000116455	WDR77	-1.08	1.99E-47	Down
ENSG00000271992.1	AL354872.2	1.89	5.32E-05	Up	ENSG00000116761	CTH	1.28	4.13E-31	Up

ENSG00000260088.1	DDX59-AS1	1.16	5.91E-03	Up	ENSG00000118197	DDX59	1.22	1.75E-36	Up
ENSG00000227220.1	AL133346.1	-2.64	1.04E-62	Down	ENSG00000118523	CTGF	-2.52	3.10E-261	Down
ENSG00000256694.1	AC026369.2	4.55	5.93E-03	Up	ENSG00000120645	IQSEC3	4.52	3.59E-06	Up
ENSG00000246130.1	AC107959.2	4.52	6.49E-30	Up	ENSG00000120889	TNFRSF10B	1.88	5.92E-81	Up
ENSG00000267131.1	AC005746.2	4.78	1.11E-03	Up	ENSG00000121068	TBX2	5.84	2.91E-110	Up
ENSG00000250751.1	AC015795.1	-1.00	7.84E-03	Down	ENSG00000121104	FAM117A	-1.19	1.45E-18	Down
ENSG00000239775.1	AC017116.1	2.23	5.24E-14	Up	ENSG00000122678	POLM	-1.05	3.82E-21	Down
ENSG00000237768.2	AL731563.3	-1.33	5.07E-13	Down	ENSG00000122884	P4HA1	-1.16	1.81E-76	Down
ENSG00000267379.1	AC008569.1	-1.03	4.55E-11	Down	ENSG00000123146	CD97	-1.14	5.66E-24	Down
ENSG00000249641.2	HOXC13-AS	5.30	4.93E-08	Up	ENSG00000123364	HOXC13	4.04	7.49E-06	Up
ENSG00000269125.1	AL137002.1	2.60	1.60E-04	Up	ENSG00000126231	PROZ	1.89	2.49E-07	Up
ENSG00000256341.1	AP006333.2	-2.37	2.83E-04	Down	ENSG00000126500	FLRT1	-2.25	1.90E-05	Down
ENSG00000232220.2	AC008440.1	-1.26	9.03E-27	Down	ENSG00000126583	PRKCG	1.90	6.89E-03	Up
ENSG00000268262.1	AC011445.1	-2.48	8.41E-09	Down	ENSG00000128011	LRFN1	-1.96	9.61E-20	Down
ENSG00000270147.1	AC068620.2	-1.25	3.63E-08	Down	ENSG00000128059	PPAT	-1.02	5.53E-38	Down
ENSG00000232530.1	LIF-AS1	2.55	6.31E-10	Up	ENSG00000128342	LIF	2.13	3.56E-61	Up
ENSG00000272582.1	AL031587.3	4.01	5.59E-21	Up	ENSG00000128346	C22orf23	2.48	4.71E-85	Up
ENSG00000232363.1	AL021391.1	5.08	8.73E-04	Up	ENSG00000128408	RIBC2	2.85	2.09E-34	Up
ENSG00000239480.1	AC073517.1	5.11	1.99E-03	Up	ENSG00000128563	PRKRIP1	1.03	5.84E-19	Up
ENSG00000242902.1	FLNC-AS1	2.58	5.98E-07	Up	ENSG00000128591	FLNC	3.08	1.33E-102	Up
ENSG00000253559.1	OSGEPL1-AS1	1.00	3.47E-03	Up	ENSG00000128694	OSGEPL1	-1.03	2.71E-17	Down
ENSG00000228403.1	AC035139.1	4.62	2.90E-03	Up	ENSG00000128815	WDFY4	3.54	8.25E-32	Up
ENSG00000255308.1	CSRP3-AS1	1.80	3.74E-08	Up	ENSG00000129173	E2F8	2.01	7.02E-137	Up
ENSG00000229299.2	AL121845.1	2.57	8.55E-18	Up	ENSG00000130584	ZBTB46	1.62	2.34E-10	Up
ENSG00000272078.1	AL139423.1	2.56	4.42E-85	Up	ENSG00000130940	CASZ1	2.81	4.55E-138	Up
ENSG00000232259.1	AL158166.2	1.82	6.59E-07	Up	ENSG00000132334	PTPRE	1.94	6.94E-111	Up
ENSG00000227076.1	AL158166.1	1.65	4.85E-08	Up	ENSG00000132334	PTPRE	1.94	6.94E-111	Up
ENSG00000261202.1	Z83847.1	1.93	9.47E-03	Up	ENSG00000133477	FAM83F	1.62	1.20E-43	Up
ENSG00000253837.1	AC090197.1	-2.04	2.74E-23	Down	ENSG00000134013	LOXL2	-2.27	2.25E-126	Down
ENSG00000256006.1	AC084117.1	-4.87	1.05E-03	Down	ENSG00000134333	LDHA	-2.68	0.00E+00	Down
ENSG00000235121.1	AL645504.1	4.99	1.33E-03	Up	ENSG00000134369	NAV1	-1.66	4.47E-14	Down
ENSG00000256897.1	AC018410.1	2.32	6.39E-04	Up	ENSG00000134574	DDB2	3.83	0.00E+00	Up
ENSG00000232814.2	COL4A2-AS1	-1.24	3.25E-09	Down	ENSG00000134871	COL4A2	-1.17	1.39E-33	Down
ENSG00000257671.1	KRT7-AS	-1.28	5.14E-51	Down	ENSG00000135480	KRT7	-1.33	6.66E-83	Down
ENSG00000257181.1	AC025423.4	4.33	0.00E+00	Up	ENSG00000135678	CPM	3.93	0.00E+00	Up
ENSG00000257181.1	AC025423.4	4.33	0.00E+00	Up	ENSG00000135679	MDM2	4.82	0.00E+00	Up
ENSG00000256325.1	AC025423.1	3.69	5.00E-05	Up	ENSG00000135679	MDM2	4.82	0.00E+00	Up
ENSG00000243155.1	AL162431.1	1.68	8.57E-80	Up	ENSG00000135823	STX6	1.63	5.25E-85	Up
ENSG00000243155.1	AL162431.1	1.68	8.57E-80	Up	ENSG00000135835	KIAA1614	2.01	3.95E-12	Up
ENSG00000232586.1	KIAA1614-AS1	2.96	1.29E-51	Up	ENSG00000135835	KIAA1614	2.01	3.95E-12	Up
ENSG00000214184.3	GCC2-AS1	1.00	6.31E-06	Up	ENSG00000135968	GCC2	1.04	1.78E-44	Up
ENSG00000257202.1	AC084398.2	2.58	3.49E-49	Up	ENSG00000136048	DRAM1	2.54	4.32E-135	Up

ENSG00000244161.1	FLNB-AS1	-1.50	1.35E-50	Down	ENSG00000136068	FLNB	-1.53	8.24E-25	Down
ENSG00000235837.1	AC073333.1	-1.56	8.12E-34	Down	ENSG00000136261	BZW2	-1.76	7.74E-108	Down
ENSG00000239775.1	AC017116.1	2.23	5.24E-14	Up	ENSG00000136279	DBNL	-1.09	2.35E-50	Down
ENSG00000259539.1	AC051619.5	1.28	1.30E-03	Up	ENSG00000137857	DUOX1	2.31	3.70E-51	Up
ENSG00000230928.1	AL139241.1	3.09	5.56E-03	Up	ENSG00000138131	LOXL4	1.18	4.42E-04	Up
ENSG00000255958.1	AC115676.1	1.57	1.22E-03	Up	ENSG00000139112	GABARAPL1	1.26	7.89E-39	Up
ENSG00000257023.1	AC087241.2	4.23	7.83E-03	Up	ENSG00000139163	ETNK1	1.52	1.11E-79	Up
ENSG00000257225.1	AC079601.2	-1.85	9.03E-67	Down	ENSG00000139174	PRICKLE1	-1.94	4.57E-44	Down
ENSG00000257453.1	AC011611.3	-1.32	7.62E-27	Down	ENSG00000139289	PHLDA1	-1.37	9.32E-32	Down
ENSG00000258086.1	AC079313.1	-1.44	3.49E-08	Down	ENSG00000139572	GPR84	4.36	8.88E-03	Up
ENSG00000272418.1	AC090607.4	1.17	1.56E-12	Up	ENSG00000140403	DNAJA4	1.10	5.98E-26	Up
ENSG00000260252.1	AC009087.1	1.28	2.52E-13	Up	ENSG00000140830	TXNL4B	1.03	2.97E-20	Up
ENSG00000260650.1	AC010542.1	5.94	7.70E-08	Up	ENSG00000140932	CMTM2	5.37	2.03E-06	Up
ENSG00000266872.1	AC015688.6	2.03	4.04E-45	Up	ENSG00000141068	KSR1	2.13	1.06E-32	Up
ENSG00000264273.1	AC107982.2	1.84	3.21E-05	Up	ENSG00000141127	PRPSAP2	1.07	2.70E-47	Up
ENSG00000262413.1	AC145207.2	-1.52	1.41E-114	Down	ENSG00000141522	ARHGDIA	-1.46	1.45E-164	Down
ENSG00000232010.1	DNMT3L-AS1	6.68	6.14E-07	Up	ENSG00000142182	DNMT3L	6.04	4.80E-08	Up
ENSG00000255441.1	AC008750.2	1.84	3.46E-05	Up	ENSG00000142512	SIGLEC10	2.30	2.01E-10	Up
ENSG00000254760.1	AC008750.1	1.80	9.05E-03	Up	ENSG00000142512	SIGLEC10	2.30	2.01E-10	Up
ENSG00000204666.3	AC010624.1	5.28	3.11E-39	Up	ENSG00000142528	ZNF473	1.32	2.61E-95	Up
ENSG00000237058.1	MMEL1-AS1	4.10	9.46E-03	Up	ENSG00000142606	MMEL1	-1.27	4.08E-08	Down
ENSG00000233485.1	FHAD1-AS1	2.47	2.87E-03	Up	ENSG00000142621	FHAD1	2.36	2.35E-09	Up
ENSG00000228917.1	AL591806.1	4.90	2.18E-05	Up	ENSG00000143217	PVRL4	6.00	2.18E-248	Up
ENSG00000235897.1	TM4SF19-AS1	-1.49	6.51E-18	Down	ENSG00000145107	TM4SF19	-1.97	1.89E-06	Down
ENSG00000272347.1	AC116351.2	6.60	7.21E-07	Up	ENSG00000145506	NKD2	4.71	5.19E-75	Up
ENSG00000253258.1	AC068228.2	-1.69	1.01E-04	Down	ENSG00000147689	FAM83A	-1.34	7.04E-34	Down
ENSG00000235865.2	GSN-AS1	-1.20	2.39E-08	Down	ENSG00000148180	GSN	-1.56	8.48E-124	Down
ENSG00000255471.1	AP001528.1	-4.29	4.46E-03	Down	ENSG00000150687	PRSS23	-2.18	4.32E-202	Down
ENSG00000273474.1	AL157392.4	3.04	4.56E-03	Up	ENSG00000151474	FRMD4A	-1.42	7.63E-23	Down
ENSG00000259941.1	AC084782.1	1.65	6.43E-09	Up	ENSG00000151575	TEX9	1.36	2.54E-23	Up
ENSG00000253559.1	OSGEPL1-AS1	1.00	3.47E-03	Up	ENSG00000151687	ANKAR	1.18	1.66E-13	Up
ENSG00000231080.1	AL592161.1	2.28	8.23E-04	Up	ENSG00000152763	WDR78	1.05	1.40E-06	Up
ENSG00000253744.1	AC025442.1	1.28	4.70E-11	Up	ENSG00000153914	SREK1	1.19	3.77E-50	Up
ENSG00000265750.1	AC090772.3	1.59	2.80E-41	Up	ENSG00000154040	CABYR	2.85	3.43E-171	Up
ENSG00000263873.1	AP003396.5	-1.65	9.82E-110	Down	ENSG00000154096	THY1	-1.89	2.72E-124	Down
ENSG00000254568.1	AP003501.1	-1.79	5.94E-03	Down	ENSG00000154133	ROBO4	-2.09	9.86E-12	Down
ENSG00000226441.2	PLCL2-AS1	3.46	2.77E-03	Up	ENSG00000154822	PLCL2	4.56	3.92E-57	Up
ENSG00000259955.1	AC008741.1	1.54	2.10E-11	Up	ENSG00000155592	ZKSCAN2	1.67	3.43E-27	Up
ENSG00000272081.1	AC008972.2	2.71	7.91E-08	Up	ENSG00000157107	FCHO2	1.47	5.45E-58	Up
ENSG00000228838.1	AL355483.1	-1.37	3.27E-04	Down	ENSG00000157193	LRP8	-1.99	1.56E-81	Down
ENSG00000231542.1	TAB3-AS1	2.85	1.44E-10	Up	ENSG00000157625	TAB3	2.96	7.17E-90	Up
ENSG00000235512.1	TAB3-AS2	2.79	1.74E-56	Up	ENSG00000157625	TAB3	2.96	7.17E-90	Up

ENSG00000228037.1	AL139246.3	8.82	1.00E-12	Up	ENSG00000157870	FAM213B	-1.39	1.46E-29	Down
ENSG00000256811.1	AC079360.1	2.92	1.15E-03	Up	ENSG00000158104	HPD	1.96	6.36E-04	Up
ENSG00000225062.1	CATIP-AS1	2.42	1.07E-07	Up	ENSG00000158428	C2orf62	3.76	7.26E-18	Up
ENSG00000226526.1	AL049569.1	-1.94	2.95E-33	Down	ENSG00000159363	ATP13A2	-1.78	2.12E-148	Down
ENSG00000269292.1	AC093503.2	-1.21	1.35E-59	Down	ENSG00000160013	PTGIR	-1.44	1.44E-03	Down
ENSG00000232010.1	DNMT3L-AS1	6.68	6.14E-07	Up	ENSG00000160223	ICOSLG	2.38	2.54E-33	Up
ENSG00000228404.1	AP001468.1	-1.70	1.30E-06	Down	ENSG00000160284	SPATC1L	-1.17	7.48E-15	Down
ENSG00000228404.1	AP001468.1	-1.70	1.30E-06	Down	ENSG00000160285	LSS	-2.44	3.01E-92	Down
ENSG00000268729.1	AC020922.2	1.35	2.90E-04	Up	ENSG00000160469	BRSK1	1.22	1.72E-24	Up
ENSG00000258086.1	AC079313.1	-1.44	3.49E-08	Down	ENSG00000161638	ITGA5	-1.56	6.34E-67	Down
ENSG00000258086.1	AC079313.1	-1.44	3.49E-08	Down	ENSG00000161642	ZNF385A	2.27	1.98E-162	Up
ENSG00000261898.2	AC091153.4	-1.30	2.10E-10	Down	ENSG00000161920	MED11	-1.30	4.11E-21	Down
ENSG00000262899.1	AC004232.1	1.06	9.42E-04	Up	ENSG00000162086	ZNF75A	1.37	8.54E-31	Up
ENSG00000255126.1	AP003064.1	1.20	7.55E-11	Up	ENSG00000162174	ASRGL1	1.03	2.57E-19	Up
ENSG00000255478.1	AP000944.1	2.69	4.23E-06	Up	ENSG00000162241	SLC25A45	3.05	1.99E-28	Up
ENSG00000272482.1	AC254633.1	5.39	6.55E-09	Up	ENSG00000162496	DHRS3	3.73	6.04E-120	Up
ENSG00000230415.1	LINC01786	1.25	5.19E-03	Up	ENSG00000162572	SCNN1D	2.48	5.38E-52	Up
ENSG00000273204.1	AC104506.1	1.09	5.40E-03	Up	ENSG00000162694	EXTL2	-1.57	4.19E-35	Down
ENSG00000261468.1	AC096921.2	-2.60	3.32E-25	Down	ENSG00000163513	TGFBR2	-2.08	1.86E-79	Down
ENSG00000241111.1	AC092040.2	1.81	1.52E-25	Up	ENSG00000163637	PRICKLE2	1.85	2.25E-16	Up
ENSG00000226017.2	PRICKLE2-AS3	1.92	1.15E-03	Up	ENSG00000163637	PRICKLE2	1.85	2.25E-16	Up
ENSG00000238186.1	AL603839.2	1.28	2.23E-14	Up	ENSG00000164002	EXO5	1.34	1.25E-64	Up
ENSG00000227278.1	AL603839.1	1.45	1.03E-38	Up	ENSG00000164002	EXO5	1.34	1.25E-64	Up
ENSG00000261668.1	AC093591.2	1.82	1.68E-22	Up	ENSG00000164070	HSPA4L	2.03	8.70E-140	Up
ENSG00000230698.1	AC105935.2	-1.53	7.03E-07	Down	ENSG00000164078	MST1R	-1.53	8.20E-66	Down
ENSG00000250309.2	AC008453.1	4.23	5.95E-03	Up	ENSG00000164591	MYOZ3	4.99	1.18E-03	Up
ENSG00000239775.1	AC017116.1	2.23	5.24E-14	Up	ENSG00000164708	PGAM2	2.07	4.50E-12	Up
ENSG00000269899.1	AC025857.2	-2.19	6.98E-08	Down	ENSG00000164733	CTSB	-1.04	2.08E-69	Down
ENSG00000225981.1	AC102953.1	6.59	3.06E-06	Up	ENSG00000164877	MICALL2	1.59	1.11E-99	Up
ENSG00000231964.1	AL731567.1	5.87	9.07E-06	Up	ENSG00000165406	8-Mar	1.08	2.87E-10	Up
ENSG00000240291.1	AL450384.2	1.71	4.06E-39	Up	ENSG00000165995	CACNB2	1.82	8.03E-19	Up
ENSG00000265579.1	AC023301.1	-1.88	6.87E-15	Down	ENSG00000166342	NETO1	-1.23	9.98E-17	Down
ENSG00000258232.2	AC125611.3	-1.66	1.86E-54	Down	ENSG00000167553	TUBA1C	-1.86	2.49E-140	Down
ENSG00000253715.1	AC083841.2	3.89	3.24E-03	Up	ENSG00000167656	LY6D	3.59	9.53E-04	Up
ENSG00000260107.1	AC005606.1	1.12	7.17E-31	Up	ENSG00000167962	ZNF598	1.08	2.13E-55	Up
ENSG00000269926.1	DDIT4-AS1	-1.44	2.29E-66	Down	ENSG00000168209	DDIT4	-1.52	1.13E-168	Down
ENSG00000258377.1	AL139099.2	-1.13	3.49E-38	Down	ENSG00000168282	MGAT2	-1.25	2.62E-59	Down
ENSG00000272182.1	AC135507.1	-1.41	1.87E-23	Down	ENSG00000168291	PDHB	-1.36	1.63E-42	Down
ENSG00000233611.3	AC019068.1	2.98	8.87E-03	Up	ENSG00000168505	GBX2	3.82	2.53E-06	Up
ENSG00000266872.1	AC015688.6	2.03	4.04E-45	Up	ENSG00000168961	LGALS9	3.45	2.22E-05	Up
ENSG00000273110.1	AL162591.2	4.31	4.76E-04	Up	ENSG00000169291	SHE	4.86	6.39E-05	Up
ENSG00000253645.1	AC108863.2	-1.24	1.07E-23	Down	ENSG00000169495	HTRA4	7.45	3.22E-09	Up

ENSG00000253645.1	AC108863.2	-1.24	1.07E-23	Down	ENSG00000169499	PLEKHA2	-1.37	1.04E-13	Down
ENSG00000240219.1	AL512306.2	4.26	6.00E-16	Up	ENSG00000170382	LRRN2	4.62	7.56E-05	Up
ENSG00000223947.1	AC016738.1	-1.36	2.88E-11	Down	ENSG00000170485	NPAS2	-1.31	7.69E-20	Down
ENSG00000227279.1	AC110015.1	-1.15	1.05E-14	Down	ENSG00000170558	CDH2	-1.20	2.05E-41	Down
ENSG00000262001.1	DLGAP1-AS2	1.99	1.05E-66	Up	ENSG00000170579	DLGAP1	4.17	2.50E-07	Up
ENSG00000242207.1	HOXB-AS4	2.73	4.21E-03	Up	ENSG00000170689	HOXB9	2.42	9.29E-12	Up
ENSG00000203362.2	POLH-AS1	2.30	1.90E-16	Up	ENSG00000170734	POLH	2.76	4.09E-141	Up
ENSG00000255310.2	AF131215.5	1.36	4.11E-14	Up	ENSG00000171044	XKR6	1.54	1.21E-23	Up
ENSG00000269918.1	AF131215.6	1.20	3.22E-09	Up	ENSG00000171044	XKR6	1.54	1.21E-23	Up
ENSG00000272933.1	AL391121.1	2.22	8.82E-101	Up	ENSG00000171206	TRIM8	1.19	8.97E-52	Up
ENSG00000271781.1	AC026740.1	2.79	1.13E-15	Up	ENSG00000171368	TPPP	1.79	8.60E-07	Up
ENSG00000231705.1	AL451069.2	3.82	4.65E-03	Up	ENSG00000171813	PWWP2B	1.02	2.29E-22	Up
ENSG00000271787.1	AC104794.5	2.21	3.04E-23	Up	ENSG00000172059	KLF11	2.24	5.50E-36	Up
ENSG00000256879.1	AC129102.1	5.52	4.52E-04	Up	ENSG00000172572	PDE3A	4.63	7.12E-13	Up
ENSG00000273402.1	AC004908.3	1.48	8.24E-03	Up	ENSG00000172748	ZNF596	1.93	5.34E-40	Up
ENSG00000255404.1	AP001266.1	3.64	1.72E-21	Up	ENSG00000172818	OVOL1	2.60	2.39E-07	Up
ENSG00000265408.1	AC009084.1	2.97	9.69E-144	Up	ENSG00000172828	CES3	4.74	4.11E-147	Up
ENSG00000265408.1	AC009084.1	2.97	9.69E-144	Up	ENSG00000172831	CES2	2.86	0.00E+00	Up
ENSG00000259863.1	SH3RF3-AS1	-1.47	8.31E-27	Down	ENSG00000172985	SH3RF3	-1.34	7.68E-18	Down
ENSG00000245385.2	AP003396.1	-1.27	1.68E-24	Down	ENSG00000173456	RNF26	-1.27	6.22E-51	Down
ENSG00000246130.1	AC107959.2	4.52	6.49E-30	Up	ENSG00000173535	TNFRSF10C	3.41	2.26E-50	Up
ENSG00000260892.1	AC105020.4	1.14	2.41E-04	Up	ENSG00000173546	CSPG4	1.14	9.93E-11	Up
ENSG00000255478.1	AP000944.1	2.69	4.23E-06	Up	ENSG00000173825	TIGD3	1.84	6.04E-14	Up
ENSG00000224818.1	AC096677.2	3.45	1.27E-98	Up	ENSG00000174307	PHLDA3	3.52	2.07E-253	Up
ENSG00000267356.1	AC006557.3	1.41	8.72E-10	Up	ENSG00000175322	ZNF519	1.12	2.01E-12	Up
ENSG00000260944.1	FOXC2-AS1	-1.20	5.21E-04	Down	ENSG00000176692	FOXC2	-1.03	2.81E-14	Down
ENSG00000261888.1	AC144831.1	5.10	2.29E-17	Up	ENSG00000176845	METRNL	2.75	5.71E-228	Up
ENSG00000266456.1	AP001178.3	2.42	3.83E-19	Up	ENSG00000176912	C18orf56	3.19	2.19E-37	Up
ENSG00000263727.1	AP001178.1	3.04	7.36E-04	Up	ENSG00000176912	C18orf56	3.19	2.19E-37	Up
ENSG00000260912.1	AL158206.1	4.05	1.49E-279	Up	ENSG00000177076	ACER2	3.91	6.41E-69	Up
ENSG00000269915.1	AP006621.4	1.28	7.36E-25	Up	ENSG00000177106	EPS8L2	1.23	1.41E-124	Up
ENSG00000267646.1	AC008543.5	3.65	7.40E-03	Up	ENSG00000177599	ZNF491	2.61	2.62E-18	Up
ENSG00000255648.1	AC087242.1	5.00	7.66E-04	Up	ENSG00000177938	CAPZA3	5.68	4.14E-05	Up
ENSG00000268186.1	ZNF114-AS1	3.19	3.85E-03	Up	ENSG00000178150	ZNF114	1.70	9.88E-16	Up
ENSG00000256462.1	AL732437.1	4.33	3.09E-11	Up	ENSG00000178363	CALML3	4.42	5.09E-09	Up
ENSG00000272183.1	AC005041.3	1.52	1.12E-03	Up	ENSG00000179528	LBX2	2.06	8.27E-17	Up
ENSG00000257702.3	LBX2-AS1	2.07	7.48E-53	Up	ENSG00000179528	LBX2	2.06	8.27E-17	Up
ENSG00000232220.2	AC008440.1	-1.26	9.03E-27	Down	ENSG00000179820	MYADM	-1.58	9.60E-47	Down
ENSG00000262624.1	AC113189.1	-1.59	2.19E-06	Down	ENSG00000181284	TMEM102	-1.76	2.60E-29	Down
ENSG00000244268.1	AC117394.2	2.41	8.20E-03	Up	ENSG00000181467	RAP2B	1.13	5.34E-30	Up
ENSG00000263342.1	AC003688.3	-4.39	9.35E-03	Down	ENSG00000181856	SLC2A4	-3.26	7.72E-09	Down
ENSG00000256249.1	AC026333.3	1.81	1.38E-18	Up	ENSG00000182782	HCAR2	1.19	1.64E-05	Up

ENSG00000234478.1	ACBD3-AS1	1.06	2.67E-17	Up	ENSG00000182827	ACBD3	1.33	1.68E-58	Up
ENSG00000246877.1	DNM1P35	3.60	4.33E-17	Up	ENSG00000182950	ODF3L1	4.56	1.61E-22	Up
ENSG00000254812.1	AC067930.2	1.83	1.68E-05	Up	ENSG00000183309	ZNF623	1.31	1.63E-42	Up
ENSG00000268292.1	AC006547.3	1.45	3.86E-34	Up	ENSG00000183597	TANGO2	1.28	4.76E-34	Up
ENSG00000244578.1	LINC01391	4.59	2.46E-03	Up	ENSG00000183770	FOXL2	3.76	6.27E-10	Up
ENSG00000257622.1	AL512356.1	1.87	4.70E-43	Up	ENSG00000183828	NUDT14	1.49	5.57E-33	Up
ENSG00000261532.1	AC009065.8	-1.08	7.27E-16	Down	ENSG00000184207	PGP	-1.43	2.62E-51	Down
ENSG00000257622.1	AL512356.1	1.87	4.70E-43	Up	ENSG00000184916	JAG2	1.93	1.02E-166	Up
ENSG00000231864.2	AL807752.3	-1.90	2.84E-42	Down	ENSG00000186193	SAPCD2	-1.76	4.10E-34	Down
ENSG00000273117.1	AC144652.1	-1.11	2.61E-05	Down	ENSG00000186480	INSIG1	-3.01	0.00E+00	Down
ENSG00000256007.1	ARAP1-AS1	1.20	6.94E-26	Up	ENSG00000186635	ARAP1	1.02	4.43E-52	Up
ENSG00000256633.1	AP005019.1	2.45	9.32E-07	Up	ENSG00000186642	PDE2A	2.99	1.78E-30	Up
ENSG00000261215.1	AL162231.4	1.63	4.47E-14	Up	ENSG00000187186	RP11-195F19.5	1.18	1.61E-04	Up
ENSG00000259827.1	AC026461.1	-1.15	2.94E-13	Down	ENSG00000187193	MT1X	-1.26	2.20E-21	Down
ENSG00000244953.1	AC087521.1	6.45	9.47E-07	Up	ENSG00000187479	C11orf96	5.24	7.89E-33	Up
ENSG00000224969.1	AL645608.1	2.29	3.84E-03	Up	ENSG00000187608	ISG15	1.21	2.19E-24	Up
ENSG00000246740.2	PLA2G4E-AS1	3.14	1.54E-03	Up	ENSG00000188089	PLA2G4E	4.08	6.43E-05	Up
ENSG00000272508.1	AL136982.6	4.46	2.68E-03	Up	ENSG00000188100	FAM25A	4.18	7.87E-03	Up
ENSG00000260196.1	AC124798.1	1.56	5.75E-38	Up	ENSG00000188211	NCR3LG1	1.44	1.43E-09	Up
ENSG00000268896.1	AC009955.3	2.80	3.34E-05	Up	ENSG00000188760	TMEM198	1.51	3.27E-09	Up
ENSG00000267510.1	AC011451.1	1.86	1.51E-17	Up	ENSG00000196110	ZNF699	1.53	4.95E-24	Up
ENSG00000268108.1	AC008687.2	2.17	4.75E-06	Up	ENSG00000196337	CGB7	4.30	3.07E-19	Up
ENSG00000255438.2	AL354813.1	2.46	1.61E-33	Up	ENSG00000196562	SULF2	2.73	4.62E-152	Up
ENSG00000267345.1	AC010632.1	1.68	2.51E-05	Up	ENSG00000197050	ZNF420	1.01	2.77E-24	Up
ENSG00000264769.1	AC145207.8	1.15	1.64E-21	Up	ENSG00000197063	MAFG	1.13	4.95E-44	Up
ENSG00000254064.1	AC105206.2	-1.47	5.34E-04	Down	ENSG00000197181	PIWIL2	3.31	9.93E-05	Up
ENSG00000235159.1	AL121672.2	1.42	7.20E-03	Up	ENSG00000197182	FLJ27365	-1.18	8.16E-14	Down
ENSG00000258424.1	AL512791.1	-1.36	9.47E-32	Down	ENSG00000198668	CALM1	-1.28	1.46E-59	Down
ENSG00000271714.1	AC010501.2	1.92	1.15E-06	Up	ENSG00000198780	FAM169A	1.04	1.02E-17	Up
ENSG00000241886.1	AC112496.1	3.16	5.62E-11	Up	ENSG00000198814	GK	2.49	3.35E-95	Up
ENSG00000229331.1	GK-IT1	4.09	8.84E-03	Up	ENSG00000198814	GK	2.49	3.35E-95	Up
ENSG00000243055.1	GK-AS1	2.47	4.72E-29	Up	ENSG00000198814	GK	2.49	3.35E-95	Up
ENSG00000258749.1	AL110504.1	-1.31	1.42E-32	Down	ENSG00000205476	CCDC85C	-1.27	1.06E-18	Down
ENSG00000272323.1	AC026801.2	1.10	8.71E-03	Up	ENSG00000205838	TTC23L	2.39	7.30E-04	Up
ENSG00000230736.2	AL021937.1	2.27	7.55E-06	Up	ENSG00000205853	RFPL3S	2.85	1.85E-04	Up
ENSG00000269989.1	AC036176.3	3.84	2.64E-05	Up	ENSG00000206075	SERPINB5	1.31	1.36E-85	Up
ENSG00000272682.1	AC004471.2	2.65	4.32E-03	Up	ENSG00000206203	TSSK2	1.16	5.75E-06	Up
ENSG00000261996.1	AC004706.1	4.24	1.06E-52	Up	ENSG00000212734	C17orf100	2.69	4.12E-34	Up
ENSG00000235897.1	TM4SF19-AS1	-1.49	6.51E-18	Down	ENSG00000213123	TCTEX1D2	1.01	2.22E-06	Up
ENSG00000228544.1	CCDC183-AS1	1.29	8.46E-04	Up	ENSG00000213213	CCDC183	1.29	2.38E-04	Up
ENSG00000263171.1	AC026954.3	1.98	7.56E-39	Up	ENSG00000213859	KCTD11	1.81	1.48E-36	Up
ENSG00000261215.1	AL162231.4	1.63	4.47E-14	Up	ENSG00000213927	CCL27	3.28	3.19E-06	Up

ENSG00000253445.1	AC027309.1	1.53	4.08E-09	Up	ENSG00000214357	NEURL1B	1.37	4.50E-07	Up
ENSG00000268108.1	AC008687.2	2.17	4.75E-06	Up	ENSG00000225950	NTF4	1.36	4.30E-12	Up
ENSG00000268287.1	AC008687.3	1.41	9.06E-03	Up	ENSG00000225950	NTF4	1.36	4.30E-12	Up
ENSG00000228404.1	AP001468.1	-1.70	1.30E-06	Down	ENSG00000235878	AP001468.1	-1.93	2.55E-11	Down
ENSG00000262116.1	AC009134.1	-2.06	1.33E-04	Down	ENSG00000237515	SHISA9	-1.07	1.12E-08	Down
ENSG00000273474.1	AL157392.4	3.04	4.56E-03	Up	ENSG00000239665	RP11-295P9.3	1.23	3.57E-04	Up
ENSG00000267727.1	AC008738.5	1.97	6.07E-05	Up	ENSG00000245848	CEBPA	2.15	2.01E-08	Up
ENSG00000267580.1	AC008738.3	2.29	1.62E-14	Up	ENSG00000245848	CEBPA	2.15	2.01E-08	Up
ENSG00000254574.1	AC105219.3	4.52	8.30E-03	Up	ENSG00000255181	CCDC166	4.29	3.45E-03	Up
ENSG00000256249.1	AC026333.3	1.81	1.38E-18	Up	ENSG00000255398	HCAR3	2.00	1.16E-19	Up
ENSG00000259006.1	AC092143.2	1.22	1.01E-10	Up	ENSG00000258839	MC1R	1.89	1.63E-03	Up
ENSG00000271781.1	AC026740.1	2.79	1.13E-15	Up	ENSG00000268885	AC026740.1	1.20	2.59E-09	Up

Table S4.4: Gene ontology (GO) for *cis*-targeted genes.

GO term ID	q-value	Set size	Candidate containde	GO term name
GO:0005515	2.06E-16	11866	487 (4.1%)	protein binding
GO:0044424	7.68E-14	14513	553 (3.8%)	intracellular part
GO:0005622	7.68E-14	14539	553 (3.8%)	intracellular
GO:0005829	3.34E-12	5109	253 (5.0%)	cytosol
GO:0044444	1.73E-11	9698	407 (4.2%)	cytoplasmic part
GO:0005737	2.49E-11	11575	463 (4.0%)	cytoplasm
GO:0043229	3.21E-11	12754	496 (3.9%)	intracellular organelle
GO:0043227	5.37E-10	12507	484 (3.9%)	membrane-bounded organelle
GO:0043231	1.41E-08	10999	434 (4.0%)	intracellular membrane-bounded organelle
GO:0044446	1.94E-07	9279	373 (4.0%)	intracellular organelle part
GO:0043233	6.48E-07	5283	234 (4.4%)	organelle lumen
GO:0071704	7.88E-07	11025	428 (3.9%)	organic substance metabolic process
GO:0044237	7.88E-07	10637	415 (3.9%)	cellular metabolic process
GO:0044238	7.88E-07	10663	415 (3.9%)	primary metabolic process
GO:0048522	1.11E-06	5324	242 (4.6%)	positive regulation of cellular process
GO:0070013	1.31E-06	5283	234 (4.4%)	intracellular organelle lumen
GO:0005634	2.53E-06	7415	308 (4.2%)	nucleus
GO:0044877	3.17E-06	1094	69 (6.3%)	protein-containing complex binding
GO:0005654	9.81E-06	3520	166 (4.7%)	nucleoplasm
GO:0006807	1.10E-05	10174	393 (3.9%)	nitrogen compound metabolic process
GO:0080090	2.03E-05	6071	261 (4.3%)	regulation of primary metabolic process
GO:0043228	2.19E-05	4260	189 (4.5%)	non-membrane-bounded organelle
GO:0043230	2.19E-05	2166	110 (5.1%)	extracellular organelle
GO:0031981	2.90E-05	4134	186 (4.5%)	nuclear lumen
GO:0070062	3.11E-05	2142	110 (5.1%)	extracellular exosome
GO:0044260	3.22E-05	8256	333 (4.1%)	cellular macromolecule metabolic process
GO:0048518	3.22E-05	6051	258 (4.3%)	positive regulation of biological process
GO:0044428	3.37E-05	4521	199 (4.4%)	nuclear part
GO:0043170	3.62E-05	9445	370 (3.9%)	macromolecule metabolic process
GO:1903561	3.76E-05	2164	110 (5.1%)	extracellular vesicle
GO:0051641	3.90E-05	2871	138 (4.8%)	cellular localization
GO:0043232	4.12E-05	4250	188 (4.4%)	intracellular non-membrane-bounded organelle
GO:0031323	5.50E-05	6130	260 (4.3%)	regulation of cellular metabolic process
GO:0051171	6.62E-05	5904	251 (4.3%)	regulation of nitrogen compound metabolic process
GO:0005912	6.75E-05	540	39 (7.2%)	adherens junction
GO:0031982	6.81E-05	3851	172 (4.5%)	vesicle
GO:0019222	6.85E-05	6671	276 (4.2%)	regulation of metabolic process
GO:0060255	7.55E-05	6156	259 (4.2%)	regulation of macromolecule metabolic process
GO:0070161	8.86E-05	556	39 (7.0%)	anchoring junction

GO:0009894	1.10E-04	906	58 (6.4%)	regulation of catabolic process
GO:0060341	1.10E-04	886	57 (6.4%)	regulation of cellular localization
GO:0044267	1.28E-04	5155	222 (4.3%)	cellular protein metabolic process
GO:0097458	1.53E-04	1713	88 (5.1%)	neuron part
GO:0009058	1.71E-04	6185	253 (4.1%)	biosynthetic process
GO:0030055	1.72E-04	413	31 (7.5%)	cell-substrate junction
GO:0050789	1.80E-04	11539	428 (3.7%)	regulation of biological process
GO:0019899	1.94E-04	2277	115 (5.1%)	enzyme binding
GO:0005924	2.10E-04	409	31 (7.6%)	cell-substrate adherens junction
GO:0005925	3.41E-04	406	31 (7.6%)	focal adhesion
GO:0048519	3.67E-04	5219	221 (4.3%)	negative regulation of biological process
GO:2001233	4.47E-04	391	33 (8.4%)	regulation of apoptotic signaling pathway
GO:0042176	4.47E-04	382	32 (8.4%)	regulation of protein catabolic process
GO:0043209	4.51E-04	53	9 (17.0%)	myelin sheath
GO:0031252	4.81E-04	399	29 (7.3%)	cell leading edge
GO:0050839	5.08E-04	493	36 (7.3%)	cell adhesion molecule binding
GO:0005856	5.29E-04	2170	105 (4.9%)	cytoskeleton
GO:0070727	5.87E-04	1862	95 (5.1%)	cellular macromolecule localization
GO:0019538	5.87E-04	5886	242 (4.1%)	protein metabolic process
GO:1901576	5.87E-04	6112	249 (4.1%)	organic substance biosynthetic process
GO:0044249	5.87E-04	6026	246 (4.1%)	cellular biosynthetic process
GO:1901564	6.01E-04	6932	277 (4.0%)	organonitrogen compound metabolic process
GO:0007049	6.91E-04	1792	89 (5.0%)	cell cycle
GO:0050794	7.42E-04	10850	404 (3.7%)	regulation of cellular process
GO:0033554	7.42E-04	1936	96 (5.0%)	cellular response to stress
GO:0050790	7.42E-04	2294	110 (4.8%)	regulation of catalytic activity
GO:0032268	7.88E-04	2556	124 (4.9%)	regulation of cellular protein metabolic process
GO:0009056	7.96E-04	2550	118 (4.6%)	catabolic process
GO:0010604	9.02E-04	3268	150 (4.6%)	positive regulation of macromolecule metabolic process
GO:0048523	1.07E-03	4670	199 (4.3%)	negative regulation of cellular process
GO:0051246	1.08E-03	2809	132 (4.7%)	regulation of protein metabolic process
GO:0042995	1.17E-03	2168	101 (4.7%)	cell projection
GO:0043005	1.21E-03	1309	69 (5.3%)	neuron projection
GO:0044248	1.43E-03	2260	107 (4.8%)	cellular catabolic process
GO:1901362	1.46E-03	4434	189 (4.3%)	organic cyclic compound biosynthetic process
GO:0034613	1.46E-03	1851	93 (5.0%)	cellular protein localization
GO:0035556	1.47E-03	2792	127 (4.6%)	intracellular signal transduction
GO:0097190	1.47E-03	587	38 (6.5%)	apoptotic signaling pathway
GO:0032879	1.47E-03	2663	122 (4.6%)	regulation of localization
GO:1901575	1.47E-03	2120	101 (4.8%)	organic substance catabolic process
GO:1903827	1.56E-03	511	36 (7.1%)	regulation of cellular protein localization
GO:0031329	1.56E-03	791	49 (6.2%)	regulation of cellular catabolic process

GO:0051173	1.56E-03	3128	142 (4.6%)	positive regulation of nitrogen compound metabolic process
GO:0043085	1.60E-03	1413	75 (5.3%)	positive regulation of catalytic activity
GO:0043412	1.67E-03	4303	184 (4.3%)	macromolecule modification
GO:0009893	1.67E-03	3537	156 (4.4%)	positive regulation of metabolic process
GO:0036211	1.93E-03	4097	176 (4.3%)	protein modification process
GO:0051235	1.94E-03	316	24 (7.6%)	maintenance of location
GO:0008219	2.05E-03	2202	102 (4.7%)	cell death
GO:0016043	2.05E-03	6398	252 (4.0%)	cellular component organization
GO:0034641	2.18E-03	6494	256 (4.0%)	cellular nitrogen compound metabolic process
GO:0120025	2.31E-03	2098	98 (4.7%)	plasma membrane bounded cell projection
GO:0031325	2.57E-03	3251	145 (4.5%)	positive regulation of cellular metabolic process
GO:0006464	2.57E-03	4097	176 (4.3%)	cellular protein modification process
GO:0006508	2.93E-03	1861	91 (4.9%)	proteolysis
GO:0051651	3.06E-03	95	11 (11.6%)	maintenance of location in cell
GO:0006950	3.06E-03	3973	165 (4.2%)	response to stress
GO:0034654	3.20E-03	4222	178 (4.3%)	nucleobase-containing compound biosynthetic process
GO:0032507	3.23E-03	74	10 (13.5%)	maintenance of protein location in cell
GO:0006139	3.33E-03	5810	231 (4.0%)	nucleobase-containing compound metabolic process
GO:0018130	3.34E-03	4285	180 (4.2%)	heterocycle biosynthetic process
GO:0070482	3.44E-03	344	25 (7.3%)	response to oxygen levels
GO:0044770	3.64E-03	535	34 (6.4%)	cell cycle phase transition
GO:0009968	3.66E-03	1183	64 (5.4%)	negative regulation of signal transduction
GO:0008092	3.84E-03	958	54 (5.6%)	cytoskeletal protein binding
GO:0034645	4.00E-03	4867	200 (4.1%)	cellular macromolecule biosynthetic process
GO:1901360	4.20E-03	6220	244 (4.0%)	organic cyclic compound metabolic process
GO:0012501	4.21E-03	2070	96 (4.7%)	programmed cell death
GO:0044271	4.29E-03	4906	201 (4.1%)	cellular nitrogen compound biosynthetic process
GO:0043169	4.42E-03	4290	179 (4.2%)	cation binding
GO:0046907	4.42E-03	1834	87 (4.8%)	intracellular transport
GO:0006996	4.42E-03	3859	162 (4.2%)	organelle organization
GO:0051649	4.45E-03	2203	101 (4.6%)	establishment of localization in cell
GO:0006725	4.69E-03	6015	236 (4.0%)	cellular aromatic compound metabolic process
GO:0019438	4.78E-03	4296	179 (4.2%)	aromatic compound biosynthetic process
GO:0048585	4.78E-03	1539	77 (5.0%)	negative regulation of response to stimulus
GO:0051445	4.88E-03	47	8 (17.0%)	regulation of meiotic cell cycle
GO:1903046	5.03E-03	189	16 (8.5%)	meiotic cell cycle process
GO:0030029	5.03E-03	728	41 (5.6%)	actin filament-based process
GO:0065009	5.03E-03	3198	136 (4.3%)	regulation of molecular function
GO:0046483	5.06E-03	5967	234 (4.0%)	heterocycle metabolic process
GO:0033036	5.38E-03	3041	130 (4.3%)	macromolecule localization
GO:0009057	5.44E-03	1376	70 (5.1%)	macromolecule catabolic process

GO:1901565	5.44E-03	1284	66 (5.2%)	organonitrogen compound catabolic process
GO:0008104	5.68E-03	2708	119 (4.4%)	protein localization
GO:0044093	5.68E-03	1755	83 (4.7%)	positive regulation of molecular function
GO:0010467	6.16E-03	5440	218 (4.0%)	gene expression
GO:0051128	6.16E-03	2498	113 (4.5%)	regulation of cellular component organization
GO:0051716	6.75E-03	7471	282 (3.8%)	cellular response to stimulus
GO:0051015	6.98E-03	193	17 (8.8%)	actin filament binding
GO:0072595	7.15E-03	39	7 (17.9%)	maintenance of protein localization in organelle
GO:0010941	7.15E-03	1651	80 (4.9%)	regulation of cell death
GO:0009892	7.15E-03	2890	127 (4.4%)	negative regulation of metabolic process
GO:0010033	7.49E-03	3173	135 (4.3%)	response to organic substance
GO:0023051	7.49E-03	3531	148 (4.2%)	regulation of signaling
GO:0030036	7.49E-03	639	37 (5.8%)	actin cytoskeleton organization
GO:0044403	7.75E-03	784	43 (5.5%)	symbiont process
GO:0044430	7.77E-03	1656	78 (4.7%)	cytoskeletal part
GO:0045185	7.94E-03	105	11 (10.5%)	maintenance of protein location
GO:0030163	8.35E-03	918	50 (5.5%)	protein catabolic process
GO:0001944	8.44E-03	684	40 (5.8%)	vasculature development
GO:0006915	8.70E-03	1933	90 (4.7%)	apoptotic process
GO:0009059	8.70E-03	5010	201 (4.0%)	macromolecule biosynthetic process
GO:0036293	8.76E-03	320	23 (7.2%)	response to decreased oxygen levels
GO:0023057	8.76E-03	1293	65 (5.0%)	negative regulation of signaling
GO:0010646	8.76E-03	3496	148 (4.2%)	regulation of cell communication
GO:0045569	8.91E-03	5	3 (60.0%)	TRAIL binding
GO:0072358	9.23E-03	693	40 (5.8%)	cardiovascular system development
GO:0031589	9.28E-03	337	23 (6.8%)	cell-substrate adhesion
GO:0097708	9.53E-03	2306	102 (4.4%)	intracellular vesicle
GO:0022603	9.55E-03	1005	53 (5.3%)	regulation of anatomical structure morphogenesis
GO:0051640	9.83E-03	698	39 (5.6%)	organelle localization
GO:0006457	9.95E-03	227	17 (7.5%)	protein folding
GO:0006793	9.96E-03	3235	136 (4.2%)	phosphorus metabolic process
GO:0042641	1.01E-02	72	9 (12.5%)	actomyosin
GO:0044448	1.08E-02	175	15 (8.6%)	cell cortex part
GO:0051321	1.08E-02	250	18 (7.2%)	meiotic cell cycle
GO:0022402	1.08E-02	1326	63 (4.8%)	cell cycle process
GO:0001568	1.09E-02	656	37 (5.6%)	blood vessel development
GO:0033043	1.10E-02	1282	66 (5.2%)	regulation of organelle organization
GO:0012505	1.11E-02	4478	178 (4.0%)	endomembrane system
GO:1902494	1.13E-02	1374	65 (4.7%)	catalytic complex
GO:0035295	1.15E-02	996	51 (5.1%)	tube development
GO:0009628	1.19E-02	1151	56 (4.9%)	response to abiotic stimulus
GO:0009653	1.19E-02	2560	109 (4.3%)	anatomical structure morphogenesis

GO:0001776	1.19E-02	86	9 (10.5%)	leukocyte homeostasis
GO:0044419	1.19E-02	833	43 (5.2%)	interspecies interaction between organisms
GO:0031410	1.21E-02	2303	102 (4.4%)	cytoplasmic vesicle
GO:0001666	1.30E-02	308	21 (6.8%)	response to hypoxia
GO:0035239	1.30E-02	809	43 (5.3%)	tube morphogenesis
GO:0048732	1.33E-02	437	28 (6.4%)	gland development
GO:0002009	1.35E-02	483	30 (6.2%)	morphogenesis of an epithelium
GO:0070997	1.42E-02	333	22 (6.6%)	neuron death
GO:0016222	1.45E-02	2	2 (100.0%)	procollagen-proline 4-dioxygenase complex
GO:0043167	1.49E-02	6263	241 (3.9%)	ion binding
GO:0030864	1.51E-02	80	9 (11.2%)	cortical actin cytoskeleton
GO:0010605	1.53E-02	2653	118 (4.5%)	negative regulation of macromolecule metabolic process
GO:0009896	1.53E-02	419	28 (6.7%)	positive regulation of catabolic process
GO:0031324	1.53E-02	2532	113 (4.5%)	negative regulation of cellular metabolic process
GO:0072656	1.53E-02	5	3 (60.0%)	maintenance of protein location in mitochondrion
GO:0010648	1.53E-02	1289	65 (5.1%)	negative regulation of cell communication
GO:0007010	1.54E-02	1328	65 (4.9%)	cytoskeleton organization
GO:0019219	1.55E-02	4070	168 (4.2%)	regulation of nucleobase-containing compound metabolic process
GO:0060548	1.55E-02	977	52 (5.3%)	negative regulation of cell death
GO:0090304	1.55E-02	5174	204 (4.0%)	nucleic acid metabolic process
GO:0070887	1.55E-02	3148	131 (4.2%)	cellular response to chemical stimulus
GO:0001525	1.55E-02	489	29 (5.9%)	angiogenesis
GO:0043067	1.62E-02	1527	74 (4.8%)	regulation of programmed cell death
GO:0032386	1.62E-02	429	28 (6.5%)	regulation of intracellular transport
GO:0051172	1.63E-02	2369	106 (4.5%)	negative regulation of nitrogen compound metabolic process
GO:0010811	1.65E-02	118	12 (10.2%)	positive regulation of cell-substrate adhesion
GO:0002832	1.65E-02	44	7 (15.9%)	negative regulation of response to biotic stimulus
GO:0051603	1.65E-02	705	40 (5.7%)	proteolysis involved in cellular protein catabolic process
GO:0044463	1.67E-02	1452	67 (4.6%)	cell projection part
GO:0005615	1.74E-02	3347	136 (4.1%)	extracellular space
GO:0030011	1.77E-02	17	4 (23.5%)	maintenance of cell polarity
GO:0048729	1.77E-02	612	34 (5.6%)	tissue morphogenesis
GO:0031647	1.77E-02	277	19 (6.9%)	regulation of protein stability
GO:0042127	1.78E-02	1601	75 (4.7%)	regulation of cell proliferation
GO:0030155	1.81E-02	661	36 (5.5%)	regulation of cell adhesion
GO:0044772	1.82E-02	495	30 (6.1%)	mitotic cell cycle phase transition
GO:0072331	1.83E-02	220	17 (7.7%)	signal transduction by p53 class mediator
GO:0099177	1.83E-02	429	27 (6.3%)	regulation of trans-synaptic signaling
GO:0033267	1.85E-02	377	24 (6.4%)	axon part
GO:0044257	1.92E-02	759	42 (5.5%)	cellular protein catabolic process
GO:0009889	1.95E-02	4246	171 (4.1%)	regulation of biosynthetic process

GO:0005911	1.98E-02	446	26 (5.8%)	cell-cell junction
GO:0000278	2.03E-02	935	47 (5.0%)	mitotic cell cycle
GO:0009966	2.06E-02	3144	132 (4.2%)	regulation of signal transduction
GO:0043632	2.07E-02	624	36 (5.8%)	modification-dependent macromolecule catabolic process
GO:0051174	2.07E-02	1714	80 (4.7%)	regulation of phosphorus metabolic process
GO:0006796	2.20E-02	3208	134 (4.2%)	phosphate-containing compound metabolic process
GO:0048856	2.23E-02	5790	220 (3.8%)	anatomical structure development
GO:0051130	2.25E-02	1233	61 (5.0%)	positive regulation of cellular component organization
GO:0043029	2.30E-02	38	6 (15.8%)	T cell homeostasis
GO:0002040	2.30E-02	115	11 (9.6%)	sprouting angiogenesis
GO:0016032	2.30E-02	721	39 (5.4%)	viral process
GO:0048514	2.30E-02	576	33 (5.7%)	blood vessel morphogenesis
GO:0007050	2.38E-02	243	17 (7.0%)	cell cycle arrest
GO:0040017	2.39E-02	533	31 (5.8%)	positive regulation of locomotion
GO:0044265	2.45E-02	1141	56 (4.9%)	cellular macromolecule catabolic process
GO:0140013	2.48E-02	172	14 (8.1%)	meiotic nuclear division
GO:0006928	2.51E-02	2079	89 (4.3%)	movement of cell or subcellular component
GO:0034059	2.59E-02	4	2 (66.7%)	response to anoxia
GO:0120038	2.73E-02	1452	67 (4.6%)	plasma membrane bounded cell projection part
GO:0019904	2.77E-02	710	39 (5.5%)	protein domain specific binding
GO:1902531	2.78E-02	1841	84 (4.6%)	regulation of intracellular signal transduction
GO:0022604	2.78E-02	478	29 (6.1%)	regulation of cell morphogenesis
GO:0051345	2.92E-02	762	41 (5.4%)	positive regulation of hydrolase activity
GO:0010498	2.92E-02	461	28 (6.1%)	proteasomal protein catabolic process
GO:0001738	2.92E-02	98	10 (10.3%)	morphogenesis of a polarized epithelium
GO:0022612	2.95E-02	120	11 (9.2%)	gland morphogenesis
GO:0044281	2.95E-02	2011	86 (4.3%)	small molecule metabolic process
GO:0007165	2.96E-02	6053	227 (3.8%)	signal transduction
GO:0098805	3.01E-02	1660	73 (4.4%)	whole membrane
GO:0098576	3.01E-02	4	2 (50.0%)	lumenal side of membrane
GO:0031932	3.01E-02	12	3 (25.0%)	TORC2 complex
GO:0098693	3.07E-02	115	11 (9.6%)	regulation of synaptic vesicle cycle
GO:0051252	3.08E-02	3795	154 (4.1%)	regulation of RNA metabolic process
GO:0015629	3.10E-02	492	31 (6.3%)	actin cytoskeleton
GO:0051338	3.14E-02	954	48 (5.0%)	regulation of transferase activity
GO:0048870	3.20E-02	1623	71 (4.4%)	cell motility
GO:0051674	3.20E-02	1623	71 (4.4%)	localization of cell
GO:0002260	3.28E-02	62	7 (11.3%)	lymphocyte homeostasis
GO:0009967	3.34E-02	1579	73 (4.6%)	positive regulation of signal transduction
GO:0016310	3.34E-02	2299	100 (4.4%)	phosphorylation
GO:0051272	3.34E-02	514	30 (5.8%)	positive regulation of cellular component movement

GO:0007164	3.42E-02	80	8 (10.1%)	establishment of tissue polarity
GO:0006082	3.54E-02	1097	52 (4.8%)	organic acid metabolic process
GO:0061245	3.54E-02	48	6 (12.5%)	establishment or maintenance of bipolar cell polarity
GO:0007155	3.59E-02	1389	62 (4.5%)	cell adhesion
GO:0000313	3.59E-02	87	8 (9.2%)	organellar ribosome
GO:0022008	3.67E-02	1580	72 (4.6%)	neurogenesis
GO:0016192	3.70E-02	2125	92 (4.4%)	vesicle-mediated transport
GO:0043624	3.85E-02	215	16 (7.4%)	cellular protein complex disassembly
GO:0072413	3.87E-02	58	7 (12.1%)	signal transduction involved in mitotic cell cycle checkpoint
GO:0045785	3.88E-02	395	24 (6.1%)	positive regulation of cell adhesion
GO:0072395	3.88E-02	74	8 (10.8%)	signal transduction involved in cell cycle checkpoint
GO:0007059	3.89E-02	318	19 (6.0%)	chromosome segregation
GO:0031648	3.94E-02	44	6 (13.6%)	protein destabilization
GO:0007015	3.97E-02	397	24 (6.1%)	actin filament organization
GO:1904880	4.03E-02	3	2 (66.7%)	response to hydrogen sulfide
GO:0043436	4.03E-02	1077	52 (4.8%)	oxoacid metabolic process
GO:0030427	4.03E-02	167	12 (7.2%)	site of polarized growth
GO:0098984	4.03E-02	343	20 (5.8%)	neuron to neuron synapse
GO:0071214	4.06E-02	326	20 (6.2%)	cellular response to abiotic stimulus
GO:0104004	4.06E-02	326	20 (6.2%)	cellular response to environmental stimulus
GO:0022411	4.08E-02	533	29 (5.4%)	cellular component disassembly
GO:0010556	4.11E-02	4031	161 (4.0%)	regulation of macromolecule biosynthetic process
GO:0033365	4.11E-02	907	46 (5.1%)	protein localization to organelle
GO:0051402	4.14E-02	227	16 (7.1%)	neuron apoptotic process
GO:0010468	4.17E-02	4492	177 (4.0%)	regulation of gene expression
GO:0046872	4.21E-02	4197	173 (4.2%)	metal ion binding
GO:0045296	4.21E-02	329	23 (7.0%)	cadherin binding
GO:0002020	4.21E-02	126	12 (9.5%)	protease binding
GO:0005178	4.21E-02	127	12 (9.4%)	integrin binding
GO:0019752	4.23E-02	987	49 (5.0%)	carboxylic acid metabolic process
GO:0006351	4.23E-02	3645	147 (4.1%)	transcription, DNA-templated
GO:0061919	4.25E-02	484	26 (5.4%)	process utilizing autophagic mechanism
GO:0097159	4.26E-02	6118	230 (3.8%)	organic cyclic compound binding
GO:1901363	4.26E-02	6031	227 (3.8%)	heterocyclic compound binding
GO:0072401	4.26E-02	73	8 (11.0%)	signal transduction involved in DNA integrity checkpoint
GO:0072422	4.26E-02	73	8 (11.0%)	signal transduction involved in DNA damage checkpoint
GO:1990778	4.26E-02	305	20 (6.6%)	protein localization to cell periphery
GO:0010942	4.26E-02	671	36 (5.4%)	positive regulation of cell death
GO:0097435	4.27E-02	657	34 (5.2%)	supramolecular fiber organization
GO:0023014	4.27E-02	907	44 (4.9%)	signal transduction by protein phosphorylation
GO:0071310	4.31E-02	2601	109 (4.2%)	cellular response to organic substance

GO:0035090	4.31E-02	10	3 (30.0%)	maintenance of apical/basal cell polarity
GO:0043278	4.33E-02	32	5 (15.6%)	response to morphine
GO:0016070	4.46E-02	4644	181 (3.9%)	RNA metabolic process
GO:0051129	4.46E-02	701	37 (5.3%)	negative regulation of cellular component organization
GO:0031326	4.46E-02	4174	165 (4.0%)	regulation of cellular biosynthetic process
GO:0044502	4.46E-02	3	2 (66.7%)	positive regulation of signal transduction in other organism
GO:2000638	4.46E-02	3	2 (66.7%)	regulation of SREBP signaling pathway
GO:1905114	4.47E-02	567	31 (5.5%)	cell surface receptor signaling pathway involved in cell-cell signaling
GO:0006810	4.57E-02	5116	195 (3.8%)	transport
GO:0071889	4.62E-02	29	5 (17.2%)	14-3-3 protein binding
GO:0045197	4.63E-02	45	6 (13.3%)	establishment or maintenance of epithelial cell apical/basal polarity
GO:0072332	4.64E-02	76	8 (10.5%)	intrinsic apoptotic signaling pathway by p53 class mediator
GO:0032774	4.64E-02	3705	148 (4.0%)	RNA biosynthetic process
GO:0045199	4.65E-02	10	3 (30.0%)	maintenance of epithelial cell apical/basal polarity
GO:0014072	4.65E-02	32	5 (15.6%)	response to isoquinoline alkaloid
GO:0006555	4.65E-02	20	4 (20.0%)	methionine metabolic process
GO:0019058	4.65E-02	293	19 (6.5%)	viral life cycle
GO:0045786	4.69E-02	574	31 (5.5%)	negative regulation of cell cycle
GO:0072522	4.69E-02	272	18 (6.6%)	purine-containing compound biosynthetic process
GO:0031175	4.69E-02	959	47 (4.9%)	neuron projection development
GO:1990089	4.70E-02	53	6 (11.5%)	response to nerve growth factor
GO:1903047	4.72E-02	789	39 (5.0%)	mitotic cell cycle process
GO:0051347	4.73E-02	639	34 (5.3%)	positive regulation of transferase activity
GO:0001726	4.84E-02	172	13 (7.6%)	ruffle
GO:0044283	4.89E-02	742	37 (5.0%)	small molecule biosynthetic process
GO:0030030	4.89E-02	1545	68 (4.4%)	cell projection organization
GO:0046394	4.95E-02	408	24 (5.9%)	carboxylic acid biosynthetic process
GO:0048699	4.97E-02	1483	67 (4.5%)	generation of neurons
GO:0051336	4.97E-02	1273	59 (4.6%)	regulation of hydrolase activity
GO:0001736	4.97E-02	80	8 (10.1%)	establishment of planar polarity
GO:0016053	4.99E-02	409	24 (5.9%)	organic acid biosynthetic process
GO:0044819	4.99E-02	63	7 (11.1%)	mitotic G1/S transition checkpoint
GO:0017022	5.01E-02	67	8 (11.9%)	myosin binding
GO:0019900	5.01E-02	724	39 (5.4%)	kinase binding
GO:0000902	5.01E-02	1017	49 (4.8%)	cell morphogenesis
GO:0035088	5.05E-02	48	6 (12.5%)	establishment or maintenance of apical/basal cell polarity
GO:0005938	5.07E-02	301	20 (6.6%)	cell cortex
GO:0030863	5.07E-02	107	10 (9.3%)	cortical cytoskeleton
GO:0015630	5.07E-02	1179	56 (4.8%)	microtubule cytoskeleton
GO:0097517	5.07E-02	60	7 (11.7%)	contractile actin filament bundle

GO:0043901	5.08E-02	175	13 (7.5%)	negative regulation of multi-organism process
GO:0060429	5.09E-02	1227	57 (4.7%)	epithelium development
GO:0000165	5.14E-02	896	44 (4.9%)	MAPK cascade
GO:0006986	5.14E-02	176	13 (7.5%)	response to unfolded protein
GO:0006974	5.14E-02	850	42 (5.0%)	cellular response to DNA damage stimulus
GO:1990090	5.14E-02	50	6 (12.2%)	cellular response to nerve growth factor stimulus
GO:0071453	5.14E-02	177	13 (7.4%)	cellular response to oxygen levels
GO:0044839	5.14E-02	217	15 (6.9%)	cell cycle G2/M phase transition
GO:0030182	5.14E-02	1338	61 (4.6%)	neuron differentiation
GO:0051726	5.14E-02	1139	53 (4.7%)	regulation of cell cycle
GO:1901214	5.19E-02	299	19 (6.4%)	regulation of neuron death
GO:0006839	5.23E-02	238	16 (6.7%)	mitochondrial transport
GO:0061024	5.24E-02	879	42 (4.8%)	membrane organization
GO:0060706	5.24E-02	25	4 (16.0%)	cell differentiation involved in embryonic placenta development
GO:0006735	5.24E-02	25	4 (16.0%)	NADH regeneration
GO:0044783	5.38E-02	64	7 (10.9%)	G1 DNA damage checkpoint
GO:0031333	5.39E-02	136	11 (8.1%)	negative regulation of protein complex assembly
GO:0048583	5.47E-02	4227	163 (3.9%)	regulation of response to stimulus
GO:0006790	5.47E-02	367	21 (5.8%)	sulfur compound metabolic process
GO:0051668	5.47E-02	147	11 (7.5%)	localization within membrane
GO:0007166	5.47E-02	3008	120 (4.0%)	cell surface receptor signaling pathway

Chapter V: Conclusions and Implications

Overall, this dissertation utilized molecular and toxicogenomic approaches to investigate biological responses to PM from traffic-related and natural emissions. In the literature review in Chapter I, we assessed the current scientific evidence by searching the keywords of "traffic related air pollution", "particulate matter", "human health", and "metabolic syndrome" from 1980 to 2018 of traffic-related PM-induced cardiometabolic syndrome. It was an initial step to formulate research questions about the traffic-related PM and their health effects. Our findings reveal consistent correlations between traffic-related PM exposure and measured cardiometabolic health endpoints. We found that the development of cardiometabolic symptoms can occur through chronic systemic inflammation and increased oxidative stress. We suggested that additional research was needed to investigate the detailed chemical composition of PM constituents, atmospheric transformations, and the modes of action to induce adverse health effects. Furthermore, we highlighted that future studies could explore the roles of genetic and epigenetic factors in influencing cardiometabolic health outcomes by integrating multi-omics approaches (e.g., genomics, epigenomics, and transcriptomics) to provide a comprehensive assessment of biological perturbations caused by traffic-related PM. Based on our literature review, we designed our experiments and selected gasoline exhaust particles as our source of exposure in Chapter II.

We assessed the toxicological potencies of PM emissions from a modern vehicle equipped with a gasoline direct injection (GDI) engine when operated on eight different fuels with varying aromatic hydrocarbon and ethanol contents. Testing was conducted over

the LA92 driving cycle, using a chassis dynamometer with a constant volume sampling system, where particles were collected onto Teflon filters. The extracted PM constituents were analyzed for their oxidative potential using the dithiothreitol (DTT) chemical assay and exposure-induced gene expression in human lung cells. Different trends of DTT activities were seen when testing PM samples in 100% aqueous buffer solutions versus elevated fraction of methanol in aqueous buffers (50:50), indicating the effect of solubility of organic PM constituents on the measured oxidative potential. The Higher aromatic content in fuels corresponded to higher DTT activities in PM. In the literature review we observed that chronic systemic inflammation and increased oxidative stress are the main identified pathways leading to cardiometabolic disease. Therefore, we selected a few biomarkers related to oxidative stress and inflammation Each of the selected biomarkers was significantly altered with the gasoline exhaust particles exposure. Exposure to PM exhaust upregulated the expression of *HMOX-1*, but downregulated the expression of *IL-6*, *TNF-α*, *CCL5* and *NOS2* in BEAS-2B cells. The principal component regression analysis revealed different patterns of correlations. Aromatics content contributed to more significant PAH-mediated *IL-6* downregulation, whereas ethanol content was associated with decreased downregulation of *IL-6*. Our findings highlighted the key role of fuel composition in modulating the toxicological responses to GDI PM emissions. Chapter II confirms the findings of our literature review that inflammation and oxidative stress are two important pathways for traffic-related PM-induced health outcomes.

In the Chapters III and IV, we studied DMSe-derived SOA, a novel natural source of PM. The major source of DMSe compounds is through microbial transformation and plant

metabolism in aquatic and terrestrial environments. We investigated the processes of DMSe oxidation leading to SOA formation and the pulmonary health effects induced by exposure to DMSe-derived SOA. In Chapter III, we characterized the chemical composition and formation yields of SOA produced from the oxidation of DMSe with OH radicals and O_3 in controlled chamber experiments. Further, we profiled the transcriptome-wide gene expression changes in human lung cells after exposure to DMSe-derived SOA. The oxidative potential of DMSe-derived SOA, as measured by the DTT assay, suggested the presence of oxidizing moieties in DMSe-derived SOA at levels higher than in typical ambient aerosols. Compared to our traffic-related PM (Chapter II), DMSe-derived SOA has more oxidative potential capacity. Utilizing RNA sequencing (RNA-Seq) techniques, gene expression profiling followed by pathway enrichment analysis revealed several major biological pathways perturbed by DMSe-derived SOA, including elevated genotoxicity and p53-mediated stress responses, as well as downregulated cholesterol biosynthesis, glycolysis, and interleukin IL-4/IL-13 signaling. Chapter III highlights the significance of DMSe-derived SOA as a stressor in human airway epithelial cells.

In Chapter IV, we extended our study at the lncRNA level because recent evidence has suggested that lncRNAs can play important role and act as a potential epigenetic factor in gene expression regulation. We performed integrative analyses of lncRNA–mRNA coexpression in the human lung cell exposed to DMSe-derived SOA and identified a total of 971 differentially expressed lncRNAs in the human lung cells exposed to SOA derived from O_3 and OH oxidized DMSe. Gene ontology network analysis of *cis*-targeted genes showed significant enrichment of DNA damage, apoptosis, and p53-mediated stress

response pathways. In addition, four *trans*-acting lncRNAs known to be associated with human carcinogenesis, including *PINCR*, *PICART1*, *DLGAP1-AS2*, and *LINC01629*, also differentially expressed in human lung cells treated with DMSe-SOA. Overall, Chapter IV highlights the potential regulatory role of lncRNAs in altering gene expression induced by DMSe-SOA exposure.

Taken together, our findings conclude that oxidative stress and inflammatory biomarkers play a pivotal role in the health outcomes from traffic-related PM. Traffic-related PM can be linked to the global public health of PM for vulnerable people who live in urban areas and are hence exposed to higher levels of traffic-related PM. Through our literature review, the elderly (especially for women), children, genetically susceptible individuals, and people with pre-existing conditions were identified as vulnerable groups. The oxidative potential and health outcomes induced by natural DMSe-derived SOA can have important implications for both urban and rural people. Due to higher volatilization rate of methylated Se under warmer temperature, DMSe-derived SOA emissions potentially can increase in warmer region. Furthermore, because of the relatively long lifetime of the DMSe-derived SOA (~7-10 days), their ability to travel further distances, and its toxicological potency, DMSe-derived SOA is potentially a new environmental pollutant. We identified some major pathways including genotoxicity and p53-mediated pathways that are perturbed by DMSe-derived SOA. Additionally, we investigated the potential role of lncRNAs in DMSe-derived SOA exposed lung cells and found that lncRNAs might regulate gene expression through both *cis* and *trans* mechanism. Therefore, our identified mRNA and lncRNA could serve as potential biomarkers for lung diseases.

Further functional validation at the phenotype level is recommended for future studies to demonstrate the effects of gasoline exhaust particles and DMSe-derived SOA exposure from both genetic and epigenetic perspectives. Moreover, results from these studies will ultimately inform regulators about health effects due to PM exposure from traffic and natural emissions and help determining strategies to minimize the health risks from PM exposure.

References

1. Anderson, J. O.; Thundiyil, J. G.; Stolbach, A., Clearing the air: a review of the effects of particulate matter air pollution on human health. *J. Med. Toxicol.* **2012,** *8*, (2), 166-175.

2. Kampa, M.; Castanas, E., Human health effects of air pollution. *Environ. Pollut.* **2008,** *151*, 362-367.

3. Bell, M. L.; Davis, D. L., Reassessment of the lethal London fog of 1952: novel indicators of acute and chronic consequences of acute exposure to air pollution. *Environ. Health Perspect.* **2001,** *109*, (suppl 3), 389-394.

4. EPA, U., "Overview of the Clean Air Act and Air Pollution". https://www.epa.gov/clean-air-act-overview Accessed on May 23, 2019.

5. Esworthy, R. In *Air quality: EPA's 2013 changes to the particulate matter (PM) standard*, 2013; Library of Congress, Congressional Research Service: 2013.

6. Kim, K.-H.; Kabir, E.; Kabir, S., A review on the human health impact of airborne particulate matter. *Environ. Int.* **2015,** *74*, 136-143.

7. Hallquist, M.; Wenger, J.; Baltensperger, U.; Rudich, Y.; Simpson, D.; Claeys, M.; Dommen, J.; Donahue, N.; George, C.; Goldstein, A., The formation, properties and impact of secondary organic aerosol: current and emerging issues. *Atmos. Chem. Phys.* **2009,** *9*, (14), 5155-5236.

8. Lin, Y.-H.; Arashiro, M.; Clapp, P. W.; Cui, T.; Sexton, K. G.; Vizuete, W.; Gold, A.; Jaspers, I.; Fry, R. C.; Surratt, J. D., Gene Expression Profiling in Human Lung Cells Exposed to Isoprene-Derived Secondary Organic Aerosol. *Environ. Sci. Technol.* **2017,** *51*, (14), 8166-8175.

9. Ahmed, C.; Jiang, H.; Chen, J.; Lin, Y.-H.; Ahmed, C. M. S.; Jiang, H.; Chen, J. Y.; Lin, Y.-H., Traffic-Related Particulate Matter and Cardiometabolic Syndrome: A Review. *Atmosphere* **2018,** *9*, (9), 336-336.

10. Organization, W. H., Health effects of particulate matter. Policy implications for countries in Eastern Europe. Caucasus and central Asia. *World Health Organization Regional Office for Europe, Copenhagen* **2013**, http://www.euro.who.int/__data/assets/pdf_file/0006/189051/Health-effects-of-particulate-matter-final-Eng.pdf Accessed on May 23, 2019.

11. Board, S. C. A. Q. M. D. G., PM controls 2016 AQMP White Paper. In 2016.

12. von Stackelberg, K.; Buonocore, J.; Bhave, P. V.; Schwartz, J. A., Public health impacts of secondary particulate formation from aromatic hydrocarbons in gasoline. *Environ. Health* **2013,** *12*, (1), 19.

13. Hallquist, M.; Wenger, J. C.; Baltensperger, U.; Rudich, Y.; Simpson, D.; Claeys, M.; Dommen, J.; Donahue, N.; George, C.; Goldstein, A.; physics, The formation, properties and impact of secondary organic aerosol: current and emerging issues. *Atmos. Chem.* **2009,** *9*, (14), 5155-5236.

14. Jiang, H.; Jang, M., Dynamic Oxidative Potential of Atmospheric Organic Aerosol under Ambient Sunlight. *Environ. Sci. Technol.* **2018,** *52*, (13), 7496-7504.

15. Neeman, E. M.; Moreno, J. R. A.; Huet, T. R., The gas phase structure of α-pinene, a main biogenic volatile organic compound. *J. Chem. Phys.* **2017,** *147*, (21), 214305.

16. Ullah, H.; Liu, G.; Yousaf, B.; Ali, M. U.; Irshad, S.; Abbas, Q.; Ahmad, R., A comprehensive review on environmental transformation of selenium: recent advances and research perspectives. *Environ. Geochem. Health* **2018**, 1-33.

17. Gupta, M.; Gupta, S., An overview of selenium uptake, metabolism, and toxicity in plants. *Front. Plant. Sci.* **2017,** *7*, 2074.

18. Barnes, I.; Hjorth, J.; Mihalopoulos, N., Dimethyl Sulfide and Dimethyl Sulfoxide and Their Oxidation in the Atmosphere. *Chem. Rev.* **2006,** *106*, (3), 940-975.

19. Atkinson, R.; Aschmann, S. M.; Hasegawa, D.; Thompson-Eagle, E. T.; Frankenberger, W. T., Kinetics of the atmospherically important reactions of dimehtyl selenide. *Environ. Sci. Technol.* **1990,** *24*, (9).

20. Thron, R. W., Direct and indirect exposure to air pollution. *Otolaryngology-Head and Neck Surgery* **1996,** *114*, (2), 281-285.

21. Franklin, B. A.; Brook, R.; Arden Pope, C., Air Pollution and Cardiovascular Disease. *Curr. Prob. Cardiol.* **2015,** *40*, (5), 207-238.

22. Xia, T.; Zhu, Y.; Mu, L.; Zhang, Z.-F.; Liu, S., Pulmonary diseases induced by ambient ultrafine and engineered nanoparticles in twenty-first century. *Nat. Sci. Rev.* **2016,** *3*, (4), 416-429.

23. Organization, W. H., Ambient (outdoor) air quality and health. **2018**, https://www.who.int/en/news-room/fact-sheets/detail/ambient-(outdoor)-air-quality-and-health.

24. Silverman, D. T.; Samanic, C. M.; Lubin, J. H.; Blair, A. E.; Stewart, P. A.; Vermeulen, R.; Coble, J. B.; Rothman, N.; Schleiff, P. L.; Travis, W. D.; Ziegler, R. G.; Wacholder, S.; Attfield, M. D., The diesel exhaust in miners study: A nested case-control study of lung cancer and diesel exhaust. *J. Nation. Cancer Inst.* **2012,** *104*, (11), 855-868.

25. Zheng, X.; Wu, Y.; Zhang, S.; Hu, J.; Zhang, K. M.; Li, Z.; He, L.; Hao, J., Characterizing particulate polycyclic aromatic hydrocarbon emissions from diesel vehicles using a portable emissions measurement system. *Sci. Rep.* **2017,** *7*, (1), 1-12.

26. Brook, R. D.; Urch, B.; Dvonch, J. T.; Bard, R. L.; Speck, M.; Keeler, G.; Morishita, M.; Marsik, F. J.; Kamal, A. S.; Kaciroti, N., Insights into the mechanisms and mediators of the effects of air pollution exposure on blood pressure and vascular function in healthy humans. *Hypertension* **2009,** *54*, (3), 659-667.

27. Langrish, J. P.; Mills, N. L.; Chan, J. K.; Leseman, D. L.; Aitken, R. J.; Fokkens, P. H.; Cassee, F. R.; Li, J.; Donaldson, K.; Newby, D. E., Beneficial cardiovascular effects of reducing exposure to particulate air pollution with a simple facemask. *Part. Fibre Toxicol.* **2009,** *6*, (1), 8.

28. Brook, R. D.; Xu, X.; Bard, R. L.; Dvonch, J. T.; Morishita, M.; Kaciroti, N.; Sun, Q.; Harkema, J.; Rajagopalan, S., Reduced metabolic insulin sensitivity following sub-acute exposures to low levels of ambient fine particulate matter air pollution. *Sci. Total Environ.* **2013,** *448*, 66-71.

29. Arashiro, M.; Lin, Y.-H.; Zhang, Z.; Sexton, K. G.; Gold, A.; Jaspers, I.; Fry, R. C.; Surratt, J. D., Effect of secondary organic aerosol from isoprene-derived hydroxyhydroperoxides on the expression of oxidative stress response genes in human bronchial epithelial cells. *Environ. Sci. Process Impacts* **2018,** *20*, (2), 332-339.

30. Cohen, A. J.; Brauer, M.; Burnett, R.; Anderson, H. R.; Frostad, J.; Estep, K.; Balakrishnan, K.; Brunekreef, B.; Dandona, L.; Dandona, R.; Feigin, V.; Freedman, G.; Hubbell, B.; Jobling, A.; Kan, H.; Knibbs, L.; Liu, Y.; Martin, R.; Morawska, L.; Pope, C. A.; Shin, H.; Straif, K.; Shaddick, G.; Thomas, M.; van Dingenen, R.; van Donkelaar, A.; Vos, T.; Murray, C. J. L.; Forouzanfar, M. H., Estimates and 25-year trends of the global burden of disease attributable to ambient air pollution: an analysis of data from the Global Burden of Diseases Study 2015. *The Lancet* **2017,** *389*, (10082), 1907-1918.

31. Berg, K. E.; Turner, L. R.; Benka-Coker, M. L.; Rajkumar, S.; Young, B. N.; Peel, J. L.; Clark, M. L.; Volckens, J.; Henry, C. S., Electrochemical dithiothreitol assay for large-scale particulate matter studies. *Aeros. Sci. Technol.* **2019,** *53*, (3), 268-275.

32. Charrier, J. G.; Richards-Henderson, N. K.; Bein, K. J.; McFall, A. S.; Wexler, A. S.; Anastasio, C., Oxidant production from source-oriented particulate matter – Part 1: Oxidative potential using the dithiothreitol (DTT) assay. *Atmos. Chem. Phys.* **2015,** *15*, (5), 2327-2340.

33. Gao, D.; Fang, T.; Verma, V.; Zeng, L.; Weber, R. J., A method for measuring total aerosol oxidative potential (OP) with the dithiothreitol (DTT) assay and comparisons between an urban and roadside site of water-soluble and total OP. *Atmos. Meas. Tech.* **2017,** *10*, (8), 2821-2835.

34. Fang, T.; Verma, V.; Guo, H.; King, L. E.; Edgerton, E. S.; Weber, R. J., A semi-automated system for quantifying the oxidative potential of ambient particles in aqueous extracts using the dithiothreitol (DTT) assay: results from the Southeastern Center for Air Pollution and Epidemiology (SCAPE). *Atmos. Meas. Tech.* **2015,** *8*, (1), 471-482.

35. Verma, V.; Fang, T.; Xu, L.; Peltier, R. E.; Russell, A. G.; Ng, N. L.; Weber, R. J., Organic Aerosols Associated with the Generation of Reactive Oxygen Species (ROS) by Water-Soluble PM2.5. *Environ. Sci. Technol.* **2015,** *49*, (7), 4646-4656.

36. Charrier, J. G.; Anastasio, C., On dithiothreitol (DTT) as a measure of oxidative potential for ambient particles: evidence for the importance of soluble transition metals. *Atmos. Chem. Phys.* **2012,** *12*, (5), 11317-11350.

37. Held, K. D.; Sylvester, F. C.; Hopcia, K. L.; Biaglow, J. E., Role of Fenton Chemistry in Thiol-Induced Toxicity and Apoptosis. *Rad. Res.* **1996,** *145*, (5), 542-553.

38. Cho, A. K.; Sioutas, C.; Miguel, A. H.; Kumagai, Y.; Schmitz, D. A.; Singh, M.; Eiguren-Fernandez, A.; Froines, J. R., Redox activity of airborne particulate matter at different sites in the Los Angeles Basin. *Environ. Res.* **2005,** *99*, (1), 40-47.

39. Alfadda, A. A.; Sallam, R. M., Reactive oxygen species in health and disease. *J Biomed. Biotechnol.* **2012,** *2012*, 936486.

40. Sauvain, J.-J.; Rossi, M. J.; Riediker, M., Comparison of Three Acellular Tests for Assessing the Oxidation Potential of Nanomaterials. *Aeros. Sci. Technol.* **2013,** *47*, (2), 218-227.

41. Foucaud, L.; Wilson, M. R.; Brown, D. M.; Stone, V., Measurement of reactive species production by nanoparticles prepared in biologically relevant media. *Toxicol. Lett.* **2007,** *174*, (1), 1-9.

42. Pan, C. J.; Schmitz, D. A.; Cho, A. K.; Froines, J.; Fukuto, J. M., Inherent redox properties of diesel exhaust particles: catalysis of the generation of reactive oxygen species by biological reductants. *Toxicol. Sci.* **2004,** *81*, (1), 225-32.

43. Haycock, J. W., 3D cell culture: a review of current approaches and techniques. In *3D Cell Culture*, Springer: 2011; pp 1-15.

44. van Vliet, E., Current standing and future prospects for the technologies proposed to transform toxicity testing in the 21st century. *ALTEX-Alt. Ani. Exp.* **2011,** *28*, (1), 17-44.

45. Ravi, M.; Paramesh, V.; Kaviya, S.; Anuradha, E.; Solomon, F. P. J. J. o. c. p., 3D cell culture systems: advantages and applications. *J. Cell. Phy.* **2015,** *230*, (1), 16-26.

46. Holloway, J. W.; Savarimuthu Francis, S.; Fong, K. M.; Yang, I. A., Genomics and the respiratory effects of air pollution exposure. *Respirology* **2012,** *17*, (4), 590-600.

47. Karlsson, O.; Baccarelli, A. A., Environmental health and long non-coding RNAs. *Current Environ. Health Rep.* **2016,** *3*, (3), 178-187.

48. Jirtle, R. L.; Skinner, M. K., Environmental epigenomics and disease susceptibility. *Nat. Rev. Genet.* **2007,** *8*, (4), 253.

49. Assefa, A. T.; De Paepe, K.; Everaert, C.; Mestdagh, P.; Thas, O.; Vandesompele, J., Differential gene expression analysis tools exhibit substandard performance for long non-coding RNA-sequencing data. *Genome Biol.* **2018,** *19*, (1), 96.

50. Wang, K. C.; Chang, H. Y., Molecular mechanisms of long noncoding RNAs. *Molecular Cell* **2011,** *43*, (6), 904-914.

51. Roth, M.; Usemann, J.; Bisig, C.; Comte, P.; Czerwinski, J.; Mayer, A. C. R.; Beier, K.; Rothen-Rutishauser, B.; Latzin, P.; Müller, L., Effects of gasoline and ethanol-gasoline exhaust exposure on human bronchial epithelial and natural killer cells in vitro. *Toxicol. in Vitro* **2017,** *45*, (March), 101-110.

52. Gasser, M.; Riediker, M.; Mueller, L.; Perrenoud, A.; Blank, F.; Gehr, P.; Rothen-Rutishauser, B., Toxic effects of brake wear particles on epithelial lung cells in vitro. *Part. Fibre Toxicol.* **2009,** *6*, (1), 30-30.

53. WHO, Ambient (Outdoor) Air Quality and Health (fact sheet). *September-2016.[apps. who. int/iris/bitstream/10665/250141/1/97 89241511353-eng. pdf]* **2016**.

54. Zhang, K.; Batterman, S., Air pollution and health risks due to vehicle traffic. *Sci. Total Environ.* **2013,** *450*, 307-316.

55. Lin, Y.-C.; Li, Y.-C.; Amesho, K. T.; Chou, F.-C.; Cheng, P.-C., Characterization and quantification of PM2. 5 emissions and PAHs concentration in PM2. 5 from the exhausts of diesel vehicles with various accumulated mileages. *Sci. Total Environ.* **2019,** *660*, 188-198.

56. Silverman, D. T.; Samanic, C. M.; Lubin, J. H.; Blair, A. E.; Stewart, P. A.; Vermeulen, R.; Coble, J. B.; Rothman, N.; Schleiff, P. L.; Travis, W. D.; Ziegler, R. G.;

Wacholder, S.; Attfield, M. D., The diesel exhaust in miners study: A nested case-control study of lung cancer and diesel exhaust. *J. Natl. Cancer Inst.* **2012,** *104*, (11), 855-868.

57. Ahmed, C. M. S.; Jiang, H.; Chen, J.; Lin, Y.-H., Traffic-Related Particulate Matter and Cardiometabolic Syndrome: A Review. *Atmosphere* **2018,** *9*, (9), 336-336.

58. Alkidas, A. C., Combustion advancements in gasoline engines. *Energy Convers. Manag.* **2007,** *48*, (11), 2751-2761.

59. Piock, W.; Hoffmann, G.; Berndorfer, A.; Salemi, P.; Fusshoeller, B., Strategies towards meeting future particulate matter emission requirements in homogeneous gasoline direct injection engines. *SAE International Journal of Engines* **2011,** *4*, (1), 1455-1468.

60. Karlsson, R. B.; Heywood, J. B., Piston fuel film observations in an optical access GDI engine. *SAE Transactions* **2001**, 1505-1516.

61. Saliba, G.; Saleh, R.; Zhao, Y.; Presto, A. A.; Lambe, A. T.; Frodin, B.; Sardar, S.; Maldonado, H.; Maddox, C.; May, A. A., Comparison of gasoline direct-injection (GDI) and port fuel injection (PFI) vehicle emissions: Emission certification standards, cold-start, secondary organic aerosol formation potential, and potential climate impacts. *Environ. Sci. Technol.* **2017,** *51*, (11), 6542-6552.

62. Zinola, S.; Raux, S.; Leblanc, M. *Persistent particle number emissions sources at the tailpipe of combustion engines*; 0148-7191; SAE Technical Paper: 2016.

63. Karavalakis, G.; Short, D.; Vu, D.; Russell, R.; Hajbabaei, M.; Asa-Awuku, A.; Durbin, T. D., Evaluating the effects of aromatics content in gasoline on gaseous and particulate matter emissions from SI-PFI and SIDI vehicles. *Environ. Sci. Technol.* **2015,** *49*, (11), 7021-7031.

64. Chan, T. W.; Lax, D.; Gunter, G. C.; Hendren, J.; Kubsh, J.; Brezny, R., Assessment of the fuel composition impact on black carbon mass, particle number size distributions, solid particle number, organic materials, and regulated gaseous emissions from a light-duty gasoline direct injection truck and passenger car. *Energy & Fuels* **2017,** *31*, (10), 10452-10466.

65. Yang, J.; Roth, P.; Durbin, T. D.; Johnson, K. C.; Asa-Awuku, A.; Cocker III, D. R.; Karavalakis, G., Investigation of the Effect of Mid-And High-Level Ethanol Blends on the Particulate and the Mobile Source Air Toxic Emissions from a Gasoline Direct Injection Flex Fuel Vehicle. *Energy & Fuels* **2018,** *33*, (1), 429-440.

66. Peng, J.; Hu, M.; Du, Z.; Wang, Y.; Zheng, J.; Zhang, W.; Yang, Y.; Qin, Y.; Zheng, R.; Xiao, Y., Gasoline aromatics: a critical determinant of urban secondary organic aerosol formation. *Atmos. Chem. Phys.* **2017,** *17*, (17), 10743-10752.

67. Yao, C.; Dou, Z.; Wang, B.; Liu, M.; Lu, H.; Feng, J.; Feng, L., Experimental study of the effect of heavy aromatics on the characteristics of combustion and ultrafine particle in DISI engine. *Fuel* **2017,** *203*, 290-297.

68. Yang, J.; Roth, P.; Durbin, T.; Karavalakis, G., Impacts of gasoline aromatic and ethanol levels on the emissions from GDI vehicles: Part 1. Influence on regulated and gaseous toxic pollutants. *Fuel* **2019,** *252*, 799-811.

69. Aikawa, K.; Sakurai, T.; Jetter, J. J., Development of a predictive model for gasoline vehicle particulate matter emissions. *SAE International Journal of Fuels Lubricants* **2010,** *3*, (2), 610-622.

70. Leach, F.; Stone, R.; Richardson, D. *The Influence of Fuel Properties on Particulate Number Emissions from a Direct Injection Spark Ignition Engine*; 0148-7191; SAE Technical Paper: 2013.

71. Sobotowski, R. A.; Butler, A. D.; Guerra, Z., A pilot study of fuel impacts on PM emissions from light-duty gasoline vehicles. *SAE Int. J. Fuels Lubri.* **2015,** *8*, (1), 214-233.

72. Barrientos, E. J.; Anderson, J. E.; Maricq, M. M.; Boehman, A. L., Particulate matter indices using fuel smoke point for vehicle emissions with gasoline, ethanol blends, and butanol blends. *Combus. Flame* **2016,** *167*, 308-319.

73. Fatouraie, M.; Frommherz, M.; Mosburger, M.; Chapman, E.; Li, S.; McCormick, R.; Fioroni, G. *Investigation of the impact of fuel properties on particulate number emission of a modern gasoline direct injection engine*; 0148-7191; SAE Technical Paper: 2018.

74. Fushimi, A.; Kondo, Y.; Kobayashi, S.; Fujitani, Y.; Saitoh, K.; Takami, A.; Tanabe, K., Chemical composition and source of fine and nanoparticles from recent direct injection gasoline passenger cars: Effects of fuel and ambient temperature. *Atmos. Environ.* **2016,** *124*, 77-84.

75. Catapano, F.; Sementa, P.; Vaglieco, B. M., Air-fuel mixing and combustion behavior of gasoline-ethanol blends in a GDI wall-guided turbocharged multi-cylinder optical engine. *Renew. Energy* **2016,** *96*, 319-332.

76. Jin, D.; Choi, K.; Myung, C.-L.; Lim, Y.; Lee, J.; Park, S., The impact of various ethanol-gasoline blends on particulates and unregulated gaseous emissions characteristics from a spark ignition direct injection (SIDI) passenger vehicle. *Fuel* **2017,** *209*, 702-712.

77. Mirowsky, J.; Hickey, C.; Horton, L.; Blaustein, M.; Galdanes, K.; Peltier, R. E.; Chillrud, S.; Chen, L. C.; Ross, J.; Nadas, A.; Lippmann, M.; Gordon, T., The effect of

particle size, location and season on the toxicity of urban and rural particulate matter. *Inhal. Toxicol.* **2013,** *25*, (13), 747-757.

78. Usemann, J.; Roth, M.; Bisig, C.; Comte, P.; Czerwinski, J.; Mayer, A. C.; Latzin, P.; Müller, L., Gasoline particle filter reduces oxidative DNA damage in bronchial epithelial cells after whole gasoline exhaust exposure in vitro. *Sci. Rep.* **2018,** *8*, (1), 2297.

79. Bisig, C.; Comte, P.; Güdel, M.; Czerwinski, J.; Mayer, A.; Müller, L.; Petri-Fink, A.; Rothen-Rutishauser, B., Assessment of lung cell toxicity of various gasoline engine exhausts using a versatile in vitro exposure system. *Environ. Pollut.* **2018,** *235*, 263-271.

80. Yang, J.; Roth, P.; Durbin, T. D.; Shafer, M. M.; Hemming, J.; Antkiewicz, D. S.; Asa-Awuku, A.; Karavalakis, G., Emissions from a flex fuel GDI vehicle operating on ethanol fuels show marked contrasts in chemical, physical and toxicological characteristics as a function of ethanol content. *Sci. Total Environ.* **2019,** *683*, 749-761.

81. Yang, J.; Roth, P.; Ruehl, C. R.; Shafer, M. M.; Antkiewicz, D. S.; Durbin, T. D.; Cocker, D.; Asa-Awuku, A.; Karavalakis, G., Physical, chemical, and toxicological characteristics of particulate emissions from current technology gasoline direct injection vehicles. *Sci. Total Environ.* **2019,** *650*, 1182-1194.

82. Maikawa, C. L.; Zimmerman, N.; Rais, K.; Shah, M.; Hawley, B.; Pant, P.; Jeong, C. H.; Delgado-Saborit, J. M.; Volckens, J.; Evans, G.; Wallace, J. S.; Godri Pollitt, K. J., Murine precision-cut lung slices exhibit acute responses following exposure to gasoline direct injection engine emissions. *Sci. Total Environ.* **2016,** *568*, (August), 1102-1109.

83. Libalova, H.; Rossner, P.; Vrbova, K.; Brzicova, T.; Sikorova, J.; Vojtisek-Lom, M.; Beranek, V.; Klema, J.; Ciganek, M.; Neca, J.; Machala, M.; Topinka, J., Transcriptional response to organic compounds from diverse gasoline and biogasoline fuel emissions in human lung cells. *Toxicol. in vitro* **2018,** *48*, (February), 329-341.

84. Bisig, C.; Roth, M.; Müller, L.; Comte, P.; Heeb, N.; Mayer, A.; Czerwinski, J.; Petri-Fink, A.; Rothen-Rutishauser, B., Hazard identification of exhausts from gasoline-ethanol fuel blends using a multi-cellular human lung model. *Environ. Res.* **2016,** *151*, (May), 789-796.

85. Pratt, M. M.; John, K.; MacLean, A. B.; Afework, S.; Phillips, D. H.; Poirier, M. C., Polycyclic aromatic hydrocarbon (PAH) exposure and DNA adduct semi-quantitation in archived human tissues. *Int J Environ Res Public Health* **2011,** *8*, (7), 2675-2691.

86. Vineis, P.; Husgafvel-Pursiainen, K., Air pollution and cancer: biomarker studies in human populations †. *Carcinogenesis* **2005,** *26*, (11), 1846-1855.

87. Kung, T.; Murphy, K. A.; White, L. A., The aryl hydrocarbon receptor (AhR) pathway as a regulatory pathway for cell adhesion and matrix metabolism. *Biochem. Pharmacol.* **2009,** *77*, 536-546.

88. Puga, A.; Ma, C.; Marlowe, J. L., The aryl hydrocarbon receptor cross-talks with multiple signal transduction pathways. *Biochem. Pharmacol.* **2009,** *77*, (4), 713-722.

89. Xue, W.; Warshawsky, D., Metabolic activation of polycyclic and heterocyclic aromatic hydrocarbons and DNA damage: A review. *Toxicol. Appl. Pharmacol.* **2005,** *206*, (1), 73-93.

90. Jiang, H.; Ahmed, C. M. S.; Canchola, A.; Chen, J. Y.; Lin, Y.-H., Use of Dithiothreitol Assay to Evaluate the Oxidative Potential of Atmospheric Aerosols. *Atmosphere* **2019,** *10*, (10), 571.

91. Yang, J.; Roth, P.; Durbin, T. D.; Johnson, K. C.; Cocker, D. R.; Asa-Awuku, A.; Brezny, R.; Geller, M.; Karavalakis, G., Gasoline Particulate Filters as an Effective Tool to Reduce Particulate and Polycyclic Aromatic Hydrocarbon Emissions from Gasoline Direct Injection (GDI) Vehicles: A Case Study with Two GDI Vehicles. *Environ. Sci. Technol.* **2018,** *52*, (5), 3275-3284.

92. Yang, J.; Roth, P.; Zhu, H.; Durbin, T. D.; Karavalakis, G., Impacts of gasoline aromatic and ethanol levels on the emissions from GDI vehicles: Part 2. Influence on particulate matter, black carbon, and nanoparticle emissions. *Fuel* **2019,** *252*, 812-820.

93. Kramer, A.; Rattanavaraha, W.; Zhang, Z.; Gold, A.; Surratt, J.; Lin, Y., Assessing the oxidative potential of isoprene-derived epoxides and secondary organic aerosol. *Atmos. Environ.* **2016,** *130*, 211-218.

94. Li, Q.; Wyatt, A.; Kamens, R. M., Oxidant generation and toxicity enhancement of aged-diesel exhaust. *Atmos. Environ.* **2009,** *43*, (5), 1037-1042.

95. Cho, A. K.; Sioutas, C.; Miguel, A. H.; Kumagai, Y.; Schmitz, D. A.; Singh, M.; Eiguren-Fernandez, A.; Froines, J. R., Redox activity of airborne particulate matter at different sites in the Los Angeles Basin. *Environ. Res.* **2005,** *99*, (1), 40-47.

96. Lemaire, R.; Therssen, E.; Desgroux, P., Effect of ethanol addition in gasoline and gasoline–surrogate on soot formation in turbulent spray flames. *Fuel* **2010,** *89*, (12), 3952-3959.

97. Saffari, A.; Daher, N.; Shafer, M. M.; Schauer, J. J.; Sioutas, C., Seasonal and spatial variation in dithiothreitol (DTT) activity of quasi-ultrafine particles in the Los Angeles Basin and its association with chemical species. *J. Environ. Sci. Health, Part A* **2014,** *49*, (4), 441-451.

98. Li, N.; Sioutas, C.; Cho, A.; Schmitz, D.; Misra, C.; Sempf, J.; Wang, M.; Oberley, T.; Froines, J.; Nel, A., Ultrafine particulate pollutants induce oxidative stress and mitochondrial damage. *Environ. Health Perspect.* **2003,** *111*, (4), 455-460.

99. Cheung, K. L.; Polidori, A.; Ntziachristos, L.; Tzamkiozis, T.; Samaras, Z.; Cassee, F. R.; Gerlofs, M.; Sioutas, C., Chemical characteristics and oxidative potential of particulate matter emissions from gasoline, diesel, and biodiesel cars. *Environ. Sci. Technol.* **2009,** *43*, (16), 6334-6340.

100. Geller, M. D.; Ntziachristos, L.; Mamakos, A.; Samaras, Z.; Schmitz, D. A.; Froines, J. R.; Sioutas, C., Physicochemical and redox characteristics of particulate matter (PM) emitted from gasoline and diesel passenger cars. *Atmos. Environ.* **2006,** *40*, (36), 6988-7004.

101. Savjani, K. T.; Gajjar, A. K.; Savjani, J. K., Drug solubility: importance and enhancement techniques. *ISRN pharmaceutics* **2012,** *2012*.

102. Dahan, A.; Miller, J. M., The solubility–permeability interplay and its implications in formulation design and development for poorly soluble drugs. *The AAPS journal* **2012,** *14*, (2), 244-251.

103. Bates, J. T.; Weber, R. J.; Abrams, J.; Verma, V.; Fang, T.; Klein, M.; Strickland, M. J.; Sarnat, S. E.; Chang, H. H.; Mulholland, J. A.; Tolbert, P. E.; Russell, A. G., Reactive Oxygen Species Generation Linked to Sources of Atmospheric Particulate Matter and Cardiorespiratory Effects. *Environ. Sci. Technol.* **2015,** *49*, (22), 13605-13612.

104. ISO, P., 10993–5: 2009 Biological Evaluation of Medical Devices—Part 5: Tests for In Vitro Cytotoxicity. *ISO: Geneva, Switzerland* **2009**.

105. Libalova, H.; Rossner, P.; Vrbova, K.; Brzicova, T.; Sikorova, J.; Vojtisek-Lom, M.; Beranek, V.; Klema, J.; Ciganek, M.; Neca, J.; Pencikova, K.; Machala, M.; Topinka, J., Comparative analysis of toxic responses of organic extracts from diesel and selected alternative fuels engine emissions in human lung BEAS-2B cells. *Int. J. Mol. Sci.* **2016,** *17*, (11), 1-24.

106. Livak, K. J.; Schmittgen, T. D., Analysis of relative gene expression data using real-time quantitative PCR and the 2-ΔΔCT method. *Methods* **2001,** *25*, (4), 402-408.

107. Luo, Y.; Zhu, L.; Fang, J.; Zhuang, Z.; Guan, C.; Xia, C.; Xie, X.; Huang, Z., Size distribution, chemical composition and oxidation reactivity of particulate matter from gasoline direct injection (GDI) engine fueled with ethanol-gasoline fuel. *Appl. Therm. Eng.* **2015,** *89*, 647-655.

108. Muñoz, M.; Heeb, N. V.; Haag, R.; Honegger, P.; Zeyer, K.; Mohn, J.; Comte, P.; Czerwinski, J., Bioethanol blending reduces nanoparticle, PAH, and alkyl-and nitro-PAH emissions and the genotoxic potential of exhaust from a gasoline direct injection flex-fuel vehicle. *Environ. Sci. Technol.* **2016,** *50*, (21), 11853-11861.

109. Jensen, B. A.; Leeman, R. J.; Schlezinger, J. J.; Sherr, D. H., Aryl hydrocarbon receptor (AhR) agonists suppress interleukin-6 expression by bone marrow stromal cells: an immunotoxicology study. *Environ. Health* **2003,** *2*, (1), 16.

110. Billiard, S. M.; Timme-Laragy, A. R.; Wassenberg, D. M.; Cockman, C.; Di Giulio, R. T., The role of the aryl hydrocarbon receptor pathway in mediating synergistic developmental toxicity of polycyclic aromatic hydrocarbons to zebrafish. *Toxicol. Sci.* **2006,** *92*, (2), 526-536.

111. Park, K.; Lee, J.-H.; Cho, H.-C.; Cho, S.-Y.; Cho, J.-W., Down-regulation of IL-6, IL-8, TNF-α and IL-1β by glucosamine in HaCaT cells, but not in the presence of TNF-α. *Oncol. Lett.* **2010,** *1*, (2), 289-292.

112. Manzano-León, N.; Serrano-Lomelin, J.; Sánchez, B. N.; Quintana-Belmares, R.; Vega, E.; Vázquez-López, I.; Rojas-Bracho, L.; López-Villegas, M. T.; Vadillo-Ortega, F.; de Vizcaya-Ruiz, A.; Perez, I. R.; O'Neill, M. S.; Osornio-Vargas, A. R., TNFα and IL-6 responses to particulate matter in vitro: Variation according to PM size, season, and polycyclic aromatic hydrocarbon and soil content. *Environ. Health Perspect.* **2016,** *124*, (4), 406-412.

113. Aldinucci, D.; Colombatti, A., The inflammatory chemokine CCL5 and cancer progression. *Mediators Inflamm.* **2014,** *2014*.

114. Asano, K.; Chee, C. B.; Gaston, B.; Lilly, C. M.; Gerard, C.; Drazen, J. M.; Stamler, J. S., Constitutive and inducible nitric oxide synthase gene expression, regulation, and activity in human lung epithelial cells. *Proc. Natl. Acad. Sci. U.S.A.* **1994,** *91*, (21), 10089-93.

115. Uetani, K.; Arroliga, M. E.; Erzurum, S. C., Double-stranded rna dependence of nitric oxide synthase 2 expression in human bronchial epithelial cell lines BET-1A and BEAS-2B. *Am J Respir Cell Mol Biol* **2001,** *24*, (6), 720-726.

116. Machado, F. S.; Souto, J. T.; Rossi, M. A.; Esper, L.; Tanowitz, H. B.; Aliberti, J.; Silva, J. S., Nitric oxide synthase-2 modulates chemokine production by Trypanosoma cruzi-infected cardiac myocytes. *Microbes and Infection* **2008,** *10*, (14), 1558-1566.

117. Kelleher, Z. T.; Potts, E. N.; Brahmajothi, M. V.; Foster, M. W.; Auten, R. L.; Foster, W. M.; Marshall, H. E. J. A. J. o. P.-L. C., NOS2 regulation of LPS-induced airway inflammation via S-nitrosylation of NF-κB p65. *Am. J. Physiol. Lung Cell Mol. Physiol.* **2011,** *301*, (3), L327-L333.

118. Kong, L.-Y.; Luster, M. I.; Dixon, D.; O'Grady, J.; Rosenthal, G. J., Inhibition of lung immunity after intratracheal instillation of benzo (a) pyrene. *Am. J. Respir. Crit. Care Med.* **1994,** *150*, (4), 1123-1129.

119. Happo, M. S.; Hirvonen, M.-R.; Hälinen, A. I.; Jalava, P. I.; Pennanen, A. S.; Sillanpää, M.; Hillamo, R.; Salonen, R. O., Chemical compositions responsible for inflammation and tissue damage in the mouse lung by coarse and fine particulate samples from contrasting air pollution in Europe. *Inhal. Toxicol.* **2008,** *20*, (14), 1215-1231.

120. Happo, M. S.; Uski, O.; Jalava, P. I.; Kelz, J.; Brunner, T.; Hakulinen, P.; Mäki-Paakkanen, J.; Kosma, V.-M.; Jokiniemi, J.; Obernberger, I., Pulmonary inflammation and tissue damage in the mouse lung after exposure to PM samples from biomass heating appliances of old and modern technologies. *Sci. Total Environ.* **2013,** *443*, 256-266.

121. Tuet, W. Y.; Chen, Y.; Fok, S.; Champion, J. A.; Ng, N. L., Inflammatory responses to secondary organic aerosols (SOA) generated from biogenic and anthropogenic precursors. *Atmos. Chem. Phys.* **2017,** *17*, (18), 11423-11440.

122. Rao, X.; Zhong, J.; Brook, R. D.; Rajagopalan, S., Effect of particulate matter air pollution on cardiovascular oxidative stress pathways. *Antioxid. Redox Signal.* **2018,** *28*, (9), 797-818.

123. Sapcariu, S. C.; Kanashova, T.; Dilger, M.; Diabaté, S.; Oeder, S.; Passig, J.; Radischat, C.; Buters, J.; Sippula, O.; Streibel, T.; Paur, H. R.; Schlager, C.; Mülhopt, S.; Stengel, B.; Rabe, R.; Harndorf, H.; Krebs, T.; Karg, E.; Gröger, T.; Weiss, C.; Dittmar, G.; Hiller, K.; Zimmermann, R., Metabolic profiling as well as stable isotope assisted metabolic and proteomic analysis of RAW 264.7 macrophages exposed to ship engine aerosol emissions: Different effects of heavy fuel oil and refined diesel fuel. *PLoS ONE* **2016,** *11*, (6), 1-22.

124. Mehdi, Y.; Hornick, J.-L.; Istasse, L.; Dufrasne, I., Selenium in the environment, metabolism and involvement in body functions. *Molecules* **2013,** *18*, (3), 3292.

125. Winkel, L. H. E.; Johnson, C. A.; Lenz, M.; Grundl, T.; Leupin, O. X.; Amini, M.; Charlet, L., Environmental selenium research: from microscopic processes to global understanding. *Environ. Sci. Technol.* **2012,** *46*, (2), 571-579.

126. Ullah, H.; Liu, G.; Yousaf, B.; Ali, M. U.; Irshad, S.; Abbas, Q.; Ahmad, R., A comprehensive review on environmental transformation of selenium: recent advances and research perspectives. *Environ. Geochem. Health* **2019,** *41*, (2), 1003-1036.

127. Wen, H.; Carignan, J., Reviews on atmospheric selenium: emissions, speciation and fate. *Atmos. Environ.* **2007,** *41*, (34), 7151-7165.

128. Guadayol, M.; Cortina, M.; Guadayol, J. M.; Caixach, J., Determination of dimethyl selenide and dimethyl sulphide compounds causing off-flavours in bottled mineral waters. *Water Res.* **2016,** *92*, 149-55.

129. Wadgaonkar, S. L.; Nancharaiah, Y. V.; Esposito, G.; Lens, P. N., Environmental impact and bioremediation of seleniferous soils and sediments. *Crit. Rev. Biotechnol.* **2018,** *38*, (6), 941-956.

130. Frie, A. L.; Dingle, J. H.; Ying, S. C.; Bahreini, R., The effect of a receding saline lake (the Salton Sea) on airborne particulate matter composition. *Environ. Sci. Technol.* **2017,** *51*, (15), 8283-8292.

131. Blazina, T.; Läderach, A.; Jones, G. D.; Sodemann, H.; Wernli, H.; Kirchner, J. W.; Winkel, L. H., Marine primary productivity as a potential indirect source of selenium and other trace elements in atmospheric deposition. *Environ. Sci. Technol.* **2016,** *51*, (1), 108-118.

132. Kaur, N.; Sharma, S.; Kaur, S.; Nayyar, H., Selenium in agriculture: a nutrient or contaminant for crops? *Arch. Agron. Soil Sci.* **2014,** *60*, (12), 1593-1624.

133. Reeves, M.; Hoffmann, P., The human selenoproteome: recent insights into functions and regulation. *Cell. Mol. Life Sci.* **2009,** *66*, (15), 2457-2478.

134. Karlson, U.; Frankenberger, W. T., Volatilization of selenium from agricultural evaporation pond sediments. *Sci. Total Environ.* **1990,** *92*, 41-54.

135. Cherdwongcharoensuk, D.; Henrique, R.; Upatham, S.; Pereira, A. S.; Águas, A. P., Tubular kidney damage and centrilobular liver injury after intratracheal instillation of dimethyl selenide. *Toxicol. Pathol.* **2005,** *33*, (2), 225-229.

136. Atkinson, R.; Aschmann, S. M.; Hasegawa, D.; Thompson-Eagle, E. T.; Frankenberger, W. T., Kinetics of the atmospherically important reactions of dimehtyl selenide. *Environ. Sci. Technol.* **1990,** *24*, (9), 1326-1332.

137. Rael, R. M.; Tuzaon, E. C.; Frankenberger, W. T., Gas-phase reactions of dimethyl selenide with ozone and the hydroxyl and nitrate radicals. *Atmos. Environ.* **1996,** *30*, (8), 1221-1232.

138. Dingle, J. H.; Zimmerman, S.; Frie, A. L.; Min, J.; Jung, H.; Bahreini, R., Complex refractive index, single scattering albedo, and mass absorption coefficient of secondary organic aerosols generated from oxidation of biogenic and anthropogenic precursors. *Aerosol Sci. Technol.* **2019,** *53 (4)*, 449-463, doi: 10.1080/02786826.2019.1571680.

139. Canagaratna, M. R.; Jayne, J. T.; Jimenez, J. L.; Allan, J. D.; Alfarra, M. R.; Zhang, Q.; Onasch, T. B.; Drewnick, F.; Coe, H.; Middlebrook, A. M.; Delia, A.; Williams, L. R.; Trimborn, A. M.; Northway, M. J.; DeCarlo, P. F.; Kolb, C. E.; Davidovits, P.; Worsnop, D. R., Chemical and microphysical characterization of ambient aerosols with the aerodyne aerosol mass spectrometer. *Mass Spectrom. Rev.* **2007,** *26*, 185-222.

140. Bahreini, R.; Keywood, M. D.; Ng, N. L.; Varutbangkul, V.; Gao, S.; Flagan, R. C.; Seinfeld, J. H.; Worsnop, D. R.; Jimenez, J. L., Measurements of secondary organic aerosol from oxidation of cycloalkenes, terpenes, and m-xylene using an Aerodyne aerosol mass spectrometer. *Environ. Sci. Technol.* **2005,** *39*, (15), 5674-5688.

141. DeCarlo, P. F.; Slowik, J. G.; Worsnop, D. R.; Davidovits, P.; Jimenez, J. L., Particle morphology and density characterization by combined mobility and aerodynamic measurements. part 1: theory. *Aerosol Sci. Technol.* **2004,** *38*, 1185–1205, doi: 10.1080/027868290903907.

142. Bahreini, R.; Middlebrook, A. M.; Brock, C. A.; de Gouw, J. A.; McKeen, S. A.; Williams, L. R.; Daumit, K. E.; Lambe, A. T.; Massoli, P.; Canagaratna, M. R.; Ahmadov, R.; Carrasquillo, A. J.; Cross, E. S.; Ervens, B.; Holloway, J. S.; Hunter, J. F.; Onasch, T. B.; Pollack, I. B.; Roberts, J. M.; Ryerson, T. B.; Warneke, C.; Davidovits, P.; Worsnop, D. R.; Kroll, J. H., Mass spectral analysis of organic aerosol formed downwind of the deepwater horizon oil spill: field studies and laboratory confirmations. *Environ. Sci. Technol.* **2012,** *46*, (15), 8025-8034.

143. Reddel, R. R.; Ke, Y.; Gerwin, B. I.; McMenamin, M. G.; Lechner, J. F.; Su, R. T.; Brash, D. E.; Park, J.-B.; Rhim, J. S.; Harris, C. C., Transformation of human bronchial epithelial cells by infection with SV40 or adenovirus-12 SV40 hybrid virus, or transfection via strontium phosphate coprecipitation with a plasmid containing SV40 early region genes. *Cancer Res.* **1988,** *48*, (7), 1904-1909.

144. Andrews, S., A quality control tool for high throughput sequence data. FastQC. **2014**, http://www.bioinformatics.babraham.ac.uk/projects/fastqc/.

145. Bolger, A. M.; Lohse, M.; Usadel, B. J. B., Trimmomatic: a flexible trimmer for Illumina sequence data. *Bioinformatics* **2014,** *30*, (15), 2114-2120.

146. Kim, D.; Langmead, B.; Salzberg, S. L., HISAT: a fast spliced aligner with low memory requirements. *Nat. Methods* **2015,** *12*, (4), 357-60.

147. Li, H.; Handsaker, B.; Wysoker, A.; Fennell, T.; Ruan, J.; Homer, N.; Marth, G.; Abecasis, G.; Durbin, R., The sequence alignment/map format and SAMtools. *Bioinformatics* **2009,** *25*, (16), 2078-2079.

148. Liao, Y.; Smyth, G. K.; Shi, W., The Subread aligner: fast, accurate and scalable read mapping by seed-and-vote. *Nucleic Acids Res.* **2013,** *41*, (10), e108-e108.

149. Love, M. I.; Huber, W.; Anders, S., Moderated estimation of fold change and dispersion for RNA-seq data with DESeq2. *Genome Biol.* **2014,** *15*, (12), 550.

150. Ritchie, M. E.; Phipson, B.; Wu, D.; Hu, Y.; Law, C. W.; Shi, W.; Smyth, G. K., limma powers differential expression analyses for RNA-sequencing and microarray studies. *Nucleic Acids Res.* **2015,** *43*, (7), e47-e47.

151. Robinson, M. D.; McCarthy, D. J.; Smyth, G. K., edgeR: a Bioconductor package for differential expression analysis of digital gene expression data. *Bioinformatics* **2010,** *26*, (1), 139-140.

152. Costa-Silva, J.; Domingues, D.; Lopes, F. M., RNA-Seq differential expression analysis: An extended review and a software tool. *PloS ONE* **2017,** *12*, (12), e0190152.

153. Kamburov, A.; Wierling, C.; Lehrach, H.; Herwig, R., ConsensusPathDB--a database for integrating human functional interaction networks. *Nucleic Acids Res.* **2009,** *37*, (Database issue), D623-8.

154. Zhavoronkov, A.; Buzdin, A. A.; Garazha, A. V.; Borisov, N. M.; Moskalev, A. A., Signaling pathway cloud regulation for in silico screening and ranking of the potential geroprotective drugs. *Front. Genet.* **2014,** *5*, 49.

155. Bindea, G.; Mlecnik, B.; Hackl, H.; Charoentong, P.; Tosolini, M.; Kirilovsky, A.; Fridman, W.-H.; Pagès, F.; Trajanoski, Z.; Galon, J., ClueGO: a Cytoscape plug-in to decipher functionally grouped gene ontology and pathway annotation networks. *Bioinformatics* **2009,** *25*, (8), 1091-1093.

156. Cho, A. K.; Sioutas, C.; Miguel, A. H.; Kumagai, Y.; Schmitz, D. A.; Singh, M.; Eiguren-Fernandez, A.; Froines, J. R., Redox activity of airborne particulate matter at different sites in the los angeles basin. *Environ. Res.* **2005,** *99*, (1), 40-47.

157. Verma, V.; Fang, T.; Xu, L.; Peltier, R. E.; Russell, A. G.; Ng, N. L.; Weber, R. J., Organic aerosols associated with the generation of reactive oxygen species (ROS) by water-soluble PM2.5. *Environ. Sci. Technol.* **2015,** *49*, (7), 4646-4656.

158. Jiang, H.; Jang, M.; Sabo-Attwood, T.; Robinson, S. E., Oxidative potential of secondary organic aerosols produced from photooxidation of different hydrocarbons using outdoor chamber under ambient sunlight. *Atmos. Environ.* **2016,** *131*, 382-389.

159. Tuet, W. Y.; Chen, Y.; Xu, L.; Fok, S.; Gao, D.; Weber, R. J.; Ng, N. L., Chemical oxidative potential of secondary organic aerosol (SOA) generated from the

photooxidation of biogenic and anthropogenic volatile organic compounds. *Atmos. Chem. Phys.* **2017,** *17*, (2), 839-853.

160. Kroll, J. H.; Ng, N. L.; Murphy, S. M.; Flagan, R. C.; Seinfeld, J. H., Secondary organic aerosol formation from isoprene photooxidation. *Environ. Sci. Technol.* **2006,** *40*, (6), 1869-1877.

161. Lambe, A.; Chhabra, P.; Onasch, T.; Brune, W. H.; Hunter, J.; Kroll, J.; Cummings, M.; Brogan, J.; Parmar, Y.; Worsnop, D., Effect of oxidant concentration, exposure time, and seed particles on secondary organic aerosol chemical composition and yield. *Atmos. Chem. Phys.* **2015,** *15*, (6), 3063-3075.

162. Ng, N.; Chhabra, P.; Chan, A.; Surratt, J.; Kroll, J.; Kwan, A.; McCabe, D.; Wennberg, P.; Sorooshian, A.; Murphy, S., Effect of NO_x level on secondary organic aerosol (SOA) formation from the photooxidation of terpenes. *Atmos. Chem. Phys.* **2007,** *7*, (19), 5159-5174.

163. Charrier, J. G.; Richards-Henderson, N. K.; Bein, K. J.; McFall, A. S.; Wexler, A. S.; Anastasio, C., Oxidant production from source-oriented particulate matter-part 1: oxidative potential using the dithiothreitol (DTT) assay. *Atmos. Chem. Phys.* **2015,** *15*, (5), 2327-2340.

164. Charrier, J.; Anastasio, C., On dithiothreitol (DTT) as a measure of oxidative potential for ambient particles: evidence for the importance of soluble transition metals. *Atmos. Chem. Phys.* **2012,** *12*, (5), 11317.

165. Chen, J. Y.; Jiang, H.; Chen, S. J.; Cullen, C.; Ahmed, C. M. S.; Lin, Y.-H., Characterization of electrophilicity and oxidative potential of atmospheric carbonyls. *Environ. Sci.: Process. Impacts* **2019,** *21*, 856-866.

166. Reuter, S.; Gupta, S. C.; Chaturvedi, M. M.; Aggarwal, B. B., Oxidative stress, inflammation, and cancer: how are they linked? *Free Radic. Biol. Med.* **2010,** *49*, (11), 1603-16.

167. Letavayová, L.; Vlčková, V.; Brozmanová, J., Selenium: From cancer prevention to DNA damage. *Toxicology* **2006,** *227*, (1), 1-14.

168. Kung, C. P.; Murphy, M. E., The role of the p53 tumor suppressor in metabolism and diabetes. *J. Endocrinol.* **2016,** *231*, (2), R61-R75.

169. Rodin, S. N.; Rodin, A. S., Human lung cancer and p53: the interplay between mutagenesis and selection. *Proc. Natl. Acad. Sci. U.S.A.* **2000,** *97*, (22), 12244-12249.

170. Levine, A. J.; Oren, M., The first 30 years of p53: growing ever more complex. *Nat. Rev. Cancer* **2009,** *9*, 749.

171. Hu, W.; Feng, Z.; Levine, A. J., The regulation of multiple p53 stress responses is mediated through MDM2. *Genes Cancer* **2012,** *3*, (3-4), 199-208.

172. Puzio-Kuter, A. M., The role of p53 in metabolic regulation. *Genes Cancer* **2011,** *2*, (4), 385-91.

173. Wu, G. S., The functional interactions between the MAPK and p53 signaling pathways. *Cancer Biol. Ther.* **2004,** *3*, (2), 156-161.

174. Gupta, A.; Shah, K.; Oza, M. J.; Behl, T., Reactivation of p53 gene by MDM2 inhibitors: A novel therapy for cancer treatment. *Biomed. Pharmacother.* **2019,** *109*, 484-492.

175. Steinbrenner, H.; Speckmann, B.; Pinto, A.; Sies, H., High selenium intake and increased diabetes risk: experimental evidence for interplay between selenium and carbohydrate metabolism. *J. Clin. Biochem. Nutr.* **2011,** *48*, (1), 40-45.

176. Ong, S. H.; Hadari, Y. R.; Gotoh, N.; Guy, G. R.; Schlessinger, J.; Lax, I., Stimulation of phosphatidylinositol 3-kinase by fibroblast growth factor receptors is mediated by coordinated recruitment of multiple docking proteins. *Proc. Natl. Acad. Sci. U.S.A.* **2001,** *98*, (11), 6074-6079.

177. Chen, Z.; Trotman, L. C.; Shaffer, D.; Lin, H.-K.; Dotan, Z. A.; Niki, M.; Koutcher, J. A.; Scher, H. I.; Ludwig, T.; Gerald, W.; Cordon-Cardo, C.; Paolo Pandolfi, P., Crucial role of p53-dependent cellular senescence in suppression of Pten-deficient tumorigenesis. *Nature* **2005,** *436*, (7051), 725-730.

178. Webster, N. J. G.; Resnik, J. L.; Reichart, D. B.; Strauss, B.; Haas, M.; Seely, B. L., Repression of the insulin receptor promoter by the tumor suppressor gene product p53: a possible mechanism for receptor overexpression in breast cancer. *Cancer Res.* **1996,** *56*, (12), 2781.

179. Burns, J.; Manda, G. J. I. j. o. m. s., Metabolic pathways of the warburg effect in health and disease: Perspectives of choice, chain or chance. *Int. J. Mol. Sci.* **2017,** *18*, (12), 2755.

180. Seki, T.; Kumagai, T.; Kwansa-Bentum, B.; Furushima-Shimogawara, R.; Anyan, W. K.; Miyazawa, Y.; Iwakura, Y.; Ohta, N., Interleukin-4 (IL-4) and IL-13 suppress excessive neutrophil infiltration and hepatocyte damage during acute murine schistosomiasis japonica. *Infect. Immun.* **2012,** *80*, (1), 159-168.

181. Hazari, Y. M.; Bashir, A.; Habib, M.; Bashir, S.; Habib, H.; Qasim, M. A.; Shah, N. N.; Haq, E.; Teckman, J.; Fazili, K. M., Alpha-1-antitrypsin deficiency: Genetic variations, clinical manifestations and therapeutic interventions. *Mutat. Res.* **2017,** *773*, 14-25.

182. Kagan, P.; Sultan, M.; Tachlytski, I.; Safran, M.; Ben-Ari, Z., Both MAPK and STAT3 signal transduction pathways are necessary for IL-6-dependent hepatic stellate cells activation. *PLoS One* **2017,** *12*, (5), e0176173.

183. Junttila, I. S., Tuning the cytokine responses: An update on interleukin (IL)-4 and IL-13 receptor complexes. *Front. Immunol.* **2018,** *9*, 888.

184. Gour, N.; Wills-Karp, M., IL-4 and IL-13 signaling in allergic airway disease. *Cytokine* **2015,** *75*, (1), 68-78.

185. Hao, Y.; Kuang, Z.; Jing, J.; Miao, J.; Mei, L. Y.; Lee, R. J.; Kim, S.; Choe, S.; Krause, D. C.; Lau, G. W., Mycoplasma pneumoniae modulates STAT3-STAT6/EGFR-FOXA2 signaling to induce overexpression of airway mucins. *Infect. Immun.* **2014,** *82*, (12), 5246-5255.

186. Crosby, L. M.; Waters, C. M., Epithelial repair mechanisms in the lung. *Am. J. Physiol. Lung Cell. Mol. Physiol.* **2010,** *298*, (6), L715-L731.

187. Jiang, H.; Ahmed, C.; Canchola, A.; Chen, J. Y.; Lin, Y.-H., Use of dithiothreitol assay to evaluate the oxidative potential of atmospheric aerosols. *Atmosphere* **2019,** *10*, (10), 571.

188. Lin, M.; Yu, J. Z., Dithiothreitol (DTT) concentration effect and its implications on the applicability of DTT assay to evaluate the oxidative potential of atmospheric aerosol samples. *Environ. Pollut.* **2019,** *251*, 938-944.

189. De Santiago, A.; Longo, A. F.; Ingall, E. D.; Diaz, J. M.; King, L. E.; Lai, B.; Weber, R. J.; Russell, A. G.; Oakes, M., Characterization of selenium in ambient aerosols and primary emission sources. *Environ. Sci. Technol.* **2014,** *48*, (16), 8988-94.

190. Lin, Z. Q.; Cervinka, V.; Pickering, I. J.; Zayed, A.; Terry, N., Managing selenium-contaminated agricultural drainage water by the integrated on-farm drainage management system: role of selenium volatilization. *Water Res.* **2002,** *36*, (12), 3150-3160.

191. Lin, Z. Q.; Schemenauer, R. S.; Cervinka, V.; Zayed, A.; Lee, A.; Terry, N., Selenium volatilization from a soil-plant system for the remediation of contaminated water and soil in the San Joaquin Valley. *J. Environ. Qual.* **2000,** *29*, (4), 1048-1056.

192. Karlson, U.; Frankenberger, W. T.; Spencer, W. F., Physicochemical properties of dimethyl selenide and dimethyl diselenide. *J. Chem. Eng. Data* **1994,** *39*, (3), 608-610.

193. Karlson, U.; Frankenberger, W. T., Determination of gaseous selenium-75 evolved from soil. *Soil Sci. Soc. Am. J.* **1988,** *52*, (3), 678-681.

194. Mehdi, Y.; Hornick, J.-L.; Istasse, L.; Dufrasne, I., Selenium in the environment, metabolism and involvement in body functions. *Molecules* **2013,** *18*, (3), 3292-3311.

195. Cai, X.; Wang, C.; Yu, W.; Fan, W.; Wang, S.; Shen, N.; Wu, P.; Li, X.; Wang, F., Selenium exposure and cancer risk: an updated meta-analysis and meta-regression. *Sci. Rep.* **2016,** *6*, 19213.

196. Park, K.; Rimm, E. B.; Siscovick, D. S.; Spiegelman, D.; Manson, J. E.; Morris, J. S.; Hu, F. B.; Mozaffarian, D., Toenail selenium and incidence of type 2 diabetes in US men and women. *Diabetes Care* **2012,** *35*, (7), 1544-1551.

197. Tanguy, S.; Grauzam, S.; de Leiris, J.; Boucher, F., Impact of dietary selenium intake on cardiac health: experimental approaches and human studies. *Mol. Nutrition Food Res.* **2012,** *56*, (7), 1106-1121.

198. Winkel, L. H.; Johnson, C. A.; Lenz, M.; Grundl, T.; Leupin, O. X.; Amini, M.; Charlet, L., Environmental selenium research: from microscopic processes to global understanding. *Environ. Sci. Technol.* **2012,** *46*, (2), 571–579.

199. Ahmed, C. M. S.; Cui, Y.; Frie, A. L.; Burr, A.; Kamath, R.; Chen, J. Y.; Rahman, A.; Nordgren, T. M.; Lin, Y.-H.; Bahreini, R., Exposure to dimethyl selenide (DMSe)-derived secondary organic aerosol alters transcriptomic profiles in human airway epithelial cells. *Environ. Sci. Technol.* **2019,** *53*, (24), 14660-14669.

200. Karlson, U.; Frankenberger Jr, W., Volatilization of selenium from agricultural evaporation pond sediments. *Sci. Total Environ.* **1990,** *92*, 41-54.

201. Ulitsky, I.; Bartel, D. P., lincRNAs: genomics, evolution, and mechanisms. *Cell* **2013,** *154*, (1), 26-46.

202. Tang, Y.; Cheung, B. B.; Atmadibrata, B.; Marshall, G. M.; Dinger, M. E.; Liu, P. Y.; Liu, T., The regulatory role of long noncoding RNAs in cancer. *Cancer Lett.* **2017,** *391*, 12-19.

203. Bhat, S. A.; Ahmad, S. M.; Mumtaz, P. T.; Malik, A. A.; Dar, M. A.; Urwat, U.; Shah, R. A.; Ganai, N. A. J. N.-c. R. r., Long non-coding RNAs: mechanism of action and functional utility. *Non-coding RNA Res.* **2016,** *1*, (1), 43-50.

204. Ponting, C. P.; Oliver, P. L.; Reik, W., Evolution and functions of long noncoding RNAs. *Cell* **2009,** *136*, (4), 629-641.

205. Deng, X.; Feng, N.; Zheng, M.; Ye, X.; Lin, H.; Yu, X.; Gan, Z.; Fang, Z.; Zhang, H.; Gao, M., PM2. 5 exposure-induced autophagy is mediated by lncRNA loc146880 which also promotes the migration and invasion of lung cancer cells. *Acta Bioch. Bioph. Gen. Sub.* **2017,** *1861*, (2), 112-125.

206. Huang, Y.; Liu, N.; Wang, J. P.; Wang, Y. Q.; Yu, X. L.; Wang, Z. B.; Cheng, X. C.; Zou, Q. J. J. o. p., Regulatory long non-coding RNA and its functions. *J. Physiol. Biochem.* **2012,** *68*, (4), 611-618.

207. Derrien, T.; Johnson, R.; Bussotti, G.; Tanzer, A.; Djebali, S.; Tilgner, H.; Guernec, G.; Martin, D.; Merkel, A.; Knowles, D. G., The GENCODE v7 catalog of human long noncoding RNAs: analysis of their gene structure, evolution, and expression. *Genome Res.* **2012,** *22*, (9), 1775-1789.

208. Wang, K. C.; Chang, H. Y., Molecular mechanisms of long noncoding RNAs. *Mol. Cell* **2011,** *43*, (6), 904-914.

209. Rinn, J. L.; Chang, H. Y., Genome regulation by long noncoding RNAs. *Annual Review Biochem.* **2012,** *81*, 145-166.

210. Durut, N.; Scheid, O. M. J. F. i. p. s., The role of noncoding RNAs in double-strand break repair. *Front. Plant Sci.* **2019,** *10*.

211. Jackson, S. P.; Bartek, J., The DNA-damage response in human biology and disease. *Nature* **2009,** *461*, (7267), 1071-1078.

212. Hung, T.; Wang, Y.; Lin, M. F.; Koegel, A. K.; Kotake, Y.; Grant, G. D.; Horlings, H. M.; Shah, N.; Umbricht, C.; Wang, P., Extensive and coordinated transcription of noncoding RNAs within cell-cycle promoters. *Nat. Genet.* **2011,** *43*, (7), 621.

213. Huarte, M.; Guttman, M.; Feldser, D.; Garber, M.; Koziol, M. J.; Kenzelmann-Broz, D.; Khalil, A. M.; Zuk, O.; Amit, I.; Rabani, M., A large intergenic noncoding RNA induced by p53 mediates global gene repression in the p53 response. *Cell* **2010,** *142*, (3), 409-419.

214. Shi, T.; Dansen, T. B. J. A., ROS induced p53 activation: DNA damage, redox signaling or both? *Antioxid. Redox Signal.* **2020**, (ja).

215. Schmitt, A. M.; Garcia, J. T.; Hung, T.; Flynn, R. A.; Shen, Y.; Qu, K.; Payumo, A. Y.; Peres-da-Silva, A.; Broz, D. K.; Baum, R., An inducible long noncoding RNA amplifies DNA damage signaling. *Nat. Genet.* **2016,** *48*, (11), 1370.

216. Hu, W. L.; Jin, L.; Xu, A.; Wang, Y. F.; Thorne, R. F.; Zhang, X. D.; Wu, M. J. N. c. b., GUARDIN is a p53-responsive long non-coding RNA that is essential for genomic stability. *Nat. Cell Biol.* **2018,** *20*, (4), 492-502.

217. Sharma, V.; Khurana, S.; Kubben, N.; Abdelmohsen, K.; Oberdoerffer, P.; Gorospe, M.; Misteli, T., A BRCA 1□interacting lnc RNA regulates homologous recombination. *EMBO Reports* **2015,** *16*, (11), 1520-1534.

218. Loewen, G.; Jayawickramarajah, J.; Zhuo, Y.; Shan, B., Functions of lncRNA HOTAIR in lung cancer. *J. Hematol. Oncol.* **2014,** *7*, (1), 90.

219. Lin, Y.-H.; Arashiro, M.; Martin, E.; Chen, Y.; Zhang, Z.; Sexton, K. G.; Gold, A.; Jaspers, I.; Fry, R. C.; Surratt, J. D., Isoprene-derived secondary organic aerosol induces the expression of oxidative stress response genes in human lung cells. *Environ. Sci. Technol. Lett.* **2016,** *3*, (6), 250-254.

220. Ahmed, C. S.; Yang, J.; Chen, J. Y.; Jiang, H.; Cullen, C.; Karavalakis, G.; Lin, Y.-H., Toxicological responses in human airway epithelial cells (BEAS-2B) exposed to particulate matter emissions from gasoline fuels with varying aromatic and ethanol levels. *Sci. Total Environ.* **2020,** *706*, 135732.

221. Libalova, H.; Rossner Jr, P.; Vrbova, K.; Brzicova, T.; Sikorova, J.; Vojtisek-Lom, M.; Beranek, V.; Klema, J.; Ciganek, M.; Neca, J., Transcriptional response to organic compounds from diverse gasoline and biogasoline fuel emissions in human lung cells. *Toxicol. In Vitro* **2018,** *48*, 329-341.

222. Iwakiri, J.; Terai, G.; Hamada, M., Computational prediction of lncRNA-mRNA interactions by integrating tissue specificity in human transcriptome. *Biol. Direct* **2017,** *12*, (1), 15.

223. Gao, Y.; Wang, P.; Wang, Y.; Ma, X.; Zhi, H.; Zhou, D.; Li, X.; Fang, Y.; Shen, W.; Xu, Y. J. N. a. r., Lnc2Cancer v2. 0: updated database of experimentally supported long non-coding RNAs in human cancers. *Nucleic Acids Res.* **2019,** *47*, (D1), D1028-D1033.

224. Subramanian, A.; Tamayo, P.; Mootha, V. K.; Mukherjee, S.; Ebert, B. L.; Gillette, M. A.; Paulovich, A.; Pomeroy, S. L.; Golub, T. R.; Lander, E. S., Gene set enrichment analysis: a knowledge-based approach for interpreting genome-wide expression profiles. *Proc. Natl. Acad. Sci. U.S.A.* **2005,** *102*, (43), 15545-15550.

225. Ning, S.; Zhang, J.; Wang, P.; Zhi, H.; Wang, J.; Liu, Y.; Gao, Y.; Guo, M.; Yue, M.; Wang, L., Lnc2Cancer: a manually curated database of experimentally supported lncRNAs associated with various human cancers. *Nucleic Acids Res.* **2016,** *44*, (D1), D980-D985.

226. Cai, B.; Li, Z.; Ma, M.; Wang, Z.; Han, P.; Abdalla, B. A.; Nie, Q.; Zhang, X. J. F. i. p., LncRNA-Six1 encodes a micropeptide to activate Six1 in Cis and is involved in cell proliferation and muscle growth. *Front. Physiol.* **2017,** *8*, 230.

227. Li, D.; Li, F.; Jiang, K.; Zhang, M.; Han, R.; Jiang, R.; Li, Z.; Tian, Y.; Yan, F.; Kang, X., Integrative analysis of long noncoding RNA and mRNA reveals candidate lncRNAs responsible for meat quality at different physiological stages in Gushi chicken. *PloS one* **2019,** *14*, (4).

228. Jandura, A.; Krause, H. M. J. T. i. G., The new RNA world: growing evidence for long noncoding RNA functionality. *Trends Genet.* **2017,** *33*, (10), 665-676.

229. Jiang, P.; Hou, Y.; Fu, W.; Tao, X.; Luo, J.; Lu, H.; Xu, Y.; Han, B.; Zhang, J. J. P. o., Characterization of lncRNAs involved in cold acclimation of zebrafish ZF4 cells. *PloS one* **2018,** *13*, (4).

230. Zhang, H.; Chen, Z.; Wang, X.; Huang, Z.; He, Z.; Chen, Y., Long non-coding RNA: a new player in cancer. *J. Hematol. Oncol.* **2013,** *6*, (1), 37.

231. Gupta, R. A.; Shah, N.; Wang, K. C.; Kim, J.; Horlings, H. M.; Wong, D. J.; Tsai, M.-C.; Hung, T.; Argani, P.; Rinn, J. L., Long non-coding RNA HOTAIR reprograms chromatin state to promote cancer metastasis. *Nature* **2010,** *464*, (7291), 1071-1076.

232. Gutschner, T.; Hämmerle, M.; Diederichs, S. J. J. o. m. m., MALAT1—a paradigm for long noncoding RNA function in cancer. *J. Mol. Med.* **2013,** *91*, (7), 791-801.

233. Zhang, X.; Gejman, R.; Mahta, A.; Zhong, Y.; Rice, K. A.; Zhou, Y.; Cheunsuchon, P.; Louis, D. N.; Klibanski, A., Maternally expressed gene 3, an imprinted noncoding RNA gene, is associated with meningioma pathogenesis and progression. *Cancer Res.* **2010,** *70*, (6), 2350-2358.

234. Chaudhary, R.; Gryder, B.; Woods, W. S.; Subramanian, M.; Jones, M. F.; Li, X. L.; Jenkins, L. M.; Shabalina, S. A.; Mo, M.; Dasso, M., Prosurvival long noncoding RNA PINCR regulates a subset of p53 targets in human colorectal cancer cells by binding to Matrin 3. *elife* **2017,** *6*, e23244.

235. Cao, Y.; Lin, M.; Bu, Y.; Ling, H.; He, Y.; Huang, C.; Shen, Y.; Song, B.; Cao, D. J. I. j. o. o., p53-inducible long non-coding RNA PICART1 mediates cancer cell proliferation and migration. *Int. J. Oncol.* **2017,** *50*, (5), 1671-1682.

236. Miao, T.; Si, Q.; Wei, Y.; Fan, R.; Wang, J.; An, X., Identification and validation of seven prognostic long non□coding RNAs in oral squamous cell carcinoma. *Oncol. Lett.* **2020,** *20*, (1), 939-946.

237. Miao, W.; Li, N.; Gu, B.; Yi, G.; Su, Z.; Cheng, H., LncRNA DLGAP1-AS2 modulates glioma development by up-regulating YAP1 expression. *J. Biochem.* **2020,** *167*, (4), 411-418.

238. Chen, K.; Zhang, Z.; Yu, A.; Li, J.; Liu, J.; Zhang, X., lncRNA DLGAP1-AS2 Knockdown Inhibits Hepatocellular Carcinoma Cell Migration and Invasion by Regulating miR-154-5p Methylation. *BioMed Res. Int.* **2020,** *2020*.

239. Giulietti, M.; Righetti, A.; Principato, G.; Piva, F., LncRNA co-expression network analysis reveals novel biomarkers for pancreatic cancer. *Carcinogenesis* **2018,** *39*, (8), 1016-1025.

240. Chandra Gupta, S.; Nandan Tripathi, Y., Potential of long non□coding RNAs in cancer patients: From biomarkers to therapeutic targets. *Int. J. Cancer* **2017,** *140*, (9), 1955-1967.

241. Zou, Y.; Zhong, Y.; Wu, J.; Xiao, H.; Zhang, X.; Liao, X.; Li, J.; Mao, X.; Liu, Y.; Zhang, F., Long non□coding PANDAR as a novel biomarker in human cancer: A systematic review. *Cell Prolif.* **2018,** *51*, (1), e12422.

242. Jain, A. K. J. R. B., Emerging roles of long non-coding RNAs in the p53 network. *RNA Biol.* **2020**.

243. Yang, L.; Yi, K.; Wang, H.; Zhao, Y.; Xi, M., Comprehensive analysis of lncRNAs microarray profile and mRNA–lncRNA co-expression in oncogenic HPV-positive cervical cancer cell lines. *Oncotarget* **2016,** *7*, (31), 49917.

244. Gong, C.; Maquat, L. E., lncRNAs transactivate STAU1-mediated mRNA decay by duplexing with 3′ UTRs via Alu elements. *Nature* **2011,** *470*, (7333), 284-288.

245. Zhang, M.; Ma, F.; Xie, R.; Wu, Y.; Wu, M.; Zhang, P.; Peng, Y.; Zhao, J.; Xiong, J.; Li, A., Overexpression of Srcin1 contributes to the growth and metastasis of colorectal cancer. *Int. J. Oncol.* **2017,** *50*, (5), 1555-1566.

246. Jasinski-Bergner, S.; Steven, A.; Seliger, B., The Role of the RNA-Binding Protein Family MEX-3 in Tumorigenesis. *Int. J. Mol. Sci.* **2020,** *21*, (15), 5209.

247. Wan, J.; Xu, W.; Zhan, J.; Ma, J.; Li, X.; Xie, Y.; Wang, J.; Zhu, W.-g.; Luo, J.; Zhang, H., PCAF-mediated acetylation of transcriptional factor HOXB9 suppresses lung adenocarcinoma progression by targeting oncogenic protein JMJD6. *Nucleic Acids Res.* **2016,** *44*, (22), 10662-10675.

248. Hubert, J.-N.; Zerjal, T.; Hospital, F., Cancer-and behavior-related genes are targeted by selection in the Tasmanian devil (Sarcophilus harrisii). *PloS one* **2018,** *13*, (8), e0201838.

249. Jen, J.; Wang, Y.-C., Zinc finger proteins in cancer progression. *J. Biomed. Sci.* **2016,** *23*, (1), 53.

250. Zhao, C.; Zou, H.; Zhang, J.; Wang, J.; Liu, H., An integrated methylation and gene expression microarray analysis reveals significant prognostic biomarkers in oral squamous cell carcinoma. *Oncol. Rep.* **2018,** *40*, (5), 2637-2647.

251. Jang, H.-J.; Boo, H.-J.; Lee, H. J.; Min, H.-Y.; Lee, H.-Y., Chronic stress facilitates lung tumorigenesis by promoting exocytosis of IGF2 in lung epithelial cells. *Cancer Res.* **2016,** *76*, (22), 6607-6619.

252. Schones, D. E.; Leung, A.; Natarajan, R., Chromatin modifications associated with diabetes and obesity. *Arterioscler. Thromb. Vasc. Biol.* **2015,** *35*, (7), 1557-1561.

253. Reddy, M. A.; Zhang, E.; Natarajan, R., Epigenetic mechanisms in diabetic complications and metabolic memory. *Diabetologia* **2015,** *58*, (3), 443-455.

254. He, X.; Ou, C.; Xiao, Y.; Han, Q.; Li, H.; Zhou, S., LncRNAs: key players and novel insights into diabetes mellitus. *Oncotarget* **2017,** *8*, (41), 71325-71341.